Biosynthetic Derivatization of Antimicrobial Orthosomycins to Engage a Unique Ribosomal Binding Site

By

Audrey Elizabeth Yñigez-Gutierrez

Dissertation

Submitted to the Faculty of the

Graduate School of Vanderbilt University

in partial fulfillment of the requirements

for the degree of

DOCTOR OF PHILOSOPHY

in

Chemistry

February 28, 2021

Nashville, Tennessee

Approved:

Brian O. Bachmann, Ph.D

Carmelo J. Rizzo, Ph.D

Steven D. Townsend, Ph.D

Tina M. Iverson, Ph.D

A mi esposo, el amor de mi vida

“Sólo tú sabes adonde voy, sólo tú sabes muy bien quien soy.”

-Javier Martín del Campo

Acknowledgements

There are so many people to acknowledge who have helped me to complete this journey. I would like to first acknowledge all of the institutional & financial support from Vanderbilt University, the Department of Chemistry, the Vanderbilt Institute of Chemical Biology, the National Science Foundation, and the National Institutes of Health. Their support and funding of my work has allowed for the completion of this dissertation. I would also like to acknowledge my committee members, who have dedicated so much time and expertise to help train me as a scientist and researchers. I hope I can pay it forward by being as kind and thoughtful as a mentor.

A lot of credit must be attributed to the past and current members of the Vanderbilt Laboratory for Biosynthetic Studies. Much of the work presented here was made possible through collaboration and commiseration with my fellow lab members. In particular, Dr. Emilianne Limbrick who helped to train me at the bench and provide advice and support throughout my time at Vanderbilt. Additionally, Dr. Jordan Froese not only provided his synthetic expertise to help advance the project but also always helped to lighten the mood in lab. Of course, all of my fellow graduate students throughout my time in the VLBS who were always available for scientific discussion and lab high jinks, including some back of the hood chemistry. Special thanks to all of the rotation students and summer intern students who worked with me on the project. I always learned something from my students, and they often helped to advance the work through their efforts. I am extremely grateful, as well, to my mentor Dr. Brian Bachmann. His support throughout my graduate career has guided me to become a better scientist and a deeper thinker. I am deeply appreciative of my time in his lab to develop and grow as a researcher. He was always supportive of my scientific endeavors and pushed me and my project much further than I could have ever imagined.

I would also like to thank my family, especially my mother. She always supported me in my educational pursuits and was patient throughout the years when I lost my way. She is a strong, funny, and completely unique woman who has made me into the person I am today. She was my first teacher and always encouraged me to use my passion to improve the world and the lives of people around me.

Of course, none of my time here at Vanderbilt would have been possible without my husband, Mario, who took the huge leap to first move with me to San Antonio to complete my Bachelors and then to Nashville to attend graduate school. Mario has supported me with patience through the long nights studying and weekends in lab. His kindness and wisdom are an inspiration to me, as well as his resilience and grit. He is the one person who has been with me throughout all the highs and lows of completing a doctoral degree. I will never forget all of the love and support he has given me throughout these years.

Table of Contents

List of Figures

Figure **Page**

List of Tables

Table **Page**

List of Abbreviations

Abbreviation	Meaning
MOA	Mechanism of action
SAR	Structure activity relationship
6-MSA	6-methylsalicyclic acid
3-ABA	3-aminobenzoic acid
PKS	Polyketide synthase
ACP	Acyl carrier protein
SAM	S-adenosyl-L-methionine
ATP	Adenosine triphosphate
GT	Glycosyltransferase
FDH	Flavin-dependent halogenase
PCR	Polymerase chain reaction
DCIE	Dichloroisoeverninic acid
OSA	Orsellinic acid
FT-ICR	Fourier transform ion cyclotron resonance
HMBC	Heteronuclear multiple bond correlation
NMR	Nuclear magnetic resonance
LC/MS	Liquid chromatography – mass spectrometry

Chapter I

Introduction & Dissertation Statement

Secondary metabolites are produced in microorganisms and plants as a means of chemical communication and competition within a given environment. These secondary metabolites are also referred to as natural products, and they often demonstrate inherent biological activity due to their complex and diverse chemical structures. As such, they have long served as a source of therapeutics to combat human disease. From the discovery of penicillin through the golden age of antibiotic discovery, natural products have been developed for the treatment of infectious diseases, cancer, heart disease, and pain management. Nature, however, has not evolved these secondary metabolites specifically as human therapeutics. Therefore, they often suffer from poor solubility, low chemical stability, high toxicity, and poor pharmacological properties. These shortcomings can make the clinical development of natural products difficult and expensive. Due to these issues, there has been a recent shift away from developing natural products as therapeutic candidates. In Chapter II, I highlight a number of case studies demonstrating that our current toolbox of total synthesis, semi-synthesis, and biosynthetic manipulation is capable of altering and improving natural products specifically aimed at developing them as clinical candidates. In particular, we now have the ability to go back through the natural product catalog to identify previously discarded secondary metabolites and rescue them via these methods. The orthosomycins, the natural products that this dissertation focuses on, are a prime example of a discarded class of natural products that we believe can be altered and improved via biosynthetic manipulation and advnace into the clinic.

The orthosomycins are complex oligosaccharide natural products characterized by the unique oxidation state of multiple glycosidic linkages to provide spirocyclic ortho-δ-lactones,

known as orthoesters. Class I orthosomycins include the heptasaccharide orthosomcyins avilamycins and the octasaccharide orthosomycins everninomicins. Both of these analog classes demonstrate significant antibacterial activity, specifically against gram-positive pathogens relevant to human health. The orthosomycins also benefit from inhibiting bacterial growth via a novel MOA to prevent bacterial protein translation. The avilamycins have long been used as feed additives for livestock. Alternatively, everninomicin A was brought forward as a therapeutic candidate and advanced to phase III clinical trials for the treatment of antibiotic-resistant infections. Due to formulation issues, Evn A was withdrawal from clinical trials. However, due to their potent bioactivity, novel MOA, and relative safety, the orthosomycins still remain viable drug candidates to help combat the current antibiotic-resistance crisis. The research presented in this dissertation centers on elucidating key biosynthetic steps with a focus on utilizing the biosynthetic machinery to generate orthosomycin analogs with improved antibacterial activity and pharmacological properties.

Previous work on the everninomicin producer *Micromonospora carbonacea* var. *aurantiaca* focused on improving production titers, characterizing the four wildtype everninomicins produced, and developing robust genetic tools for future manipulation. The work in Chapter III highlights the development of the microporous membrane intergeneric method developed to facilitate targeted genetic deletion in *M. carbonacea* var. *aurantiaca*. In collaboration with Dr. Limbrick, this method was utilized to perform targeted gene-replacement of multiple putative methyltransferases in the everninomicin pathway. Specifically, I performed the targeted deletion of genes encoding for methyltransferases *evdM1* and *evdM5*. I completed the fermentations, extractions, and LC/MS analyses of these deletion strains to identify a total of nine novel everninomicin analogs. When combined with the work performed by Dr. Limbrick and previous work from the Bechthold group in the avilamycin pathway, the deletions and subsequent analysis of the resulting metabolites allowed the annotation of all ten methyltransferases in the

everninomicin pathway. Additionally, I completed the cloning, expression, and purification for *in vitro* characterization of enzymes EvdM5 and EvdM1 with Ms. Callie Dulin. Using the semi-purified metabolites from the respective deletion strains, we confirmed that these enzymes catalyze the attachment of methyl groups to late-stage, fully elaborated everninomicins analogs. Taken together, these results demonstrate our robust genetic deletion technique, provide novel everninomicin analogs, and establish a basis of work to access valuable analogs via genetic manipulation.

The research presented in Chapter IV focuses on investigations into the biosynthesis of the aromatic DCIE acid ring in the everninomicin pathway. At the beginning of my work, the annotation of this pathway was largely based on nucleotide homology to other pathways, including that of avilamycin. Previous work by the Bechthold group into avilamycin biosynthesis demonstrated that enzyme AviM is an iterative type I polyketide synthase (iPKS), the first of its kind described in a bacterial secondary biosynthetic pathway, responsible for synthesizing the orsellinic acid core of DCIE. However, there was no clear mechanistic understanding for the attachment of orsellinic acid to the saccharide core from the iPKS, which lacks a canonical thioesterase domain. A review of similar iPKS enzymes in related biosynthetic pathways, such as tiacumicin B and chlorothricin, did not yield a universal mechanism for the biosynthesis of these small aromatic moieties. While the results from the methyltransferase work covered in Chapter III indicated that methylation is the last biosynthetic transformation in DCIE assembly, the timing and flexibility of ring attachment or halogenation was not clear at the onset of this work. Therefore, Chapter IV presents my work to fully annotate the DCIE biosynthesis via targeted gene deletion of three putative DCIE enzymes in *Micromonospora carbonacea* var. *aurantiaca*, including an iPKS EvdD3, a flavin-dependent halogenase EvdD2, and a putative acyltransferase EvdD1. I completed the fermentation, extraction, and LC/MS and tandem MS analysis of the four novel everninomicin analogs identified from these deletion strains.

Additionally, all three of these enzymes were cloned into appropriate expression vectors for purification from *E. coli* to facilitate *in vitro* biochemical analysis. Following purification of the enzymes and the relevant everninomicin metabolites, I completed biochemical assays to confirm enzymatic substrates and to confirm biosynthetic order for DCIE assembly. In the course of this work, I discovered that EvdD1, a β-ketoacyl-ACP (KAS) III homolog, is responsible for off-loading the orsellinic acid scaffold from the iPKS EvdD3 to a key biosynthetic heptasaccharide shunt product, everninomicin Q (Evn Q). Subsequently, I focused on synthesizing a small library of *N*-acetylcysteamine thioester mimics to introduce non-natural aromatic rings to Evn Q using the transferase EvdD1 to provide wholly novel everninomicin analogs.

This dissertation presents significant advancement in the understanding of everninomicin biosynthesis. Additionally, the identification of the EvdD1 KASIII-like transferase now provides a clear pathway to access non-natural everninomicin analogs. The inherent flexibility of this enzyme indicates that it could be utilized to generate designer everninomicins with improved antibacterial activity. The ultimate focus of this dissertation is to illustrate that we now have the tools and knowledge to rescue this powerful class of natural products and utilize their activity to improve the treatment of bacterial infections in the clinic.

Chapter II

Fixing the unfixable: the arts of improving natural products for human medicine

This chapter is adapted from “Fixing the Unfixable: The Art of Optimizing Natural Products for Human Medicine” published in the Journal of Medicinal Chemistry and has been reproduced in part with the permission of my co-author, Brian O. Bachmann. Reproduced in part with permission from Ynigez-Gutierrez, A. E.; Bachmann, B. O. Fixing the unfixable: The art of optimizing natural products for human medicine. *J Med Chem* **2019**, *62*, 8412-8428. Copyright 2019 American Chemical Society.

Introduction

The complex molecular architecture and high functional density of natural products are responsible for their selective and potent interactions with a wide variety of clinically-relevant biomolecular targets. These properties contribute to the large proportion of natural product-based pharmaceuticals in the clinic.[1] However, as isolated from their source organisms, natural products sometimes possess suboptimal pharmacological properties including high toxicity, poor pharmacokinetics, rapid metabolism, and low solubility or chemical stability. Natural products have acquired a reputation for being intransigent to the contemporary optimization workflows favored by medicinal chemists due to the perception of technical challenges involved in generating targeted changes in complex natural scaffolds. Additionally, questions of supply may raise concerns for the development of natural products and their analogs for clinical applications. In this Chapter, we endeavor to counter this prevailing wisdom by providing support for the opinion that technological advances in synthetic biology and in the chemical synthesis of natural

products render these concerns obsolete. Decades of research focused on natural product biosynthesis and synthetic biology, coupled with the great strides taken in the field of organic synthesis provide powerful tools that demonstrate the ability to salvage natural product scaffolds of high complexity. This Chapter provides case studies demonstrating how several natural product scaffolds have been rescued via biosynthetic manipulation, total synthesis, semi-synthesis, or a combination of these methods. We will discuss the development of pactamycin derivatives harnessing the power of the biosynthetic machinery to access analogs with differential activity. The polyene macrolides will be presented as an example of semi-synthetic and biosynthetic manipulations applied to decrease the mammalian toxicity of a powerful natural product scaffold. The long history of semi-synthetic manipulations of the tetracycline core will also be reviewed, with an eye towards highlighting completely synthetic analogs currently in development. Geldanamycin will be considered as an example of an anti-cancer therapeutic developed via semi-synthetic manipulation and biosynthetic engineering to bypass toxicity and low solubility. The thiopeptides are an example of the advanced biosynthetic and selective semi-synthetic manipulations that can be employed to access potent antimicrobials with increased solubility. Finally, the orthosomycins will be presented as an illustration of a natural product class that were withdrawn from late-stage development due to structural issues that can now be overcome with semi-synthesis and biosynthetic engineering. These examples of a rapidly growing number of success stories highlight the potential for a renaissance in adapting the largely untapped pharmacopeia of natural products currently not optimized for application in human medicine. While the liabilities of many natural products may have appeared insurmountable in the past, our current capacity to precisely manipulate genomes encoding biosynthetic pathways and efficiently synthesize core scaffolds should motivate medicinal chemists to re-embrace natural products. Our ability to adapt natural products' molecular complexity to improve selectivity, potency, and pharmacological properties is now only limited

by our ability to see past initial structural liabilities and embrace the now conjoined arts of natural product synthesis and synthetic biology.

Case Studies in Improving Natural Products

Pactamycin

The aminocyclopentitol pactamycin is a clear example of the intricate and complex molecular diversity available from the natural product catalog. Pactamycin's highly substituted five-membered aminocyclitol core is elaborated with 6-methylsalicylic acid (6-MSA), 3-aminoacetophenone, and a 1,1-dimethylurea.[2] This complex structure directly traces to pactamycin's potent activity across all three domains as a universal protein synthesis inhibitor.[3,4] Crystal structures of pactamycin bound to the 16S rRNA region of the ribosome illustrate that the two aromatic rings lie in the E-site of the 30S ribosome, acting as mRNA mimics to prevent initiation of protein biosynthesis.[5,6] The significant structural similarity between kingdoms at the pactamycin ribosomal binding site likely accounts for its broad and potent activity across gram-positive and negative bacteria, as well as its anti-tumor activity. Unfortunately, pactamycin's broad activity is a double-edged sword, as it is also highly cytotoxic to healthy mammalian cells.[7] Therefore, development of pactamycin as a therapeutic hinges on the ability to access less toxic and/or more selective analogs. The complex architecture, dense functionalization, and chemical instability of pactamycin makes derivatization via semi-synthesis particularly challenging. However, the ability to genetically manipulate the biosynthetic machinery of the producing organism, *Streptomyces pactum*, has provided a rich source of analogs with differentiated activity profiles.

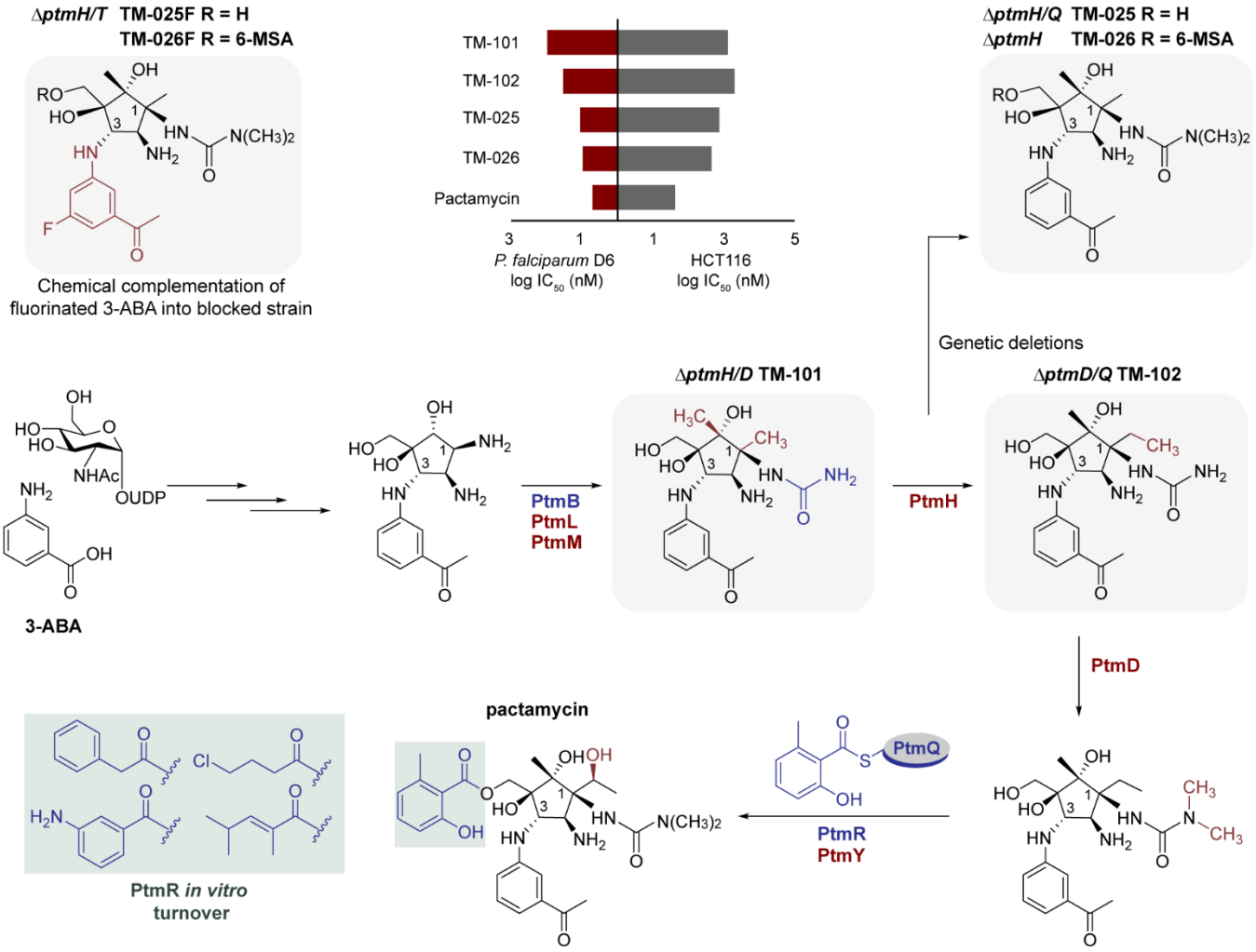

Figure 2-1. Pactamycin biosynthetic pathway with mutant analogs. Novel pactamycins produced by genetic deletion strains highlighted (gray boxes). The pactamycin derivatives show differential activity & an increased therapeutic window against *P. falciparum* as compared to human colon carcinoma cells (HCT116) (inset).

Early studies utilizing isotope labeled substrates identified the key pactamycin biosynthetic precursors for the aminocyclopentitol core, the 3-aminoacetophenone ring, and the 6-MSA ring.[8] In particular, 3-aminobenzoic acid (3-ABA) was identified as a key intermediate in 3-aminoacetophenone biosynthesis from the shikimate pathway.[9] This discovery led to chemical bypass studies of non-natural fluorinated 3-ABA derivatives to yield fluorinated pactamycin analogs, which did not demonstrate decreased cytotoxicity nor differentiated activity.[10] However, these early experiments revealed the possibility of utilizing the biosynthetic machinery to access pactamycin analogs. Advances in genome editing methodology allowed the Mahmud group to develop a robust system for gene inactivation in the pactamycin producer *S. pactum*. Using this

system, Mahmud and coworkers were able to sequentially delete key biosynthetic genes to elucidate the pactamycin biosynthetic pathway and generate a number of analogs with differentiated activity (Figure 2-1).[11] The deletion of the gene encoding the iterative polyketide synthase (iPKS) PtmQ, encoding for 6-MSA biosynthesis, revealed that this moiety may not be necessary for pactamycin bioactivity. Through further gene deletions, the Mahmud group discovered that replacement of the hydroxyethyl group at the C-1 position of the aminocyclitol core with a methyl group resulted in pactamycin analogs with significantly altered activity across domains. For example, pactamycin analogs TM-025/026 completely lacked antibacterial activity but retained eukaryotic activity against the parasite *Plasmodium falciparum*.[12] These analogs also showed divergent activity across kingdoms with significantly decreased cytotoxicity against mammalian cells. In order to further derivatize the already enhanced analogs TM-025/026, the Mahmud group deleted the gene encoding for the pyridoxal phosphate-dependent enzyme PtmT, which is responsible for the conversion of 3-dehydroshikimate to 3-ABA.[13] Thus, fluorinated 3-ABA derivatives were able to chemically bypass the 3-ABA deletion strains. The fluorinated analogs showed similar anti-plasmodial activity as their non-fluorinated equivalents.[14]

Additional deletion of genes encoding late-stage tailoring enzymes in the pactamycin biosynthetic gene cluster elucidated the key biosynthetic steps, as well provided access to additional pactamycin analogs. Double deletion strains lacking the SAM-dependent N-methyltransferase encoded by *ptmD* with previously investigated genes produced key analogs TM-101/102. Even though the des-methyl analogs were less active against *P. falciparum*, they were also less cytotoxic, demonstrating a widening therapeutic window for these typically highly toxic compounds.[15] Current progress in the development of pactamycin derivatives with decreased cytotoxicity has focused on taking advantage of the extremely flexible β-ketoacyl-ACP synthase III-like protein PtmR that installs the 6-MSA moiety at the C-9 position. As previous work has demonstrated that the 6-MSA moiety is not required for bioactivity, it is

possible to envision pactamycin analogs functionalized with diverse acyl moieties to modulate activity.[16,17] Interestingly, jogyamycin is a natural product analog of pactamycin that lacks the 6-MSA and the hydroxylethyl group at C-1.[18] This compound shows decreased antiprotozoal activity with increased cytotoxicity, indicating that while the 6-MSA may not be necessary for bioactivity it may affect selectivity, thus providing a handle for designing pactamycin analogs. In addition to the analogs accessed via biosynthesis, the total synthesis of pactamycin was accomplished by Hanessian and coworkers in 2011.[19] More recently, the Hanessian and Johnson groups have synthesized analogs of this complex class of molecules to gain a clearer understanding of structure-activity relationships (SAR).[20,21] While many of the synthetic analogs have not demonstrated increased or differentiated activity to this point, the ability to efficiently access such analogs synthetically greatly increases the pharmaceutical potential for this potent scaffold.

Polyene Macrolides

The need for less toxic natural product analogs is especially evident in the field of antifungals. The physiological similarity between mammalian and fungal cells makes developing selective antifungals a difficult needle to thread.[22] Since their discovery in the early 1950s, the polyene macrolides, including nystatin and the amphotericins, have been used as antifungals both topically and systemically. In particular, amphotericin B (AmpB) has broad activity against a number of pathogenic fungi such as *Candida albicans*, *Candida neoformans*, and *Blastomyces dermatitidis*.[23] Unfortunately, AmpB has significant nephrotoxicity coupled with poor solubility, relegating it to a drug of last-resort for systemic fungal infections.[24,25] Originally, AmpB was believed to kill fungi via assembly with sterols in the lipid membrane to create channels leading to ion and solute leakage and ultimately to cell death.[26] More recent work from the Burke laboratory suggests another potential mechanism where AmpB acts as a sterol

sponge to extract ergosterol from fungal lipid membranes.[27] Due to its mammalian toxicity and chemical lability to light, oxygen, and acid, generating AmpB or other polyene macrolide analogs with improved properties has been a long-standing goal in the natural product field.

Due to their molecular complexity, the total synthesis of polyene macrolides has been difficult, with several groups developing methods to access these potent compounds synthetically.[28,29] However, the ability to access analogs from bacterial sources via genetic manipulation coupled with elegant semi-synthetic derivatization has provided polyene macrolide analogs with increased activity and decreased toxicity. Polyene macrolide derivatization has focused on three main components of the core structure: the exocyclic carbonyl at C-16, the polyol region, and glycosyl variants at the C-19 position (Figure 2-2). Removal of the exocyclic carboxylic acid at the C-16 position via genetic deletion of the gene encoding a P450 monooxygenase in both the AmpB and nystatin biosynthetic clusters provided the C-16 methylated analogs.[30,31] The Burke group accessed this same AmpB methylated analog (MeAmB) via targeted semi-synthetic methods.[32] In all cases, the loss of the carboxylic acid did not decrease antifungal activity and instead resulted in decreased mammalian hemolysis (Figure 2-2A). Leveraging chemical synthesis, the Burke group generated a number of analogs at the C-16 position via a Curtius rearrangement to yield an oxazolidinone intermediate, which could then be opened by a variety of primary amines. In particular, the urea analogs showed increased water solubility and *in vivo* activity.[33] Zotchev and coworkers were able to investigate similar C-16 nystatin analogs by coupling biosynthetic manipulations with semi-synthesis. By deleting the gene encoding the enoylreductase domain of the NysC polyketide synthase (PKS) in nystatin producer *Streptomyces noursei*, the Zotchev group was able to access a heptaenic version of nystatin, termed S44HP, with improved antifungal activity.[34] The S44HP metabolite was further derivatized to access a large number of C-16 nystatin analogs (S44HP-SZ6,7,14) that showed similar antifungal activity to AmpB but with reduced toxicity.[35]

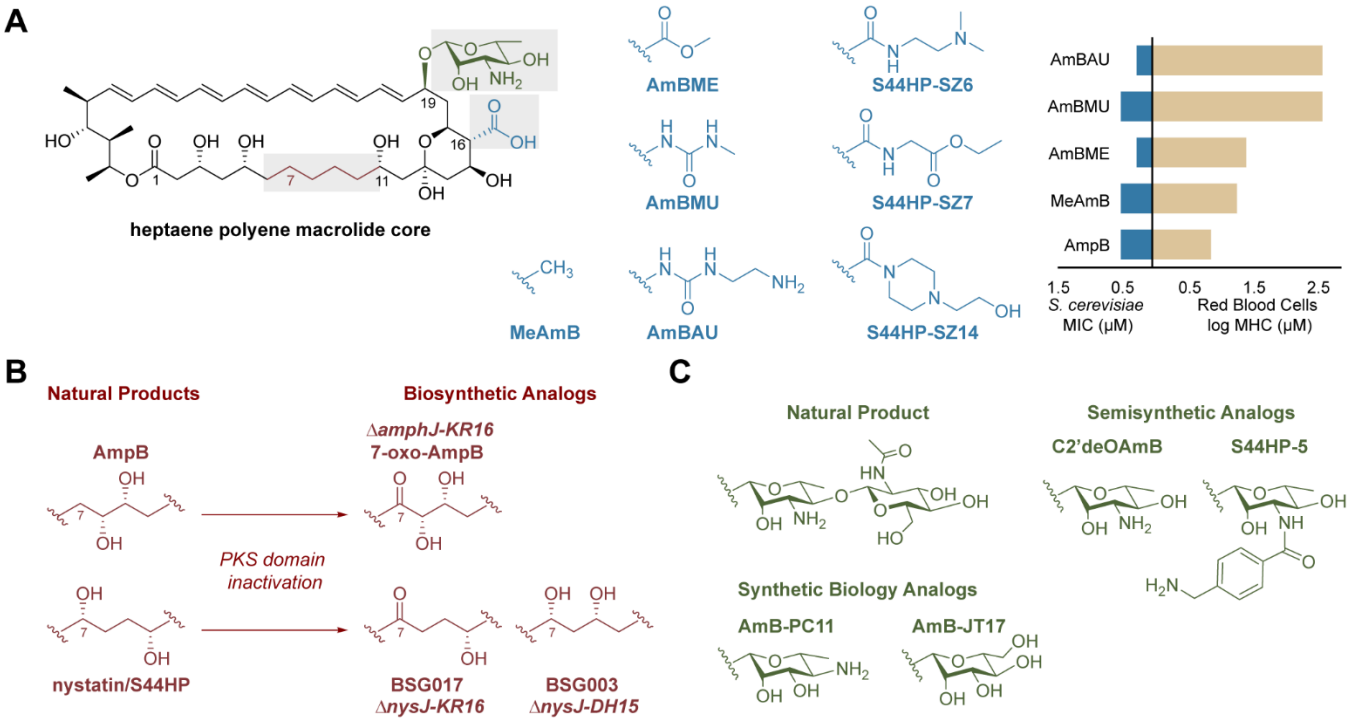

Figure 2-2. Overview of polyene macrolide analogs. Figure 2-(A) Semi-synthetic analogs at the C-16 exocyclic carbonyl (blue). Urea functionalized compounds show similar antifungal properties with decreased hemolytic properties as compared to AmpB (inset). (B) Analogs at the polyol region (red) accessed via functional deletion of genes encoding ketoreductase (KR) and/or dehydratase (DH) domains within nystatin (*nysJ*) and AmpB (*amphJ*) PKS modules. (C) Polyene macrolides with diverse sugar moieties (green) from natural sources and via derivatization.

The polyol region of the polyene macrolides has also proven to be a convenient area for derivatization via biosynthetic manipulations. The oxidation pattern between C-7 and C-10 is one of the primary differences between AmpB and nystatin. Editing portions of the genes encoding individual ketoreductase or dehydratase domains within the PKS modules, as well as post-PKS tailoring enzymes, has afforded access to analogs with diverse oxidation patterns in this region. A number of these analogs, such as 7-oxo-AmpB, retained antifungal activity with decreased hemolytic activity (Figure 2-2B).[31,36,37] The production of these derivatives through genetic manipulation, in light of the evident challenges that their synthetic production would entail, demonstrates the power of this method.

A final portion of the polyene macrolide structure under study is the mycosamine sugar at the C-19 position. Removal of this moiety, either synthetically or biosynthetically, results in a complete loss of antifungal activity.[32,38] However, there is significant room for mycosamine derivatization despite its importance in polyene macrolide activity (Figure 2-2C). Burke and coworkers were able to achieve site-selective acylation of the C-2' position of mycosamine via electronic tuning of acylation reagents.[39] This site-selective functionalization allowed for a clearer understanding of how the C-2' hydroxyl group modulates sterol binding and mammalian toxicity.[40] More complex semi-synthetic transformations, such as double reductive alkylation of the mycosamine moiety, were also found to be well tolerated.[41,42] Synthetic biology approaches have also been successful in providing access to mycosamine derivatives geared towards increasing selectivity. The Thorson group has investigated the AmpB and nystatin glycosyltransferases (GTs) for their potential to introduce glycosyl variants chemoenzymatically.[43] The *in vivo* bioengineering of polyene GTs also provided AmpB derivatives with perosamine and 6-deoxyhexose in place of mycosamine via a hybrid GT.[44] Interestingly, nature has revealed its own ability to produce analogs at this position, as the identification of nystatin-like *Pseudonocardia* polyene (NPP) illustrates. The Kim group identified NPP using targeted genome screening for polyene cytochrome P450 hydroxylases to identify novel polyene natural products.[45] Produced by the rare actinomycete *Pseudonocardia autotrophica*, NPP bears the di-saccharide mycosamine (α1-4)-*N*-acetyl-glucosamine at C-19, which results in greatly increased water solubility and decreased hemolytic activity.[46] The identification of new analogs within known natural product classes via genome mining also has the potential to revitalize underdeveloped scaffolds as these previously unknown analogs may exhibit improved activity or pharmacological properties. The polyene macrolides remain a therapeutic of last resort for serious fungal infections despite their toxicity and poor solubility. Biosynthetic and semi-synthetic techniques, however, have generated polyene macrolides with

improved activity profiles. The development of AmpB and nystatin derivatives with decreased toxicity and retained antifungal properties is quite promising for the continued development of these natural products.

Tetracyclines

The tetracycline polyketides are a class of potent natural products that have provided broad-spectrum antibacterial therapeutics for decades. Along with the eponymous tetracycline, there are three related natural products that differ only on the north side of the scaffold; these analogs initially provided a rich source of antibiotics (Figure 2-3A).[47,48] However, all natural tetracycline analogs are oxidized to introduce a hydroxyl at C-6, which is known to undergo acid-catalyzed dehydration to yield anhydrotetracycline analogs with reported nephrotoxicity.[49] Due to this structural liability, semi-synthetic analogs of the tetracycline core have been of significant interest in the field. Early work led to the discovery that the tetracyclines undergo acidic hydrogenolysis to yield 6-deoxy analogs that are resistant to dehydration while maintaining antibacterial activity.[50] This conservative change resulted in the development of the terramycin derivative, doxycycline, which remains one of the most prescribed generic antibiotics in use (Figure 2-3B). This transformation also increases the reactivity of the C-7 and C-9 positions of the 6-deoxy-tetracycline core. Nitration of the C-7 position allowed for reductive methylation to yield the alkylated amino-tetracycline analog, minocycline, with increased activity against tetracycline sensitive and resistant bacterial strains.[51]

While these second generation semi-synthetic analogs expanded the range of potential applications for the tetracyclines in the clinic, their widespread prescription has also contributed to growing tetracycline resistance. The tetracyclines inhibit protein translation by binding to the 30S ribosomal subunit to block aminoacylated tRNA from binding the ribosomal A-site.[5] Resistance to the tetracyclines is acquired via *tet* genes that encode for efflux pumps, ribosomal

protection proteins, or tetracycline destructases.[52,53] Increasing acquisition of *tet* genes prompted new investigations into tetracycline derivatization, particularly at the C-9 position. The American Cyanamid Company led the way with expanded investigations into the potent glycylcyclines by developing an efficient route of nitration, reduction, and acylation of minocycline at the C-9 position to provide analogs with increased antibacterial activity against tetracycline resistant strains.[54,55] A 9-*t*-butylglycylamido minocycline derivative bypassed major tetracycline resistance mechanisms *in vivo* and *in vitro*, resulting in its approval for use in the clinic as tigecycline (Figure 2-3C).[56] Due to an FDA black-box warning, tigecycline is now an antibiotic of last resort used to combat only the most serious of bacterial infections.[57] Recently, omadacycline, a novel minocycline derivative, was approved by the FDA for treatment of acute skin infections and bacterial pneumonia.[58] Developed at Paratek Pharmaceuticals, omadacycline is a C9-aminomethylcycline with potent activity against tetracycline resistant strains and improved oral bioavailability compared to tigecycline.[59] Another novel aminomethylcycline, sarecycline, was also recently approved as a targeted spectrum tetracycline for treatment of acne vulgaris. Sarecycline contains a C-7 modification that is unique among tetracycline derivatives. Recent crystal structures of sarecycline bound to the ribosome indicate that the C7-[methoxy(methyl)amino]methyl group protrudes into the messenger RNA binding channel to improve stabilization and increase efficacy, thus providing evidence that C-7 modifications may provide an additional route to develop novel tetracycline derivatives.[60] Sarecycline also shows decreased activity against gram-negative bacilli, which are associated with healthy intestinal flora.[61] The development of novel semi-synthetic tetracycline analogs demonstrates the continued importance of this natural product scaffold in the clinic.

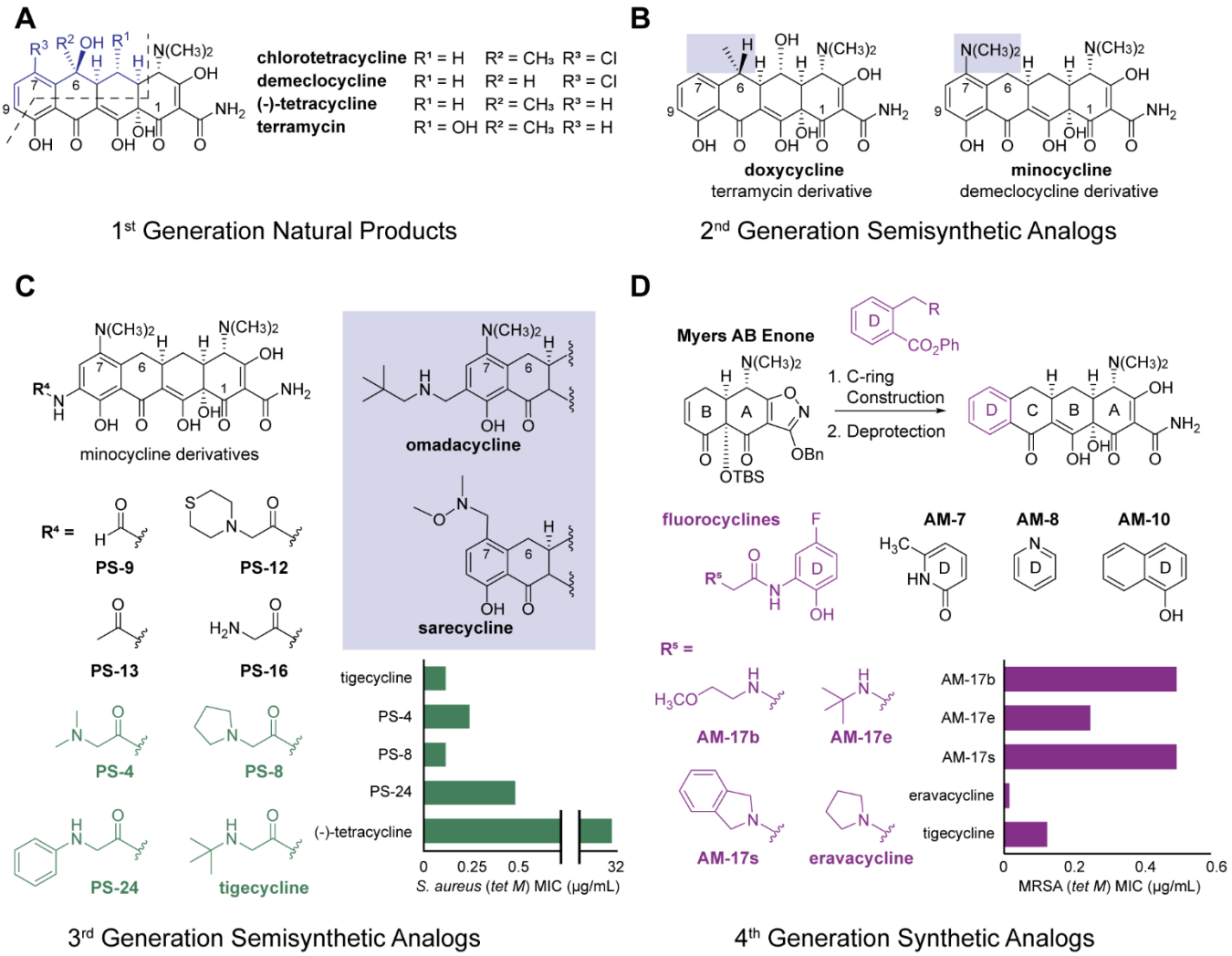

Figure 2-3. Profile of tetracycline analogs. (A) First generation of tetracycline and related natural products. (B) Second generation semi-synthetic 6-deoxy analogs. (C) Third generation semi-synthetic glycylcyclines showing increased activity towards resistant bacteria (inset). Minocycline semi-synthetic derivatives, omadacycline and sarecycline, are highlighted (blue box). (D) Fourth generation fluorocycline derivatives accessed via total synthesis with increased activity towards tetracycline-resistant, methicillin-resistant *Staphylococcus aureus* (MRSA) (inset).

Despite the decades of semi-synthetic derivatization, a scalable and efficient fully synthetic route to the tetracyclines has lagged due to their molecular complexity. From Woodward's first racemic synthesis of sancycline in 1968 to the first enantioselective synthesis of (-)-tetracycline from the Takahashi group in 2000, total synthesis of the tetracyclines has been stymied by lengthy synthetic sequences and low overall yields.[47,62,63] However, this trend was disrupted in 2005 with work from the Myers laboratory. Their approach focused on a tricyclic AB enone

precursor that allowed access to enantiopure tetracycline in a total of 17 steps with 1.1% overall yield.[64] Importantly, this route also allowed for the facile synthesis of numerous tetracycline derivatives through a late-stage addition of the D-ring (Figure 2-3D). A number of these novel tetracycline derivatives showed increased antimicrobial activity against a broad bacterial panel.[65] Along with the development of a more efficient route to the AB enone, the Myers group was able to access approximately 50 tetracycline analogs, including pentacyclines, with excellent antibacterial properties.[66] This work eventually led to the founding of Tetraphase, which continues to develop tetracycline antibiotics. In particular, Tetraphase has focused on the glycylcycline-related fluorocycline analogs, which demonstrate potent antibacterial activity.[67] One such analog, eravacycline, was recently approved for treatment of complicated intra-abdominal infection and urinary tract infections.[68,69] The successful derivatization of the tetracyclines should serve as a powerful reminder of the potential for semi-synthesis and total synthesis to complement one another in the development of natural products for pharmaceutical applications. The past and continued successes of semi-synthetic techniques to develop improved tetracycline analogs informed the total synthesis endeavors by identifying vital points of derivatization. Neither of these techniques must stand alone as we continue to search for new therapeutics from the natural product arsenal.

Geldanamycin

Natural products with anticancer activity often stall in development due to toxicity to non-cancerous cells. A prime example of such a natural product is the macrocyclic lactam geldanamycin. Since its discovery from *Streptomyces hygroscopicus* extracts in 1970, its potency as an extremely active anticancer agent has made geldanamycin a compound of intense study.[70] Despite this, hepatotoxicity along with low stability and bioavailability have made natural geldanamycin a poor choice as a therapeutic.[71] Geldanamycin's antitumor activity,

however, spurred countless investigations into its mechanism of action (MOA), eventually leading to identification of its target. Geldanamycin prevents binding of ATP to the N-terminus of heat shock protein 90 (Hsp90), which is a prevalent molecular chaperone.[72,73] Cancer cells are especially sensitive to geldanamycin due to increased binding to the Hsp90 heterodimers that are overexpressed in tumors.[74] Therefore, the search for improved geldanamycin analogs lacking hepatotoxicity but retaining activity became an area of intense focus.

Multiple groups have investigated total synthetic routes not only to geldanamycin but also to related ansamycin scaffolds.[75] The first total synthesis of an ansamycin natural product, herbimycin A, was completed by the Tatsuta group.[76] Subsequently, Andrus and coworkers completed the first total synthesis of geldanamycin with their work demonstrating the difficultly in accessing the final C-17 methoxy benzoquinone moiety.[77,78] A number of different protecting groups were investigated by Andrus, as well as the Panek group, to reliably achieve the final deprotection to yield the desired *p*-benzoquinone.[79,80] Panek and coworkers were able to extend their synthetic route to access other ansamycin natural product, with a particular focus on non-benzoquinone analogs such as reblastatin and autolytimycin.[81] Despite these robust efforts, a facile method to access geldanamycin analogs has thus far eluded the field, with only a handful of synthetic analogs reported.[82]

Semi-synthetic methods, however, have demonstrated significant utility for the derivatization of geldanamycin. The α,β-unsaturated quinone was immediately recognized as a redox liability of the core structure but also as a potentially powerful site of reactivity. A large number of analogs were readily accessed at the C-17 position by displacing the methoxy group to form 17-amino-17-demethoxygeldanamycin analogs. Derivatization at this position provided analogs with increased *in vitro* activity and decreased overall toxicity, especially the 17-allylamino derivative (17-AAG).[83] Subsequent work focused on increasing solubility and bioavailability, with the 17-(2-dimethylaminoethyl)amino derivative (17-DMAG) showing potent activity and increased

solubility (Figure 2-4B).[84] Overall, the C-17 position appears to be particularly open to derivatization with a large panel of moieties being well-tolerated.[85] Other areas of the geldanamycin scaffold proved less amenable to modification, such as the C-7 carbamate of the ansa-ring, which was determined to be crucial for Hsp90 binding following screening of various substituents.[86] The geldanamycin derivatives 17-AAG and 17-DMAG were eventually brought to clinical trials as tanespimycin and alvespimycin respectively, but neither were advanced for use in the clinic.[87]

Contemporaneously, Kosan Biosciences developed genomic tools to study and manipulate the biosynthetic pathway of geldanamycin in the producer *S. hygroscopicus*. Analogs were accessed by substituting heterologous acyltransferase (AT) domains within the geldanamycin PKS via gene editing. This work yielded a number of geldanamycin analogs with derivatized ansa chains (C-1 to C-16) and contributed to the understanding of the vital interactions between AT domains within PKS proteins (Figure 2-4C). Most importantly perhaps, these compounds illustrated that the hydroquinone form of geldanamycin was as active as the quinone form, thus providing a new avenue for derivatization.[88,89] The Kirschning group focused on accessing related geldanamycin analogs via feeding precursors to a 3-amino-5-hydroxybenzoic acid (AHBA) blocked-mutant of the producer strain (Figure 2-4D). Removal of AHBA production via mutagenesis allowed for supplementation of diverse amino-benzoic acid starting units for geldanamycin incorporation, as AHBA serves as the starter unit for the type I PKS amide synthase in geldanamycin biosynthesis.[90] This work facilitated access to a range of geldanamycin analogs showing differential activity across a number of cancer cell lines and providing a more nuanced understanding of the hydroquinone's SAR in Hsp90 binding.[91,92] Previous semi-synthetic manipulations of the geldanamycin scaffold eventually resulted in the advancement of a number of clinical candidates. Despite not advancing to the clinic, the SAR

data gathered from previous efforts continues to inform the current work towards biosynthetically generated analogs focused on leveraging the Hsp90 target in anticancer treatment.

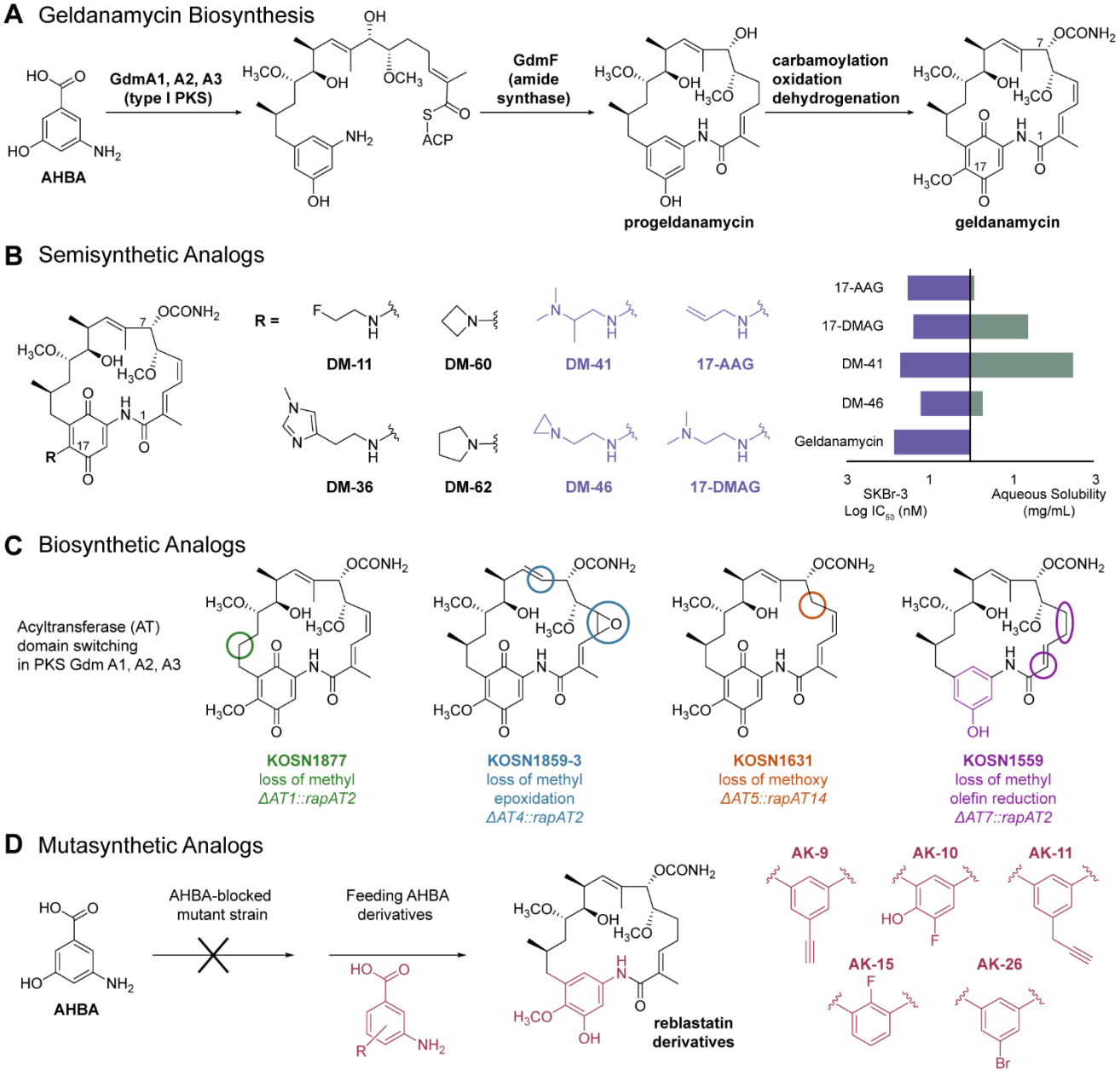

Figure 2-4. Overview of geldanamycin analogs. (A) Geldanamycin biosynthesis. (B) Geldanamycin analogs accessed via semi-synthesis. Alkyl amine analogs show similar activity against human breast cancer cell line (SKBr-3) and increased aqueous solubility as compared to the wildtype geldanamycin compound (inset). (C) Geldanamycin derivatives with ansa chain modifications from acyltransferase (AT) domain switching in the polyketide synthase (PKS) modules of Gdm A1, A2, and A3. (D) Reblastatin analogs accessed via mutasynthetic manipulations and precursor supplementation.

Thiopeptides

The thiopeptides are a class of complex ribosomally synthesized and post-translationally modified peptides (RiPPs).[93,94] These compounds all contain a polyazole cluster with a central nitrogen heterocycle, the oxidation state of which provides the structural classification system.[95] Thiopeptides are sulfur-rich and contain heavily modified side chains off of the peptide core. Despite their ubiquity and high potency against gram-positive pathogenic strains, no thiopeptide is currently approved for use in the clinic. This is likely due to their extremely poor solubility and bioavailability. However, the thiopeptides are known to inhibit bacterial protein synthesis through novel binding sites at the ribosome. Certain thiopeptide classes bind the 23S ribosomal RNA at the L11 binding domain of the 50S ribosomal subunit to abrogate tRNA translocation.[96,97] Conversely, other classes of thiopeptides have been show to bind the bacterial elongation factor Tu (Ef-Tu), preventing the initiation of peptide synthesis.[98] There have been extensive investigations into the derivatization of thiopeptides with the goal of increasing activity and solubility in order to capitalize on their unique MOA and potent activity.[99]

Thiostrepton (Tsr), a series *b* thiopeptide, is the parent of this class of macrocycles. It was first isolated in 1954 from *Streptomyces azureus* and has subsequently been found to be produced by *Streptomyces hawaiiensis* and *Streptomyces laurentii*.[100] Similar to all thiopeptides, Tsr suffers from poor solubility, preventing its use in the clinic. Unfortunately, access to analogs via total synthesis is difficult with only one total synthesis published from Nicolaou and coworkers.[101] However, valuable Tsr analogs have been accessed via biosynthetic manipulations and targeted semi-synthesis. The Kelly group developed a fosmid Tsr expression strain in the homologous producer *S. laurentii* to allow for engineering of the biosynthetic gene cluster.[102] Using this system, Kelly and coworkers replaced amino acids throughout the macrocyclic core in order to investigate the flexibility of the biosynthetic machinery as well as access novel Tsr analogs. Initial replacement of the threonine at the 7-position of the Tsr

propeptide stunted the biosynthesis of the quinaldic acid (QA) macrocycle to provide analogs with significantly decreased antibacterial activity.[103] However, subsequent amino acid substitutions of the alanines at the 4- and 2-position of the propeptide provided Tsr analogs with increased aqueous solubility as compared to the parent compound.[104,105] Importantly, many of these analogs retain the potent antibacterial activity observed with Tsr. More thorough investigations into the QA macrocycle have also yielded valuable Tsr analogs. To this end, the Liu group performed genetic functional analysis to identify the five enzymes involved in converting L-tryptophan to QA in *S. laurentii*.[106] It was confirmed that production of Tsr could be restored to these mutant strains via chemical complementation with the quinaldic acid ketone precursor. Encouraged by these results, the Liu group investigated the incorporation of non-natural QA precursors through chemical complementation in mutated strains to access Tsr analogs. Their work focused on modulating the interactions between the QA portion of Tsr and the 23S rRNA of the 50S ribosome to generate pharmaceutically relevant Tsr analogs with increased antibacterial activity and solubility (Figure 2-5).[107] Further work combined these improvements with modifications to the C-terminus of Tsr via a double-mutant strain lacking TsrB, a carboxylesterase responsible for C-terminal tailoring.[108] Therefore, Liu and coworkers were able to access Tsr analogs with differentiated QA moieties and methyl ester C-termini that demonstrated potency against methicillin-resistant *Staphylococcus aureus* (MRSA) and vancomycin-resistant *Enterococcus faecium* (VRE).[109] Biosynthetic manipulations have provided access to a variety of Tsr analogs with increased activity and drug-like properties, which would have been difficult to achieve synthetically.

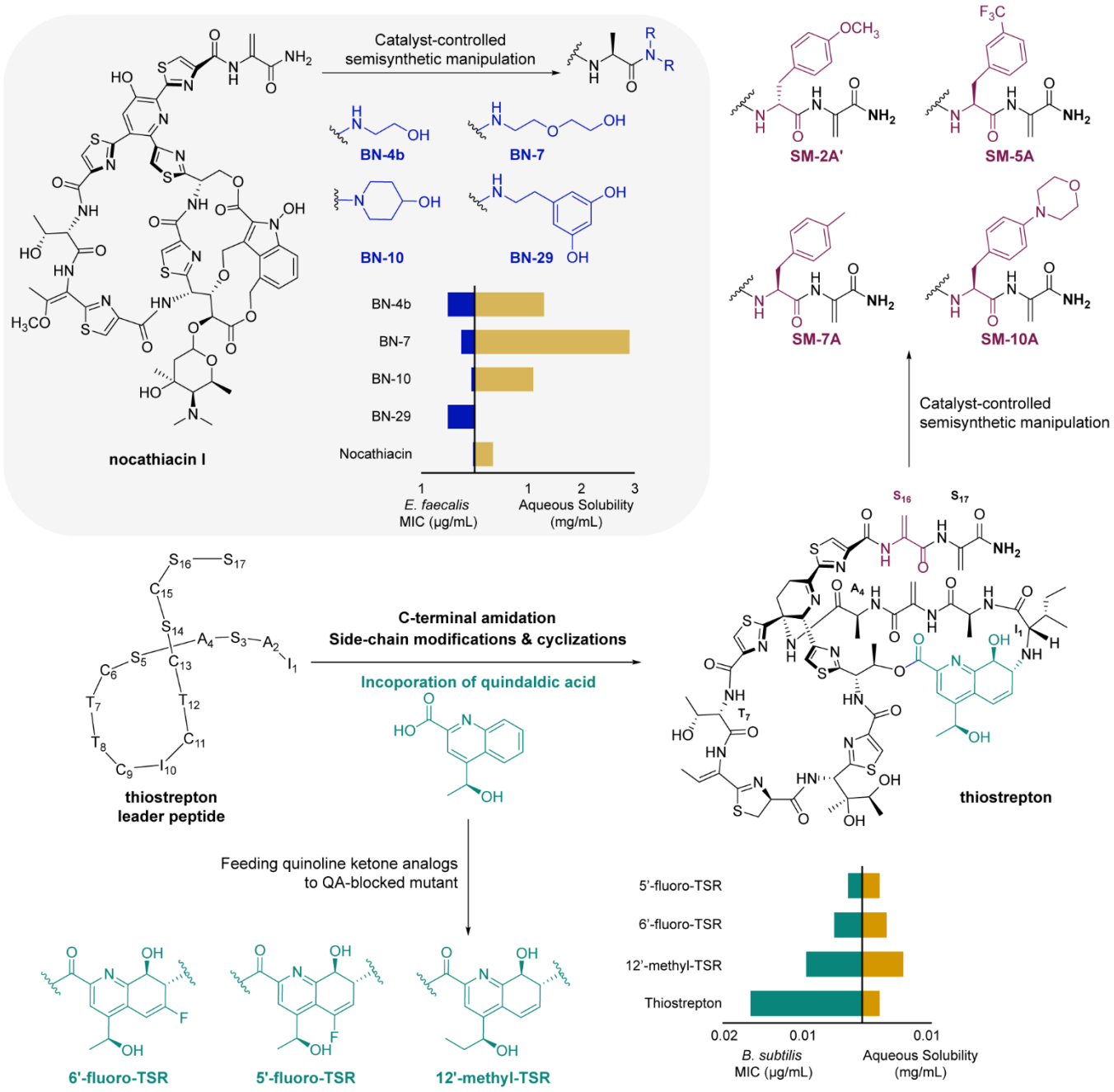

Figure 2-5. Overview of thiopeptide analogs accessed via biosynthetic manipulation and semi-synthesis. Thiostrepton QA-analogs show increased aqueous solubility and antimicrobial activity against *B. subtilis* as compared to the parent compound (inset). Derivatives of nocathiacin I, accessed via stereoselective catalysis, have greatly increased solubility with retention of activity against *E. faecalis*.

Due to the complexity and dense functionalization of the thiopeptides, targeted semi-synthesis of the scaffold is difficult to achieve. Recently, however, the Miller group successfully utilized catalyst-controlled site- and stereoselective functionalization to access Tsr derivatives.

A rhodium catalyzed conjugate arylation was optimized to selectively functionalize the subterminal dehydroalanine residue at the C-terminus in a fully deprotected Tsr substrate (Figure 2-5). Further, diastereoselectivity was also achieved by varying the proton source and base to provide Tsr derivatives with retained antibiotic activity.[110] Catalyst-controlled semi-synthetic routes have also been successful for the derivatization of the *e* series thiopeptide nocathiacin. Nocathiacin is produced by *Nocardia* sp. and *Amycolatopsis* sp. MJ347-81F4 and is highly active against a number of drug-resistant gram-positive bacteria.[111,112] Bristol-Meyers Squibb dedicated considerable semi-synthetic effort to increasing the solubility of nocathiacin in an attempt to capitalize on its activity. While nocathiacin is less complex than thiostrepton, it contains multiple functional groups that make selective late-stage functionalization challenging. Initial conjugations to the C-terminus dehydroalanine side-chain introduced a variety of amines and thiol Michael adducts, resulting in derivatives with increased water solubility.[113,114] However, all of these nocathiacin analogs were produced as diastereomeric mixtures, thus increasing production costs. Therefore, a method for asymmetric hydrogenation of the dehydroalanine olefin was developed using a rhodium catalyst to achieve high diastereomeric excess.[115] Subsequent derivatization of the C-terminus end provided compounds with greatly increased solubility and high antibacterial activity (Figure 2-5, gray inset).

Similar strategies have also been employed for the development of series *d* thiopeptides. Initial investigations into the thiocillin thiopeptides revealed the overall biosynthetic logic of these natural products.[116,117] These discoveries aided in the biosynthetic manipulation of the producing strain, *Bacillus cereus* ATCC 14579, to allow for SAR studies to be performed on the thiocillins. The Walsh laboratory substituted alanine for all residues in the thiocillin prepeptide and substituted serine for all cysteine residues to evaluate scaffold incorporation and, when successful, the antibiotic activity of analogs.[118,119] The inherent flexibility in these pathways has allowed for more recent work from Bower and coworkers focusing on the promiscuous enzymes

involved in thiopeptide biosynthesis to access novel analogs.[120,121] Conversely, a semi-synthetic strategy was employed by Novartis for the development of related thiopeptide GE2270A. Modifications at the C-terminus allowed for the introduction of an *N*-alkylated urethane moiety, greatly increasing aqueous solubility with a retention of antimicrobial activity.[122,123] One of these derivatives, LFF571, was advanced to clinical trials as an oral treatment for *Clostridium difficile*, where it showed noninferiority to vancomycin.[124,125] These examples show the power of the selective functionalization of complex natural products to access derivatives with improved pharmacological properties.

Orthosomycins

The orthosomycins are natural products first identified from the extracts of soil-dwelling actinobacteria and are comprised of two main classes.[126] Class I orthosomycins include oligosaccharides containing at least one dichloroisoeverninic (DCIE) acid ester, and class II orthosomycins are pseudotrisaccharides with aminocyclitol cores. Both orthosomycin classes contain the unique oxidation of at least one glycosidic bond to provide the eponymous orthoester linkages between saccharide residues. The class I orthosomycins have additional rare structural features such as a large proportion of deoxy sugars, a first-in-class nitrosugar, complex methylation patterns, and a further unique methylenedioxy bridge on the terminal eurekanate sugar.[127] These features endow the orthosomycins with potent bioactivity, and class I orthosomycins, in particular, have been the focus of intense study for their potential application to combat bacterial infections. The two main members of this class are the avilamycins and the everninomicins. The avilamycins are produced by *Streptomyces viridochromogenes* Tü57 and are heptasaccharides that contain a single DCIE ester. There are currently sixteen naturally occurring avilamycin derivatives described in the literature, with the most significant differences between these analogs being centered on the G- and H-rings.[128,129] In comparison, the

everninomicins are octasaccharides that contain up to two DCIE esters and are produced by variants of *Micromonospora carbonacea*. The everninomicins differ from the avilamycins most notably by their terminal nitrosugar, evernitrose.[130] Approximately fourteen natural everninomicin analogs have been described to date, demonstrating nature's ability to generate a large library of these complex natural products. Both the everninomicins and the avilamycins show potent antibacterial activity against a number of pathogens relevant to human health. This bioactivity has led to the avilamycins finding an application as feedstock additives for poultry and swine to prevent infection and improve growth.[131,132] The everninomicins, on the other hand, were developed as clinical therapeutics by the Schering-Plough Corporation.[133] In particular, the analog everninomicin A (Evn A, Ziracin) was found to be highly active against gram-positive pathogens such as *Staphylococcus aureus*, *Streptococcus pneumoniae*, and *Clostridium difficile*.[134] Unfortunately, due to difficulties in developing a robust formulation, Evn A was withdrawal from phase III clinical studies in 2000.[135]

The withdrawal of Evn A from clinical trials due to poor reproducibility in formulation highlights a common hindrance to natural product candidates. The inability to rapidly generate analogs with a goal towards improving solubility and pharmacological properties can result in prime clinical candidates being discarded. Despite this setback for the orthosomycins, this class of natural products has remained of interest due to their novel MOA. Everninomicin resistant *Strep. pneumoniae* isolates provided strong evidence that the orthosomycins act as translation inhibitors.[136] While the bacterial ribosome is a common macromolecular target of natural products, many of these molecules bind to the peptidyl transferase center leading to cross-resistance between drug classes.[137] However, it was discovered that everninomicin's binding site on the 50S ribosomal subunit was not inhibited in competition assays with other known ribosome targeting molecules, making them prime clinical candidates.[138] Further studies confirmed the orthosomycins inhibit translation via a unique interaction with the 50S hairpins 89

and 91, as well as the ribosomal protein L16.[139-141] More recently, however, a complete picture of the 50S ribosomal subunit binding site for the orthosomycins has been obtained via X-ray and cyro-EM structures.[142,143] From these structures, the unique binding site of the orthosomycins is now fully elaborated to provide a snapshot of the extended oligosaccharide structure bound to the ribosome. Many of these interactions had been elucidated via previous biochemical studies, such as the interaction of the heptasaccharide core (rings B-H) in the minor groove of hairpins 89 and 91. The structures also identified a crucial interaction between the western DCIE ring and the ribosomal protein L16; in particular, the aromatic ring has direct interaction with residues Arg-51, Arg-55, and Arg-59. This observation aligns with previously identified orthosomycin resistant mutants with altered residues at these positions and demonstrates the importance of the DCIE ester moiety for bioactivity, which will be further explored in Chapter IV.[136,140,144] The ribosome structures provide a map to facilitate the development of this powerful class of natural products for the clinic via focused SAR studies.

The obvious clinical applications of the orthosomycins coupled with their unique and complex structures have made this class of natural products a target for total synthesis. The Nicolaou group completed a total synthesis of Evn A that required the development of methodology for the stereocontrolled synthesis of 1,1'-disaccharides and the unique orthoesters.[145-150] Unfortunately, this total synthetic route, while impressive, was not amenable to the generation of analogs nor was it focused on improving everninomicin activity or pharmacology. Conversely, during the development of Evn A, the Schering-Plough Corporation spent considerable effort to identify semi-synthetic methods to derivatize the everninomicin scaffold. These efforts were complicated by the acid lability of the orthoester linkages, which are absolutely necessary for antibiotic activity.[133] A key difference between the avilamycins and the everninomicins is the presence of the nitrosugar, evernitrose, on the latter. The lack of the evernitrose sugar on the avilamycins does not appear to greatly differentiate its antibiotic activity

from the everninomicins, and both orthosomycins retain significant gram-positive activity against a number of strains. Ganguly and coworkers determined that while the evernitrose sugar was not required for activity, it could be a useful handle for semi-synthetic derivatization. In particular, they sought to improve the pharmacokinetic properties of the everninomicins to increase *in vivo* potency. Initial semi-synthetic efforts utilized electrochemical modifications using tetraethylammonium fluoroborate to provide Evn D analogs with altered evernitrose sugars. In particular, everninomicin-7 (evn-7) was found to have significantly improved pharmacokinetics with retention of antibiotic activity.[151] While the lower N-oxidation congeners of Evn D and Evn A were observable in fermentation extracts in low levels, Ganguly and coworkers developed reduction protocols to specifically reduce the nitro of evernitrose. With reliable access to the amino derivative, later termed everninomicin E (Evn E), they were able to access everninomicin N-acyl derivatives termed Evn D-20,22-24.[152] The N-acetyl derivative Evn D-20, in particular, showed improved pharmacokinetic properties coupled with high antibiotic activity. This methodology was applied to the Evn A scaffold to further probe the SAR of the evernitrose sugar. Amino acid derivatives were coupled to the amino congener of Evn A to provide access to derivatives Evn A-20, 21, 24; Ganguly and coworkers found that this position was amenable to the introduction of fairly large groups without a loss of activity (Figure 2-6A).[153] These observations align with currently available everninomicin-50S ribosome structures showing minimal direct interactions between the evernitrose sugar and the ribosome due to its orientation up and away from the binding site. Also of note, both of the nitro congeners Evn A and Evn D, show potent activity against a wide variety of gram-positive pathogens, but they do not demonstrate significant gram-negative activity.[134,154-156] The workers at Schering-Plough reported the reduced Evn A amino analog showed modulated activity towards gram-negative species while abolishing gram-positive activity.[157] These results indicate that the evernitrose

sugar may be exploited towards activity modulation and to expand the potential application of the everninomicins in the clinic.

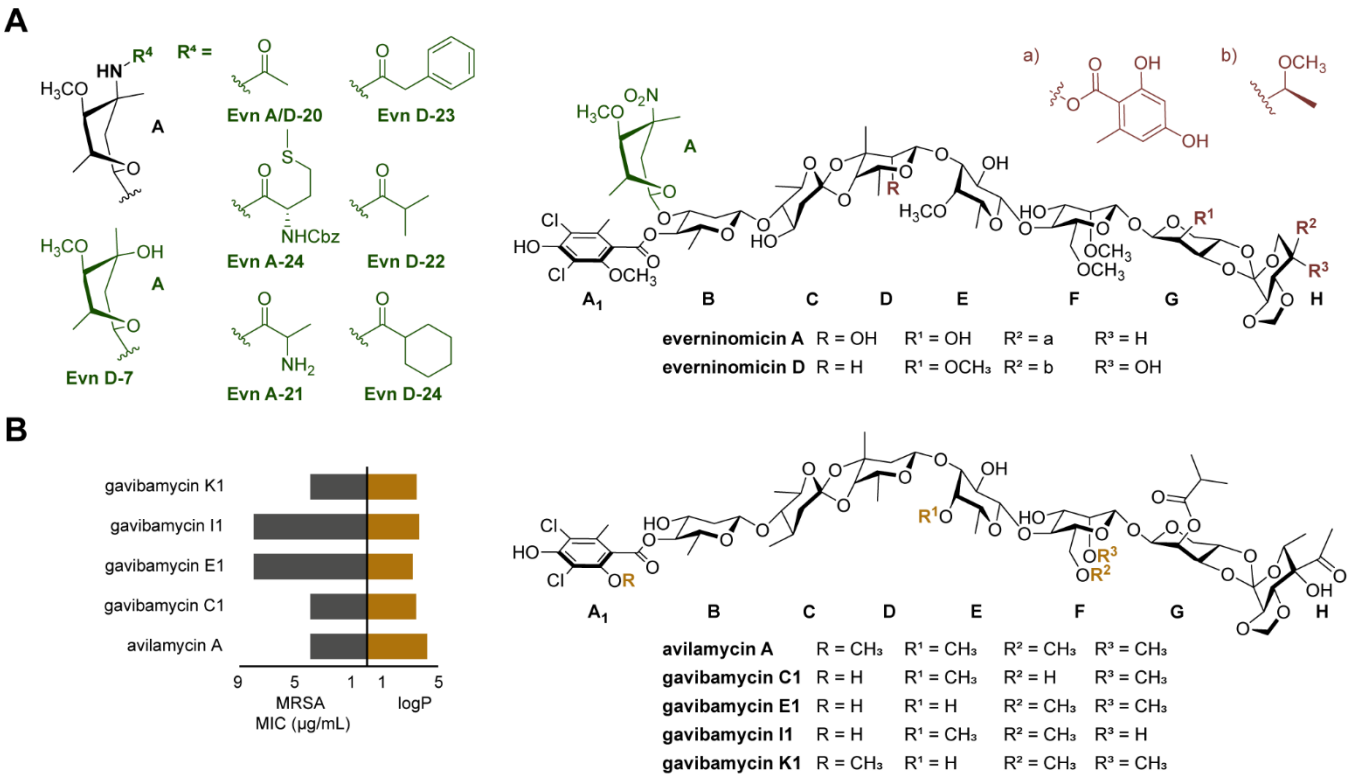

Figure 2-6. Overview of orthosomycins and relevant analogs. (A) Structures of wildtype everninomicins A and D with semi-synthetic analogs of the evernitrose sugar (green). (B) Avilamycin A and gavibamycin analogs accessed via biosynthetic manipulation. The n-octanol-water partition (P) is decreased in gavibamycin analogs as compared to parent avilamycin A, showing increased aqueous solubility. These analogs also show similar activity against methicillin-resistant *S. aureus* (MRSA) (inset).

Despite obstacles to develop orthosomycin analogs with improved structural features, recent work to elucidate the biosynthetic pathways of these complex natural products now provides an alternative pathway to once again advance these molecules as therapeutics. While significant efforts were expended to bring everninomicin to the clinic, many basic questions concerning orthosomycin biosynthesis remained unanswered. The Bechthold group endeavored to investigate orthosomycin biosynthesis by developing a PCR method to amplify and identify genes responsible for the biosynthesis of deoxysugar moieties.[158] This methodology allowed

identification of the avilamycin gene cluster in the producing strain *Strep. viridochromogenes* Tü57 and genetic disruption via insertional inactivation.[159] The gene encoding for a putative methyltransferase *aviG4* was inactivated individually and in double mutations with the putative halogenase gene *aviH* to provide four novel metabolites termed the gavibamycins, which retained their antibiotic activity against a number of human pathogenic strains.[160] Subsequent genetic deletions of methyltransferases provided access to fifteen gavibamycin analogs with differing methylation patterns across the avilamycin scaffold. While not all of these analogs were stable enough to be isolated, the Bechthold group was able to analyze a number of the gavibamycins' solubility and antibiotic activity (Figure 2-6B).[161] Gavibamycin E1, lacking the methyl groups at the ortho hyroxyl of DCIE and the C-4 hydroxyl of D-fucose (E-ring), showed a 10-fold increase in water solubility with a relative retention of antibiotic activity as compared to the wildtype avilamycin A. These initial orthosomycin biosynthetic studies demonstrate that orthosomycins can be favorable modified via gene cluster alterations. Additional gene inactivation by Bechthold and coworkers identified key biosynthetic proteins such as the rRNA methyltransferases responsible for self-resistance, the oxidases responsible for the formation of the orthoester linkages, and the enzymes involved in the formation and attachment of the unique, terminal eurekanate sugar (H-ring).[162-166] While none of these gene deletions provided additional analogs with improved activity or solubility, the further annotation of the biosynthetic pathway allowed for subsequent work on the everninomicins.

Bachmann and coworkers were especially interested in discovering the biosynthetic mechanisms for the construction of the everninomicins' defining features, the evernitrose sugar and the orthoester bonds. Their work identified and characterized a flavin-dependent nitrososynthase responsible for the double oxidation required to convert the amino variant of evernitrose to the nitroso.[167] Structural characterization confirmed the preferred enzymatic substrates and mechanism for oxidation of the amino sugar.[168] In addition to the identification of

key enzymatic transformation *in vitro*, the Bachmann laboratory also developed robust methods for the reproducible manipulation of the everninomicin biosynthetic pathway in the producer *Micromonospora carbonacea* var. *aurantiaca*. This producing strain generates the four oxidation states of evernitrose, everninomicins D-G (Evn D-G). Bachmann and coworkers were able to adapt the Gust PCR-targeted λ-red recombination system to perform targeted gene inactivation in this producing strain.[169] They performed targeted disruptions of the genes encoding for two of the three α-ketoglutarate oxygenases, *evdO1* and *evdMO1*, believed to be responsible for the formation of the unique orthoester linkages.[170] These genetic deletions did not yield any detectable everninomicin metabolites to provide insight into the oxygenases substrates. However, through a collaboration with the Iverson laboratory, the crystal structures of a number of these oxygenases were obtained with enzymes from the avilamycin, everninomicin, and the class II orthosomycin hygromycin B pathways represented. The synthesis of all of the potential substrates for the oxygenases proved impractical for *in vitro* analysis; however, a low-micromolar affinity was measured between hygromycin B and its putative oxygenase HygX. This result indicated that HygX catalyzes the formation of the orthoester bond as the final biosynthetic step. These results were later confirmed by Sun and coworkers via deletion of the gene *hygX* in the hygromycin B producer *Streptomyces hygroscopicus* subsp. *hygroscopicus* DSM 40578. Deletion of *hygX* provided access to the ring-open metabolite hygromycin C, which was subsequently shown to undergo cyclization in the presence of purified HygX.[171]

The orthosomycins are complex natural product scaffolds with potent antibacterial activity. While the avilamycins are currently used as livestock additives, the everninomicins were developed as candidates for use in the clinic. Unfortunately, poor reproducibility in Evn A formulation led to their discontinuation in phase III clinical trials despite their potency and reported safety. While the total synthesis of Evn A (Ziracin) was completed by Nicolaou and coworkers, this methodology was not capable of allowing quick access to relevant analogs with

retained activity and improved properties. The Bechthold group elucidated multiple biosynthetic steps via insertional genetic inactivation and generated a number of analogs, termed the gavibamycins, with improved solubility and retention of antibiotic activity. Likewise, the Bachmann laboratory has successfully utilized targeted genetic deletion in *Micromonospora carbonacea* var. a*urantiaca* and *in vitro* expression and analysis to investigate key biosynthetic transformations. The accumulation of this biosynthetic knowledge in addition to the recent elucidation of the unique MOA of the orthosomycins provides a pathway to the development of novel orthosomycin analogs focused on improving this powerful class of molecules for deployment in the clinic.

Additional Case Studies

The six case studies illustrated in this Perspective represent only a small portion of the many examples of therapeutics derived from natural products via synthesis, semi-synthesis, and/or biosynthetic manipulation. An important example of continued development of natural products are the macrolides, which have provided a rich source of therapeutics since their discovery. Multiple generations of macrolide derivatives have now been accessed via semi-synthesis from the parent compound erythromycin.[172,173] Additionally, investigations into the biosynthetic machinery deoxyerythronolide B synthase (DEBS) yielded the discovery of multi-modular PKS systems responsible for the biosynthesis of many natural products and allowed for manipulation of these pathways to access macrolide analogs.[174,175] Despite multiple generations of macrolides currently in the clinic, there is a continued need for analogs that can overcome widespread resistance. Novel screening techniques that use the bacterial ribosome to template *in situ* click chemistry may provide improved macrolide scaffolds with increased potency against resistant strains.[176,177] In addition, semi-synthetic techniques now stand to be complemented by total synthetic methods from the Myers laboratory using a scalable route to easily access

macrolides of varying ring size and substitution patterns.[178,179] Thus, the ability to access novel macrolides able to bypass growing resistance is likely on the horizon.

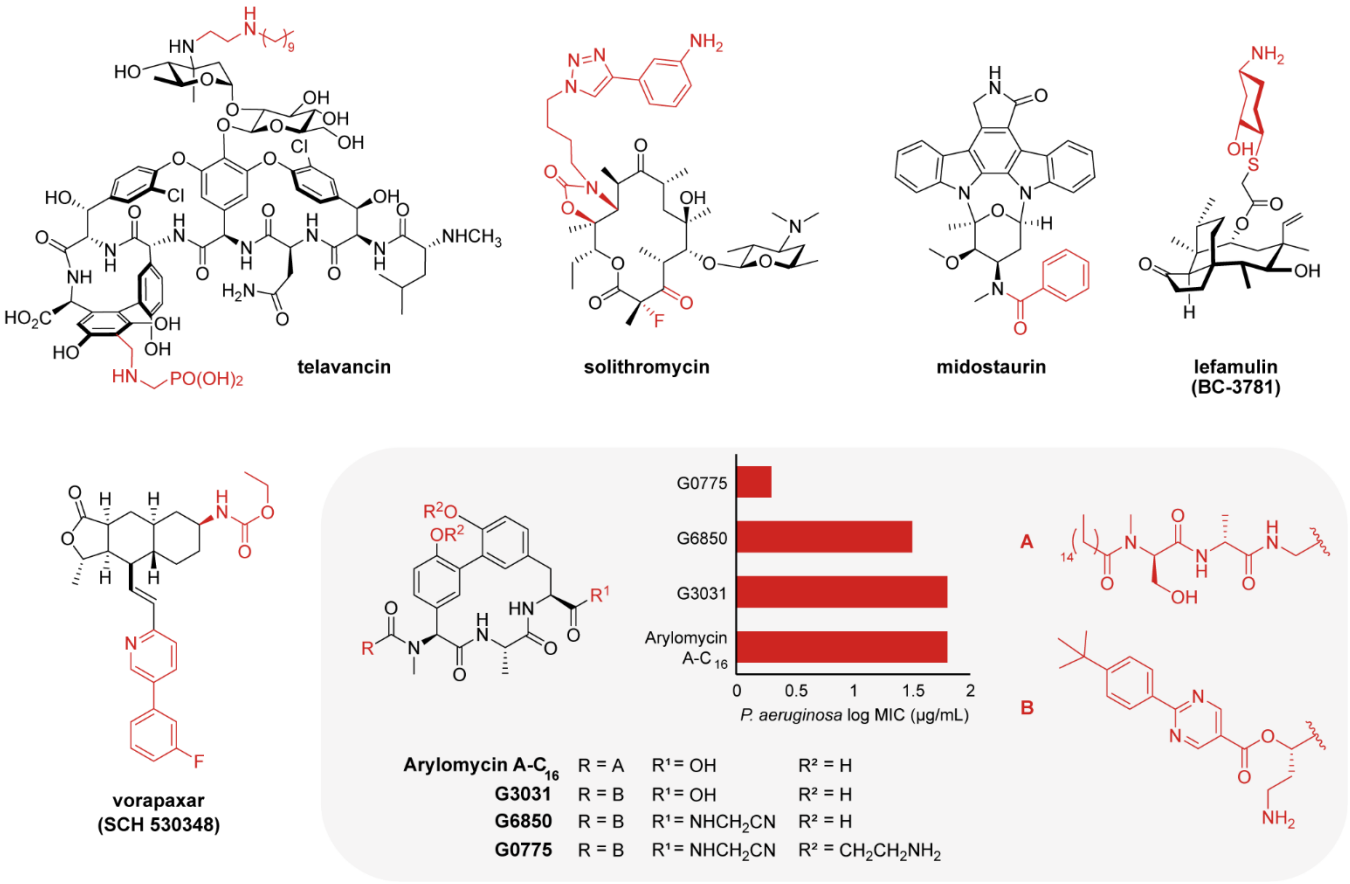

Figure 2-7. Natural product derivatives accessed via biosynthetic manipulation, semi-synthesis, or total synthesis (changes to scaffold highlighted in red). Telavancin is a first-generation glycopeptide derivative accessed via semi-synthesis from vancomycin. The macrolide solithromycin is accessed in 9 steps from clarithromycin. Midostaurin is an N-benzoyl-staurosporine analog approved for treatment of acute myeloid leukemia. Total synthesis allows access to vorapaxar, a himbacine analog, employed in the treatment of coronary heart disease. Generation of arylomycin A-C_{16} analogs yielded compound G0775, which shows increased activity against gram-negative pathogen *P. aeruginosa* (gray inset).

The glycopeptide antibiotics are another well-known example of successful semi-synthetic derivatization of a natural product scaffold. Vancomycin and teicoplanin antibiotics are used in the clinic in their natural form. However, both of these scaffolds have been improved upon to introduce additional generations of glycopeptides into the clinic with increased potency and *in*

vivo stability.[180] Telavancin, a vancomycin derivative, shows enhanced potency and improved bioavailability (Figure 2-7).[181] Other second generation glycopeptides, such as dalbavancin and oritavancin, benefit from greatly extended half-lives to allow for less frequent dosing. Oritavancin is a derivative of chloroeremomycin with an alkyl chain on the vancosamine amino group and an aminosugar on the phenylserine hydroxyl. These changes resulted in extended drug half-life and retention of activity against vancomycin-resistant *Staph. aureus* (VRSA) and enterococci (VRE).[182] Total synthesis of the glycopeptides has been advanced by a number of groups allowing access to more complex analogs and the development of powerful synthetic tools.[183] Boger and coworkers have used total synthesis to generate vancomycin derivatives specifically designed to act via multiple mechanisms of action. These analogs show increased potency against vancomycin-resistant strains and decreased susceptibility to resistance due to their multiple bacterial targets.[184] Additionally, site-selective alterations of multiple glycopeptide scaffolds via non-enzymatic catalysis have allowed for targeted changes in the pursuit of active analogs.[185-187] Recently, further elucidation of key late-stage biosynthetic steps from the Seyedsayamdost group has allowed for *in vitro* biosynthesis of the aglycone core from the 7-mer precursor peptide. This chemoenzymatic approach may allow access to additional vancomycin analogs in the future.[188,189]

The lipopeptides are a powerful class of natural products that have undergone a recent renaissance for clinical use. The cyclic lipopeptide daptomycin showed potent antibacterial activity *in vitro* and *in vivo*, but was discontinued due to adverse side effects. However, later development by Cubist Pharmaceuticals was able to overcome these adverse outcomes by altering the dosing schedule to allow daptomycin to make it to the clinic.[190] Additional members of the lipopeptide class, the arylomycins, were first isolated from *Streptomyces* sp. Tü 6075 in 2002 and demonstrated activity against gram-positive organisms.[191] It was eventually discovered that the arylomycins act via inhibition of the essential bacterial type I signal peptidase

(SPase). Subsequently, Romesberg and coworkers investigated which portions of the arylomycin scaffold are necessary for activity via the total synthesis of arylomycin analogs.[192-194] This work led to a scalable synthetic route focusing on C-H functionalization of the arylomycin core to access analogs with increased potency that bypass resistance incurred by SPase mutations.[195] Genentech has also investigated the arylomycins, specifically aiming to broaden their activity for gram-negative organisms. Targeted modifications of the N-terminal lipopeptide tail, the C-terminal carboxylic acid, and the two phenols located on the macrocycle resulted in the compound G0775, which is significantly more potent than the parent compound, arylomycin A-C_{16}, against gram-negative ESKAPE pathogens.[196] Specifically, G0775 showed a 500-fold increase in potency against *E. coli* and a 32-fold increase against *A. baumannii* (Figure 2-7, gray inset). Subsequent SAR studies led to the development of a further derivative, GDC-5338, as the best candidate for the treatment of gram-negative infections.[197]

The ability to access analogs of complex scaffolds via semi-synthesis has also been applied to the mutilins, fungal diterpene natural products. The mutilins inhibit protein synthesis by binding to a unique site on the 50S ribosome, which overlaps both the A- and P-sites of the peptidyl transfer center (PTC).[198] The mutilins were not initially developed for human clinical use due to issues of instability, toxicity, and poor bioavailability.[199] Semi-synthetically derived analogs of the C-14 side chain allowed for the diversification of this class and led to the development of tiamulin for veterinary use.[200] Subsequently, a topical formulation of the semi-synthetic retapamulin was developed at GlaxoSmithKline, also using the C-14 side chain as the primary area of derivatization.[201,202] More recent work from Nabriva Therapeutics introduced a thioether at the C-14 side chain and led to the development of lefamulin (BC-3781), an orally available mutilin derivative recently approved for community-acquired bacterial pneumonia, making it the first systemic mutilin in the clinic. (Figure 2-7).[203-205] While these semi-synthetic derivatives have brought the mutilins into the clinic, the investigation of more diverse mutilin analogs requires a

scalable synthetic route. Modular synthetic routes to the mutilins allow for increased scale with the potential to allow development of more complex derivatives.[206,207] Additionally, the Herzon group has developed a route utilizing C-H activation to access analogs at the C-17 and C-20 positions, while also allowing for further investigations into the activity of the gram-negative 12-*epi*-pleuromutilins.[208] These efforts will likely allow access to more diverse mutilin analogs with potential for clinical use.

Natural products continue to be a rich source of antimicrobials in the clinic. However, natural product development is not restricted to antibiotics, as shown by the development of the antiplatelet therapeutic vorapaxar. Developed at Schering-Plough, vorapaxar (SCH 530348) is an analog of the tetracyclic piperidine alkaloid himbacine (Figure 2-7).[209] Initially investigated for its potent antagonist effects for muscarine receptors, research was stymied by a lack of reliable availability of the compound. Therefore, access to himbacine, and subsequent analogs, was reliant on total synthesis.[210,211] Chackalamannil and coworkers used their scalable synthetic route to develop substituted pyridine derivatives of himbacine that showed increased binding to the protease-activated receptor-1 (PAR-1).[212,213] PAR-1 is a thrombin activated G-protein-coupled receptor involved in platelet activation, making it a valuable antiplatelet target for the treatment of cardiovascular disease. Subsequent derivatization of himbacine added an ethyl carbamate at the C-7 position of the tricyclic core, which further improved potency and oral availability.[214] Vorapaxar is a first-in-class PAR-1 antagonist and is a vital tool in the treatment of coronary heart disease.[215]

In the area of cancer therapeutics, the alkaloid indolocarbazoles were identified as promising inhibitors of protein kinases.[216,217] Staurosporine, the first indolocarbazole described, is a potent, but promiscuous, inhibitor of protein kinases. A biosynthetic precursor of staurosporine (K252a), however, was found to specifically inhibit protein kinase C (PKC), which is commonly dysregulated in cancers.[218] Therefore, development of the indocolocarbazoles focused on

increasing selectivity to inhibit specific PKC isozymes.[219] Semi-synthetic modifications of staurosporine via N-alkylation/acylation allowed access to a number of analogs with increased selectivity for PKC.[220] Subsequently, midostaurin, an N-benzoyl-staurosporine derivative, was found to have *in vivo* antitumor activity and to inhibit angiogenesis, eventually leading to its development as a therapeutic to treat acute myeloid leukemia (Figure 2-7).[221,222] While other indolocarbazole derivatives were developed and showed increased protein kinase selectivity, they did not advance to the clinic due to lack of efficacy.[223,224] However, a number of indolocarbazoles are of continued interest due to their antibacterial activity and DNA topoisomerase inhibition, potentially leaving space for additional therapeutic analogs to be advanced.[225]

Discussion

Recent innovations in synthetic biology and chemical synthesis have lowered many perceived barriers to natural product-based drug development. Across all classes of secondary metabolites it is now possible to produce scale quantities of natural products and targeted structural analogs using these technologies. Eliciting changes in potency, toxicity, cell-type selectivity, and pharmacokinetic properties is now well precedented using these methods. Innovations in synthetic methodology now permit rapid and efficient access to potent natural product cores, allowing for the production of analogs that can overcome the structural liabilities of their parent compounds.[226,227] No compound exemplifies these innovations more clearly than the most structurally complex drug accessed via total synthesis on the market, eribulin. A simplified derivative of the natural product halichondrin B, eribulin is an antimicrotubule agent for the treatment of metastatic breast cancer.[228] Its advancement to the clinic was directly due to the ability to access analogs via total synthesis since it was only available in limited amounts

from the natural source, a marine sponge. In conjunction with advances in synthetic chemistry, the ongoing innovations in the biosynthetic arts include inexpensive genome sequencing, gene synthesis, and increasingly facile genetic manipulation of the biosynthetic machinery via advances in genomic editing, such as CRISPR/Cas9 technology.[229-231] Additionally, the increased competence to selectively alter natural products via targeted semi-synthesis also has the potential to revitalize the field.[232] By combining these efforts through collaboration and cross-disciplinary training, we can continue to develop natural product analogs with novel activity and improved profiles.[233,234]

There are pressing clinical needs that require the adaption and improvement of natural products for human medicine. Antibiotic resistance is a critical threat, and historically, natural products have provided the most successful entrée. There is also a need for target and cell-type selectivity in non-infectious diseases such as cancer and neurodegenerative diseases.[235] It is now feasible to greatly expand and improve existing scaffolds to develop new generations of therapeutics and to potentially adapt previously discarded scaffolds using the current state of the art. Within the complexity and functional richness of natural products' structures are the necessary properties to engender target specificity. In particular, the large size and conformation of many natural products facilitates addressing "undruggable" targets, such as protein-protein interactions, that are not easily affected by small molecules. By taking advantage of advances in chemical synthesis and synthetic biology, we can continue to make optimal use of natural products to improve human health.

Acknowledgements

The authors would like to acknowledge support from the National Institutes of Health (no. R01GM092218 awarded to B.O.B. and T32 GM065086-13 awarded to A.E.Y). A.E.Y. received additional funding from the NSF GRFP under Grant No. 1445197.

References

1. Newman, D. J.; Cragg, G. M. Natural products as sources of new drugs from 1981 to 2014. *J Nat Prod* **2016**, *79*, 629-661.

2. Wiley, P. F.; Jahnke, H. K.; MacKellar, F. A.; Kelly, R. B.; Argoudelis, A. D. Structure of pactamycin. *J. Org. Chem.* **1970**, *35*, 1420-1425.

3. Tejedor, F.; Amils, R.; Ballesta, J. P. G. Pactamycin binding site on archaebacterial and eukaryotic ribosomes. *Biochemistry* **1987**, *26*, 652-656.

4. Mankin, A. S.; Garrett, R. A. Chloramphenicol resistance mutations in the single 23s rrna gene of the archaeon *halobacterium halobium*. *Journal of Bacteriology* **1991**, *173*, 3559-3563.

5. Brodersen, D. E.; Clemons, W. M.; Carter, A. P.; Morgan-Warren, R. J.; Wimberly, B. T.; Ramakrishnan, V. The structural basis for the action of the antibiotics tetracycline, pactamycin, and hygromycin b on the 30s ribosomal subunit. *Cell* **2000**, *103*, 1143-1154.

6. Ballesta, J. P. G.; Cundliffe, E. Site-specific methylation of 16s rrna caused by pct, a pactamycin resistance determinant from the producing organism, *streptomyces pactum*. *J. Bacteriol.* **1991**, *173*, 7213-7218.

7. Bhuyan, B. K.; Dietz, A.; Smith, C. G. Pactamycin, a new antitumor antibiotic. I. Discovery and biological properties. *Antimicrob. Agents Chemother.* **1962**, *1961*, 184-190.

8. Weller, D. D.; Rinehart, K. L. Biosynthesis of the antitumor antibiotic pactamycin. A methionine-derived ethyl group and a c7n unit. *Journal of the American Chemical Society* **1978**, *100*, 6757-6760.

9. Rinehart, K. L., Jr.; Potgieter, M.; Delaware, D. L.; Seto, H. Direct evidence from multiple carbon-13-labeling and homonuclear decoupling for the labeling pattern by glucose of the *m*-aminobenzoyl (c7n) unit of pactamycin. *J. Am. Chem. Soc.* **1981**, *103*, 2099-2101.

10. Adams, E. S.; Rinehart, K. L. Directed biosynthesis of 5''-fluoropactamycin in *streptomyces pactum*. *J. Antibiot.* **1994**, *47*, 1456-1465.

11. Ito, T.; Roongsawang, N.; Shirasaka, N.; Lu, W.; Flatt, P. M.; Kasanah, N.; Miranda, C.; Mahmud, T. Deciphering pactamycin biosynthesis and engineered production of new pactamycin analogues. *ChemBioChem* **2009**, *10*, 2253-2265.

12. Lu, W.; Roongsawang, N.; Mahmud, T. Biosynthetic studies and genetic engineering of pactamycin analogs with improved selectivity toward malarial parasites. *Chem. Biol. (Cambridge, MA, U. S.)* **2011**, *18*, 425-431.

13. Hirayama, A.; Eguchi, T.; Kudo, F. A single plp-dependent enzyme pctv catalyzes the transformation of 3-dehydroshikimate into 3-aminobenzoate in the biosynthesis of pactamycin. *ChemBioChem* **2013**, *14*, 1198-1203.

14. Almabruk, K. H.; Lu, W.; Li, Y.; Abugreen, M.; Kelly, J. X.; Mahmud, T. Mutasynthesis of fluorinated pactamycin analogues and their antimalarial activity. *Org. Lett.* **2013**, *15*, 1678-1681.

15. Abugrain, M. E.; Lu, W.; Li, Y.; Serrill, J. D.; Brumsted, C. J.; Osborn, A. R.; Alani, A.; Ishmael, J. E.; Kelly, J. X.; Mahmud, T. Interrogating the tailoring steps of pactamycin biosynthesis and accessing new pactamycin analogues. *ChemBioChem* **2016**, *17*, 1585-1588.

16. Abugrain, M. E.; Brumsted, C. J.; Osborn, A. R.; Philmus, B.; Mahmud, T. A highly promiscuous ss-ketoacyl-acp synthase (kas) iii-like protein is involved in pactamycin biosynthesis. *ACS Chem. Biol.* **2017**, *12*, 362-366.

17. Eida, A. A.; Mahmud, T. The secondary metabolite pactamycin with potential for pharmaceutical applications: Biosynthesis and regulation. *Appl Microbiol Biotechnol* **2019**, *103*, 4337-4345.

18. Iwatsuki, M.; Nishihara-Tsukashima, A.; Ishiyama, A.; Namatame, M.; Watanabe, Y.; Handasah, S.; Pranamuda, H.; Marwoto, B.; Matsumoto, A.; Takahashi, Y.; Otoguro, K.; Omura, S. Jogyamycin, a new antiprotozoal aminocyclopentitol antibiotic, produced by *streptomyces* sp. A-wm-jg-16.2. *J Antibiot (Tokyo)* **2012**, *65*, 169-171.

19. Hanessian, S.; Vakiti, R. R.; Dorich, S.; Banerjee, S.; Lecomte, F.; DelValle, J. R.; Zhang, J.; Deschenes-Simard, B. Total synthesis of pactamycin. *Angew Chem Int Ed* **2011**, *50*, 3497-3500.

20. Hanessian, S.; Vakiti, R. R.; Chattopadhyay, A. K.; Dorich, S.; Lavallee, C. Probing functional diversity in pactamycin toward antibiotic, antitumor, and antiprotozoal activity. *Bioorg. Med. Chem.* **2013**, *21*, 1775-1786.

21. Sharpe, R. J.; Malinowski, J. T.; Sorana, F.; Luft, J. C.; Bowerman, C. J.; DeSimone, J. M.; Johnson, J. S. Preparation and biological evaluation of synthetic and polymer-encapsulated congeners of the antitumor agent pactamycin: Insight into functional group effects and biological activity. *Bioorg. Med. Chem.* **2015**, *23*, 1849-1857.

22. Denning, D. W.; Hope, W. W. Therapy for fungal diseases: Opportunities and priorities. *Trends Microbiol* **2010**, *18*, 195-204.

23. Jambor, W. P.; Steinberg, B. A.; Suydam, L. O. Amphotericins a and b: Two new antifungal antibiotics possessing high activity against deep-seated and superficial mycoses. *Antibiot Annu* **1955**, *3*, 574-578.

24. Dutcher, J. D. The discovery and development of amphotericin b. *Diseases of the Chest* **1968**, *54*, 296-298.

25. Sawaya, B. P.; Briggs, J. P.; Schnermann, J. Amphotericin b nephrotoxicity: The adverse consequences of altered membrane properties. *J. Am. Soc. Nephrol.* **1995**, *6*, 154-164.

26. Hartsel, S. C.; Hatch, C.; Ayenew, W. How does amphotericin b work?: Studies on model membrane systems. *Journal of Liposome Research* **1993**, *3*, 377-408.

27. Gray, K. C.; Palacios, D. S.; Dailey, I.; Endo, M. M.; Uno, B. E.; Wilcock, B. C.; Burke, M. D. Amphotericin primarily kills yeast by simply binding ergosterol. *Proc. Natl. Acad. Sci. U. S. A.* **2012**, *109*, 2234-2239.

28. Nicolaou, K. C.; Daines, R. A.; Ogawa, Y.; Chakraborty, T. K. Total synthesis of amphotericin b. 3. The final stages. *J. Am. Chem. Soc.* **1988**, *110*, 4696-4705.

29. Carreira, E. M.; Cereghetti, D. M. Amphotericin b: 50 years of chemistry and biochemistry. *Synthesis* **2006**, 914-942.

30. Carmody, M.; Murphy, B.; Byrne, B.; Power, P.; Rai, D.; Rawlings, B.; Caffrey, P. Biosynthesis of amphotericin derivatives lacking exocyclic carboxyl groups. *J Biol Chem* **2005**, *280*, 34420-34426.

31. Brautaset, T.; Sletta, H.; Nedal, A.; Borgos, S. E. F.; Degnes, K. F.; Bakke, I.; Volokhan, O.; Sekurova, O. N.; Treshalin, I. D.; Mirchink, E. P.; Dikiy, A.; Ellingsen, T. E.; Zotchev, S. B. Improved antifungal polyene macrolides via engineering of the nystatin biosynthetic genes in *streptomyces noursei*. *Chem. Biol. (Cambridge, MA, U. S.)* **2008**, *15*, 1198-1206.

32. Palacios, D. S.; Anderson, T. M.; Burke, M. D. A post-pks oxidation of the amphotericin b skeleton predicted to be critical for channel formation is not required for potent antifungal activity. *J. Am. Chem. Soc.* **2007**, *129*, 13804-13805.

33. Davis, S. A.; Vincent, B. M.; Endo, M. M.; Whitesell, L.; Marchillo, K.; Andes, D. R.; Lindquist, S.; Burke, M. D. Nontoxic antimicrobials that evade drug resistance. *Nat Chem Biol* **2015**, *11*, 481-487.

34. Bruheim, P.; Borgos, S. E. F.; Tsan, P.; Sletta, H.; Ellingsen, T. E.; Lancelin, J.-M.; Zotchev, S. B. Chemical diversity of polyene macrolides produced by *streptomyces noursei* atcc 11455 and recombinant strain erd44 with genetically altered polyketide synthase nysc. *Antimicrob. Agents Chemother.* **2004**, *48*, 4120-4129.

35. Preobrazhenskaya, M. N.; Olsufyeva, E. N.; Solovieva, S. E.; Tevyashova, A. N.; Reznikova, M. I.; Luzikov, Y. N.; Terekhova, L. P.; Trenin, A. S.; Galatenko, O. A.; Treshalin, I. D.; Mirchink, E. P.; Bukhman, V. M.; Sletta, H.; Zotchev, S. B. Chemical modification and biological evaluation of new semisynthetic derivatives of 28,29-didehydronystatin a1 (s44hp), a genetically engineered antifungal polyene macrolide antibiotic. *J. Med. Chem.* **2009**, *52*, 189-196.

36. Power, P.; Dunne, T.; Murphy, B.; Lochlainn, L. N.; Rai, D.; Borissow, C.; Rawlings, B.; Caffrey, P. Engineered synthesis of 7-oxo- and 15-deoxy-15-oxo-amphotericins: Insights into structure-activity relationships in polyene antibiotics. *Chem. Biol. (Cambridge, MA, U. S.)* **2008**, *15*, 78-86.

37. Brautaset, T.; Sletta, H.; Degnes, K. F.; Sekurova, O. N.; Bakke, I.; Volokhan, O.; Andreassen, T.; Ellingsen, T. E.; Zotchev, S. B. New nystatin-related antifungal polyene macrolides with altered polyol region generated via biosynthetic engineering of *streptomyces noursei*. *Appl. Environ. Microbiol.* **2011**, *77*, 6636-6643.

38. Byrne, B.; Carmody, M.; Gibson, E.; Rawlings, B.; Caffrey, P. Biosynthesis of deoxyamphotericins and deoxyamphoteronolides by engineered strains of *streptomyces nodosus*. *Chem. Biol.* **2003**, *10*, 1215-1224.

39. Wilcock, B. C.; Uno, B. E.; Bromann, G. L.; Clark, M. J.; Anderson, T. M.; Burke, M. D. Electronic tuning of site-selectivity. *Nat Chem* **2012**, *4*, 996-1003.

40. Wilcock, B. C.; Endo, M. M.; Uno, B. E.; Burke, M. D. C2'-oh of amphotericin b plays an important role in binding the primary sterol of human cells but not yeast cells. *J Am Chem Soc* **2013**, *135*, 8488-8491.

41. Volmer, A. A.; Szpilman, A. M.; Carreira, E. M. Synthesis and biological evaluation of amphotericin b derivatives. *Nat Prod Rep* **2010**, *27*, 1329-1349.

42. Preobrazhenskaya, M. N.; Olsufyeva, E. N.; Tevyashova, A. N.; Printsevskaya, S. S.; Solovieva, S. E.; Reznikova, M. I.; Trenin, A. S.; Galatenko, O. A.; Treshalin, I. D.; Pereverzeva, E. R.; Mirchink, E. P.; Zotchev, S. B. Synthesis and study of the antifungal activity of new mono- and disubstituted derivatives of a genetically engineered polyene antibiotic 28,29-didehydronystatin a1 (s44hp). *J. Antibiot.* **2010**, *63*, 55-64.

43. Zhang, C.; Albermann, C.; Fu, X.; Thorson, J. S. The *in vitro* characterization of the iterative avermectin glycosyltransferase avebi reveals reaction reversibility and sugar nucleotide flexibility. *J. Am. Chem. Soc.* **2006**, *128*, 16420-16421.

44. Hutchinson, E.; Murphy, B.; Dunne, T.; Breen, C.; Rawlings, B.; Caffrey, P. Redesign of polyene macrolide glycosylation: Engineered biosynthesis of 19-(*o*)-perosaminyl-amphoteronolide b. *Chem. Biol. (Cambridge, MA, U. S.)* **2010**, *17*, 174-182.

45. Kim, B.-G.; Lee, M.-J.; Seo, J.; Hwang, Y.-B.; Lee, M.-Y.; Han, K.; Sherman, D. H.; Kim, E.-S. Identification of functionally clustered nystatin-like biosynthetic genes in a rare actinomycetes, *pseudonocardia autotrophica*. *J. Ind. Microbiol. Biotechnol.* **2009**, *36*, 1425-1434.

46. Lee, M.-J.; Kong, D.; Han, K.; Sherman, D. H.; Bai, L.; Deng, Z.; Lin, S.; Kim, E.-S. Structural analysis and biosynthetic engineering of a solubility-improved and less-hemolytic nystatin-like polyene in *pseudonocardia autotrophica*. *Appl. Microbiol. Biotechnol.* **2012**, *95*, 157-168.

47. Rossiter, S. E.; Fletcher, M. H.; Wuest, W. M. Natural products as platforms to overcome antibiotic resistance. *Chem. Rev.* **2017**, *117*, 12415-12474.

48. Liu, F.; Myers, A. G. Development of a platform for the discovery and practical synthesis of new tetracycline antibiotics. *Curr. Opin. Chem. Biol.* **2016**, *32*, 48-57.

49. Benitz, K. F.; Diermeier, H. F. Renal toxicity of tetracycline degradation products. *Proc. Soc. Exp. Biol. Med.* **1964**, *115*, 930-935.

50. McCormick, J. R. D.; Jensen, E. R.; Miller, P. A.; Doerschuk, A. P. 6-deoxytetracyclines. Further studies on the relation between structure and antibacterial activity in the tetracycline series. *J. Am. Chem. Soc.* **1960**, *82*, 3381-3388.

51. Martell, M. J., Jr.; Boothe, J. H. 6-deoxytetracyclines. Vii. Alkylated aminotetracyclines possessing unique antibacterial activity. *J. Med. Chem.* **1967**, *10*, 44-46.

52. Chopra, I.; Roberts, M. Tetracycline antibiotics: Mode of action, applications, molecular biology, and epidemiology of bacterial resistance. *Microbiol Mol Biol Rev* **2001**, *65*, 232-260.

53. Forsberg, K. J.; Patel, S.; Wencewicz, T. A.; Dantas, G. The tetracycline destructases: A novel family of tetracycline-inactivating enzymes. *Chem Biol* **2015**, *22*, 888-897.

54. Sum, P.-E.; Petersen, P. Synthesis and structure-activity relationship of novel glycylcycline derivatives leading to the discovery of gar-936. *Bioorg. Med. Chem. Lett.* **1999**, *9*, 1459-1462.

55. Sum, P. E.; Lee, V. J.; Testa, R. T.; Hlavka, J. J.; Ellestad, G. A.; Bloom, J. D.; Gluzman, Y.; Tally, F. P. Glycylcyclines. 1. A new generation of potent antibacterial agents through modification of 9-aminotetracyclines. *J. Med. Chem.* **1994**, *37*, 184-188.

56. Petersen, P. J.; Jacobus, N. V.; Weiss, W. J.; Sum, P. E.; Testa, R. T. In vitro and in vivo antibacterial activities of a novel glycylcycline, the 9-t-butylglycylamido derivative of minocycline (gar-936). *Antimicrobial Agents and Chemotherapy* **1999**, *43*, 738-744.

57. Dixit, D.; Madduri, R. P.; Sharma, R. The role of tigecycline in the treatment of infections in light of the new black box warning. *Expert Rev Anti Infect Ther* **2014**, *12*, 397-400.

58. Barber, K. E.; Bell, A. M.; Wingler, M. J. B.; Wagner, J. L.; Stover, K. R. Omadacycline enters the ring: A new antimicrobial contender. *Pharmacotherapy* **2018**, *38*, 1194-1204.

59. Honeyman, L.; Ismail, M.; Nelson, M. L.; Bhatia, B.; Bowser, T. E.; Chen, J.; Mechiche, R.; Ohemeng, K.; Verma, A. K.; Cannon, E. P.; Macone, A.; Tanaka, S. K.; Levy, S. Structure-activity relationship of the aminomethylcyclines and the discovery of omadacycline. *Antimicrob Agents Chemother* **2015**, *59*, 7044-7053.

60. Batool, Z.; Lomakin, I. B.; Polikanov, Y. S.; Bunick, C. G. Sarecycline interferes with trna accommodation and tethers mrna to the 70s ribosome. *Proc Natl Acad Sci U S A* **2020**, *117*, 20530-20537.

61. Zhanel, G.; Critchley, I.; Lin, L.-Y.; Alvandi, N. Microbiological profile of sarecycline, a novel targeted spectrum tetracycline for the treatment of acne vulgaris. *Antimicrobial Agents and Chemotherapy* **2019**, *63*, e01297-01218.

62. Korst, J. J.; Johnston, J. D.; Butler, K.; Bianco, E. J.; Conover, L. H.; Woodward, R. B. The total synthesis of dl-6-demethyl-6-deoxytetracycline. *J. Amer. Chem. Soc.* **1968**, *90*, 439-457.

63. Tatsuta, K.; Yoshimoto, T.; Gunji, H.; Okado, Y.; Takahashi, M. The first total synthesis of natural (-)-tetracycline. *Chem. Lett.* **2000**, *29*, 646-647.

64. Charest, M. G.; Siegel, D. R.; Myers, A. G. Synthesis of (−)-tetracycline. *Journal of the American Chemical Society* **2005**, *127*, 8292-8293.

65. Charest, M. G.; Lerner, C. D.; Brubaker, J. D.; Siegel, D. R.; Myers, A. G. A convergent enantioselective route to structurally diverse 6-deoxytetracycline antibiotics. *Science (Washington, DC, U. S.)* **2005**, *308*, 395-398.

66. Sun, C.; Wang, Q.; Brubaker, J. D.; Wright, P. M.; Lerner, C. D.; Noson, K.; Charest, M.; Siegel, D. R.; Wang, Y.-M.; Myers, A. G. A robust platform for the synthesis of new tetracycline antibiotics. *J. Am. Chem. Soc.* **2008**, *130*, 17913-17927.

67. Xiao, X.-Y.; Hunt, D. K.; Zhou, J.; Clark, R. B.; Dunwoody, N.; Fyfe, C.; Grossman, T. H.; O'Brien, W. J.; Plamondon, L.; Ronn, M.; Sun, C.; Zhang, W.-Y.; Sutcliffe, J. A. Fluorocyclines. 1. 7-fluoro-9-pyrrolidinoacetamido-6-demethyl-6-deoxytetracycline: A potent, broad spectrum antibacterial agent. *J. Med. Chem.* **2012**, *55*, 597-605.

68. Zhang, W. Y.; Che, Q.; Crawford, S.; Ronn, M.; Dunwoody, N. A divergent route to eravacycline. *J Org Chem* **2017**, *82*, 936-943.

69. Mullard, A. 2018 fda drug approvals. *Nat Rev Drug Discov* **2019**, *18*, 85-89.

70. De Boer, C.; Meulman, P. A.; Wnuk, R. J.; Peterson, D. H. Geldanamycin, a new antibiotic. *J. Antibiot.* **1970**, *23*, 442-447.

71. Supko, J. G.; Hickman, R. L.; Grever, M. R.; Malspeis, L. Preclinical pharmacologic evaluation of geldanamycin as an antitumor agent. *Cancer Chemotherapy and Pharmacology* **1995**, *36*, 305-315.

72. Whitesell, L.; Mimnaugh, E. G.; De Costa, B.; Myers, C. E.; Neckers, L. M. Inhibition of heat shock protein hsp90-pp60v-src heteroprotein complex formation by benzoquinone ansamycins: Essential role for stress proteins in oncogenic transformation. *Proceedings of the National Academy of Sciences* **1994**, *91*, 8324-8328.

73. Stebbins, C. E.; Russo, A. A.; Schneider, C.; Rosen, N.; Hartl, F. U.; Pavletich, N. P. Crystal structure of an hsp90-geldanamycin complex: Targeting of a protein chaperone by an antitumor agent. *Cell* **1997**, *89*, 239-250.

74. Kamal, A.; Thao, L.; Sensintaffar, J.; Zhang, L.; Boehm, M. F.; Fritz, L. C.; Burrows, F. J. A high-affinity conformation of hsp90 confers tumor selectivity on hsp90 inhibitors. *Nature (London, U. K.)* **2003**, *425*, 407-410.

75. Franke, J.; Eichner, S.; Zeilinger, C.; Kirschning, A. Targeting heat-shock-protein 90 (hsp90) by natural products: Geldanamycin, a show case in cancer therapy. *Nat Prod Rep* **2013**, *30*, 1299-1323.

76. Nakata, M.; Osumi, T.; Ueno, A.; Kimura, T.; Tamai, T.; Tatsuta, K. Total synthesis of herbimycin a. *Tetrahedron Letters* **1991**, *32*, 6015-6018.

77. Andrus, M. B.; Meredith, E. L.; Simmons, B. L.; Soma Sekhar, B. B. V.; Hicken, E. J. Total synthesis of (+)-geldanamycin and (−)-*o*-quinogeldanamycin with use of asymmetric *anti*- and *syn*-glycolate aldol reactions. *Organic Letters* **2002**, *4*, 3549-3552.

78. Andrus, M. B.; Meredith, E. L.; Hicken, E. J.; Simmons, B. L.; Glancey, R. R.; Ma, W. Total synthesis of (+)-geldanamycin and (−)-o-quinogeldanamycin: Asymmetric glycolate aldol reactions and biological evaluation. *The Journal of Organic Chemistry* **2003**, *68*, 8162-8169.

79. Andrus, M. B.; Hicken, E. J.; Meredith, E. L.; Simmons, B. L.; Cannon, J. F. Selective synthesis of the *para*-quinone region of geldanamycin. *Org. Lett.* **2003**, *5*, 3859-3862.

80. Qin, H.-L.; Panek, J. S. Total synthesis of the hsp90 inhibitor geldanamycin. *Org. Lett.* **2008**, *10*, 2477-2479.

81. Wrona, I. E.; Gozman, A.; Taldone, T.; Chiosis, G.; Panek, J. S. Synthesis of reblastatin, autolytimycin, and non-benzoquinone analogues: Potent inhibitors of heat shock protein 90. *J. Org. Chem.* **2010**, *75*, 2820-2835.

82. Andrus, M. B.; Wong, Y.; Liu, J.; Beebe, K.; Neckers, L. M. Synthesis and evaluation of 8,9-amido analogs of geldanamycin. *Tetrahedron Letters* **2009**, *50*, 6705-6708.

83. Schnur, R. C.; Corman, M. L.; Gallaschun, R. J.; Cooper, B. A.; Dee, M. F.; Doty, J. L.; Muzzi, M. L.; Moyer, J. D.; DiOrio, C. I.; et, a. Inhibition of the oncogene product p185erbb-2 *in vitro* and *in vivo* by geldanamycin and dihydrogeldanamycin derivatives. *J. Med. Chem.* **1995**, *38*, 3806-3812.

84. Tian, Z. Q.; Liu, Y.; Zhang, D.; Wang, Z.; Dong, S. D.; Carreras, C. W.; Zhou, Y.; Rastelli, G.; Santi, D. V.; Myles, D. C. Synthesis and biological activities of novel 17-aminogeldanamycin derivatives. *Bioorg. Med. Chem.* **2004**, *12*, 5317-5329.

85. Le Brazidec, J.-Y.; Kamal, A.; Busch, D.; Thao, L.; Zhang, L.; Timony, G.; Grecko, R.; Trent, K.; Lough, R.; Salazar, T.; Khan, S.; Burrows, F.; Boehm, M. F. Synthesis and biological evaluation of a new class of geldanamycin derivatives as potent inhibitors of hsp90. *Journal of Medicinal Chemistry* **2004**, *47*, 3865-3873.

86. Rastelli, G.; Tian, Z.-Q.; Wang, Z.; Myles, D.; Liu, Y. Structure-based design of 7-carbamate analogs of geldanamycin. *Bioorg. Med. Chem. Lett.* **2005**, *15*, 5016-5021.

87. Dimopoulos, M.-A.; Mitsiades, C. S.; Anderson, K. C.; Richardson, P. G. Tanespimycin as antitumor therapy. *Clinical Lymphoma, Myeloma and Leukemia* **2011**, *11*, 17-22.

88. Patel, K.; Piagentini, M.; Rascher, A.; Tian, Z.-Q.; Buchanan, G. O.; Regentin, R.; Hu, Z.; Hutchinson, C. R.; McDaniel, R. Engineered biosynthesis of geldanamycin analogs for hsp90 inhibition. *Chemistry & Biology* **2004**, *11*, 1625-1633.

89. Buchanan, G. O.; Regentin, R.; Piagentini, M.; Rascher, A.; McDaniel, R.; Galazzo, J. L.; Licari, P. J. Production of 8-demethylgeldanamycin and 4,5-epoxy-8-

demethylgeldanamycin from a recombinant strain of *streptomyces hygroscopicus*. *J. Nat. Prod.* **2005**, *68*, 607-610.

90. Eichner, S.; Floss, H. G.; Sasse, F.; Kirschning, A. New, highly active nonbenzoquinone geldanamycin derivatives by using mutasynthesis. *ChemBioChem* **2009**, *10*, 1801-1805.

91. Bułyszko, I.; Dräger, G.; Klenge, A.; Kirschning, A. Evaluation of the synthetic potential of an ahba knockout mutant of the rifamycin producer *amycolatopsis mediterranei*. *Chemistry – A European Journal* **2015**, *21*, 19231-19242.

92. Mohammadi-Ostad-Kalayeh, S.; Stahl, F.; Scheper, T.; Kock, K.; Herrmann, C.; Heleno Batista, F. A.; Borges, J. C.; Sasse, F.; Eichner, S.; Ongouta, J.; Zeilinger, C.; Kirschning, A. Heat shock proteins revisited: Using a mutasynthetically generated reblastatin library to compare the inhibition of human and *leishmania* hsp90s. *ChemBioChem* **2018**, *19*, 562-574.

93. Kelly, W. L.; Pan, L.; Li, C. Thiostrepton biosynthesis: Prototype for a new family of bacteriocins. *J. Am. Chem. Soc.* **2009**, *131*, 4327-4334.

94. Liao, R.; Duan, L.; Lei, C.; Pan, H.; Ding, Y.; Zhang, Q.; Chen, D.; Shen, B.; Yu, Y.; Liu, W. Thiopeptide biosynthesis featuring ribosomally synthesized precursor peptides and conserved posttranslational modifications. *Chem. Biol. (Cambridge, MA, U. S.)* **2009**, *16*, 141-147.

95. Bagley, M. C.; Dale, J. W.; Merritt, E. A.; Xiong, X. Thiopeptide antibiotics. *Chem. Rev. (Washington, DC, U. S.)* **2005**, *105*, 685-714.

96. Cameron, D. M.; Thompson, J.; March, P. E.; Dahlberg, A. E. Initiation factor if2, thiostrepton and micrococcin prevent the binding of elongation factor g to the *escherichia coli* ribosome. *Journal of Molecular Biology* **2002**, *319*, 27-35.

97. Harms, J. M.; Wilson, D. N.; Schluenzen, F.; Connell, S. R.; Stachelhaus, T.; Zaborowska, Z.; Spahn, C. M. T.; Fucini, P. Translational regulation via l11: Molecular switches on the ribosome turned on and off by thiostrepton and micrococcin. *Mol. Cell* **2008**, *30*, 26-38.

98. Heffron, S. E.; Jurnak, F. Structure of an ef-tu complex with a thiazolyl peptide antibiotic determined at 2.35 å resolution: Atomic basis for ge2270a inhibition of ef-tu. *Biochemistry* **2000**, *39*, 37-45.

99. Just-Baringo, X.; Albericio, F.; Alvarez, M. Thiopeptide engineering: A multidisciplinary effort towards future drugs. *Angew. Chem., Int. Ed.* **2014**, *53*, 6602-6616.

100. Pagano, J. F.; Weinstein, M. J.; Stout, H. A.; Donovick, R. Thiostrepton, a new antibiotic. I. *In vitro* studies. *Antibiot. Annu.* **1956**, 554-559.

101. Nicolaou, K. C.; Zak, M.; Safina, B. S.; Estrada, A. A.; Lee, S. H.; Nevalainen, M. Total synthesis of thiostrepton. Assembly of key building blocks and completion of the synthesis. *J. Am. Chem. Soc.* **2005**, *127*, 11176-11183.

102. Li, C.-X.; Zhang, F.-F.; Kelly, W. L. Heterologous production of thiostrepton a and biosynthetic engineering of thiostrepton analogs. *Mol. BioSyst.* **2011**, *7*, 82-90.

103. Li, C.; Zhang, F.; Kelly, W. L. Mutagenesis of the thiostrepton precursor peptide at thr7 impacts both biosynthesis and function. *Chem. Commun. (Cambridge, U. K.)* **2012**, *48*, 558-560.

104. Zhang, F.; Kelly, W. L. Saturation mutagenesis of tsra ala4 unveils a highly mutable residue of thiostrepton a. *ACS Chem. Biol.* **2015**, *10*, 998-1009.

105. Zhang, F.; Li, C.; Kelly, W. L. Thiostrepton variants containing a contracted quinaldic acid macrocycle result from mutagenesis of the second residue. *ACS Chem. Biol.* **2016**, *11*, 415-424.

106. Duan, L.; Wang, S.; Liao, R.; Liu, W. Insights into quinaldic acid moiety formation in thiostrepton biosynthesis facilitating fluorinated thiopeptide generation. *Chem. Biol. (Cambridge, MA, U. S.)* **2012**, *19*, 443-448.

107. Wang, S.; Zheng, Q.; Wang, J.; Zhao, Z.; Li, Q.; Yu, Y.; Wang, R.; Liu, W. Target-oriented design and biosynthesis of thiostrepton-derived thiopeptide antibiotics with improved pharmaceutical properties. *Organic Chemistry Frontiers* **2015**, *2*, 106-109.

108. Liao, R.; Liu, W. Thiostrepton maturation involving a deesterification-amidation way to process the c-terminally methylated peptide backbone. *J. Am. Chem. Soc.* **2011**, *133*, 2852-2855.

109. Wang, S.; Zheng, Q.; Wang, J.; Chen, D.; Yu, Y.; Liu, W. Concurrent modifications of the c-terminus and side ring of thiostrepton and their synergistic effects with respect to improving antibacterial activities. *Org. Chem. Front.* **2016**, *3*, 496-500.

110. Key, H. M.; Miller, S. J. Site- and stereoselective chemical editing of thiostrepton by rh-catalyzed conjugate arylation: New analogues and collateral enantioselective synthesis of amino acids. *J Am Chem Soc* **2017**, *139*, 15460-15466.

111. Leet, J. E.; Li, W.; Ax, H. A.; Matson, J. A.; Huang, S.; Huang, R.; Cantone, J. L.; Drexler, D.; Dalterio, R. A.; Lam, K. S. Nocathiacins, new thiazolyl peptide antibiotics from *nocardia* sp. Ii. Isolation, characterization, and structure determination. *J. Antibiot.* **2003**, *56*, 232-242.

112. Sasaki, T.; Otani, T.; Matsumoto, H.; Unemi, N.; Hamada, M.; Takeuchi, T.; Hori, M. Mj347-81f4 a & b, novel antibiotics from *amycolatopsis* sp.: Taxonomic characteristics, fermentation, and antimicrobial activity. *J. Antibiot.* **1998**, *51*, 715-721.

113. Naidu, B. N.; Sorenson, M. E.; Zhang, Y.; Kim, O. K.; Matiskella, J. D.; Wichtowski, J. A.; Connolly, T. P.; Li, W.; Lam, K. S.; Bronson, J. J.; Pucci, M. J.; Clark, J. M.; Ueda, Y. Nocathiacin i analogues: Synthesis, in vitro and in vivo biological activity of novel semi-synthetic thiazolyl peptide antibiotics. *Bioorg. Med. Chem. Lett.* **2004**, *14*, 5573-5577.

114. Naidu, B. N.; Sorenson, M. E.; Bronson, J. J.; Pucci, M. J.; Clark, J. M.; Ueda, Y. Synthesis, in vitro, and in vivo antibacterial activity of nocathiacin i thiol-michael adducts. *Bioorg. Med. Chem. Lett.* **2005**, *15*, 2069-2072.

115. Naidu, B. N.; Sorenson, M. E.; Matiskella, J. D.; Li, W.; Sausker, J. B.; Zhang, Y.; Connolly, T. P.; Lam, K. S.; Bronson, J. J.; Pucci, M. J.; Yang, H.; Ueda, Y. Synthesis and

antibacterial activity of nocathiacin i analogues. *Bioorg. Med. Chem. Lett.* **2006**, *16*, 3545-3549.

116. Wieland Brown, L. C.; Acker, M. G.; Clardy, J.; Walsh, C. T.; Fischbach, M. A. Thirteen posttranslational modifications convert a 14-residue peptide into the antibiotic thiocillin. *Proc. Natl. Acad. Sci. U. S. A.* **2009**, *106*, 2549-2553.

117. Bowers, A. A.; Walsh, C. T.; Acker, M. G. Genetic interception and structural characterization of thiopeptide cyclization precursors from *bacillus cereus*. *J. Am. Chem. Soc.* **2010**, *132*, 12182-12184.

118. Acker, M. G.; Bowers, A. A.; Walsh, C. T. Generation of thiocillin variants by prepeptide gene replacement and *in vivo* processing by *bacillus cereus*. *J. Am. Chem. Soc.* **2009**, *131*, 17563-17565.

119. Bowers, A. A.; Acker, M. G.; Koglin, A.; Walsh, C. T. Manipulation of thiocillin variants by prepeptide gene replacement: Structure, conformation, and activity of heterocycle substitution mutants. *Journal of the American Chemical Society* **2010**, *132*, 7519-7527.

120. Gober, J. G.; Ghodge, S. V.; Bogart, J. W.; Wever, W. J.; Watkins, R. R.; Brustad, E. M.; Bowers, A. A. P450-mediated non-natural cyclopropanation of dehydroalanine-containing thiopeptides. *ACS Chem. Biol.* **2017**, *12*, 1726-1731.

121. Fleming, S. R.; Bartges, T. E.; Vinogradov, A. A.; Kirkpatrick, C. L.; Goto, Y.; Suga, H.; Hicks, L. M.; Bowers, A. A. Flexizyme-enabled benchtop biosynthesis of thiopeptides. *Journal of the American Chemical Society* **2019**, *141*, 758-762.

122. LaMarche, M. J.; Leeds, J. A.; Dzink-Fox, J.; Gunderson, K.; Krastel, P.; Memmert, K.; Patane, M. A.; Rann, E. M.; Schmitt, E.; Tiamfook, S.; Wang, B. 4-aminothiazolyl analogs of ge2270 a: Antibacterial lead finding. *J. Med. Chem.* **2011**, *54*, 2517-2521.

123. LaMarche, M. J.; Leeds, J. A.; Amaral, K.; Brewer, J. T.; Bushell, S. M.; Dewhurst, J. M.; Dzink-Fox, J.; Gangl, E.; Goldovitz, J.; Jain, A.; Mullin, S.; Neckermann, G.; Osborn, C.; Palestrant, D.; Patane, M. A.; Rann, E. M.; Sachdeva, M.; Shao, J.; Tiamfook, S.; Whitehead, L.; Yu, D. Antibacterial optimization of 4-aminothiazolyl analogues of the natural product ge2270 a: Identification of the cycloalkylcarboxylic acids. *J. Med. Chem.* **2011**, *54*, 8099-8109.

124. LaMarche, M. J.; Leeds, J. A.; Amaral, A.; Brewer, J. T.; Bushell, S. M.; Deng, G.; Dewhurst, J. M.; Ding, J.; Dzink-Fox, J.; Gamber, G.; Jain, A.; Lee, K.; Lee, L.; Lister, T.; McKenney, D.; Mullin, S.; Osborne, C.; Palestrant, D.; Patane, M. A.; Rann, E. M.; Sachdeva, M.; Shao, J.; Tiamfook, S.; Trzasko, A.; Whitehead, L.; Yifru, A.; Yu, D.; Yan, W.; Zhu, Q. Discovery of lff571: An investigational agent for *clostridium difficile* infection. *J Med Chem* **2012**, *55*, 2376-2387.

125. Mullane, K.; Lee, C.; Bressler, A.; Buitrago, M.; Weiss, K.; Dabovic, K.; Praestgaard, J.; Leeds, J. A.; Blais, J.; Pertel, P. Multicenter, randomized clinical trial to compare the safety and efficacy of lff571 and vancomycin for *clostridium difficile* infections. *Antimicrob Agents Chemother* **2015**, *59*, 1435-1440.

126. Wright, D. E. The orthosomycins, a new family of antibiotics. *Tetrahedron* **1979**, *35*, 1207-1237.

127. McCranie, E. K.; Bachmann, B. O. Bioactive oligosaccharide natural products. *Natural Product Reports* **2014**, *31*, 1026-1042.

128. Buzzetti, F.; Eisenber.F; Grant, H. N.; Kellersc.W; Voser, W.; Zahner, H. Avilamycin. *Experientia* **1968**, *24*, 320-&.

129. Mertz, J. L.; Peloso, J. S.; Barker, B. J.; Babbitt, G. E.; Occolowitz, J. L.; Simson, V. L.; Kline, R. M. Isolation and structural identification of 9 avilamycins. *J Antibiot* **1986**, *39*, 877-887.

130. Ganguly, A. K.; Sarre, O. Z.; Reimann, H. Chemistry of everninomicin antibiotics. Iii. Evernitrose, a naturally occurring nitro sugar from everninomicins. *Journal of the American Chemical Society* **1968**, *90*, 7129-7130.

131. Williams, R. B. Intercurrent coccidiosis and necrotic enteritis of chickens: Rational, integrated disease management by maintenance of gut integrity. *Avian Pathol* **2005**, *34*, 159-180.

132. Jones, D. J.; Mowrey, D. H.; Anderson, D. B.; Wellenreiter, R. H. Effect of various levels of avilamycin on the performance of growing-finishing swine. *J. Anim. Sci.* **1987**, *65*, 881-885.

133. Ganguly, A. K. Ziracin, a novel oligosaccharide antibiotic. *J Antibiot* **2000**, *53*, 1038-1044.

134. Foster, D. R.; Rybak, M. J. Pharmacologic and bacteriologic properties of sch-27899 (ziracin), an investigational antibiotic from the everninomicin family. *Pharmacotherapy: The Journal of Human Pharmacology and Drug Therapy* **1999**, *19*, 1111-1117.

135. Ganguly, A. K. Challenges in drug discovery at schering-plough research institute: A personal reflection. *Annu. Rep. Med. Chem.* **2013**, *48*, 3-14.

136. Adrian, P. V.; Zhao, W.; Black, T. A.; Shaw, K. J.; Hare, R. S.; Klugman, K. P. Mutations in ribosomal protein l16 conferring reduced susceptibility to evernimicin (sch27899): Implications for mechanism of action. *Antimicrobial Agents and Chemotherapy* **2000**, *44*, 732-738.

137. Wilson, D. N. Ribosome-targeting antibiotics and mechanisms of bacterial resistance. *Nature Reviews Microbiology* **2014**, *12*, 35-48.

138. McNicholas, P. M.; Najarian, D. J.; Mann, P. A.; Hesk, D.; Hare, R. S.; Shaw, K. J.; Black, T. A. Evernimicin binds exclusively to the 50s ribosomal subunit and inhibits translation in cell-free systems derived from both gram-positive and gram-negative bacteria. *Antimicrobial Agents and Chemotherapy* **2000**, *44*, 1121-1126.

139. Belova, L.; Tenson, T.; Xiong, L.; McNicholas, P. M.; Mankin, A. S. A novel site of antibiotic action in the ribosome: Interaction of evernimicin with the large ribosomal subunit. *Proc Natl Acad Sci U S A* **2001**, *98*, 3726-3731.

140. Aarestrup, F. M.; Jensen, L. B. Presence of variations in ribosomal protein l16 corresponding to susceptibility of enterococci to oligosaccharides (avilamycin and evernimicin). *Antimicrobial Agents and Chemotherapy* **2000**, *44*, 3425-3427.

141. McNicholas, P. M.; Mann, P. A.; Najarian, D. J.; Miesel, L.; Hare, R. S.; Black, T. A. Effects of mutations in ribosomal protein l16 on susceptibility and accumulation of evernimicin. *Antimicrob Agents Chemother* **2001**, *45*, 79-83.

142. Krupkin, M.; Wekselman, I.; Matzov, D.; Eyal, Z.; Diskin Posner, Y.; Rozenberg, H.; Zimmerman, E.; Bashan, A.; Yonath, A. Avilamycin and evernimicin induce structural changes in rproteins ul16 and ctc that enhance the inhibition of a-site trna binding. *Proceedings of the National Academy of Sciences* **2016**, *113*, E6796-E6805.

143. Arenz, S.; Juette, M. F.; Graf, M.; Nguyen, F.; Huter, P.; Polikanov, Y. S.; Blanchard, S. C.; Wilson, D. N. Structures of the orthosomycin antibiotics avilamycin and evernimicin in complex with the bacterial 70s ribosome. *Proceedings of the National Academy of Sciences* **2016**, *113*, 7527-7532.

144. Zarazaga, M.; Tenorio, C.; Del Campo, R.; Ruiz-Larrea, F.; Torres, C. Mutations in ribosomal protein l16 and in 23s rrna in enterococcus strains for which evernimicin mics differ. *Antimicrobial Agents and Chemotherapy* **2002**, *46*, 3657-3659.

145. Nicolaou, K. C.; Rodríguez, R. M.; Mitchell, H. J.; Suzuki, H.; Fylaktakidou, K. C.; Baudoin, O.; van Delft, F. L. Total synthesis of everninomicin 13,384-1—part 1: Retrosynthetic analysis and synthesis of the a1b(a)c fragment. *Chemistry – A European Journal* **2000**, *6*, 3095-3115.

146. Nicolaou, K. C.; Mitchell, H. J.; Suzuki, H.; Rodríguez, R. M.; Baudoin, O.; Fylaktakidou, K. C. Total synthesis of everninomicin 13,384-1—part 1: Synthesis of the a1b(a)c fragment. *Angewandte Chemie International Edition* **1999**, *38*, 3334-3339.

147. Nicolaou, K. C.; Mitchell, H. J.; Fylaktakidou, K. C.; Rodríguez, R. M.; Suzuki, H. Total synthesis of everninomicin 13,384-1—part 2: Synthesis of the fgha2 fragment. *Chemistry – A European Journal* **2000**, *6*, 3116-3148.

148. Nicolaou, K. C.; Rodríguez, R. M.; Fylaktakidou, K. C.; Suzuki, H.; Mitchell, H. J. Total synthesis of everninomicin 13,384-1—part 2: Synthesis of the fgha2 fragment. *Angewandte Chemie International Edition* **1999**, *38*, 3340-3345.

149. Nicolaou, K. C.; Mitchell, H. J.; Rodríguez, R. M.; Fylaktakidou, K. C.; Suzuki, H.; Conley, S. R. Total synthesis of everninomicin 13,384-1—part 3: Synthesis of the de fragment and completion of the total synthesis. *Chemistry – A European Journal* **2000**, *6*, 3149-3165.

150. Nicolaou, K. C.; Fylaktakidou, K. C.; Mitchell, H. J.; van Delft, F. L.; Rodríguez, R. M.; Conley, S. R.; Jin, Z. Total synthesis of everninomicin 13,384-1—part 4: Explorations of methodology; stereocontrolled synthesis of 1,1′-disaccharides, 1,2-seleno migrations in carbohydrates, and solution- and solid-phase synthesis of 2-deoxy glycosides and orthoesters. *Chemistry – A European Journal* **2000**, *6*, 3166-3185.

151. Ganguly, A. K.; Kabasakalian, P.; Morton, J.; Sarre, O.; Westcott, A.; Kalliney, S.; Mangiaracina, P.; Papaphilippou, A. Electrochemical modification of everninomicin d. *Journal of the Chemical Society, Chemical Communications* **1980**, 56-58.

152. Ganguly, A. K.; Girijavallabhan, V. M.; Miller, G. H.; Sarre, O. Z. Chemical modification of everninomicins. *J Antibiot (Tokyo)* **1982**, *35*, 561-570.

153. Ganguly, A. K.; McCormick, J. L.; Saksena, A. K.; Das, P. R.; Chan, T.-M. Chemical modifications and structure activity studies of ziracin and related everninomicin antibiotics. *Bioorganic & Medicinal Chemistry Letters* **1999**, *9*, 1209-1214.

154. Cormican, M. G.; Marshall, S. A.; Jones, R. N. Preliminary interpretive criteria for disk diffusion susceptibility testing of sch 27899, a compound in the everninomicin class of antimicrobial agents. *Diagn. Microbiol. Infect. Dis.* **1995**, *23*, 157-160.

155. Jones, R. N.; Barrett, M. S. Antimicrobial activity of sch 27899, oligosaccharide member of the everninomycin class with a wide gram-positive spectrum. *Clinical Microbiology and Infection* **1995**, *1*, 35-43.

156. Sanders, W. E.; Sanders, C. C. Microbiological characterization of everninomicin-b and everninomicin-d. *Antimicrobial Agents and Chemotherapy* **1974**, *6*, 232-238.

157. Waitz, J. A.; Horan, A. C.: Micromonospora carbonacea var africana. Google Patents, 1988.

158. Decker, H.; Gaisser, S.; Pelzer, S.; Schneider, P.; Westrich, L.; Wohlleben, W.; Bechthold, A. A general approach for cloning and characterizing dndp-glucose dehydratase genes from actinomycetes. *FEMS Microbiol. Lett.* **1996**, *141*, 195-201.

159. Gaisser, S.; Trefzer, A.; Stockert, S.; Kirschning, A.; Bechthold, A. Cloning of an avilamycin biosynthetic gene cluster from streptomyces viridochromogenes tü57. *Journal of Bacteriology* **1997**, *179*, 6271-6278.

160. Weitnauer, G.; Mühlenweg, A.; Trefzer, A.; Hoffmeister, D.; Süßmuth, R. D.; Jung, G.; Welzel, K.; Vente, A.; Girreser, U.; Bechthold, A. Biosynthesis of the orthosomycin antibiotic avilamycin a: Deductions from the molecular analysis of the avi biosynthetic gene cluster of streptomyces viridochromogenes tü57 and production of new antibiotics. *Chemistry & Biology* **2001**, *8*, 569-581.

161. Weitnauer, G.; Hauser, G.; Hofmann, C.; Linder, U.; Boll, R.; Pelz, K.; Glaser, S. J.; Bechthold, A. Novel avilamycin derivatives with improved polarity generated by targeted gene disruption. *Chemistry & Biology* **2004**, *11*, 1403-1411.

162. Mosbacher, T. G.; Bechthold, A.; Schulz, G. E. Crystal structure of the avilamycin resistance-conferring methyltransferase avira from streptomyces viridochromogenes. *Journal of Molecular Biology* **2003**, *329*, 147-157.

163. Treede, I.; Jakobsen, L.; Kirpekar, F.; Vester, B.; Weitnauer, G.; Bechthold, A.; Douthwaite, S. The avilamycin resistance determinants avira and avirb methylate 23s rrna at the guanosine 2535 base and the uridine 2479 ribose. *Molecular Microbiology* **2003**, *49*, 309-318.

164. Mosbacher, T. G.; Bechthold, A.; Schulz, G. E. Structure and function of the antibiotic resistance-mediating methyltransferase avirb from streptomyces viridochromogenes. *Journal of Molecular Biology* **2005**, *345*, 535-545.

165. Treede, I.; Hauser, G.; Mühlenweg, A.; Hofmann, C.; Schmidt, M.; Weitnauer, G.; Glaser, S.; Bechthold, A. Genes involved in formation and attachment of a two-carbon chain as a component of eurekanate, a branched-chain sugar moiety of avilamycin a. *Applied and Environmental Microbiology* **2005**, *71*, 400-406.

166. Hofmann, C.; Boll, R.; Heitmann, B.; Hauser, G.; Durr, C.; Frerich, A.; Weitnauer, G.; Glaser, S. J.; Bechthold, A. Genes encoding enzymes responsible for biosynthesis of l-lyxose and attachment of eurekanate during avilamycin biosynthesis. *Chemistry & Biology* **2005**, *12*, 1137-1143.

167. Hu, Y.; Al-Mestarihi, A.; Grimes, C. L.; Kahne, D.; Bachmann, B. O. A unifying nitrososynthase involved in nitrosugar biosynthesis. *J Am Chem Soc* **2008**, *130*, 15756-15757.

168. Vey, J. L.; Al-Mestarihi, A.; Hu, Y.; Funk, M. A.; Bachmann, B. O.; Iverson, T. M. Structure and mechanism of orf36, an amino sugar oxidizing enzyme in everninomicin biosynthesis. *Biochemistry* **2010**, *49*, 9306-9317.

169. Gust, B.; Challis, G. L.; Fowler, K.; Kieser, T.; Chater, K. F. Pcr-targeted streptomyces gene replacement identifies a protein domain needed for biosynthesis of the sesquiterpene soil odor geosmin. *Proc Natl Acad Sci U S A* **2003**, *100*, 1541-1546.

170. McCulloch, K. M.; McCranie, E. K.; Smith, J. A.; Sarwar, M.; Mathieu, J. L.; Gitschlag, B. L.; Du, Y.; Bachmann, B. O.; Iverson, T. M. Oxidative cyclizations in orthosomycin biosynthesis expand the known chemistry of an oxygenase superfamily. *Proc Natl Acad Sci U S A* **2015**, *112*, 11547-11552.

171. Li, S.; Zhang, J.; Liu, Y.; Sun, G.; Deng, Z.; Sun, Y. Direct genetic and enzymatic evidence for oxidative cyclization in hygromycin b biosynthesis. *ACS Chem Biol* **2018**.

172. Bright, G. M.; Nagel, A. A.; Bordner, J.; Desai, K. A.; Dibrino, J. N.; Nowakowska, J.; Vincent, L.; Watrous, R. M.; Sciavolino, F. C. Synthesis, *in vitro* and *in vivo* activity of novel 9-deoxo-9a-aza-9a-homoerythromycin a derivatives; a new class of macrolide antibiotics, the azalides. *J. Antibiot.* **1988**, *41*, 1029-1047.

173. Fernandes, P.; Martens, E.; Bertrand, D.; Pereira, D. The solithromycin journey-it is all in the chemistry. *Bioorg Med Chem* **2016**, *24*, 6420-6428.

174. Khosla, C. Harnessing the biosynthetic potential of modular polyketide synthases. *Chem. Rev. (Washington, D. C.)* **1997**, *97*, 2577-2590.

175. Park, S. R.; Han, A. R.; Ban, Y.-H.; Yoo, Y. J.; Kim, E. J.; Yoon, Y. J. Genetic engineering of macrolide biosynthesis: Past advances, current state, and future prospects. *Appl. Microbiol. Biotechnol.* **2010**, *85*, 1227-1239.

176. Glassford, I.; Teijaro, C. N.; Daher, S. S.; Weil, A.; Small, M. C.; Redhu, S. K.; Colussi, D. J.; Jacobson, M. A.; Childers, W. E.; Buttaro, B.; Nicholson, A. W.; MacKerell, A. D., Jr.;

Cooperman, B. S.; Andrade, R. B. Ribosome-templated azide-alkyne cycloadditions: Synthesis of potent macrolide antibiotics by in situ click chemistry. *J Am Chem Soc* **2016**, *138*, 3136-3144.

177. Jin, X.; Daher, S. S.; Lee, M.; Buttaro, B.; Andrade, R. B. Ribosome-templated azide-alkyne cycloadditions using resistant bacteria as reaction vessels: *In cellulo* click chemistry. *ACS Med. Chem. Lett.* **2018**, *9*, 907-911.

178. Seiple, I. B.; Zhang, Z.; Jakubec, P.; Langlois-Mercier, A.; Wright, P. M.; Hog, D. T.; Yabu, K.; Allu, S. R.; Fukuzaki, T.; Carlsen, P. N.; Kitamura, Y.; Zhou, X.; Condakes, M. L.; Szczypinski, F. T.; Green, W. D.; Myers, A. G. A platform for the discovery of new macrolide antibiotics. *Nature* **2016**, *533*, 338-345.

179. Hogan, P. C.; Chen, C.-L.; Mulvihill, K. M.; Lawrence, J. F.; Moorhead, E.; Rickmeier, J.; Myers, A. G. Large-scale preparation of key building blocks for the manufacture of fully synthetic macrolide antibiotics. *J. Antibiot.* **2018**, *71*, 318-325.

180. Blaskovich, M. A. T.; Hansford, K. A.; Butler, M. S.; Jia, Z.; Mark, A. E.; Cooper, M. A. Developments in glycopeptide antibiotics. *ACS Infect Dis* **2018**, *4*, 715-735.

181. Leadbetter, M. R.; Adams, S. M.; Bazzini, B.; Fatheree, P. R.; Karr, D. E.; Krause, K. M.; Lam, B. M. T.; Linsell, M. S.; Nodwell, M. B.; Pace, J. L.; Quast, K.; Shaw, J.-P.; Soriano, E.; Trapp, S. G.; Villena, J. D.; Wu, T. X.; Christensen, B. G.; Judice, J. K. Hydrophobic vancomycin derivatives with improved adme properties: Discovery of telavancin (td-6424). *J. Antibiot.* **2004**, *57*, 326-336.

182. Bouza, E.; Burillo, A. Oritavancin: A novel lipoglycopeptide active against gram-positive pathogens including multiresistant strains. *Int. J. Antimicrob. Agents* **2010**, *36*, 401-407.

183. Okano, A.; Isley, N. A.; Boger, D. L. Total syntheses of vancomycin-related glycopeptide antibiotics and key analogues. *Chem. Rev.* **2017**, *117*, 11952-11993.

184. Okano, A.; Isley, N. A.; Boger, D. L. Peripheral modifications of [ψ[ch(2)nh]tpg(4)]vancomycin with added synergistic mechanisms of action provide durable and potent antibiotics. *Proc. Natl. Acad. Sci. U. S. A.* **2017**, *114*, E5052-E5061.

185. Fowler, B. S.; Laemmerhold, K. M.; Miller, S. J. Catalytic site-selective thiocarbonylations and deoxygenations of vancomycin reveal hydroxyl-dependent conformational effects. *J Am Chem Soc* **2012**, *134*, 9755-9761.

186. Han, S.; Miller, S. J. Asymmetric catalysis at a distance: Catalytic, site-selective phosphorylation of teicoplanin. *J. Am. Chem. Soc.* **2013**, *135*, 12414-12421.

187. Pathak, T. P.; Miller, S. J. Chemical tailoring of teicoplanin with site-selective reactions. *J. Am. Chem. Soc.* **2013**, *135*, 8415-8422.

188. Ozturk, S.; Forneris, C. C.; Nguy, A. K. L.; Sorensen, E. J.; Seyedsayamdost, M. R. Modulating oxyb-catalyzed cross-coupling reactions in vancomycin biosynthesis by incorporation of diverse d-tyr analogues. *J Org Chem* **2018**, *83*, 7309-7317.

189. Forneris, C. C.; Seyedsayamdost, M. R. In vitro reconstitution of oxyc activity enables total chemoenzymatic syntheses of vancomycin aglycone variants. *Angew Chem Int Ed* **2018**, *57*, 8048-8052.

190. Baltz, R. H.; Miao, V.; Wrigley, S. K. Natural products to drugs: Daptomycin and related lipopeptide antibiotics. *Nat Prod Rep* **2005**, *22*, 717-741.

191. Schimana, J.; Gebhardt, K.; Holtzel, A.; Schmid, D. G.; Sussmuth, R.; Muller, J.; Pukall, R.; Fiedler, H.-P. Biosynthetic capacities of actinomycetes arylomycins a and b, new biaryl-bridged lipopeptide antibiotics produced by *streptomyces* sp. Tu 6075. I. Taxonomy, fermentation, isolation and biological activities. *J. Antibiot.* **2002**, *55*, 565-570.

192. Roberts, T. C.; Smith, P. A.; Cirz, R. T.; Romesberg, F. E. Structural and initial biological analysis of synthetic arylomycin a2. *Journal of the American Chemical Society* **2007**, *129*, 15830-15838.

193. Liu, J.; Luo, C.; Smith, P. A.; Chin, J. K.; Page, M. G. P.; Paetzel, M.; Romesberg, F. E. Synthesis and characterization of the arylomycin lipoglycopeptide antibiotics and the crystallographic analysis of their complex with signal peptidase. *J. Am. Chem. Soc.* **2011**, *133*, 17869-17877.

194. Liu, J.; Smith, P. A.; Steed, D. B.; Romesberg, F. Efforts toward broadening the spectrum of arylomycin antibiotic activity. *Bioorg. Med. Chem. Lett.* **2013**, *23*, 5654-5659.

195. Peters, D. S.; Romesberg, F. E.; Baran, P. S. Scalable access to arylomycins via c-h functionalization logic. *J. Am. Chem. Soc.* **2018**, *140*, 2072-2075.

196. Smith, P. A.; Koehler, M. F. T.; Girgis, H. S.; Yan, D.; Chen, Y.; Chen, Y.; Crawford, J. J.; Durk, M. R.; Higuchi, R. I.; Kang, J.; Murray, J.; Paraselli, P.; Park, S.; Phung, W.; Quinn, J. G.; Roberts, T. C.; Rouge, L.; Schwarz, J. B.; Skippington, E.; Wai, J.; Xu, M.; Yu, Z.; Zhang, H.; Tan, M. W.; Heise, C. E. Optimized arylomycins are a new class of gram-negative antibiotics. *Nature* **2018**, *561*, 189-194.

197. Wong, N.; Petronijevic, F.; Hong, A. Y.; Linghu, X.; Kelly, S. M.; Hou, H.; Cravillion, T.; Lim, N. K.; Robinson, S. J.; Han, C.; Molinaro, C.; Sowell, C. G.; Gosselin, F. Stereocontrolled synthesis of arylomycin-based gram-negative antibiotic gdc-5338. *Org Lett* **2019**, *21*, 9099-9103.

198. Davidovich, C.; Bashan, A.; Auerbach-Nevo, T.; Yaggie, R. D.; Gontarek, R. R.; Yonath, A. Induced-fit tightens pleuromutilins binding to ribosomes and remote interactions enable their selectivity. *Proc. Natl. Acad. Sci. U. S. A.* **2007**, *104*, 4291-4296.

199. Novak, R. Are pleuromutilin antibiotics finally fit for human use? *Ann N Y Acad Sci* **2011**, *1241*, 71-81.

200. Egger, H.; Reinshagen, H. New pleuromutilin derivatives with enhanced antimicrobial activity. Ii. Structure-activity correlations. *J. Antibiot.* **1976**, *29*, 923-927.

201. Rittenhouse, S.; Biswas, S.; Broskey, J.; McCloskey, L.; Moore, T.; Vasey, S.; West, J.; Zalacain, M.; Zonis, R.; Payne, D. Selection of retapamulin, a novel pleuromutilin for topical use. *Antimicrob. Agents Chemother.* **2006**, *50*, 3882-3885.

202. Jacobs, M. R. Retapamulin: A semisynthetic pleuromutilin compound for topical treatment of skin infections in adults and children. *Future Microbiol.* **2007**, *2*, 591-600.

203. Veve, M. P.; Wagner, J. L. Lefamulin: Review of a promising novel pleuromutilin antibiotic. *Pharmacotherapy* **2018**, *38*, 935-946.

204. Goethe, O.; Heuer, A.; Ma, X.; Wang, Z.; Herzon, S. B. Antibacterial properties and clinical potential of pleuromutilins. *Nat. Prod. Rep.* **2019**, *36*, 220-247.

205. Chahine, E. B.; Sucher, A. J. Lefamulin: The first systemic pleuromutilin antibiotic. *Ann Pharmacother* **2020**, *54*, 1203-1214.

206. Murphy, S. K.; Zeng, M.; Herzon, S. B. A modular and enantioselective synthesis of the pleuromutilin antibiotics. *Science* **2017**, *356*, 956-959.

207. Farney, E. P.; Feng, S. S.; Schafers, F.; Reisman, S. E. Total synthesis of (+)-pleuromutilin. *J Am Chem Soc* **2018**, *140*, 1267-1270.

208. Ma, X.; Kucera, R.; Goethe, O. F.; Murphy, S. K.; Herzon, S. B. Directed c-h bond oxidation of (+)-pleuromutilin. *J Org Chem* **2018**, *83*, 6843-6892.

209. Pinhey, J.; Ritchie, E.; Taylor, W. The chemical constituents of *himantandra* (*galbulimima*) species. Iv. The structures of himbacine, himbeline, himandravine, and himgravine. *Australian Journal of Chemistry* **1961**, *14*, 106-134.

210. Hart, D. J.; Wu, W.-L.; Kozikowski, A. P. Total syntheses of (+)-himbacine and (+)-himbeline. *J. Am. Chem. Soc.* **1995**, *117*, 9369-9370.

211. Chackalamannil, S.; Davies, R. J.; Asberom, T.; Doller, D.; Leone, D. A highly efficient total synthesis of (+)-himbacine. *Journal of the American Chemical Society* **1996**, *118*, 9812-9813.

212. Chackalamannil, S.; Xia, Y.; Greenlee, W. J.; Clasby, M.; Doller, D.; Tsai, H.; Asberom, T.; Czarniecki, M.; Ahn, H.-S.; Boykow, G.; Foster, C.; Agans-Fantuzzi, J.; Bryant, M.; Lau, J.; Chintala, M. Discovery of potent orally active thrombin receptor (protease activated receptor 1) antagonists as novel antithrombotic agents. *Journal of Medicinal Chemistry* **2005**, *48*, 5884-5887.

213. Chelliah, M. V.; Chackalamannil, S.; Xia, Y.; Eagen, K.; Clasby, M. C.; Gao, X.; Greenlee, W.; Ahn, H.-S.; Agans-Fantuzzi, J.; Boykow, G.; Hsieh, Y.; Bryant, M.; Palamanda, J.; Chan, T.-M.; Hesk, D.; Chintala, M. Heterotricyclic himbacine analogs as potent, orally active thrombin receptor (protease activated receptor-1) antagonists. *J. Med. Chem.* **2007**, *50*, 5147-5160.

214. Chackalamannil, S.; Wang, Y.; Greenlee, W. J.; Hu, Z.; Xia, Y.; Ahn, H.-S.; Boykow, G.; Hsieh, Y.; Palamanda, J.; Agans-Fantuzzi, J.; Kurowski, S.; Graziano, M.; Chintala, M. Discovery of a novel, orally active himbacine-based thrombin receptor antagonist (sch 530348) with potent antiplatelet activity. *Journal of Medicinal Chemistry* **2008**, *51*, 3061-3064.

215. Gryka, R. J.; Buckley, L. F.; Anderson, S. M. Vorapaxar: The current role and future directions of a novel protease-activated receptor antagonist for risk reduction in atherosclerotic disease. *Drugs R D* **2017**, *17*, 65-72.

216. Tamaoki, T.; Nomoto, H.; Takahashi, I.; Kato, Y.; Morimoto, M.; Tomita, F. Staurosporine, a potent inhibitor of phospholipidca++dependent protein kinase. *Biochem. Biophys. Res. Commun.* **1986**, *135*, 397-402.

217. Karaman, M. W.; Herrgard, S.; Treiber, D. K.; Gallant, P.; Atteridge, C. E.; Campbell, B. T.; Chan, K. W.; Ciceri, P.; Davis, M. I.; Edeen, P. T.; Faraoni, R.; Floyd, M.; Hunt, J. P.; Lockhart, D. J.; Milanov, Z. V.; Morrison, M. J.; Pallares, G.; Patel, H. K.; Pritchard, S.; Wodicka, L. M.; Zarrinkar, P. P. A quantitative analysis of kinase inhibitor selectivity. *Nat Biotechnol* **2008**, *26*, 127-132.

218. Kase, H.; Iwahashi, K.; Matsuda, Y. K-252a, a potent inhibitor of protein kinase c from microbial origin. *J. Antibiot.* **1986**, *39*, 1059-1065.

219. Gani, O. A.; Engh, R. A. Protein kinase inhibition of clinically important staurosporine analogues. *Nat Prod Rep* **2010**, *27*, 489-498.

220. Caravatti, G.; Meyer, T.; Fredenhagen, A.; Trinks, U.; Mett, H.; Fabbro, D. Inhibitory activity and selectivity of staurosporine derivatives towards protein kinase c. *Bioorg. Med. Chem. Lett.* **1994**, *4*, 399-404.

221. Fabbro, D.; Buchdunger, E.; Wood, J.; Mestan, J.; Hofmann, F.; Ferrari, S.; Mett, H.; O'Reilly, T.; Meyer, T. Inhibitors of protein kinases: Cgp 41251, a protein kinase inhibitor with potential as an anticancer agent. *Pharmacology & Therapeutics* **1999**, *82*, 293-301.

222. Stone, R. M.; Manley, P. W.; Larson, R. A.; Capdeville, R. Midostaurin: Its odyssey from discovery to approval for treating acute myeloid leukemia and advanced systemic mastocytosis. *Blood Advances* **2018**, *2*, 444-453.

223. Bourhill, T.; Narendran, A.; Johnston, R. N. Enzastaurin: A lesson in drug development. *Critical Reviews in Oncology/Hematology* **2017**, *112*, 72-79.

224. Omura, S.; Asami, Y.; Crump, A. Staurosporine: New lease of life for parent compound of today's novel and highly successful anti-cancer drugs. *J Antibiot (Tokyo)* **2018**, *71*, 688-701.

225. Sanchez, C.; Mendez, C.; Salas, J. A. Indolocarbazole natural products: Occurrence, biosynthesis, and biological activity. *Nat Prod Rep* **2006**, *23*, 1007-1045.

226. Allred, T. K.; Manoni, F.; Harran, P. G. Exploring the boundaries of "practical": De novo syntheses of complex natural product-based drug candidates. *Chem. Rev.* **2017**, *117*, 11994-12051.

227. Kuttruff, C. A.; Eastgate, M. D.; Baran, P. S. Natural product synthesis in the age of scalability. *Nat Prod Rep* **2014**, *31*, 419-432.

228. Yu, M. J.; Zheng, W.; Seletsky, B. M.; Littlefield, B. A.; Kishi, Y. Case history: Discovery of eribulin, a halichondrin b analogue that prolongs overall survival in patients with metastatic breast cancer. *Annu. Rep. Med. Chem.* **2011**, *46*, 227-241.

229. Vila-Farres, X.; Chu, J.; Inoyama, D.; Ternei, M. A.; Lemetre, C.; Cohen, L. J.; Cho, W.; Reddy, B. V.; Zebroski, H. A.; Freundlich, J. S.; Perlin, D. S.; Brady, S. F. Antimicrobials inspired by nonribosomal peptide synthetase gene clusters. *J Am Chem Soc* **2017**, *139*, 1404-1407.

230. Cobb, R. E.; Wang, Y.; Zhao, H. High-efficiency multiplex genome editing of *streptomyces* species using an engineered crispr/cas system. *ACS Synth. Biol.* **2015**, *4*, 723-728.

231. Weber, T.; Charusanti, P.; Musiol-Kroll, E. M.; Jiang, X.; Tong, Y.; Kim, H. U.; Lee, S. Y. Metabolic engineering of antibiotic factories: New tools for antibiotic production in actinomycetes. *Trends Biotechnol.* **2015**, *33*, 15-26.

232. Shugrue, C. R.; Miller, S. J. Applications of nonenzymatic catalysts to the alteration of natural products. *Chem. Rev. (Washington, DC, U. S.)* **2017**, *117*, 11894-11951.

233. Kalkreuter, E.; Williams, G. J. Engineering enzymatic assembly lines for the production of new antimicrobials. *Curr Opin Microbiol* **2018**, *45*, 140-148.

234. Wallace, S.; Balskus, E. P. Opportunities for merging chemical and biological synthesis. *Curr Opin Biotechnol* **2014**, *30*, 1-8.

235. Patridge, E.; Gareiss, P.; Kinch, M. S.; Hoyer, D. An analysis of fda-approved drugs: Natural products and their derivatives. *Drug Discov Today* **2016**, *21*, 204-207.

Chapter III

Methyltransferase contingencies in the pathway of everninomicin D antibiotics and analogs

This chapter is adapted from “Methyltransferase contingencies in the pathway of everninomicin D antibiotics and analogues” published in the journal ChemBioChem and has been reproduced with the permission of the publisher and my co-authors Emilianne M. Limbrick, Callie C. Dulin, Dagmara K. Derewacz, Jeffrey M. Spraggins, Kathryn M. McCulloch, T.M. Iverson, and Brian O. Bachmann. Reproduced with permission from Limbrick, E. M.; Ynigez-Gutierrez, A. E.; Dulin, C. C.; Derewacz, D. K.; Spraggins, J. M.; McCulloch, K. M.; Iverson, T. M.; Bachmann, B. O. Methyltransferase contingencies in the pathway of everninomicin d antibiotics and analogues. *Chembiochem* **2020**, *21*, 3349-3358.

Introduction

The majority of natural product antibiotics target central microbial cellular processes such as gene replication and transcription, the cascade of biochemical reactions that comprise cell wall biosynthesis, or ribosomal translation. Ribosomal translation inhibitors are one of the most prevalent solutions adopted by nature to generate antibiotics. This is likely due to the size, complexity, and structural divergence amongst bacterial ribosomes, which provide a wide landscape for small molecule interactions. For instance, the interface between the 30S and 50S ribosome comprises ca. 8500 Å, providing a rich and varied surface for targeting.[1] The majority of ribosome-targeting drugs address the topology of the peptidyl transferase center. For example, tetracyclines, erythromycin, and related macrolides target the interaction between

tRNA and the 30S and 23S subunits, respectively.[2-4] Successfully targeting large inter-surface macromolecular interactions may require larger surface area ligands, and selective ribosome-targeting natural products are often relatively large and structurally complex molecules.

These properties have complicated the mapping of structure-activity relationships in these classes and motivated the development of synthetic methods to create diversity within these scaffolds. In the tetracycline and erythromycin antibiotics classes, elegant and robust synthetic platforms have recently been developed for the efficient generation of diverse libraries, resulting in antibiotics with improved spectrum and pharmacological properties.[5,6] Modification of existing secondary metabolite scaffolds is an intense area of research.[7] However, a concise synthetic platform for many other ribosome-targeting scaffolds has yet to be devised. Everninomicins represent an antibiotic scaffold with the potential for treating MDR pathogenic infections. Everninomicins are predominantly Gram-positive targeting, orthoester-containing antibiotics (orthosomycins) produced by variants of the soil bacterium *Micromonospora carbonacea*.[8-12] Everninomicin A (Evn A, Ziracin) was advanced to phase III clinical trials before being discontinued due to difficulties in accessing a reproducible intravenous formulation.[13] However, continued development of this scaffold is of interest as members of this class possess potent activity against clinically important strains of bacteria such as methicillin-resistant staphylococci, glycopeptide-resistant enterococci, and penicillin-resistant streptococci.[14] Furthermore, Ziracin and related orthosomycins have been demonstrated to bind to a unique and distal site of the ribosome in comparison to all other antibiotics.[15,16] The prospect of improving the pharmacology of everninomicins is complicated by their structural complexity. A total chemical synthesis has been reported that involves over 130 steps, making analog generation via chemical synthesis a daunting and impractical proposal.[17-22]

An alternative to chemical synthesis entails generation of analogs via genetic recombination of the producing strains and/or late-stage scaffold modification with expressed biosynthetic

enzymes.[7] This requires understanding the function and sequence of the constituent biosynthetic pathway biotransformations and the mutability of the pathway for modifications of the scaffold. Here, we report the development of a new system for the genetic manipulation of rare actinomycetes and the application of this system to the functional analysis of genes in the biosynthesis of everninomicins in *M. carbonacea* var. *aurantiaca* (Figure A-1). In the course of these studies, we assign putative roles for several methyltransferase enzymes spanning the octasaccharide scaffold and demonstrate the generation of twelve new, previously unreported everninomicin metabolites.

Results

Development of microporous intergeneric conjugation for genetic manipulation of actinomycetes

A wide variety of mycelial actinobacteria, particularly 'rare' actinomycetes including *M. carbonacea*, do not readily form isolable spores under laboratory conditions (making protoplast generation and transformation difficult) and are sensitive to conjugal strain antibiotic counter selection with nalidixic acid (complicating bacterial conjugation). Likewise, the introduction of selection markers to facilitate conjugation, as has been done in gram-negative *Pseudomonas* species, has not been fully realized in actinobacteria.[23] Correspondingly, we developed a method for genetic manipulation of antibiotic-producing actinomycetes via efficient genetic conjugation of mycelia without the requirement of a conjugal strain antibiotic. *M. carbonacea* var. *aurantiaca* is sensitive to nalidixic acid, the counter selection antibiotic typically used to eliminate the donor *E. coli*. As transformation using nalidixic acid was inefficient and poorly reproducible, we developed a nalidixic acid-free method to separate the exconjugants from the contaminating *E. coli*. The mixture of donor and recipient bacteria was plated on a 0.4 µm membrane mounted to a sterilized nylon washer (Figure 3-1A). The membrane/washer assembly was bonded by a

thin layer of silicone adhesive. Donor *E. coli* is unable to diffuse through the pores of the membrane, whereas ex-conjugate antibiotic-resistant actinomycetes can penetrate pores into the agar subsurface, thereby facilitating isolation of apramycin-resistant exconjugants.[24] After nine days of incubation at 30 °C, the membrane/washer assembly was removed, revealing individual, monoclonal colonies that did not require additional isolation steps (Figure 3-1B). Scanning electron microscopy imaging of the conjugal 'lagoon' demonstrated that the top of the membrane was covered in a dense mixture of *E. coli* and *M. carbonacea* (Figure 3-1C) while the underside contained only *M. carbonacea* mycelia, because it was able to penetrate the membrane (Figure 3-1D) and diffusively grow into the agar.

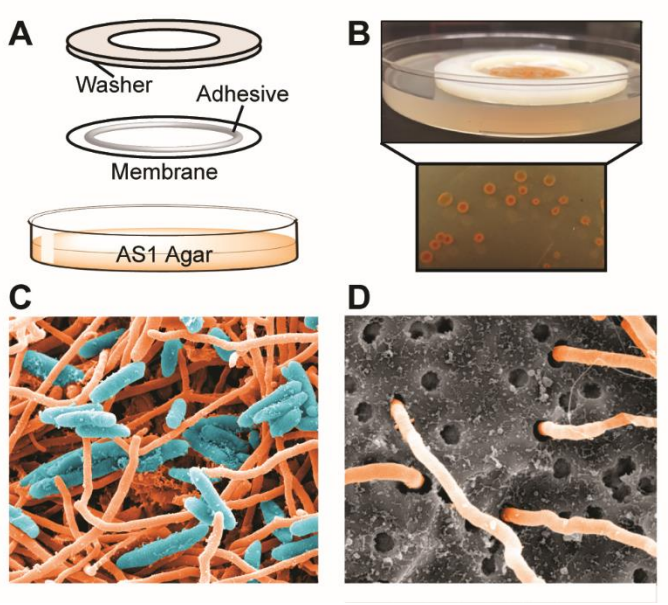

Figure 3-1. Transformation of *M. carbonacea* var. *aurantiaca* by microporous intergeneric conjugation. (A) Schematic of washer/membrane assembly. (B) Appearance of conjugation plates 9 days after transformation. Insert: pure *M. carbonac*ea var. *aurantiaca* colonies are visible within agar after removal of membrane assembly. (C) SEM image of top of membrane (magnification 10,000 x). Donor *E. coli* are colored teal. Recipient *M. carbonacea* are colored orange. (D) SEM image of bottom of membrane (magnification 20,000 x).

To generate a suitable complementation plasmid for use in *M. carbonacea* var. *aurantiaca* (*vide infra*), a pSET152 derivative was designed and synthesized. The constitutive promoter

ermE* was inserted upstream of a multiple cloning site and the apramycin resistance gene [*aac(3)IV*] was replaced with the hygromycin B resistance marker [*hyg*] to generate the new complementation plasmid, pSET152ermE (map shown in Figure A-2).[25]

Functional analysis of everninomicin methyltransferases provides novel everninomicin metabolites

Functional analysis of the everninomicin gene cluster and analog synthesis were performed by generating targeted gene replacements of four genes (*evdM1*, *evdM2*, *evdM3*, and *evdM5*) from the evd pathway using a two-step lambda-red mediated gene replacement method.[26,27] The genes of interest were individually replaced on a cosmid containing most of the evd gene cluster in *E. coli*. The modified cosmids were then transformed into *M. carbonacea* var. *aurantiaca* using microporous conjugation, wherein two rounds of homologous recombination resulted in precise replacement of the target gene with the apramycin resistance cassette. Double crossover mutants were confirmed by PCR or Southern hybridization analysis (Figure A-3). Extracts from production cultures of each gene-replacement mutant were generated via solid phase extraction and analyzed by liquid chromatography mass spectrometry (LC/MS).

LC/MS analysis of the putative central D-ring C-methyltransferase *ΔevdM3::aac(3)IV* extracts revealed a loss of production of full length Evn D – G (**1-4**). However, we observed three new metabolites, which we termed Evn H, J, and K (**5-7**), with masses 1523.5, 1493.5, and 1507.5, respectively (Figure 3-2). Genetic complementation with *evdM3* resulted in production of a metabolite, Evn L (**8**), with a mass of 1537.5, consistent with restoration of a methyl group (Figure A-4). The LC/MS analysis of *ΔevdM2::aac(3)IV* (Figure 3-2) did not reveal *m/z* consistent with the production of any desmethyl analogs. Genetic complementation of *evdM2* did not result in the restoration of any everninomicin analogs (data not shown).

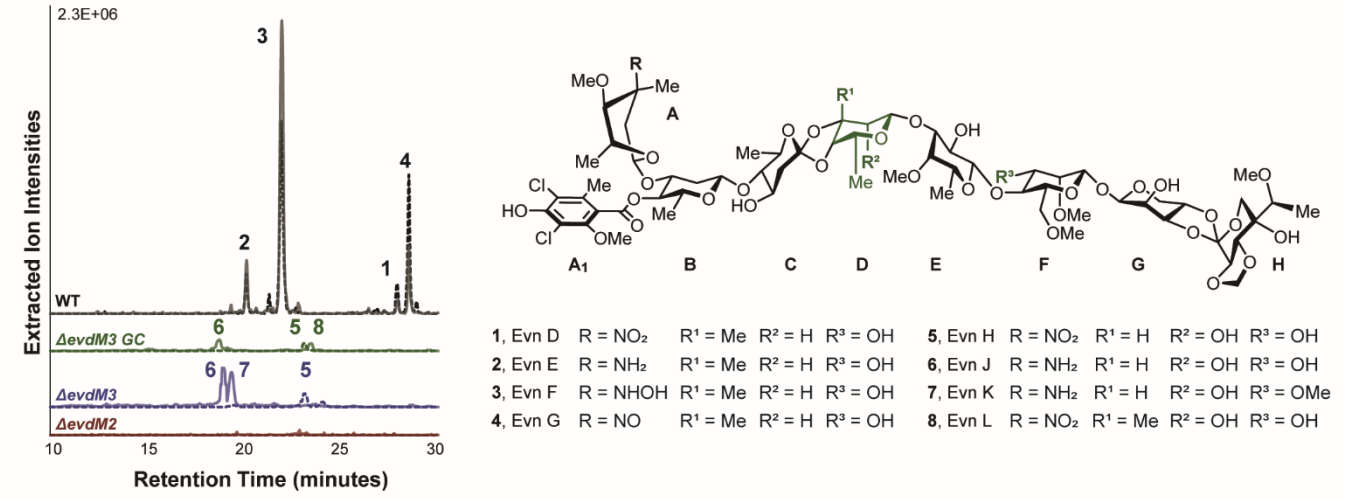

Figure 3-2. Analysis of genetic replacements of *evdM2* and *evdM3*. LC/MS analysis of wild type *M. carbonacea* var. *aurantiaca*, gene replacements *evdM3* (*ΔevdM3::aac(3)IV*), *evdM2* (*ΔevdM2::aac(3)IV*), and genetic complementation of *evdM3* gene replacement (*ΔevdM3::aac(3)IV* GC). The chromatogram shows summed ion intensities in negative mode (dotted lines, [-H]) and positive mode (solid lines, [+H]) for Ever D – G and new metabolites. Everninomicin masses in this study are found in Table A-1.

Three new metabolites, Evn H, J, and K (**5-7**), accumulated in the *evdM3* mutant strain. Structure determination of the most abundant amino functional metabolites Evn J (**6**) and Evn K (**7**) was accomplished using high-resolution mass spectrometric fragmentation via a Fourier Transform Ion Cyclotron Resonance (FT-ICR) mass spectrometer (Figures A-5 – 6). The neutral nitro-functional congener Evn H (**5**), though demonstrating lower ionization efficiency than cationic Evn J (**6**) and K (**7**), was the most abundant metabolite in *ΔevdM3::aac(3)IV* extracts (indicated via UV absorption), and its structure is partially consistent with Evn J (**6**) and K (**7**) via mass spectrometric fragmentation analysis (Figure A-7). Mass spectra suggest that all three congeners, Evn H, J, and K (**5-7**), lack the C-3 methyl of the D-ring as well as the C-2 O-methyl on the G-ring. The new D-ring structure was confirmed using multidimensional NMR analysis of Evn H (**5**) (Figures A-8 – 13; Table A-2). Specifically, a new six contiguous spin 6-deoxy hexose system was identified in Evn H (**5**). The coupling constant (J = 1.9, 2.8 Hz) suggests that the

relative stereochemistry of H-23 to H-22 and H-24 is syn, consistent with 6-deoxy-D-glucose substitution. The position of the new deoxyglucose D-ring spin system was confirmed via Heteronuclear Multiple Bond Correlation (HMBC) correlation between the anomeric position of the D-ring and C-3 of the E-ring. Notably, the hydroxyl group at the C-2 position of the D-ring is found in other everninomicins (e.g. Ziracin) and everninomicin B in *M. carbonacea* var. *aurantiaca*.[28] Unexpectedly, the F-ring of Evn K (**7**) was determined to be O-methylated at C-3, which has not been previously reported in everninomicin variants.

Evn H (**5**) was purified and tested for activity against *S. aureus* subsp. *aureus* Rosenbach in a broth microdilution assay. Everninomicin A (Ziracin) was used as a benchmark and had an MIC of 1 µg/mL in line with literature values. The most abundant metabolite from *ΔevdM3::aac(3)IV* was somewhat less active against *S. aureus* with an MIC of 16 µg/mL.

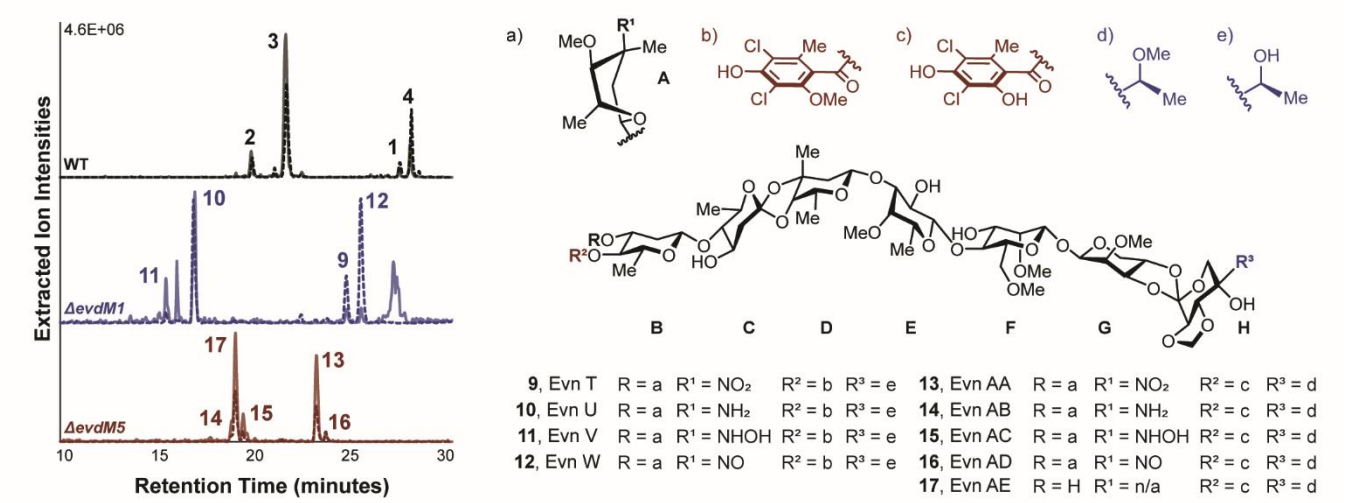

Figure 3-3. Analysis of genetic replacements of *evdM1* and *evdM5*. LC/MS analysis of wild type *M. carbonacea* var. *aurantiaca*, gene replacements *evdM1* (*ΔevdM1::aac(3)IV*) and *evdM5* (*ΔevdM5::aac(3)IV*). The chromatogram shows summed ion intensities in negative mode (dotted lines, [-H]) and positive mode (solid lines, [+H]) for Ever D–G (1-4) and new metabolites (9-17). Everninomicin masses in this study are found in Table A-1.

The extract from the deletion strain of the putative eurekanate (H-ring) O-methyltransferase *ΔevdM1::aac(3)IV* also revealed a loss of production of Evn D – G (**1-4**). Additionally, four new

compounds were identified with masses 1521.5, 1491.5, 1507.5, 1504.5, which were termed Evn T, U, V, and W (**9-12**), respectively (Figure 3-3). These masses were consistent with the expected desmethyl analogs (Figures A-14 – 17). FT-ICR mass spectrometer was used to further analyze the four new metabolites accumulated in the *ΔevdM1::aac(3)IV* strain. The data indicate that all four congeners lack an O-methyl group on either the G-ring or H-ring. However, the molecules proved resistant to fragmentation to provide the H-ring mass fragment, thus preventing conclusive assignment of the methyltransferase from this genetic deletion alone (Figure A-15). We then attempted to perform mild acidic methanolysis to access the individual methyl glycosides for MS analysis; however, this method also did not provide the necessary fragments to confirm the loss of the methyl group to the H-ring.[29,30] Finally, the extract from the deletion strain of the putative dichloroisoeverninic acid (A_1-ring) O-methyltransferase, *ΔevdM5::aac(3)IV*, was analyzed. Five new metabolites were observed with the masses 1521.5, 1491.5, 1507.5, 1504.5, and 1334.4, which were termed Evn AA, AB, AC, AD, and AE (**13-17**), respectively (Figure 3-3). The mass spectrometric fragmentation analysis confirmed that four of these metabolites, Evn AA-AD (**13-16**), lacked the O-methyl group at the C-2 position of the A_1-ring (Figures A-18 – 21). The fifth metabolite, Evn AE (**17**), is consistent with the loss of the C-2 O- methyl of the A_1-ring as well as the loss of the entire evernitrose sugar (A-ring) (Figure A-22). The loss of the evernitrose sugar is unlikely a result of the *evdM5* deletion and rather represents the accumulation of the desmethyl analogs of a notable shunt product, Evn M (**18**) (formerly known as ‘everninomicin-2’), which was previously observed by us and others.[31]

Methyltransferases EvdM1 and EvdM5 methylate advanced everninomicin intermediates in vitro

EvdM1 and EvdM5 were cloned into appropriate expression vectors and over-expressed in *E. coli* under optimized conditions (Figure A-23). Following purification, the two

methyltransferases were evaluated for their ability to catalyze the addition of a methyl group to the metabolites isolated from their respective gene replacement mutant strains.

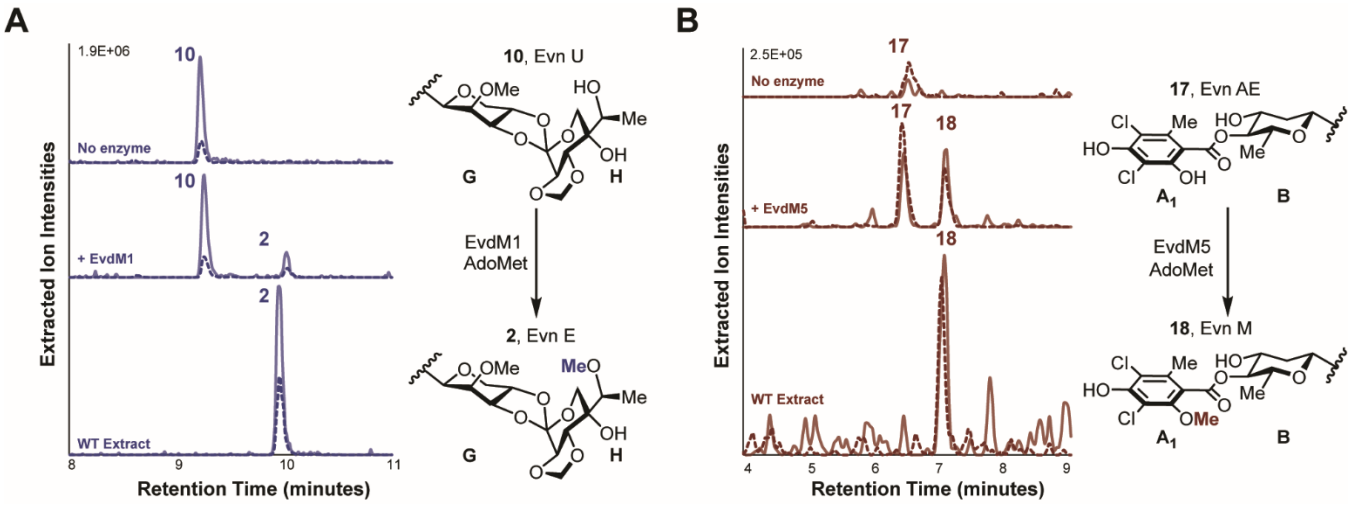

Figure 3-4. *In vitro* evaluation of methyltransferases EvdM1 and EvdM5. (A) LC/MS analysis of EvdM1 conversion of Evn U (10) to Evn E (2) via addition of a methyl group at C4'-OH position of the eurekanate sugar (H-ring). No conversion was observed for a boiled enzyme control. (B) LC/MS analysis of EvdM5 conversion of Evn AE (17) to Evn M (18) at the C2-OH position of dichloroisoverninic acid (A_1-ring). No conversion observed for a no enzyme control. The chromatograms shows summed ion intensities in negative mode (dotted line, [-H]) and positive mode (solid line, [+H]). Everninomicin masses in this study are found in Table A-1.

EvdM1 was incubated with Evn U (**10**), the amino congener lacking a methyl group on the C4'-OH of the eurekanate, and the required cofactor S-adenosyl methionine. Following incubation, we observed, via LC/MS, a mass shift of 14 Da to Evn E (**2**) (Figure 3-4A). Subsequent tandem MS confirmed the addition of a methyl group at the G-ring or H-ring to covert the deletion metabolite Evn U (**10**) to the wildtype Evn E (**2**) metabolite (Figure A-24). While MS/MS data was unable to conclusively assign the position of this methylation as occurring at the H-ring, co-elution of the reaction product with authentic Evn E (**2**) supports proposed regiochemistry. Additionally, EvdM5 was incubated with the *ΔevdM5* metabolite Evn AE (**17**), which lacks the entire evernitrose sugar (A-ring) and the O-methyl group on the dicholoroisoeverninic acid, under similar assay conditions. We were able to observe a shift in

mass of Evn AE (**17**) of 14 Da, indicating that a methyl group was appended by the methyltransferase EvdM5 to yield Evn M (**18**) (Figure 3-4B). Despite repeated attempts, no turnover was observed between EvdM5 and any of the other *ΔevdM5::aac(3)IV* metabolites Evn AA-AD (**13-16**). This implies that methyltransferase access to the ortho hydroxyl position of dichloroisoeverninic acid (A_1-ring) is blocked by the evernitrose sugar (A-ring), suggesting that evernitrose is appended last in the biosynthetic pathway, subsequent to complete dichloroisoeverninic acid elaboration.

Discussion

Our long-term goal is to understand and improve ribosomal interactions and *in vivo* pharmacology of everninomicin-type orthosomycins by generating structural analogs across the scaffold. This goal requires understanding the sequence of events encoded by the approximately 50-gene biosynthetic pathway, the mechanisms and constraints of novel constituent transformations, and assessing the mutability of the octasaccharide biosynthetic pathway to modifications.

There are ten methyltransferases required in the biosynthesis of everninomicins, eight O-methyltransferases and two C-methyltransferases. Herein we report new insight into the roles of these methyltransferases, allowing assignment of the putative function of all the methyltransferases and underlining the potential mutability of the pathway (Figure 3-5A/B). Comparison to analysis of the closely-related avilamycin pathway allows for increased confidence in our assignment of the everninomicin methyltransferases (Figure 3-5C). Homologs of five of these methyltransferases were previously functionally investigated in the avilamycin gene cluster via targeted gene disruption and stand in agreement with our functional analyses (Table 2-1). Subsequent to developing an efficient new genetic system based on intergeneric

bacterial conjugation, we targeted several methyltransferase homologs in the everninomicin pathway. We chose to directly analyze four methyltransferases hypothesized to provide a broad range of des-methyl everninomicin analogs across the octasaccharide scaffold. In particular, we chose to characterize EvdM1, which has no homolog in the avilamycin gene cluster. Conversely, we also deleted three genes, *evdM2*, *evdM3*, and *evdM5*, with homology to the previously investigated avilamycin pathway to confirm their function in the everninomicin pathway. Thus, we were able to successfully generate replacements of *evdM1*, *evdM2*, *evdM3*, *evdM5*, and to confirm the precision of their replacement by PCR and/or Southern hybridization analysis.

Inactivation of the putative C-methyltransferase *evdM3* resulted in the accumulation of three previously unreported metabolites. These metabolites lacked the methyl group at C-3 of the D-ring mycarose, as expected, but they also possessed an additional hydroxyl group. tereochemical analysis revealed that the D-ring had been substituted with an alternate sugar, 6-deoxyglucose. Notably, there are multiple everninomicins reported that possess a hydroxyl at this position, suggesting this may be a naturally variable position. Everninomcin A produced by the *africana* variant and everninomicin B produced by the *aurantiaca* variant both incorporate 6-deoxyglucose as the D-ring.[28] Genetic complementation of *evdM3* resulted in the accumulation of a compound whose mass was consistent with restoration of the C-3 methyl of the D-ring, although the compound was not produced in sufficient quantities to allow NMR characterization. Taken together, these data suggest that there is flexibility both in the putative glycosyltransferase forming the C-D ring linkage and the proposed synthase oxidizing the glycosidic linkage to the orthoester. In the avilamycin pathway, the functional role of the only C-methyltransferase (*aviG1*) in mycarose (D-ring) biosynthesis was also assigned by genetic studies.[32] While no new avilamycin intermediates were observed in the *aviG1* mutant, genetic complementation was able to restore avilamycin production, indicating that the avilamycin glycosyltransferase forming the C-D ring linage may not have the ability to incorporate D-ring variants.

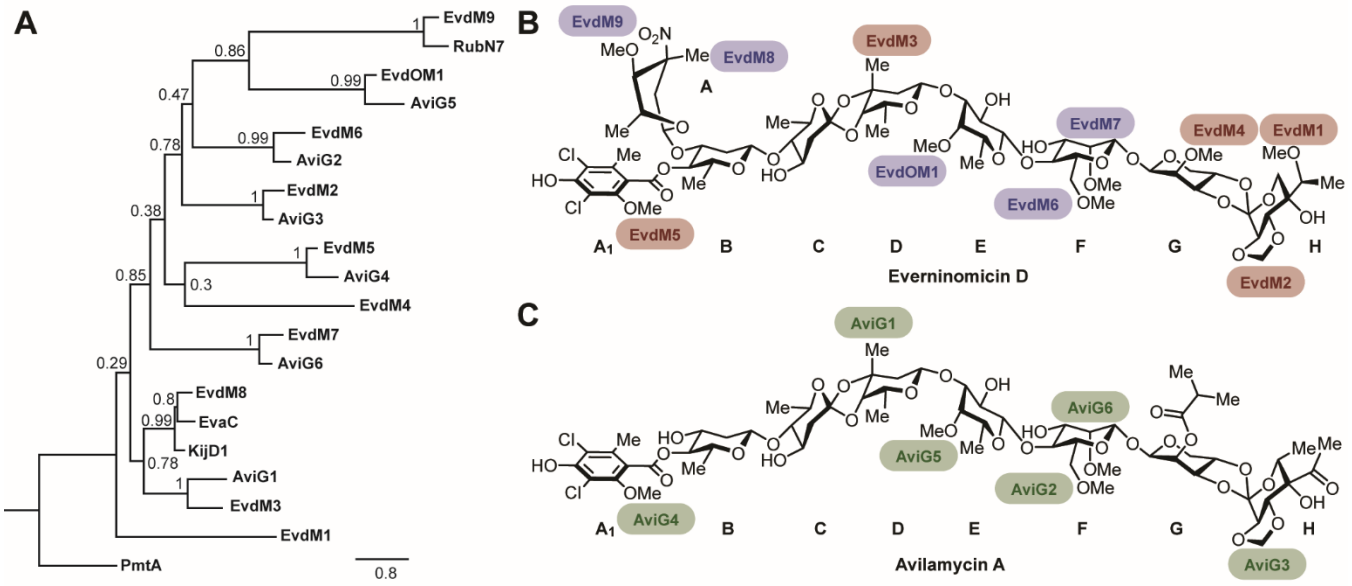

Figure 3-5. Assignment of methyltransferases for orthosomycin biosynthesis. (A) Phylogenetic tree of orthosomycin methyltransferase enzymes. Numbers are FastTree support values from inferred maximum-likelihood. (B) Structure of everninomicin D with assignment of all ten methyltransferases. Enzymes characterized in this study highlighted in red. (C) Structure of related orthosomycin avilamycin A with assignment of all six methyltransferases.

Table 3-1. Assignment of Evn methyltransferases.

Evn Methyltransferase	Relevant Homologs[a]	Functional Genetic Analysis	Biochemical/Structural Analysis	Methylation Location Assignment[b]
EvdM1	None	This work	This work	H-ring C4' O-MT
EvdM2	AviG3 (69%)	This work	None	H-ring C2/C3 O-MT
EvdM3	AviG1 (45%)	This work, AviG1	None	D-ring C3 C-MT
EvdM4	None	This work	None	G-ring C2 O-MT
EvdM5	AviG4 (60%)	This work, AviG4	This work	A_1-ring C2 O-MT
EvdM6	AviG2 (57%)	AviG2	None	F-ring C6 O-MT
EvdM7	AviG6 (66%)	AviG6	None	F-ring C2 O-MT
EvdM8	EvaC (67%) KijD1 (71%)	None	EvaC, KijD1	A-ring C3 C-MT
EvdM9	RubN7 (61%)	None	RubN7	A-ring C4 O-MT
EvdMO1	AviG5 (62%)	AviG5	EvdMO1	E-ring C4 O-MT

[a]Identity % in parenthesis
[b]Evn ring, carbon position, O-methyltransferase (O-MT) or C-methyltransferase (C-MT)

Unexpectedly, Evn H, J, and K (**5-7**) from *ΔevdM3::aac(3)IV* also indicate loss of the O-methyl on C-2 of the G-ring. The gene *evdM4*, which encodes a putative O-methyltransferase, is located directly downstream of *evdM3* in the biosynthetic gene cluster (Figure A-1). There are

no close homologs of *evdM4* in the avilamycin gene cluster, indicating that this methyltransferase is unique to the everninomicin gene cluster. Everninomicins have an O-methyl at C-2 of the G-ring, while avilamycin has an isovalerate ester at this position. Our data are consistent with attenuated expression of *evdM4* resulting from upstream gene replacement, and it is likely that EvdM4 is the O-methyltransferase responsible for methylation at the C-2 position of the G-ring. Conversely, the targeted replacement of *evdM2* with the apramycin cassette produced no identifiable full length everninomicins.

Further comparison of the structures of everninomicin (excluding evernitrose) and avilamycin reveals only two O-methyl groups that are present in everninomicin but not avilamycin: at C-2 of the G-ring and C-4' of the H ring. The analysis of the *evdM3* replacement above has identified EvdM4 as the likely O-methyltransferase responsible for catalyzing the methylation at C-2 of the G-ring. Replacement of the gene encoding *evdM1* yielded four novel everninomicin metabolites. MS/MS analyses demonstrated that these metabolites are all lacking the methyl group on either the G- or H-ring, but the assignment could not be conclusively stated based on the MS/MS data alone. However, co-elution with of the reaction product of EvdM1 with authentic Evn E (**2**) is consistent with proposed regiochemistry. Furthermore, based on our results from the *evdM3* replacement, EvdM1 is the only remaining O-methyltransferase with no homology to the avilamycin pathway and likely transfers the methyl group to the C-4' position of the H-ring in the everninomicin pathway. Likewise, our data from *evdM5* deletion provided five everninomicin metabolites all lacking the O-methyl group at the C-2 position of dichloroisoeverninic acid (A_1-ring). These data are consistent with the metabolites observed from the deletion of the homologous avilamycin protein, AviG4, demonstrating that both proteins methylate the ortho hydroxyl group of the precursor to dichloroisoeverninic acid.[33]

Based on the results of these experiments, as well as homology to the methyltransferases characterized in the avilamycin and other characterized pathways, we are able to putatively

assign, the function of the ten methyltransferases from the everninomicin pathway (Figure A-1). The roles of EvdM1, EvdM2, EvdM3, EvdM4, and EvdM5 were assigned based on the results of gene replacement studies as discussed above. EvdM6 is homologous to AviG2, which was shown to methylate the C-6 hydroxyl of the F-ring via functional analysis in the avilamycin pathway. Additionally, EvdM7 shares sequence homology with AviG6, which has been shown to methylate the C-2 hydroxyl of the F-ring.[34] EvdM8 appears to encode a C-3 methyltransferase with sequence homology to C-methyltransferases EvaC and KijD1. EvaC and KijD1 methylate the C-3 positions of TDP-L-epivancosamine and TDP-L-kijanose, respectively, which are nitro sugar precursors closely related to evernitrose.[35-37] Therefore, EvdM8 is likely responsible for methylating the C-3 position of evernitrose. Based on sequence similarity to the O-methyltransferase from the rubradirin pathway, RubN7, EvdM9 encodes the O-methyltransferase responsible for methylating the C-4 hydroxyl of evernitrose.[38] Finally, *evdMO1* encodes a fusion protein with an N-terminal O-methyltransferase with homology to *aviG5*, the product of which methylates the C-4 hydroxyl of the E-ring of avilamycin.[34,39] The C-terminal portion of EvdMO1 is homologous to the oxidase EveO1 in *M. carbonacea* var. *africana*, wherein it is not observed as a fusion protein. A summary of the methyltransferases assigned in this study is found in Table 2-1.

Conclusions

We developed an efficient genetic system for manipulating *Micromonospora* via bacterial conjugation that overcomes the limiting requirements of protoplasts and antibiotic counter selection. This method can in principle be applied to any mycelial actinomycetes and will facilitate analysis and modification of a large number of biosynthetic pathways previously considered to be intractable, adding an important tool to the actinomyces genetic toolkit.[40] Microporous

intergeneric conjugation was applied to the analysis of the everninomicin gene cluster, and gene replacement experiments allowed assignment of functional roles for four methyltransferase genes. Unlike in the avilamycin pathway, deletion of the C-3 methyltransferase acting on the on the D-ring resulted in the incorporation of a different deoxysugar at this position and did not adversely affect the subsequent formation of the orthoester linkage between the C- and D-rings, despite the significant structural changes in the vicinity of the orthoester linkage. These data indicate that the glycosyltransferase appending the D-ring sugar is flexible towards multiple glycosyl donors, and the orthoester synthase functioning to oxidize the C-D ring glycosidic bond has substrate flexibility, which is important in generating analogs as the orthoester linkage is required for activity. Furthermore, the glycosyltransferases throughout the scaffold demonstrated tolerance to polysaccharide modifications, and two distal methyltransferases were capable of methylation of advanced biosynthetic intermediates. These data show promise for future application of SAM analogs in the generation of unnatural congeners. The data presented herein show that the everninomicin gene cluster of *M. carbonacea* var. *aurantiaca* is adaptable for creating new antibacterial compounds across the length of the entire scaffold via biosynthetic analog synthesis.

Materials & Methods

Bacterial Strains and Culture Conditions

E. coli strains were grown in Luria-Bertani (LB) broth (10% tryptone, 5% yeast extract, 10% NaCl) or LB agar (10% tryptone, 5% yeast extract, 10% NaCl, 2% agar). *Micromonospora carbonacea* var. *aurantiaca* (NRRL 2997) and replacement mutants were grown tryptone soya broth (3% Oxoid TSB) and on TSB agar (3% Oxoid TSB, 2% agar). Intergeneric conjugations were performed on solid AS1 media (0.1% yeast extract, 0.5% soluble starch, 0.02% L-alanine,

0.02% L-arginine, 0.05% L-asparagine, 0.25% NaCl, 1% Na_2SO_4, 2% agar at pH 7.5, supplemented with 10 mM $MgCl_2$). Apramycin (50 µg/ml), nalidixic acid (25 µg/ml), chloramphenicol (30 µg/ml), and kanamycin (50 µg/ml) were used when required for selection as described in Methods Details.

Generation of Gene Replacements in E. coli

The genes *evdM2*, *evdM3*, *evdM1*, and *evdM5* were individually deleted on cosmids using a PCR-targeting gene replacement strategy [13b]. Lambda-red competent cells were prepared by inoculating 1% of a fresh overnight culture of *E. coli* BW25113/pIJ790 containing Evn cosmids into 10 mL LB medium containing 20 mM $MgSO_4$, 10mM L-arabinose, and kanamycin. The culture was grown with shaking at 30 °C to an OD_{600} = 0.6. Cells were recovered by centrifugation at 3000 x g for 10 minutes at 4 °C and the pellet was washed three times with 10 mL ice-cold 10% glycerol, resuspended in 100 µL ice-cold 10% glycerol, and kept on ice.

The gene replacement cassette containing the apramycin resistance marker (*aac(3)IV*), oriT, and FRT regions was amplified by PCR using the primers listed in Table A-3. The 1.4 kb PCR products were then directly transformed via electroporation into the arabinose-induced strain BW25113/pIJ790 containing the cosmid, in which lambda-red mediated homologous recombination enabled replacement of the gene of interest. Transformed *E. coli* were plated on LB agar containing apramycin and incubated overnight at 37 °C to promote loss of the temperature sensitive plasmid pIJ790. Colonies from these plates were inoculated into liquid LB containing apramycin and grown with shaking overnight at 37 °C. The gene replacements were confirmed by PCR using primers DelUp and DelDn to confirm integration of apramycin cassette and subsequently by sequencing. PCR amplification using primers NeoUp and NeoDn confirmed identified double crossover strains. The resultant cosmids were transformed via electroporation into the non-methylating *E. coli* strain ET12567 containing plasmid pUZ8002, which contains the

genes necessary for conjugal transfer of the cosmid. The gene replacements in *E. coli* were maintained at 37 °C in liquid LB medium containing kanamycin, apramycin, and chloramphenicol.

Generation of Gene Replacements in M. carbonacea var. Aurantiaca

M. carbonacea var. *aurantiaca* was grown on TSB agar for 7 days at 30 °C. Conjugal acceptor mycelia were prepared by inoculating a loop of mycelia into 10 mL of TSB medium in a 50 mL Falcon tube and incubating with shaking at 30 °C for 5 days. The culture was then centrifuged at 3000 x g for 10 minutes and the pellet resuspended in 2 mL fresh TSB. 150 µL aliquots were transferred into sterile 1.5 mL Eppendorf tubes and homogenized using a sterile plastic cell homogenizer. Donor *E. coli* ET12567/pUZ8002 cells containing the gene replacement were prepared by inoculating 1% of a freshly prepared overnight LB culture into 10 mL LB medium in a 50 mL Falcon tube containing apramycin and kanamycin, and grown to an OD_{600} = 0.6 at 37 °C with shaking. The culture was centrifuged at 3000 x g for 10 minutes, and the pellet was washed three times with 10 mL fresh LB. After the final wash, the pellet was resuspended in 150 µL LB. Next, 50 µL of donor *E. coli* was added to 150 µL of recipient *M. carbonacea*. Prior to plating, a sterile 0.4 µm membrane was attached to a sterile plastic washer using silicon glue. After drying, each membrane-washer apparatus was placed on an AS1 plate. The mixture of bacteria was plated on top of the membrane-washer setup. After 16 hours of incubation at 30 °C, apramycin (50 µg/mL) was added to the bacteria mixture on top of the assembly to select for apramycin-resistant exconjugants. Alternatively the apparatus can be transferred to agar containing apramycin added pre-cooling. After 7-9 days of incubation at 30 °C, membranes were removed and colonies were streaked onto TSB plates containing apramycin.

Double-crossover mutants were identified by testing for kanamycin sensitivity. To confirm, PCR amplification was also used to identify kanamycin (primers NeoUp and NeoDn) and

apramycin (primers AprUp and AprDn) resistance genes. Alternatively, double-crossover mutants in *M. carbonacea* were confirmed by Southern hybridization. Gene specific probes were designed upstream of the genes of interest. The *evdM2* probe (782 bp) was amplified using primers EvdM2-Southern-For and EvdM2-Southern-Rev. The *evdM3* probe (574 bp) was amplified using primers EvdM3-Southern-For and EvdM3-Southern-Rev. An 884 bp probe specific to the apramycin resistance gene was also designed and amplified using primers Apr-Southern-For and Apr Southern-Rev. All probes were labeled with digoxigenin using the DIG High Prime DNA Labeling and Detection Starter Kit II (Roche Diagnostics GmbH, Mannheim Germany). Hybridization and detection were also performed using the DIG Starter Kit.

Production and Extraction of Everninomicin Metabolites

Seed cultures were generated by inoculating a loop of mycelia from a fresh TSB plate into 100 mL of 2997 germination medium (0.3% beef extract, 0.5% tryptose, 0.1% dextrose, 2.4% soluble starch, 0.5% yeast extract, 0.1% calcium carbonate, and for mutants 50 µg/mL apramycin) and grown with shaking for 5 days at 30 °C in a 500 mL Erlenmeyer flask. For production of everninomicins, 25 mL of the seed culture was added to 500 mL production medium (0.5% yeast extract, 0.1% corn steep solids, 0.1% calcium carbonate, 3% glucose) in a 2 L baffled Fernbach flask and grown with shaking at 30 °C for 10 days. Diaion HP-20 resin (100 mL, previously pre-equilibrated with methanol and washed with water) was added to the fermentation cultures and incubated for 60 minutes with shaking. The resin and mycelia were collected by centrifugation at 3000 x g. The pellets were extracted first with 250 mL methanol for 60 minutes then 250 mL acetone for 60 minutes. The methanol and acetone fractions were combined and evaporated to dryness by rotary evaporation. The resulting crude oily extract was filtered through a fritted glass funnel containing silica gel (9 x 2 cm) in methylene chloride via

vacuum filtration, eluted with methanol and concentrated to dryness. Extracts were resuspended at a final concentration of 200 mg/mL in HPLC grade methanol prior to analysis by LC/MS.

HPLC/MS of Crude Extracts

The extracts were analysed in both negative and positive ion modes using a TSQ Quantum Access Max triple stage quadrupole mass spectrometer (Thermo Scientific, Waltham, MA) equipped with a HESI II electrospray ionization source. Injections of 20 µl were separated on Luna C18(2) column (250 x 4.6 mm; Phenomenex) using either a Finnigan Surveyor LC Pump Plus (Thermo Scientific) or an Accela Pump (Thermo Scientific). Mobile phases were: (A) 95% water/5% acetonitrile with 10 mM ammonium acetate and (B) 5% water/95% acetonitrile with 10 mM ammonium acetate. Gradient conditions were: 0-1 min, 100% A; 1-20 min, linear gradient to 100% B; 20-26 min, 100% B; 26-7 min, linear gradient to 100% A; 27-30 min, 100% A. The flow rate was maintained at 1 ml/min with 15 µl sent to an Accela PDA detector (Thermo Scientific) and 5 µl subjected to mass spectral analysis. Nitrogen was used for both the auxiliary and sheath gas, set to 10 psi and 54 psi respectively. For positive ion mode: capillary temperature 275 °C; spray voltage 4.5 kV; capillary offset 35 V; tube lens voltage 133 V; skimmer offset 5 V. For negative ion mode: capillary temperature 275 °C; spray voltage 3.0 kV; capillary offset -35 V; tube lens voltage -132 V; skimmer offset 5 V.

Isolation and Purification of Everninomicin Analogs

The first dimension of separation for crude extracts was size-exclusion chromatography using a Sephadex LH20 column in methanol. Fractions were analyzed by LC/MS, and the fractions containing everninomicins were combined and separated by RP-HPLC using a linear gradient. Mobile phases were: (A) 99% water/1% acetonitrile with 10 mM ammonium acetate, pH = 8 and (B) 5% water/95% acetonitrile with 10 mM ammonium acetate, pH = 8.

Fragmentation Analysis of Everninomicins

Structural identification was performed using a 15T solariX FT-ICR mass spectrometer (Bruker Daltonics, Billerica, MA, USA) to provide both accurate mass measurements and tandem mass spectrometry fragmentation patterns.[41] External mass calibration was performed prior to analysis (ESI-L Tuning Mix, Agilent Technologies, Santa Clara, CA). Evn H, J, and K (**5-7**) were detected as $[M+Na]^+$ (m/z 1546.4919, -1.01 ppm), $[M+H]^+$ (m/z 1494.5341, 0.03 ppm), and $[M+H]^+$ (m/z 1508.5493, 0.36 ppm) by electrospray ionization respectively. Each ion was isolated in the source region of the instrument (quadrupole isolation window: 1.5 Da), accumulated in the collisional hexapole (10-40 s), and fragmented by sustained off-resonance irradiation collision induced dissociation (SORI-CID) in the ICR cell using pulsed argon (pulse length: 0.25 s, frequency offset: 500 Hz, SORI Power: 2.8-3.1%).[42] The structures of Evn T-W (**9-12**) and AA-AE (**13-17**) were confirmed using the TSQ Quantum Access Max triple stage quadrupole mass spectrometer and parameters described above. Collision energies of 20 V – 30 V with a skimmer offset of 5 V were employed in positive mode to fragment these metabolites.

Genetic Complementation of Replacement Strains

For complementation of *ΔevdM3::aac(3)IV*, the *evdM3* gene was amplified by PCR using the primers listed in Table A-3. The PCR products were subsequently cloned into the NdeI and EcoRV sites of pSET152ermE. This complementation plasmid was transformed into the conjugal *E. coli* strain ET12567/pUZ8002. Conjugation between the donor *E. coli* and recipient *M. carbonacea* was performed in the same manner as listed above, except that apramycin and hygromycin were added after 16 hours of incubation to select for mutants that contained the gene replacement as well as the genetic complementation plasmid. Crude extracts of the complemented strains were prepared and analyzed by HPLC/MS as described.

Scanning Electron Microscopy

Conjugations were performed in the same manner as with the *E. coli* donor strain ET12567/pUZ8002 containing plasmid pSET152. Specimens were processed for scanning electron microscopy (SEM) and imaged in the Vanderbilt Cell Imaging Shared Resource-Research Electron Microscopy facility. Membranes were removed from plates and fixed in 2.5% gluteraldehyde in 0.1M cacodylate buffer, pH 7.4 at room temperature (RT) 1 hour then transferred to 4 ºC, overnight. The samples were washed in 0.1 M cacodylate buffer, then incubated 1 hour in 1% osmium tetraoxide at RT, then washed with 0.1 M cacodylate buffer. Subsequently, the samples were dehydrated through a graded ethanol series and then three exchanges of 100% ethanol. Prior to critical point drying, the filters were cut in half and surface side was carefully noted. The two pieces of filter were then dried in the same cassette and placed in the Tousimis Samdri-PVT-3D critical point dryer. The filters were subsequently mounted on aluminum stubs with carbon adhesive tabs, paying careful attention to the orientation of the filter. The samples were sputter coated with gold/palladium target using the Cressington Sputter Coater (Watford, England (UK). After coating for 90 seconds, the samples were imaged using the Quanta 250ESEM.

Protein Expression and Purification

The genes *evdM1* and *evdM5* were amplified from the EveD cosmid via PCR using the primers EvdM1-For/Rev and EvdM5-For/Rev, respectively (Table A-3). For EvdM5, the PCR fragment was cloned into a TOPO vector (Thermo Fisher) and transformed into *E. coli* Top10 electrocompetent cells. Putative transformants were identified using blue/white screening and confirmed via restriction digest. EvdM5 was then subcloned into the expression vector pET28a(+) using the restriction sites NdeI and BamHI. The resulting vector was transformed into

E. coli BL21 (DE3). For EvdM1, the PCR amplified fragment was directly cloned into a linearized pET28a(+) vector (NdeI, BamHI) using Gibson assembly.

For expression, *E. coli* cultures were grown to OD_{600} = 0.4-0.6 at 37 °C in LB broth containing kanamycin. Cultures were cooled on ice for 20 minutes followed by induction with 1 mM IPTG. EvdM1 cultures were allowed to shake for 3 hours at 16 °C before being harvesting. EvdM5 cultures were allowed shake for approximately 16 hours at 16 °C before harvesting. Cells were harvested via centrifugation at 3,000 X g for 30 minutes at 4 °C. Pellets were resuspended in 15 mL of lysis buffer A (50 mM Tris, 300 mM NaCl, 5 mM imidazole; pH 7.4) and 5 mg/mL lysozyme and frozen at -80 °C overnight. Subsequently, the pellets were defrosted and 10 mL DNAse was added. The samples were lysed via passage through a French Press (x 2). Crude lysates were clarified by centrifugation at 10,000 x g for 50 minutes. The supernatants were loaded onto a 5 mL HisTrap FF Crude nickel affinity column (GE Healthcare Life Sciences) and eluted on AKTA fast protein liquid chromatography (FPLC) system using elution buffer B (500 mM Tris, 300 mM NaCl, 500 mM imidazole; pH 7.4). Based on the UV trace from the FPLC, the relevant fractions were combined and concentrated to approximately 2 mL using Amicon® Ultra Centrifugal Filters with the appropriate size filter. Concentrated fractions were then desalted and solvent exchanged into protein storage buffer (10% glycerol, 1 mM DTT, 20 mM HEPES, pH 7.5) using a 5 mL HiTrap Desalting column (GE Healthcare Life Sciences). Protein aliquots were flash frozen in ethanol and CO_2 (s) and stored at -80 °C.

Biochemical Methyltransferase Assays

The EvdM5 methyltransferase reactions were carried out in 25 mM HEPES (pH 7.5) with 2.5 mM $MgCl_2$ and supplemented with 0.5% (v/v) bovine serum albumin. A final concentration of 20 uM EvdM5 with 50 mg/mL of HPLC purified Evn AE (**17**) and 4.0 μM adoMet was incubated at 30 °C for 16 hours. Reactions were quenched with an equal volume of methanol to precipitate

the protein, which was removed via centrifugation. The reaction was analyzed via TSQ Quantum Access Max triple stage quadrupole mass spectrometer with instrument parameters described above except a Kinetex C18 (150 x 4.6mm; Phenomenex) column was used. A 12 minute gradient was used with conditions as follows: 0-1 min, 100% (A); 1-8 min, linear gradient to 100% (B); 8-10 min, 100% (B); 10-11 min, linear gradient to 100% (A); and 11-12 min, 100% (A). Mobile phases were 95% water/5% acetonitrile (vol/vol) with 10 mM ammonium acetate (A) and 5% water/95% acetonitrile (vol/vol) with 10 mM ammonium acetate (B).

The EvdM1 methyltransferase reactions were carried out with a final concentration of 25 uM EvdM5 in 50 mM HEPES (pH 7.5) with 10 uM $MgCl_2$, 4 mM adoMet, and 30 mg/mL of SEC-purified *ΔevdM1::aac(3)IV* extract. Assay reactions were incubated at 30 °C for 16 hours and subsequently quenched with an equal volume of methanol to precipitate the protein, which was removed via centrifugation. The reaction was analyzed via TSQ Quantum Access Max triple stage quadrupole mass spectrometer with instrument parameters described above using the Kinetex C18 (150 x 4.6mm; Phenomenex) column. A 20 minute gradient was used with conditions as follows: 0-1 min, 100% (A); 1-15 min, linear gradient to 100% (B); 15-17 min, 100% (B); 17-19 min, linear gradient to 100% (A); and 19-20 min, 100% (A). Mobile phases were 95% water/5% acetonitrile (vol/vol) with 10 mM ammonium acetate (A) and 5% water/95% acetonitrile (vol/vol) with 10 mM ammonium acetate (B).

Phylogenetic Analysis of Orthosomycin Methyltransferases

Protein sequences for all methyltransferases analyzed can be found in Table A-4. The protein sequences were uploaded to the CIPRES Science Gateway portal and aligned using MUSCLE (version 3.7).[43,44] This alignment was trimmed using Trim AI (version 1.2.59).[45] A maximum-likelihood phylogenetic tree of the methyltransferases was generated from this trimmed alignment by FastTree (version 2.1.11) using Geneious R11 (version 2020.1.2).[46]

Acknowledgements

This work was supported by the Vanderbilt Institute of Chemical Biology, the D. Stanley and Ann T. Tarbell Endowment Fund, the National Institutes of Health (no. RO1GM092218 to BOB), and an American Heart Association Grant 12GRNT11920011 (to TMI). Scanning electron microscopy was performed through the use of the VUMC Cell Imaging Shared Resource (supported by NIH grants CA68485, DK20593, DK58404, DK59637 and EY08126). JMS is supported by the NIH/NIGMS (2P41 GM103391) and DARPA (W911NF-14-2-0022). KMM was supported by T32 HL007751 from the NIH. AEY was supported by the NSF GRFP (no. 1445197) and the National Institutes of Health (no. T32 GM065086-13). The 15T FTICR MS in the Mass Spectrometry Research Center at Vanderbilt University was acquired through the National Institutes of Health Shared Instrumentation Grant Program (1S10OD012359).

References

1. Fraternali, F.; Cavallo, L. Parameter optimized surfaces (pops): Analysis of key interactions and conformational changes in the ribosome. *Nucleic Acids Research* **2002**, *30*, 2950-2960.

2. Arenz, S.; Ramu, H.; Gupta, P.; Berninghausen, O.; Beckmann, R.; Vazquez-Laslop, N.; Mankin, A. S.; Wilson, D. N. Molecular basis for erythromycin-dependent ribosome stalling during translation of the ermbl leader peptide. *Nature Communications* **2014**, *5*, 3501.

3. Dunkle, J. A.; Xiong, L.; Mankin, A. S.; Cate, J. H. Structures of the escherichia coli ribosome with antibiotics bound near the peptidyl transferase center explain spectra of drug action. *Proceedings of the National Academy of Sciences of the United States of America* **2010**, *107*, 17152-17157.

4. Brodersen, D. E.; Clemons, W. M.; Carter, A. P.; Morgan-Warren, R. J.; Wimberly, B. T.; Ramakrishnan, V. The structural basis for the action of the antibiotics tetracycline, pactamycin, and hygromycin b on the 30s ribosomal subunit. *Cell* **2000**, *103*, 1143-1154.

5. Charest, M. G.; Lerner, C. D.; Brubaker, J. D.; Siegel, D. R.; Myers, A. G. A convergent enantioselective route to structurally diverse 6-deoxytetracycline antibiotics. *Science (Washington, DC, U. S.)* **2005**, *308*, 395-398.

6. Seiple, I. B.; Zhang, Z.; Jakubec, P.; Langlois-Mercier, A.; Wright, P. M.; Hog, D. T.; Yabu, K.; Allu, S. R.; Fukuzaki, T.; Carlsen, P. N.; Kitamura, Y.; Zhou, X.; Condakes, M. L.; Szczypinski, F. T.; Green, W. D.; Myers, A. G. A platform for the discovery of new macrolide antibiotics. *Nature* **2016**, *533*, 338-345.

7. Ynigez-Gutierrez, A. E.; Bachmann, B. O. Fixing the unfixable: The art of optimizing natural products for human medicine. *J Med Chem* **2019**, *62*, 8412-8428.

8. Ganguly, A. K.; McCormick, J. L.; Saksena, A. K.; Das, P. D.; Chan, T. Chemical modifications and structure activity studies of ziracin and related everninomicin antibiotics. *Bioorganic and Medicinal Chemistry Letters* **1999**, *9*, 1209-1214.

9. Ganguly, A. K. Ziracin, a novel oligosaccharide antibiotic. *J Antibiot* **2000**, *53*, 1038-1044.

10. Marshall, S. A.; Jones, R. N.; Erwin, M. E. Antimicrobial activity of sch27899 (ziracin), a novel everninomicin derivative, tested against streptococcus spp.: Disk diffusion/etest method evaluations and quality control guidelines. The quality control study group. *Diagnostic Microbiology and Infectious Disease* **1999**, *33*, 19-25.

11. Souli, M.; Thauvin-Eliopoulos, C.; Eliopoulos, G. M. In vivo activities of evernimicin (sch 27899) against vancomycin-susceptible and vancomycin-resistant enterococci in experimental endocarditis. *Antimicrobial Agents and Chemotherapy* **2000**, *44*, 2733-2739.

12. Weinstein, M. J.; Wagman, G. H.; Oden, E. M.; Luedemann, G. M.; Sloane, P.; Murawski, A.; Marquez, J. Purification and biological studies of everninomicin b. *Antimicrobial Agents and Chemotherapy* **1965**, *5*, 821-827.

13. Ganguly, A. K. Challenges in drug discovery at schering-plough research institute: A personal reflection. *Annu. Rep. Med. Chem.* **2013**, *48*, 3-14.

14. Foster, D. R.; Rybak, M. J. Pharmacologic and bacteriologic properties of sch-27899 (ziracin), an investigational antibiotic from the everninomicin family. *Pharmacotherapy: The Journal of Human Pharmacology and Drug Therapy* **1999**, *19*, 1111-1117.

15. Krupkin, M.; Wekselman, I.; Matzov, D.; Eyal, Z.; Diskin Posner, Y.; Rozenberg, H.; Zimmerman, E.; Bashan, A.; Yonath, A. Avilamycin and evernimicin induce structural changes in rproteins ul16 and ctc that enhance the inhibition of a-site trna binding. *Proceedings of the National Academy of Sciences* **2016**, *113*, E6796-E6805.

16. Arenz, S.; Juette, M. F.; Graf, M.; Nguyen, F.; Huter, P.; Polikanov, Y. S.; Blanchard, S. C.; Wilson, D. N. Structures of the orthosomycin antibiotics avilamycin and evernimicin in complex with the bacterial 70s ribosome. *Proceedings of the National Academy of Sciences* **2016**, *113*, 7527-7532.

17. Nicolaou, K. C.; Mitchell, H. J.; Suzuki, H.; Rodríguez, R. M.; Baudoin, O.; Fylaktakidou, K. C. Total synthesis of everninomicin 13,384-1—part 1: Synthesis of the a1b(a)c fragment. *Angewandte Chemie International Edition* **1999**, *38*, 3334-3339.

18. Nicolaou, K. C.; Rodríguez, R. M.; Fylaktakidou, K. C.; Suzuki, H.; Mitchell, H. J. Total synthesis of everninomicin 13,384-1—part 2: Synthesis of the fgha2 fragment. *Angewandte Chemie International Edition* **1999**, *38*, 3340-3345.

19. Nicolaou, K. C.; Fylaktakidou, K. C.; Mitchell, H. J.; van Delft, F. L.; Rodríguez, R. M.; Conley, S. R.; Jin, Z. Total synthesis of everninomicin 13,384-1—part 4: Explorations of methodology; stereocontrolled synthesis of 1,1′-disaccharides, 1,2-seleno migrations in carbohydrates, and solution- and solid-phase synthesis of 2-deoxy glycosides and orthoesters. *Chemistry – A European Journal* **2000**, *6*, 3166-3185.

20. Nicolaou, K. C.; Mitchell, H. J.; Fylaktakidou, K. C.; Rodríguez, R. M.; Suzuki, H. Total synthesis of everninomicin 13,384-1—part 2: Synthesis of the fgha2 fragment. *Chemistry – A European Journal* **2000**, *6*, 3116-3148.

21. Nicolaou, K. C.; Mitchell, H. J.; Rodríguez, R. M.; Fylaktakidou, K. C.; Suzuki, H.; Conley, S. R. Total synthesis of everninomicin 13,384-1—part 3: Synthesis of the de fragment and completion of the total synthesis. *Chemistry – A European Journal* **2000**, *6*, 3149-3165.

22. Nicolaou, K. C.; Rodríguez, R. M.; Mitchell, H. J.; Suzuki, H.; Fylaktakidou, K. C.; Baudoin, O.; van Delft, F. L. Total synthesis of everninomicin 13,384-1—part 1: Retrosynthetic analysis and synthesis of the a1b(a)c fragment. *Chemistry – A European Journal* **2000**, *6*, 3095-3115.

23. de Lorenzo, V.; Herrero, M.; Jakubzik, U.; Timmis, K. N. Mini-tn5 transposon derivatives for insertion mutagenesis, promoter probing, and chromosomal insertion of cloned DNA in gram-negative eubacteria. *Journal of Bacteriology* **1990**, *172*, 6568-6572.

24. Gavrish, E.; Bollmann, A.; Epstein, S.; Lewis, K. A trap for in situ cultivation of filamentous actinobacteria. *Journal of microbiological methods* **2008**, *72*, 257-262.

25. Bibb, M. J.; White, J.; Ward, J. M.; Janssen, G. R. The mrna for the 23s rrna methylase encoded by the erme gene of saccharopolyspora erythraea is translated in the absence of a conventional ribosome-binding site. *Molecular Microbiology* **1994**, *14*, 533-545.

26. Gust, B.; Challis, G. L.; Fowler, K.; Kieser, T.; Chater, K. F. Pcr-targeted streptomyces gene replacement identifies a protein domain needed for biosynthesis of the sesquiterpene soil odor geosmin. *Proc Natl Acad Sci U S A* **2003**, *100*, 1541-1546.

27. Gust, B.; Chandra, G.; Jakimowicz, D.; Yuqing, T.; Bruton, C. J.; Chater, K. F.: Λ red-mediated genetic manipulation of antibiotic-producing streptomyces. In *Advances in applied microbiology*; Academic Press, 2004; Vol. Volume 54; pp 107-128.

28. Ganguly, A. K.; Saksena, A. K. Structure of everninomicin-b. *J Antibiot* **1975**, *28*, 707-709.

29. Ollis, W. D.; Smith, C.; Wright, D. E. Hydrolysis of flambamycin. The constitution of flambeurekanose. *J. Chem. Soc., Chem. Commun.* **1976**, 348-350.

30. Ollis, W. D.; Smith, C.; Wright, D. E. Methanolysis of flambamycin. The constitution of methyl eurekanate. *J. Chem. Soc., Chem. Commun.* **1976**, 347-348.

31. Ganguly, A. K.; Szmulewicz, S.; Sarre, O. Z.; Girijavallabhan, V. M. Structure of everninomicin-2. *J Chem Soc Chem Comm* **1976**, 609-611.

32. Weitnauer, G.; Gaisser, S.; Kellenberger, L.; Leadlay, P. F.; Bechthold, A. Analysis of a c-methyltransferase gene (avig1) involved in avilamycin biosynthesis in streptomyces

viridochromogenes tü57 and complementation of a saccharopolyspora erythraea erybiii mutant by avig1. *Microbiology* **2002**, *148*, 373-379.

33. Weitnauer, G.; Mühlenweg, A.; Trefzer, A.; Hoffmeister, D.; Süßmuth, R. D.; Jung, G.; Welzel, K.; Vente, A.; Girreser, U.; Bechthold, A. Biosynthesis of the orthosomycin antibiotic avilamycin a: Deductions from the molecular analysis of the avi biosynthetic gene cluster of streptomyces viridochromogenes tü57 and production of new antibiotics. *Chemistry & Biology* **2001**, *8*, 569-581.

34. Weitnauer, G.; Hauser, G.; Hofmann, C.; Linder, U.; Boll, R.; Pelz, K.; Glaser, S. J.; Bechthold, A. Novel avilamycin derivatives with improved polarity generated by targeted gene disruption. *Chemistry & Biology* **2004**, *11*, 1403-1411.

35. Chen, H.; Thomas, M. G.; Hubbard, B. K.; Losey, H. C.; Walsh, C. T.; Burkart, M. D. Deoxysugars in glycopeptide antibiotics: Enzymatic synthesis of tdp-l-epivancosamine in chloroeremomycin biosynthesis. *Proceedings of the National Academy of Sciences of the United States of America* **2000**, *97*, 11942-11947.

36. Vey, J. L.; Al-Mestarihi, A.; Hu, Y.; Funk, M. A.; Bachmann, B. O.; Iverson, T. M. Structure and mechanism of orf36, an amino sugar oxidizing enzyme in everninomicin biosynthesis. *Biochemistry* **2010**, *49*, 9306-9317.

37. Dow, G. T.; Thoden, J. B.; Holden, H. M. Structural studies on kijd1, a sugar c-3'-methyltransferase. *Protein Science* **2016**, *25*, 2282-2289.

38. Al-Mestarihi, A.; Romo, A.; Liu, H.-w.; Bachmann, B. O. Nitrososynthase-triggered oxidative carbon–carbon bond cleavage in baumycin biosynthesis. *Journal of the American Chemical Society* **2013**, *135*, 11457-11460.

39. Starbird, C. A.; Perry, N. A.; Chen, Q.; Berndt, S.; Yamakawa, I.; Loukachevitch, L. V.; Limbrick, E. M.; Bachmann, B. O.; Iverson, T. M.; McCulloch, K. M. The structure of the bifunctional everninomicin biosynthetic enzyme evdmo1 suggests independent activity of the fused methyltransferase-oxidase domains. *Biochemistry* **2018**, *57*, 6827-6837.

40. Musiol-Kroll, E. M.; Tocchetti, A.; Sosio, M.; Stegmann, E. Challenges and advances in genetic manipulation of filamentous actinomycetes - the remarkable producers of specialized metabolites. *Nat Prod Rep* **2019**, *36*, 1351-1369.

41. Marshall, A. G.; Hendrickson, C. L.; Jackson, G. S. Fourier transform ion cyclotron resonance mass spectrometry: A primer. *Mass spectrometry reviews* **1998**, *17*, 1-35.

42. Herrmann, K. A.; Somogyi, A.; Wysocki, V. H.; Drahos, L.; Vekey, K. Combination of sustained off-resonance irradiation and on-resonance excitation in ft-icr. *Analytical chemistry* **2005**, *77*, 7626-7638.

43. Miller, M. A.; Schwartz, T.; Pickett, B. E.; He, S.; Klem, E. B.; Scheuermann, R. H.; Passarotti, M.; Kaufman, S.; O'Leary, M. A. A restful api for access to phylogenetic tools via the cipres science gateway. *Evol. Bioinf. Online* **2015**, *11*, 43-48.

44. Edgar, R. C. Muscle: Multiple sequence alignment with high accuracy and high throughput. *Nucleic Acids Res.* **2004**, *32*, 1792-1797.

45. Capella-Gutierrez, S.; Silla-Martinez, J. M.; Gabaldon, T. Trimal: A tool for automated alignment trimming in large-scale phylogenetic analyses. *Bioinformatics* **2009**, *25*, 1972-1973.

46. Price, M. N.; Dehal, P. S.; Arkin, A. P. Fasttree: Computing large minimum evolution trees with profiles instead of a distance matrix. *Mol. Biol. Evol.* **2009**, *26*, 1641-1650.

Chapter IV

Genetic Functional and Enzymatic Analysis of Dichloroisoeverninic Acid Biosynthesis in Orthosomycins

The work presented in this chapter was aided by Dr. Jordan Froese, Mr. Nicolas Rosenthal, and Ms. Kathleen McClanahan and is published with their permission.

Introduction

As discussed in chapters II and III, the everninomicins are complex oligosaccharide natural products produced by the soil-dwelling actinomycetes *Micromonospora carbonacea.*[1,2] Everninomicins, as well as avilamycins, curamycins, and flabamycin, are class I orthosomycins characterized as esters of dichloroisoeverninic acid (DCIE) that contain unique orthoester linkages between carbohydrate residues.[3,4] In addition to their unique structure, many orthosomycin natural products exhibit potent antibacterial activity. In particular, everninomicin A (Evn A, Ziracin) was extensively investigated for clinical application due to its activity against multi-drug resistant Gram-positive pathogens.[5,6] Despite advancing to stage III clinical trials, Ziracin's development was discontinued due to the inability to reproducibly access an intravenous formulation.[7] Given the dire need for new antibiotics, the everninomicins are excellent candidates for revitalization as human therapeutics.

The US Centers for Disease Control estimates that over 2.8 million antibiotic-resistant infections occur annually in the United States, resulting in over 35,000 deaths.[8] Therefore, it is not hyperbole to state that we are now living in a post-antibiotic era where effective treatments against bacterial infections are not guaranteed. While the prevention of infection is the first line

of defense, the need for novel antibiotic classes with new mechanisms of action is clear. Natural products have long provided the template for pharmaceuticals, especially in the antimicrobial arena. Additionally, numerous complex natural products with suboptimal characteristics, such as low solubility, high toxicity, or poor pharmacokinetics, have been "rescued" using total synthesis, semi-synthesis, biosynthetic manipulation, or a combination of these techniques.[9] Given the decades of success in improving legacy natural product classes, some of which were covered in Chapter II, the field may also benefit by revisiting previously discarded natural products with novel scaffolds and targets due to their lack of environmental and clinical resistance. The potent activity and novel mechanism of action (MOA) of the everninomicins makes them promising candidates for such derivatization.

Initial development of Ziracin determined that protein synthesis inhibition was the likely target of the orthosomycins. Despite a plethora of high-quality biochemical experiments, the specific details of how the orthosomycins interact with the bacterial ribosome was not known until recently.[10-13] Currently, through crystallography and cryo-EM imaging, we have a comprehensive view of the orthosomycin binding site on the 50S ribosomal subunit, revealing it to be unique from all other ribosomal-targeting natural products.[14-16] The everninomicins bind in an extended conformation in the minor grooves of helices 89 and 91 formed by 23S ribosomal RNA (Figure 4-1A). This binding site extends to include interactions with the ribosomal protein uL16 and the elbow region of the A-site for tRNA. The DCIE acid moiety of everninomcin (A_1-ring) binds in a pocket formed by the side chains Arg50, Ile51, Ser54, Arg55, and Arg59 of rProtein uL16 (Figure 4-1B). Ile51 forms a hydrophobic interaction by stacking with the DCIE ring, and Ser54 forms a dipole interaction to the chlorine atom at the C5 position. The loop consisting of Arg55-63 swings in to encapsulate both DCIE and the evernitrose (A-ring) of everninomicin. The crystal structure of the *Deinococcus radiodurans* 50S subunit reveals additional interactions with DCIE specific to Gram-positive organisms. In particular, the shift in the position of Arg59 results in a structural

change in the 2 domain of the CTC protein. The Arg175 side chain of CTC shifts to allow for hydrophobic interactions between Glu179 and Arg175 with DCIE and evernitrose. This also places the CTC Glu179 residue within 3.6 angstroms of the hydroxyl group at C-4 of DCIE to form a hydrophilic (H-bond) interaction.

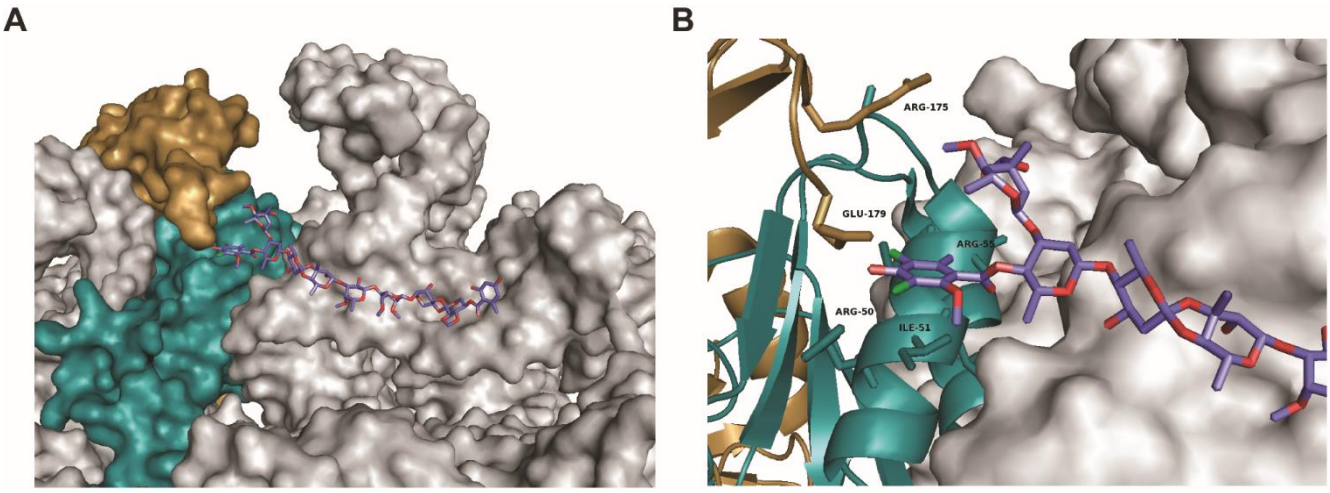

Figure 4-1. Structures of everninomicin A (Evn A) bound to the 50S ribosomal subunit. (A) Full-length Evn A bound to the ribosome (gray). Ribosomal proteins L16 (teal) and CTC (gold) form key interactions with the DCIE ring on the western portion of Evn A. (B) Zoomed in structure showing key residues from rL16 interacting with the DCIE ring. Residues from the CTC protein are shifted to accommodate DCIE and evernitrose.

These specific interactions result in the inhibition of protein synthesis in multiple ways. The binding of A-tRNA, in particular, is disrupted by the shift of uL16 Arg50/55 side chains, which normally interact with the A-tRNA G53 nucleotide during protein biosynthesis. Additionally, a comparison of the apo-50S complex with the Evn-50S complex indicates that the DCIE and D-olivose (B-ring) would directly clash with the A-tRNA elbow nucleotides G53/52 to prevent A-tRNA binding. Thus, DCIE (A_1-ring) causes structural changes to the CTC and uL16 proteins to block the A-tRNA from binding to the 50S ribosomal subunit.

Overall, DCIE (A_1-ring) plays a key role in the novel MOA of everninomicin by forming multiple interactions within the pocket between the 50S subunit, rProtein uL16, and the CTC

protein. Therefore, we seek to revitalize the everninomicins as clinical candidates by interrogating these interactions and developing analogs with improved properties. While a total synthesis of Evn A (Ziracin) has been completed, its application to access analogs is impractical as the synthesis consists of over 130 steps.[17-23] Consequently, we endeavored to grasp a fuller picture of the biosynthetic machinery responsible for everninomicin synthesis in an effort to utilize this machinery to access novel everninomicins. Previous efforts in our lab have elucidated the biosynthesis of the unique evernitrose sugar, as well as the orthoester linkages.[24,25] Chapter III reports our comprehensive functional annotation of the ten methyltransferases present in the everninomicin pathway, which play a critical role in the complex tailoring of the everninomicin scaffold.[26] In the completion of this work, we have developed a robust genetic editing system in the everninomicin producing organism, *Micromonospora carbonacea* var. *aurantiaca,* utilizing a marker-less microporous conjugation technique to avoid protoplast formation, which is difficult in non-sporulating actinomycetes. The work in this Chapter presents a detailed biosynthetic pathway for the A_1-ring DCIE portion of the everninomicins. This aromatic portion of the scaffold is the only non-saccharide moiety of everninomicin and is present in all characterized class I orthosomycins. In route to elucidating the biosynthesis of DCIE, we have accessed three new everninomicin shunt metabolites as well as generated sixteen non-natural analogs. Utilizing bioautography to quickly access antibacterial activity of these novel everninomicins, we identified two non-natural analogs for further purification, and structural and bioactivity analysis is currently underway. We have also identified key biosynthetic enzymes with clear potential for application in bioengineering and synthetic biology.

Results

A review of the everninomicin biosynthetic gene cluster in *M. car.* var. a*urantiaca* revealed

four genes putatively associated with DCIE biosynthesis. The O-methyltransferase EvdM5 was previously identified as the protein responsible for the methylation of the C-2 hydroxyl group of a DCIE precursor.[26] The remaining three genes include a flavin-dependent halogenase (*evdD2*), an iterative type I polyketide synthase (*evdD3*), and a putative β-ketoacyl-ACP (KAS) III protein (*evdD1*), which served an unclear function. The order of these enzymes and the specific enzymatic substrates were unclear when compared to homologous biosynthetic systems. Towards our goal of identifying key everninomicin biosynthetic analogs, we performed a functional analysis of the three remaining genes to clarify the biosynthetic order.

Deletion of evdD3 and evdD1 yields novel Evn Q

Iterative polyketide synthases (iPKS) were initially believed to exist primarily in fungal gene clusters. However, the first bacterial iPKS, AviM, was discovered in the orthosomycin gene cluster for avilamycin and was hypothesized to be responsible for the biosynthesis of orsellinic acid (OSA), the DCIE precursor.[27] Based on sequence similarity, we hypothesized that EvdD3 in the everninomicin pathway was responsible for the biosynthesis of OSA. Therefore, we performed a targeted gene deletion of *evdD3* using a two-step lambda-RED system and microporous membrane intergeneric conjugation.[26,28,29] Metabolites from this mutant strain were evaluated via liquid chromatography mass spectrometry (LC/MS). Following extraction of the *ΔevdD3::aac(3)IV* strain, we saw a complete loss of production for the wildtype everninomicins D-G (Evn D-G) (Figure 4-2A). We did, however, observe a novel metabolite with a mass of 1116.4, which we termed everninomicin Q (Evn Q). Utilizing tandem mass spectrometry, we determined the structure of Evn Q as a heptasaccharide late-stage everninomicin shunt product, which lacked the entire DCIE (A_1-ring) and the evernitrose sugar (A-ring) (Figure B-1). The loss of the DCIE moiety is consistent with the iPKS EvdD3 being responsible for OSA biosynthesis. The lack of the evernitrose sugar, while unexpected, is consistent with the previous observation

that addition of the A-ring is the final step in everninomicin biosynthesis.[30] Therefore, the loss of the evernitrose sugar is likely not a polar effect of the genetic disruption itself but rather results from the lack of the DCIE ring, preventing the final glycosyltransferase from recognizing its substrate to attach the evernitrose sugar.

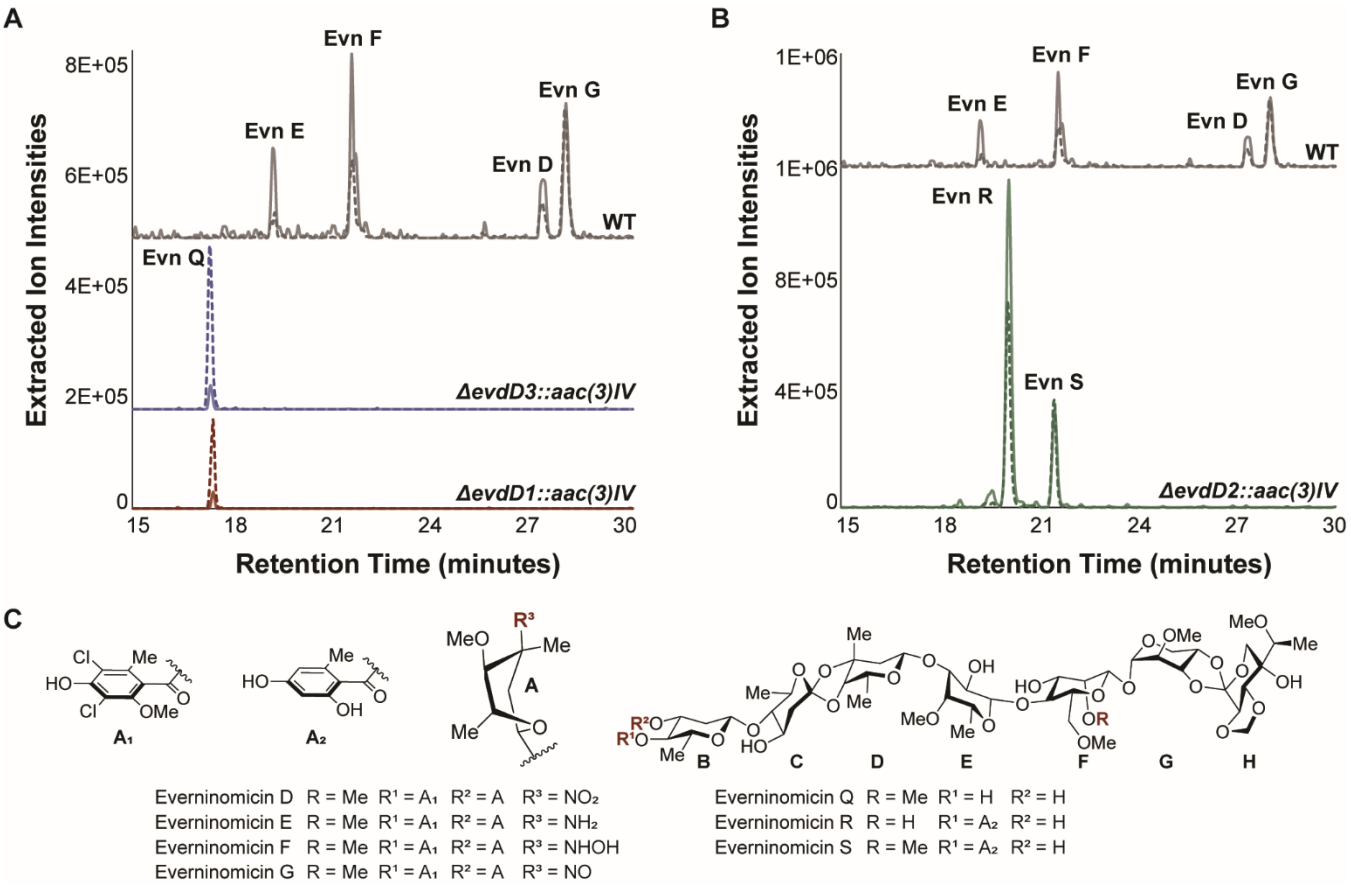

Figure 4-2.Analysis of genetic deletion of *evdD1*, *evdD3*, and *evdD2* in *Micromonospora carbonacea* var. *aurantiaca*. (A) LC/MS analysis of wildtype and deletion strains *evdD3* (*ΔevdD3::aac(3)IV*) and *evdD1* (*ΔevdD1::aac(3)IV*). (B) LC/MS analysis of wild type and deletion strain *evdD2* (*ΔevdD2::aac(3)IV*). Chromatograms show summed ion intensitites for negative mode (dotted lines) and positive mode (solid lines) for wildtype and novel Evn analogs. Everninomicin masses found in Table B-1. (C) Structures of wildtype everninomicins (Evn D-G) and novel everninomicin analogs Evn Q, R, and S.

Previous gene cluster analysis also identified a gene enconding for the putative KAS III protein EvdD1 with high sequence similarity to proteins from the pactamycin and chlorothricin pathways. Some members of this enzyme class have been shown to catalyze the initiation step

in fatty acid and PKS synthesis. Conversely, homologous enzymes have also been shown to be involved in off-loading of PKS products from the ACP domain.[31] In order to determine if EvdD1 was involved in DCIE biosynthesis, we deleted the gene *evdD1* in our producer strain. Analysis of the mutant strain *evdD1::aac(3)IV* showed an accumulation of the same heptasacchride, Evn Q, observed in the *evdD3::aac(3)IV* strain. This result indicates that EvdD1 is involved in the biosynthesis of the DCIE ring. However, its precise role and interaction with the iPKS EvdD3 was still unclear from this functional analysis.

Deletion of evdD2 produces deschloro metabolites Evn S and Evn R

The flavin-dependent halogenase (FDH) encoded by the gene *evdD2* was also evaluated via genetic deletion. LC/MS analysis revealed two novel metabolites in the extract of the mutant strain *evdD2::aac(3)IV* with masses 1252.5 and 1266.52; these two metabolites were termed everninomicin R (Evn R) and everninomicin S (Evn S), respectively (Figure 4-2B). Analysis of these novel metabolites using tandem mass spectrometry elucidated their structures as lacking the two chlorines and the methyl group on the DCIE (A_1-ring), as well as the loss of the evernitrose sugar (A-ring) entirely (Figures B-2 – 3). This observation aligns with our data from the deletion of the OSA associated proteins EvdD3 and EvdD1. The difference of 14 Da between EVR and EVS indicated the loss of a methyl group between the two metabolites. We were able to confirm via MS/MS that EVR is lacking an additional methyl group on the 2,6-di-*O*-methyl-D-mannose (F-ring) at the C-2 hydroxyl position (Figure B-2). While this result was unexpected, it is consistent with previous observations from our and other's work regarding methyltransferase assignment for orthosomycin gene clusters. Directly downstream of *evdD2* is the gene *evdM7*, which was assigned in Chapter III as the methyltransferase responsible for the O-methylation of the F-ring at the C-2 hydroxyl position. This everninomicin gene, *evdM7*, is homologous (66% identity) with *aviG6* in the avilamycin pathway, which was analyzed directly via functional

analysis and confirmed to methylate at the F-ring.[32] Thus, the metabolite Evn R is a result of unintended disruption of *evdM7* from the deletion of *evdD2*. Conversely, the loss of the methyl group at the C-2 position of the DCIE hydroxyl indicates that halogenation precedes O-methylation on the OSA scaffold. From these data alone it is not clear, however, whether EvdD2 catalyzes the addition of the chlorines while OSA is still bound to the ACP domain of EvdD3 or following attachment of OSA to the larger everninomicin scaffold, as both routes can be envisioned.[33,34]

Taken together, our functional analysis data allow for the annotation of the four genes involved in the biosynthesis of DCIE. However, this analysis alone does not resolve the issue of timing and the specific substrates necessary for each enzymatic transformation. The manner of the interactions between the iPKS EvdD3 and the KAS III transferase EvdD1 was still ambiguous from these initial data. Specifically, the involvement of EvdD1 was unclear, as the accumulation of Evn Q would be expected whether EvdD1 was responsible for loading or off-loading the ACP domain of iPKS EvdD3. Likewise, while the annotation of EvdD2 as the halogenase responsible for chlorination of the DCIE ring was confirmed, the specific substrate was still undetermined.

Acyltransferase EvdD1 catalyzes OSA transfer to Evn Q

In order to gain a more complete understanding of the biosynthetic order for DCIE, we cloned *evdD1*, *evdD3*, and *evdD2* into appropriate vectors (Methods and Materials; Figures B-4 – 7) for overexpression in *E. coli*. All three proteins were purified using Ni-affinity chromatography for *in vitro* analysis. Based on sequence homology to other KAS III-like proteins with confirmed off-loading activity, we decided to first evaluate whether EvdD1 was responsible for off-loading OSA or dichloro-OSA from the acyl carrier domain of EvdD3. Therefore, we synthesized both substrates as the *N*-acetylcysteamine (NAC) thioester, a biomimetic for the phosphopantetheine arm of acyl carrier protein domains.[35] Previously, Nicolaou and coworkers synthesized OSA via

a Gattermann formylation of orcinol followed by a Pinnick oxidation to generate the free OSA, which was then protected as an ester to allow for bis-chlorination followed by deprotection to generate dichloro-OSA.[17,23] Conversely, we utilized a Vilsmeier-Haack formylation to convert orcinol to the aldehyde and then performed a single-pot modified Pinnick oxidation-chlorination reaction to access either OSA or the dicholoro-OSA in a total of only two steps (Figure B-8).[36,37] The free acids were converted to the NAC thioester using peptide coupling.[38] Following incubation of EvdD1 with the late-stage metabolite from mutant strain *evdD3::aac(3)IV* and the NAC-thioesters, we only observed the transfer of OSA to Evn Q to provide Evn S (Figure 4-3B). This result demonstrates that the KAS III-like EvdD1 acts as an acyltransferase for the off-loading and transfer of OSA from the ACP domain of iPKS EvdD3 to the everninomicin core scaffold of Evn Q.

Comparison of the sequences of EvdD1 to other related acyltransferase proteins shows a conserved catalytic triad (Cys-His-Asp) for many members of this class. In particular, the ketosynthase homolog CerJ appears to utilize a thioester intermediate to transfer malonyl to the glycoside of cervimycin.[39] While this substrate is significantly different from the proposed aromatic OSA substrate in the everninomicin pathway, the conservation of this catalytic triad across multiple members of related acyltransferases led us to hypothesize that EvdD1 worked through a similar mechanism.[40] To verify these catalytic residues, we performed site-directed mutagenesis to access EvdD1 mutants C113S, C113A, and H293A. *In vitro* enzymatic analysis revealed that mutations at both of these positions rendered EvdD1 inactive for transfer of OSA from the NAC thioester to Evn Q (Figure 4-3B).

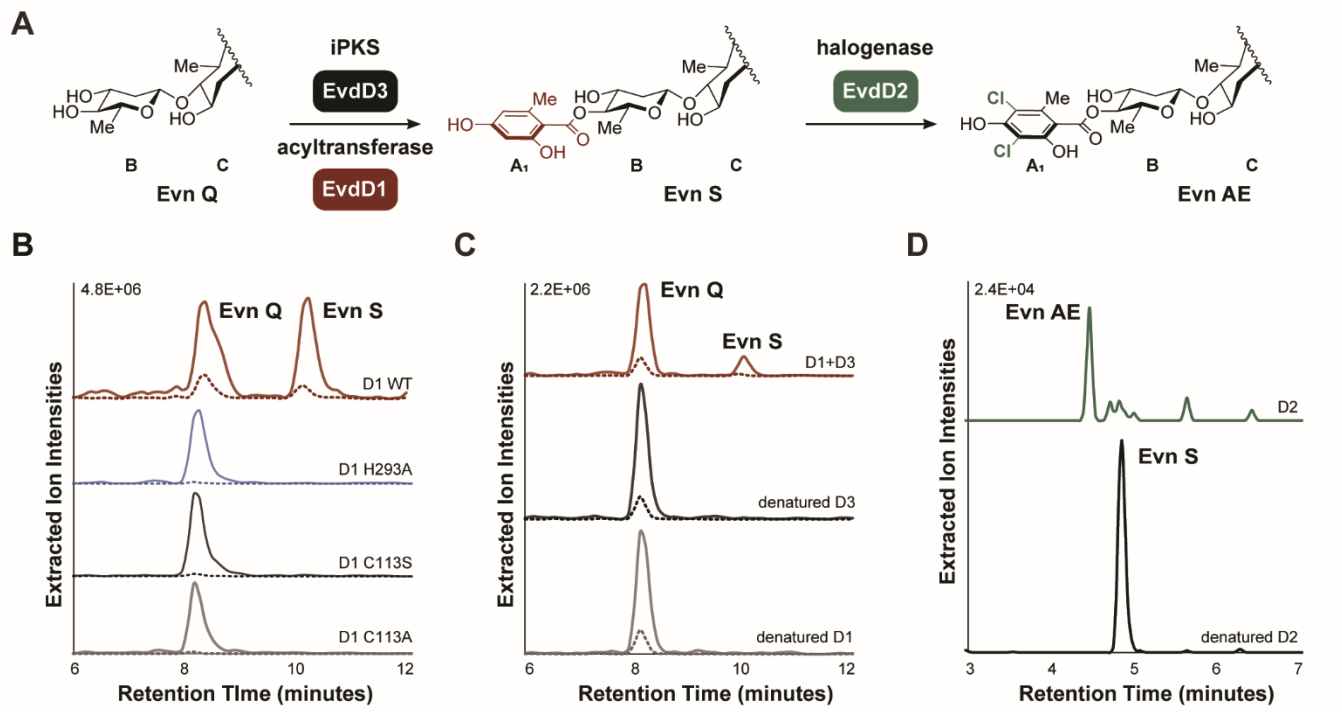

Figure 4-3. Enzymatic analysis of acyltransferase EvdD1, iPKS EvdD3, and FDH EvdD2. (A) Scheme of DCIE biosynthetic pathway reconstituted *in vitro.* (B) LC/MS analysis of acyltransferase EvdD1 attaching OSA to Evn Q *in vitro* using OSA-NAC. Mutations in the catalytic triad abrogate EvdD1's activity. (C) LC/MS analysis illustrating conversion of Evn Q to Evn S with both iPKS EvdD3 and acyltransferase EvdD1. Inactivation of either protein prevents conversion. (D) LC/MS analysis of bis-halogenation of Evn S via EvdD2. Chromatograms show summed ion intensitites for negative mode (dotted lines) and positive mode (solid lines) for Evn analogs. Everninomicin masses found in Table B-1.

Encouraged by these initial results indicating that EvdD1 interacts directly with the iPKS EvdD3 to transfer a covalently bound OSA, we sought to interrogate this interaction further. Therefore, we incubated metabolite Evn Q, acyltransferse EvdD1, and the full-length *holo*-iPKS EvdD3 with acetyl-CoA and malonyl-CoA to evaluate *in vitro* turnover. When we analyzed enzyme turnover of EvdD3 and EvdD1 via LC/MS, we observed the appearance of the Evn S peak in the chromatogram. Heat denaturation of either of the enzymes resulted in no conversion of Evn Q to Evn S, supporting our hypothesis that EvdD1 interacts directly with EvdD3 to attach OSA to Evn Q (Figure 4-3C). Of note, we could not observe the presence of free OSA *in vivo* following EvdD3 protein expression in *E. coli*, which has been observed in other iPKS systems.[41]

This result is consistent with our observation that the EvdD3 iPKS lacks a canonical thioesterase (TE) domain to catalyze the release of OSA. Additionally, no attachment of OSA to Evn Q was observed when the free acid was used *in vitro* instead of the NAC thioester. Thus, the DCIE biosynthetic pathway requires the acyltransferase EvdD1 to offload the OSA directly from the iPKS EvdD3 ACP domain and facilitate transfer to the Evn Q core (Figure 4-3A).

Halogenase EvdD2 acts as a late-stage tailoring chlorinase

We have also demonstrated *in vivo* turnover of the Evn R/S metabolites by the purified FDH EvdD2. Incubation of the EvdD2 protein, FAD, NADPH, and the oxidoreductase SsuE with semi-purified Evn S resulted in the addition of two chlorine atoms to provide everninomicin AE (Evn AE) (Figures 4-3D; B-8). These data indicate that EvdD2 acts as a tailoring halogenase only accepting the OSA substrate once it has been attached to the heptasaccharide Evn Q. However, to confirm that the true substrate for EvdD2 was not in fact the ACP-bound OSA, which has been found to be the case for chlorothricin biosynthesis, we also analyzed EvdD2 turnover with the phosphopantetheine biomimetic OSA-NAC thioester.[42] This substrate did not undergo enzymatic turnover with EvdD2, indicating that EvdD2 does not act on an ACP-bound OSA substrate. Likewise, previous evaluation of acyltransferase EvdD1 with the chemically synthesized dichloro-OSA NAC thioester and Evn Q did not yield conversion to Evn AE (Figure 4-4B). Taken together, these results confirm EvdD2 is an FDH responsible for the bis-chlorination of the orsellinic acid following its attachment to the larger everninomicin scaffold. While such tailoring halogenases are rare, they have been identified in other complex natural products containing small aromatic moieties, such as tiacumicin.[34,43]

Acyltransferase EvdD1 transfers non-natural aromatic moieties to Evn Q

Based on our previous observations that EvdD1 accepts the biomimetic *N*-acetylcysteamine

OSA in place of the ACP bound OSA, we sought to briefly explore its scope. We synthesized a small library of aromatic NAC substrates to probe the ability of EvdD1 to incorporate non-natural moieties to the Evn Q scaffold (Figures 4-4A; B-9). We initially only evaluated aromatic rings similar to OSA, such as 3- and 6-methylsalicylic acid (3MSA; 6MSA) NAC esters, or greatly simplified esters such as benzoic NAC; we were pleased to see the addition of these ring systems to the Evn Q core by EvdD1. Subsequent NAC esters were focused on replacing key substituents of the DCIE scaffold to better understand and exploit the DCIE ribosomal binding pocket in future studies. Excitingly, we were able to observe turnover for all of our chosen NAC esters following extraction of the enzymatic reaction and analysis via LC/MS (Figures 4-4B; B-10 – 14). The acyltransferase EvdD1 appears to have sufficient substrate scope to catalyze the addition of a variety of different aromatic rings to Evn Q.

In order to prioritize scale-up and purification of the novel Evn analogs with antibiotic activity, we analyzed these enzymatic reactions via bioautography.[44] The reactions were fractionated on thin layer chromatography plates subsequently overlaid with a thin layer of agar embedded with *Staphylococcus aureus*. The plates were incubated overnight and then stained with iodonitrotetrazolium (INT) to allow for visualization of zones of inhibition (Figure 4-4C). The bioautography data was coupled with the LC/MS analysis to allow for quick identification of key analogs for isolation. From these analyses, we prioritized 4-fluoro-2-methoxy-benzoic acid (AY 3.75) and 4-fluoro-2-hydroxyl-benzoic acid (AY 3.76) for scale-up reactions. Following extraction, the enzymatic turnover products were isolated using preparatory high performance liquid chromatography (HPLC). Currently, structural analysis of these novel Evn Q analogs using NMR and tandem MS to confirm their structure is ongoing. Ultimately, they will be evaluated for their antibacterial activity as compared to Evn A and Evn Q.

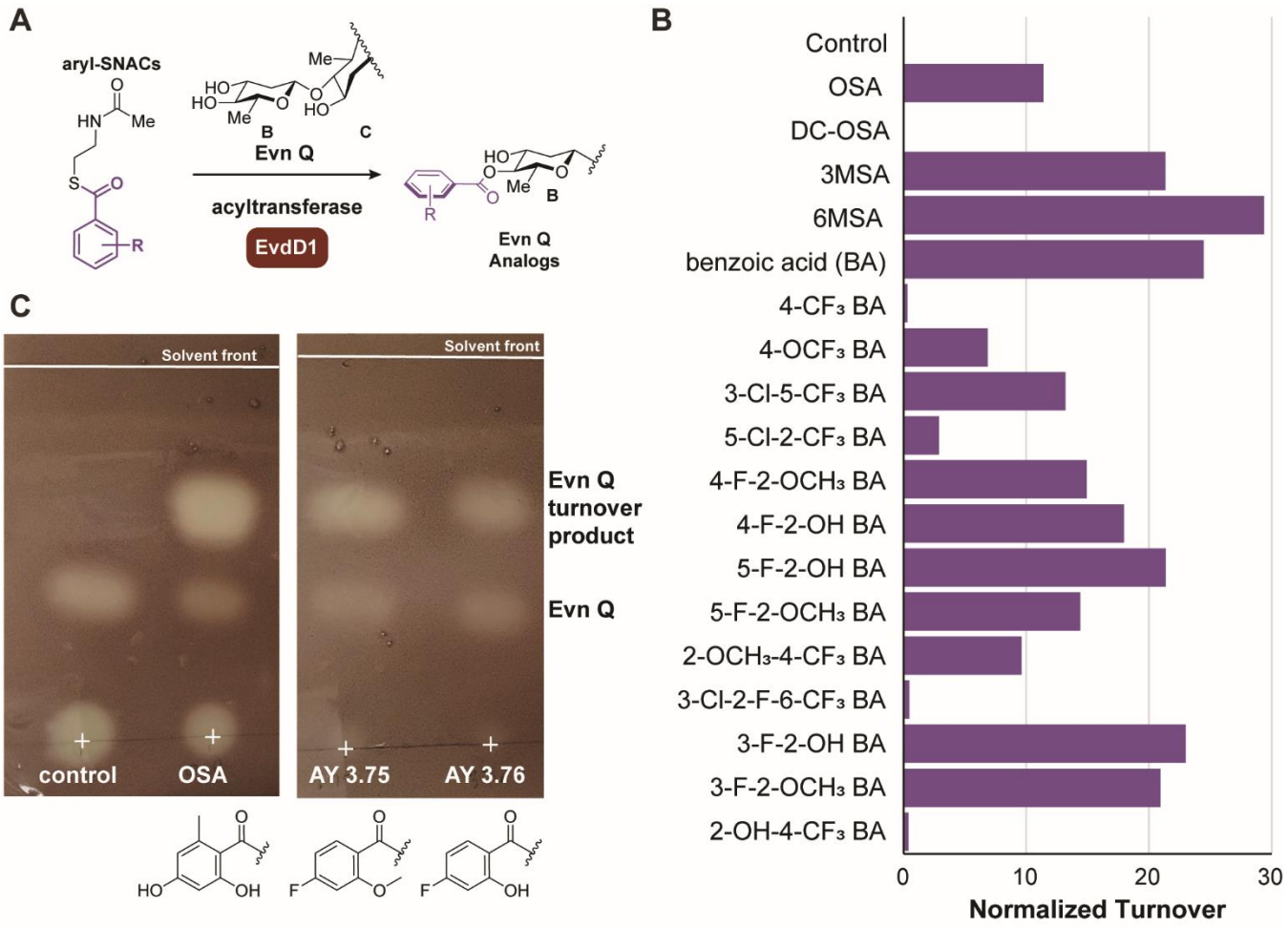

Figure 4-4. Acyltransferase EvdD1 transfers non-natural aromatic rings to Evn Qto generate novel, bioactive Evn analogs. (A) Scheme of EvdD1 transferring variable aryl-NAC groups to Evn Q. (B) Conversion rates for EvdD1 transfer for library of aryl-NACs. Areas under the curve for each extracted turnover product (negative mode) normalized to internal standard. Structures of aryl-NACs and conversion chromatograms in Figures B-9 – 14. (C) Bioautography plates demonstrating zones of inhibition for Evn Q and Evn Q turnover products. EvdD1 reactions for boiled control, OSA-NAC, AY 3.75-NAC, and AY 3.76-NAC were extracted and applied to thin layer chromatography plates. Agar embedded with *S. aureus* was overlaid and stained with INT for visualization.

We also evaluated the ability of acyltransferase EvdD1 to transfer NAC thioesters *in vivo* via chemical complementation of the mutant strain *ΔevdD3::aac(3)IV*, which lacks the iPKS EvdD3. The EvdD3 deletion strain was supplemented with NAC thioesters via pulse feeding over a ten day fermentation. Extraction of the metabolites revealed the production of wildtype Evn E for the OSA-SNAC supplemented culture (Figure B-15A). The 3-MSA and BA-NAC thioester supplemented cultures also showed incorporation of these non-natural aromatic rings into the

everninomicin scaffold (Figure B-15B). Given the inherent flexibility of EvdD1 to accept a wide variety of non-natural aromatic rings both *in vitro* and *in vivo*, we envision this protein being amenable to directed evolution to accept larger aromatic scaffolds and perhaps even aliphatic substrates as well.

Discussion

We have performed an exhaustive and comprehensive evaluation of the biosynthesis of the DCIE moeity for the orthosomycin natural product everninomicin. This fully substituted aromatic ring is found in all class I orthosomycins and plays an integral role in their novel MOA. Through functional gene analysis and biochemical assays, we can now fully annotate the DCIE biosynthetic genes and assign specific substrates for each biochemical transformation. The DCIE precursor, orsellinic acid (OSA), is synthesized by the iPKS EvdD3 from one equivalent of acetyl-CoA and three equivalents of malonyl-CoA. The ACP-bound OSA is then intercepted by the KAS III-like acyltransferase EvdD1 (Figure 4-5A). Via a covalent thioester intermediate, EvdD1 off-loads OSA from the ACP domain of EvdD3 and transfers the aromatic ring to the late-stage heptasaccharide Evn Q. The subsequent product, Evn S, is then bis-chlorinated by the FDH EvdD2, which acts as a tailoring halogenase to produce Evn AE. For the final transformation to DCIE, the SAM-dependent O-methyltransferase EvdM5 methylates the C-2 hydroxyl group to provide the fully functionalized DCIE on Evn M, a commonly observed intermediate lacking the evernitrose sugar (A-ring).[30] Full elucidation of the DCIE biosynthesis provides us with key intermediates and biocatalysts to access novel everninomicins with improved antimicrobial activity. Additionally, this work also insinuates a larger biochemical mechanism for the off-loading of iPKS proteins that lack a canonical thioesterase (TE) domain

Initially, iterative type I PKS systems were thought to exist only in fungal systems while their

non-iterative counterparts were relegated to bacteria. However, subsequent discovery of the iPKS AviM in the avilamycin pathway led to the detection of these enzymes for a large number of secondary metabolites such as calicheamicin, chlorothricin, pactamycin, tiacumicin, and others. These bacterial iPKS systems often lack the canonical thioesterase (TE) domain responsible for the release of the completed PKS product. As such, the mechanism of their release from the ACP domain was not clear. Previous work in the pactamycin and chlorothricin pathways revealed variable methods for release of products from iPKS systems. In pactamycin, a direct off-loading mechanism from the iPKS by a KAS III homolog, PtmR, to form the ester bond on the natural product scaffold was shown via genetic deletion and use of biomimetic NAC-thioesters. These data indicate that PtmR interacts directly with the iPKS PtmQ, but this was not directly observed *in vitro*. Conversely, the chlorothricin pathway has been shown to progress via a “ping pong-like” mechanism utilizing a discrete *trans* ACP domain following transfer of the aryl iPKS product, 6-methylsalicyclic acid. The two discrete acyltransferase proteins, ChlB3 and ChlB6, are responsible for transfer to and from the free-standing ACP domain.[40] While homologous PKS/KAS III systems have been found in the tiacumicin, calicheamicin, avilamycin, clorobiocin, and esmeraldin biosynthetic pathways, none of them have been fully studied nor characterized. We have been able to demonstrate the direct protein-protein interaction between the iPKS EvdD3 and the KAS III-like acyltransferase EvdD1 to off-load the OSA and transfer it to the larger natural product scaffold, indicating that this may be a common mechanism for this class of polyketide synthases.

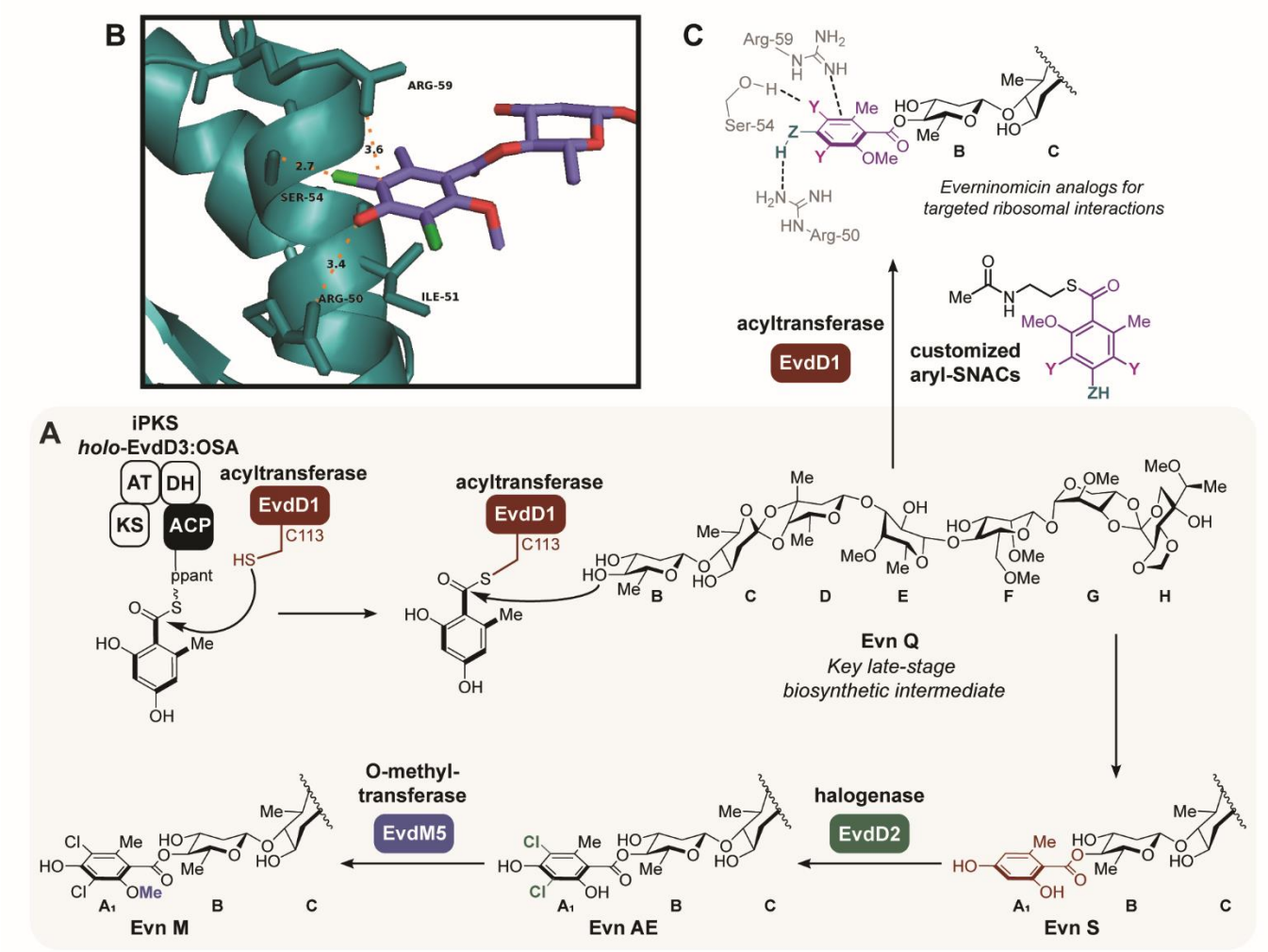

Figure 4-5. Elucidating the DCIE biosynthetic pathway to access novel analogs. (A) Wildtype biosynthesis of orsellinic acid (OSA) by iPKS EvdD3 followed by transfer of OSA via acyltransferase EvdD1 to Evn Q. Subsequent bis-halogenation and O-methylation by EvdD2 and EvdM5 to produce DCIE (tan box). (B) Crystal structure showing key interactions between avilamycin and ribosomal protein uL16. (C) Structure of key positions on the DCIE ring that can be investigated using acyltransferase EvdD1 to introduce non-natural aromatic rings to EvnQ.

In the completion of this work, we have also demonstrated that the acyltransferase EvdD1 is a valuable biocatalyst for accessing novel everninomicin analogs. With our ultimate goal of revitalizing the everninomicins as clinical candidates, access to the late-stage intermediate Evn Q and acyltransferase EvdD1 provides the tools necessary for everninomicin derivatization. In particular, we have shown that EvdD1 will transfer non-natural aromatic rings to Evn Q to produce everninomicins with atom-specific modulations at the DCIE ring. DCIE plays a key role in the novel mechanism of protein synthesis inhibition and antibacterial activity of the

everninomicins. We hypothesize that the Evn Q analogs produced here will bind to the ribosome similarly to avilamycin since they lack the evernitrose sugar. By analyzing the avilamycin-ribosome structures, we attempted to focus our NAC thioester library on compounds that could ask specific questions about the DCIE ribosomal binding pocket. For example, the C-4 hydroxyl group of DCIE forms a hydrogen bond with protein uL16 residue Arg50 (Figure 4-5B). Therefore, we replaced this hydroxyl, a metabolic liability, with bioisoteres such as fluorine and a trifluoromethyl group to maintain the H-bond interaction.[45] We also sought in investigate the dipole interaction between the chlorine at C-5 and the uL16 residue Ser54. A substitution of the more electronegative fluorine at this position may strengthen this dipole interaction. However, it is possible that fluorine may too drastically alter the electrostatics of the ring itself and disrupt the cation-π interactions with uL16 residue Arg59. Therefore, by making direct, specific changes to the ring system, we will determine how these interactions are altered via changes in bioactivity. We now have the ability to make targeted changes to the orthosomycins structure. This provides a pathway for revitalization of this powerful and potent class of molecules.

Material and Methods

General bacterial culture conditions

M. carbonacea var. *aurantiaca* wild-type and mutant strains were grown on TSB agar [Oxoid Tryptone Soy Broth; 2% (wt/vol) agar]. Germination medium was used for *M. carbonacea* var. *aurantiaca* seed cultures [0.3% beef extract, 0.5% tryptose, 0.1% dextrose, 2.4% soluble starch, 0.5% yeast extract, 0.1% calcium carbonate]. For production of everninomicin metabolites, *M. carbonacea* var. *aurantiaca* was grown in production medium [0.5% yeast extract, 0.1% corn steep solids, 0.1% calcium carbonate, 3% glucose, no antibiotic]. *E. coli* strains were grown in LB media. All *E. coli* electrocompetent strains were prepared in L broth [10 g/L tryptone, 5 g/L

yeast extract, 5 g/L NaCl]. Intergeneric conjugations utilized ASI plates [0.1% yeast extract, 0.5% soluble starch, 0.02% L-alanine, 0,02% L-arginine, 0.05% L-asparagine, 0.25% NaCl, 1% Na_2SO_4, 2% (wt/vol) agar at pH 7.5, supplemented with 10 mM $MgCl_2$]. Antibiotics were used as described below for selection: apramycin (50 µg/mL), kanamycin (50 µg/mL), and chloroamphenicol (30 µg/mL).

Gene-replacement method in E.coli

DCIE-associated genes were deleted individually from a cosmid containing the evd biosynthetic cluster using the PCR-targeted gene replacement strategy.[29] The apramycin-resistance cassette (*aac(3)IV)* was isolated from plasmid pIJ773 following digestion with Hind III and EcoR1. This cassette was amplified via PCR using the appropriate primers for each respective gene (primer sequences Table B-2). The amplified PCR product was then incubated with L-arabinose-induced BW25113/pIJ790 electrocompetent cells for forty minutes before transformation via electroporation to allow for lambda red-mediated homologous recombination. The transformed *E. coli* were plated on LB containing apramycin and incubated overnight at 30 °C. Individual colonies were inoculated into 5 mL LB containing apramycin and kanamycin to grow overnight at 30 °C with shaking. The resultant mutant cosmid was isolated and gene deletion was confirmed via sequencing and PCR. The disrupted cosmid was then transformed via electroporation into the non-methylating conjugation *E. coli* strain ET12567/ pUZ8002 and grown at 37 °C on LB agar containing kanamycin, apramycin, and chroramphenicol. Transformants were subsequently confirmed via enzymatic digestion.

Gene-replacement method in M. carbonacea var. aurantiaca

M. carbonacea var. *aurantiaca* ATCC 2997 was grown from a glycerol stock on TSB agar for 5 days at 30 °C. Mycelia were inoculated into 10 mL of TSB medium with shaking at 30 °C

for 5 days. The culture was centrifuged at 3000 x g for 10 min. The resultant pellet was resuspended in 2 mL of fresh TSB and 150 µL aliquots transferred to sterile 1.5-mL Eppendorf tubes. The donor ET12567/pUZ8002 *E. coli* were prepared by inoculating 1% of an overnight culture into 10 mL LB medium containing kanamycin and apramycin. The culture was grown at 37 °C with shaking to an OD_{600} = 0.4. The cells were recovered via centrifugation at 3000 x g for 10 minutes. The resultant pellet was washed three times with 10 mL fresh LB medium. Following the final wash, the pellet was resuspended in 150 µL of LB medium and 50 µL aliquots transferred to the Eppendorf tubes containing *M. carbonacea* var. *aurantiaca*. The donor and recipient bacteria were mixed, homogenized, and then distributed onto conjugation membrane filters (0.4 µm pores, HTTP polycarbonate, Isopore) assembled with washers on AS1 solid media. Plates were dried and then incubated overnight at 30 °C. The following day, apramycin was added to the membrane-washer assembly to give a final concentration of 35 µg/mL, plates were dried again before incubation. After 10 days of incubation at 30 °C, the conjugation lagoons were removed and any nascent colonies allowed to incubate a further 5 days at 30 °C. Potential double-crossover mutants were identified by restreaking colonies to test for apramycin resistance and kanamycin sensitivity on solid TSB medium. Mutants were also evaluated via PCR using primers Del-Up and Del-Dn for apramycin cassette insertion and primers Neo_SuperCos_For and Neo_SuperCos_Rev for kanamycin sensitivity (primer sequences Table B-2).

Production & extraction of everninomicin metabolites

M. carbonacea var. *aurantiaca* wild-type and mutant strains were grown from glycerol stocks on TSB agar for 5 days at 30 °C. A loopful of mycelia were inoculated into 10 mL of TSB medium with shaking at 30 °C for 5 days. Seed cultures were generated by inoculating 1 mL of mycelia from TSB media into 100 mL of germination medium in a 500 mL Erlenmeyer flask. Cultures

were incubated for 5 days at 30 °C with shaking. Following germination, 25 mL of the seed culture was inoculated into 500 mL of production medium in a 2 L baffled Fernbach flask. Cultures were incubated for 10 days at 30 °C with shaking. For extraction, Diaion HP-20 resin (125 mL, activated with methanol and washed with water) was added to production cultures and incubated with shaking for at least 1 hour. The resin and mycelia were collected via centrifugation and sequentially extracted with methanol and acetone. All extracts were evaporated to dryness by rotary evaporation. The crude extract was resuspended in a minimal amount of 90:10 methylene chloride:methanol and applied to silica gel (15 g) packed into a fritted glass funnel via vacuum filtration. Metabolites were eluted from silica using increasing amounts of methanol. Solution was concentrated to dryness.

HPLC/MS analysis of everninomicin metabolites

All extracts were analyzed in negative- and positive-ion modes using a TSQ Quantum Access Max triple stage quadrupole mass spectrometer (Thermo Scientific) equipped with a HESI-II electrospray ionization source. For analysis of whole extracts from wildtype and genetic deletion strains, injections (20 µL) were separated on a Luna C18(2) column (250 x 4.6 mm; Phenomenex) using an Accela Pump (Thermo Scientific). A 50 minute gradient was utilized with conditions as follows: 0-1 min, 100% (A); 1-30 min, linear gradient to 100% (B); 30-45 min, 100% (B); 45-47 min, linear gradient to 100% (A); and 47-50 min, 100% (A). For all runs, a consistent flow rate was maintained at 1 mL/min with 75 µL diverted to Accela PDA detector (Thermo Scientific) and 25 µL subjected to mass spectral analysis. The auxiliary and sheath gases were both set as nitrogen and set to 8 and 40 psi, respectively. Positive-ion mode values were as follows: capillary temperature, 350 °C; spray voltage, 4.2 kV; capillary offset, 35 V; tube lens voltage, -176 V; and no skimmer offset. Negative-ion mode values were as follows: capillary temperature, 350 °C; spray voltage, 4.2 kV; capillary offset, -35 V; tube lens voltage, 174 V; and

no skimmer offset. The structures of Evn Q, R, and S were confirmed using collision energies of 20 V – 30 V with a skimmer offset of 5 V in positive mode to fragment these metabolites.

Purification of everninomicin metabolites Evn R/S

The silica-purified extract was further purified via gravity size-exclusionary chromatography using Sephadex LH-20 resin in methanol. Fractions were analyzed via LC/MS and combined based on the presence of Evn R/S. These metabolites were further purified via preparative reverse phase HPLC with mobile phases 95% water/5% acetonitrile (vol/vol) with 10 mM ammonium acetate (A) and 5% water/95% acetonitrile (vol/vol) with 10 mM ammonium acetate (B). Injections of 0.5 mL were separated on an Xbridge Prep C18 (25 x 19 mm: Waters). A 25 minutes method at 10 mL/min was used with conditions as follows: 0-1 min, 100% (A); 1-5 min, linear gradient to 45% (A):55% (B); 5-8 min, isocratic 45% (A):55% (B); 8-17 min, linear gradient to 100% (B); 17-22 min, 100% (B); 22-23 min, linear gradient to 100% (A); and 23-25 min, 100% (A). Fractions were analyzed via LC/MS and combined based on the presence of Evn R/S.

Purification of everninomicin metabolite Evn Q

The seen and germination cultures were cultivated as described above for *ΔevdD3* cultures. Following inoculation into fermentation, the *ΔevdD3* cultures were grown for 6 days, as this was found to be optimal for Evn Q production. The mycelia were removed via centrifugation and discarded. The broth was then extracted with 90% methylene chloride/10% methanol (vol/vol) three times. The organic layers were dried over sodium sulfate and reduced under reduced pressure. This yielded a clean extract that was directly purified via preparative reverse phase HPLC with mobile phases 95% water/5% acetonitrile (vol/vol) (A) and 5% water/95% acetonitrile (vol/vol) (B). Injections of 0.5 mL were separated on an Xbridge Prep C18 (25 x 19 mm: Waters. A 25 minutes method at 10 mL/min was used with conditions as follows: 0-1 min, 100% (A); 1-

10 min, linear gradient to 35% (A):65% (B); 11-15 min, isocratic 35% (A):65% (B); 15-20 min, linear gradient to 100% (B); 20-22 min, 100% (B); 22-23 min, linear gradient to 100% (A); and 23-25 min, 100% (A). Final purification was preformed via gravity size-exclusionary chromatography using Sephadex LH-20 resin in methanol. Fractions were analyzed via LC/MS and TLC and combined based on the presence of Evn Q.

Cloning of OSA-associated enzymes

The gene *evdD2* was amplified from the CA cosmid containing the evd biosynthetic gene cluster by PCR amplification using appropriately designed primers containing NdeI and HindIII restriction sites (primer sequences Table B-2). This fragment was directly cloned into a TOPO vector (Thermo Fisher) and transformed into *E. coli* Top10 electrocompetent cells. Transformants were plated onto LB plates containing kanamycin and 5-bromo-4-chloro-3-indolyl-β-D-galactopyranoside (X-gal) for blue and white screening. Plates were incubated overnight at 37 °C. White colonies were inoculated into LB containing kanamycin and grown overnight at 37 °C with shaking. The gene was then subcloned into the expression vector pET28a(+) using DNA ligase following digestion with the appropriate restriction enzymes. The NAD(P)H:flavin oxidoreductase SsuE was cloned and expressed as previously described for biochemical analysis of halogenase EvdD2.[42]

The gene *evdD1* was amplified from the CA cosmid using primers designed for Gibson assembly (primer sequences Table B-2). This PCR fragment was directly cloned into pET28a(+) vector digested with NcoI and HindIII using the Gibson Assembly Cloning Kit (NEB). Clones were transformed into provided chemically competent cells and plated onto LB plates containing kanamycin and grown overnight at 37 °C. Transformants were confirmed via restriction digest and sequencing. Site-directed mutagenesis of AT EvdD1 was completed using the QuickChange II XL Kit (Agilent). PCR primers were designed for C113A, C113S, and H293A mutations as

outlined by Agilent (primer sequences Table B-2). Following PCR amplification, mutants were transformed into provided XL10-Gold chemically competent cells and plated on LB plates with kanamycin. Mutants were confirmed via sequencing.

The gene encoding EvdD3 was optimized for *E. coli* expression and synthesized into pMK-RQ-Bb (Invitrogen Thermo Fisher). The optimized *evdD3* gene was cloned directly into pET28a(+) using DNA ligase following digestion of both vectors with NdeI and EcoRI. Clones were transformed into electrocompetent cells and plated onto LB plates containing kanamycin and grown overnight at 37 °C. Transformants were confirmed via restriction digest and sequencing. The phosphopantetheinyl transferase Sfp already cloned into pET28a(+) was generously donated by G. J. Williams (NC State University). For co-expression with EvdD3, *sfp* was subsequently subcloned into the pCDFDuet-1 vector (Novagen) using restriction sites NdeI and XhoI. Transformation and confirmation were performed as described above.

Overproduction and purification of OSA-associated enzymes

The resulting vectors were transformed into *E. coli* BL21 (DE3) for EvdD2 or *E. coli* Tuner (DE3) for EvdD3/sfp and EvdD1 expression. Cultures were grown to OD_{600} = 0.6 at 37 °C in LB broth with kanamycin. Cultures were cooled on ice for 20 minutes followed by induction with 1 mM IPTG (BL-21) or 0.1 mM IPTG (Tuner). Cultures were allowed to shake overnight for approximately 16 hours at 16 °C. Cells were harvested via centrifugation at 3,000 X g for 30 minutes at 4 °C. Pellets were suspended in 60 mL of lysis buffer A (50 mM Tris, 300 mM NaCl, 5 mM imidazole; pH 7.4) with 30 µL DNAse. The sample was lysed via passage through a French Press (x 2). Crude lysate was clarified by centrifugation at 75,000 g for 45 minutes. The supernatant was loaded onto a 5 mL HisTrap FF Crude nickel affinity column (GE Healthcare Life Sciences) and eluted on AKTA fast protein liquid chromatography (FPLC) system using buffer B (500 mM Tris, 300 mM NaCl, 500 mM imidazole; pH 7.4). Based on the UV trace from

the FPLC, the relevant fractions were combined and concentrated to approximately 1 mL using Amicon® Ultra Centrifugal Filters with the appropriate size filter. Concentrated fractions were then desalted and solvent exchanged into protein storage buffer (1% glycerol, 1 mM DTT, 20 mM Tris, pH 8.0) using a 5 mL HiTrap Desalting column (GE Healthcare Life Sciences). Protein aliquots were flash frozen in ethanol and CO_2 (s) and stored at -80 °C.

Enzymatic Turnover Conditions for EvdD2, EvdD1, & EvdD3

The FDH EvdD2 reactions were carried out in 50 mM Tris (pH 7.8) with 100 mM NaCl. A final concentration of 10 uM EvdD2 with 500 μM of HPLC purified Evn S, 5 mM NADH, and 100 μM FAD was incubated at 30 °C for 16 hours. The oxidoreductase SsuE was supplied at a final concentration of 5 μM along with a mixture of 1 U/mL of catalase and superoxide dismutase. Reactions were quenched with an equal volume of methanol to precipitate the protein, which was removed via centrifugation. A boiled enzyme control was included for analysis. The reaction was analyzed via TSQ Quantum Access Max triple stage quadrupole mass spectrometer with instrument parameters described above except a Kinetex C18 (150 x 4.6mm; Phenomenex) column was used. A 12 minute gradient was used with conditions as follows: 0-1 min, 100% (A); 1-2 min, linear gradient to 45% (A):55% (B); 2-10 min, linear gradient to 100% (B); 10-11 min, linear gradient to 100% (A); and 11-12 min, 100% (A). Mobile phases were 95% water/5% acetonitrile (vol/vol) with 10 mM ammonium acetate (A) and 5% water/95% acetonitrile (vol/vol) with 10 mM ammonium acetate (B).

The reactions to investigate the interactions between AT EvdD1 and iPKS EvdD3 were completed in 50 mM HEPES (pH 7.5) with 10 mM $MgCl_2$ at total volume of 50 uL. The final concentrations of *holo*-EvdD3, additional Sfp, and EvdD1 were 25 uM, 5 uM, and 10 uM, respectively. Semi-purified Evn Q was at a concentration of 20 mg/mL. The final concentration of acetyl-CoA was 250 uM and malonyl-CoA was 750 uM. Reactions were incubated for 16 hours

at 30 °C then quenched with an equal volume of methanol to remove the protein. Three boiled enzyme controls were included for each enzyme individually and for both enzymes. LC/MS analysis was completed as described above with a 20 minute gradient as follows: 0-1 min, 100% (A); 1-15 min, linear gradient to 100% (B); 15-17 min, 100% (B); 17-19 min, linear gradient to 100% (A); and 19-20 min, 100% (A).

The analysis of the WT and mutant EvdD1 enzymes using OSA-SNAC were carried out in 10 mM sodium phosphate buffer (pH 7.4) with 10 mM $MgCl_2$. A semi-crude Evn Q extract was supplied at 20 mg/mL with the OSA-SNAC at 2 mM and the purified EvdD1 enzymes at a final concentration of 10 mM. Reactions were incubated for 16 hours at 30 °C then quenched with an equal volume of methanol to remove the protein. A boiled enzyme control was included for each EvdD1 variant. LC/MS analysis was completed as described above with a 12 minute gradient with conditions as follows: 0-1 min, 100% (A); 1-8 min, linear gradient to 100% (B); 8-10 min, 100% (B); 10-11 min, linear gradient to 100% (A); and 11-12 min, 100% (A).

The AT EvdD1 reactions with the NAC-thioester library were carried out in 50 mM HEPES (pH 7.5) with 5 mM $MgCl_2$ at total volume of 50 uL. Fully purified Evn Q was at a final concentration of 5 mM with AT EvdD1 at 15 mM. The NAC-thioesters in DMSO were at a final concentration of 10 mM each. These reactions were incubated at 30 °C for 2 hours then quenched with an equal volume of methanol to precipitate the protein. Following centrifugation to remove the protein, the reactions were extracted with ethyl acetate (x 3). The organic layer was removed under reduced pressure and further analysed via LC/MS, as described above, or bioautography. For the scale-up reactions, these equivalents were scaled up to 1 mL total reaction.

Antibacterial analysis via bioautography

A laboratory strain of *Staphylococcus aureus* was inoculated into 5 mL of MH-2 broth and allowed to incubate overnight with shaking at 30 °C. The following day, the overnight culture was

diluted with fresh MH-2 broth to OD_{600} = 0.09. This diluted culture was used to make a 1% inoculum into MH-2 agar maintained at 45 °C. The conditions for the EvdD1 enzymatic conversion are described above. The extracted reaction was resuspended into 15 uL Optima methanol and spotted on to Milllipore silica coated glass plates (60F-254). The mixture was eluted in 90:10 ethyl acetate:methanol in a TLC chamber. A thin layer of the MH-2 agar with *S. aureus* was applied to the plates (~1 mm thick). Once set, the plates were incubated overnight at 30 °C. For visualization, the plates were flooded with a 3 mg/mL solution of iodonitrotetrazolium (INT) in 80:20 water:ethanol.

Synthesis of 2,4-dihydroxy-6-methylbenzaldehyde

To a solution of $POCl_3$ (32.22 mmol, 2 eq) in dry DMF (80 mL) at 0 °C was slowly added a solution of 3,5-dihydroxyltoluene (16.11 mmol, 1 eq) in dry DMF (54 mL). Reaction was allowed to slowly come to room temperature overnight with stirring. Reaction was cooled to 0 °C and cautiously treated with ice water (100 mL), then with 10% aqueous NaOH to pH = 10. This solution was acidified to pH = 3 with concentrated HCl. The solution was extracted with ethyl acetate (x 3). The combined organic layers were washed with acidic brine (x 3), dried over Na_2SO_4, filtered, and concentrated under reduced pressure. The three resulting products were not purified further, rather all three were continued through the following oxidation reaction.

General synthetic experimental procedures

N-acetylcysteamine derivatives for *in vitro* studies were synthesized from materials purchased from Sigma-Aldrich, Acros Organic, or Oakwood Chemical and were used without further purification. All reactions were performed using oven dried glassware under argon atmosphere with anhydrous solvents, unless otherwise noted. Reactions were monitored by thin-layer chromatography using Milllipore silica coated glass plates (60F-254) using UV light as a

visualizing agent and ceric ammonium molybdate for development. Sorbetech silica gel (60, particle size 40-63 μm) was used for flash column chromatography.

Synthesis of 2,4-dihydroxy-6-methylbenzoic acid, orsellinic acid (OSA)

To a solution of mixture of products from the previous reaction (9.46 mmol, 1 eq) was dissolved in DMSO (31 mL) and cooled to 0 °C. To this solution, NaH_2PO_4 (23.6 mmol, 2.5 eq) in water (7 mL) at was slowly added followed by a solution of $NaClO_2$ (23.6 mmol, 2.5 eq) in water (8 mL). This solution was allowed to come to room temperature overnight with stirring. The reaction was quenched with saturated aqueous Na_2CO_3. This mixture was extracted with ethyl acetate (20 mL x 1). The aqueous phase was acidified to pH = 1 with concentrated HCl and extracted with ethyl acetate (75 mL x 3). The combined organic layers were washed with acidic brine (x 3), dried over Na_2SO_4, filtered, and concentrated under reduced pressure. Flash column chromatography (silica gel, 25 to 50% ethyl acetate in hexanes) to afford OSA in 38% yield over two steps. Conversely, OSA could also be isolated by dissolving the crude mixture in ethyl acetate followed by washing with aqueous $NaHCO_3$ pH = 8 (x 3). The aqueous layer was then acidified to pH = 2 with 1 M HCl and extracted with fresh ethyl acetate (x 3). The combined organic layers were washed with acidic water (x 3), dried over Na_2SO_4, filtered, and concentrated under reduced pressure. ^{1}H NMR (400 MHz, CD_3OD); δ = 6.18 (d, 1H), 6.13 (d, 1H), 2.48 (s, 3H). ^{13}C NMR (400 MHz, CD_3OD); δ = 173.56, 165.47, 162.22, 143.81, 110.79, 100.09, 22.83.

Synthesis of 3-chloro-4,6-dihydroxy-2-methylbenzoic acid, dichloro-orsellinic acid (DC-OSA)

2,4-dihydroxy-6-methylbenzaldehyde (6.57 mmol, 1.0 eq.) was dissolved in THF (15 mL) and cooled to 0°C. NH_2SO_3H (32.85 mmol, 5.0 eq.) was dissolved in H_2O (15 mL), added to the DMSO reaction mixture, and allowed to stir for 10 minutes. $NaClO_2$ (13.14 mmol, 2.0 eq.) was dissolved in H_2O (15.0 mL) and added to the DMSO:H_2O reaction. This reaction was allowed to

come to room temperature overnight and quenched with saturated aqueous NH_4Cl. The resultant precipitate was removed by vacuum filtration. The flow-thru was extracted with ethyl acetate (25 mL x 3). The combined organic layers were washed with acidic brine (x 3), dried over Na_2SO_4, filtered, and concentrated under reduced pressure. The crude product was purified by dissolving the product in basic water (pH 8-9), washing with ethyl acetate, then acidifying the solution to pH 1, and extracting with fresh ethyl acetate to yield the acid as a yellow powder (0.749 g, 56%). 1H NMR (400 MHz, MeOD) δ 6.34 (s, 1H), 2.64 (s, 3H).

Synthesis of N-acetylcysteamine (SNAC)

Cysteamine-HCl (8.8 mmol, 1.0 eq.), $NaHCO_3$ (26.4 mmol, 3 eq.) and KOH (8.8 mmol, 1.0 eq.) were dissolved in H_2O (44 mL). Freshly distilled acetic anhydride (8.8 mmol, 1.0 eq.) was then added and the reaction was stirred at room temperature for 2 hours. The reaction was then brought to pH 4 with concentrated HCl and extracted with ethyl acetate. The combined organic layers were dried over Na_2SO_4, filtered, and concentrated under reduced pressure. Directly prior to use, the SNAC was separated from the disulfide oxidized side-product via column chromatography (95:5 DCM/MeOH). ^{1}H NMR (400 MHz, $CDCl_3$) δ 5.913 (bs, 1H), 3.427 (q, J = 6.2 Hz, 2H), 2.642 (q, J = 6.4 Hz, 2H), 2.00 (s, 3H), 1.347 (t, J = 8.4 Hz, 1H).

General procedure for synthesis of N-acetylcysteamine thioesters

2,4-dihydroxy-6-methylbenzoic acid (0.494 mmol, 1.0 eq.) and HOBt (0.592 mmol, 1.2 eq.) were dissolved in THF (6 mL) and allowed to stir for 10 minutes. DCC (0.592 mmol, 1.2 eq.) in THF (2 mL) was then added followed by SNAC (0.987 mmol, 2 eq.) and the reaction mixture was allowed to stir for 1 hour. K_2CO_3 (0.494 mmol, 1 eq.) was added and the reaction was allowed to stir overnight. The reaction was then filtered and concentrated. The residue was dissolved in ethyl acetate, washed with $NaHCO_3$, and H_2O. The combined organic layers were

dried over Na_2SO_4, filtered, and concentrated under reduced pressure. Pure product was obtained through column chromatography (95:5 DCM/MeOH). All NAC thioesters were synthesized using the above procedure. See Appendix B for NMRs of all NAC thioesters.

Acknowledgements

The authors would like to acknowledge support from the National Institutes of Health (no. R01GM092218 awarded to B.O.B. and T32 GM065086-13 awarded to A.E.Y). A.E.Y. received additional funding from the NSF GRFP under Grant No. 1445197.

References

1. Ganguly, A. K.; Sarre, O. Z.; Greeves, D.; Morton, J. Structure of everninomicin d. *Journal of the American Chemical Society* **1975**, *97*, 1982-1985.
2. Ganguly, A. K. Ziracin, a novel oligosaccharide antibiotic. *J Antibiot* **2000**, *53*, 1038-1044.
3. Wright, D. E. The orthosomycins, a new family of antibiotics. *Tetrahedron* **1979**, *35*, 1207-1237.
4. McCranie, E. K.; Bachmann, B. O. Bioactive oligosaccharide natural products. *Natural Product Reports* **2014**, *31*, 1026-1042.
5. Jones, R. N.; Barrett, M. S. Antimicrobial activity of sch 27899, oligosaccharide member of the everninomycin class with a wide gram-positive spectrum. *Clinical Microbiology and Infection* **1995**, *1*, 35-43.
6. Foster, D. R.; Rybak, M. J. Pharmacologic and bacteriologic properties of sch-27899 (ziracin), an investigational antibiotic from the everninomicin family. *Pharmacotherapy: The Journal of Human Pharmacology and Drug Therapy* **1999**, *19*, 1111-1117.
7. Ganguly, A. K. Challenges in drug discovery at schering-plough research institute: A personal reflection. *Annu. Rep. Med. Chem.* **2013**, *48*, 3-14.
8. U.S. Department of Health and Human Services, C. Antibiotic resistance threats in the united states, 2019. **2019**.
9. Yñigez-Gutierrez, A. E.; Bachmann, B. O. Fixing the unfixable: The art of optimizing natural products for human medicine. *Journal of Medicinal Chemistry* **2019**.

10. Adrian, P. V.; Mendrick, C.; Loebenberg, D.; McNicholas, P.; Shaw, K. J.; Klugman, K. P.; Hare, R. S.; Black, T. A. Evernimicin (sch27899) inhibits a novel ribosome target site: Analysis of 23s ribosomal DNA mutants. *Antimicrobial Agents and Chemotherapy* **2000**, *44*, 3101-3106.

11. McNicholas, P. M.; Najarian, D. J.; Mann, P. A.; Hesk, D.; Hare, R. S.; Shaw, K. J.; Black, T. A. Evernimicin binds exclusively to the 50s ribosomal subunit and inhibits translation in cell-free systems derived from both gram-positive and gram-negative bacteria. *Antimicrobial Agents and Chemotherapy* **2000**, *44*, 1121-1126.

12. Belova, L.; Tenson, T.; Xiong, L.; McNicholas, P. M.; Mankin, A. S. A novel site of antibiotic action in the ribosome: Interaction of evernimicin with the large ribosomal subunit. *Proc Natl Acad Sci U S A* **2001**, *98*, 3726-3731.

13. Mikolajka, A.; Liu, H.; Chen, Y.; Starosta, A. L.; Marquez, V.; Ivanova, M.; Cooperman, B. S.; Wilson, D. N. Differential effects of thiopeptide and orthosomycin antibiotics on translational gtpases. *Chemistry & Biology* **2011**, *18*, 589-600.

14. Arenz, S.; Juette, M. F.; Graf, M.; Nguyen, F.; Huter, P.; Polikanov, Y. S.; Blanchard, S. C.; Wilson, D. N. Structures of the orthosomycin antibiotics avilamycin and evernimicin in complex with the bacterial 70s ribosome. *Proceedings of the National Academy of Sciences* **2016**, *113*, 7527-7532.

15. Krupkin, M.; Wekselman, I.; Matzov, D.; Eyal, Z.; Diskin Posner, Y.; Rozenberg, H.; Zimmerman, E.; Bashan, A.; Yonath, A. Avilamycin and evernimicin induce structural changes in rproteins ul16 and ctc that enhance the inhibition of a-site trna binding. *Proceedings of the National Academy of Sciences* **2016**, *113*, E6796-E6805.

16. Wilson, D. N. Ribosome-targeting antibiotics and mechanisms of bacterial resistance. *Nature Reviews Microbiology* **2014**, *12*, 35-48.

17. Nicolaou, K. C.; Mitchell, H. J.; Suzuki, H.; Rodríguez, R. M.; Baudoin, O.; Fylaktakidou, K. C. Total synthesis of everninomicin 13,384-1—part 1: Synthesis of the a1b(a)c fragment. *Angewandte Chemie International Edition* **1999**, *38*, 3334-3339.

18. Nicolaou, K. C.; Rodríguez, R. M.; Fylaktakidou, K. C.; Suzuki, H.; Mitchell, H. J. Total synthesis of everninomicin 13,384-1—part 2: Synthesis of the fgha2 fragment. *Angewandte Chemie International Edition* **1999**, *38*, 3340-3345.

19. Nicolaou, K. C.; Rodríguez, R. M.; Mitchell, H. J.; van Delft, F. L. Stereocontrolled synthesis of the everninomicin a1b(a)c ring framework. *Angewandte Chemie International Edition* **1998**, *37*, 1874-1876.

20. Nicolaou, K. C.; Fylaktakidou, K. C.; Mitchell, H. J.; van Delft, F. L.; Rodríguez, R. M.; Conley, S. R.; Jin, Z. Total synthesis of everninomicin 13,384-1—part 4: Explorations of methodology; stereocontrolled synthesis of 1,1′-disaccharides, 1,2-seleno migrations in carbohydrates, and solution- and solid-phase synthesis of 2-deoxy glycosides and orthoesters. *Chemistry – A European Journal* **2000**, *6*, 3166-3185.

21. Nicolaou, K. C.; Mitchell, H. J.; Fylaktakidou, K. C.; Rodríguez, R. M.; Suzuki, H. Total synthesis of everninomicin 13,384-1—part 2: Synthesis of the fgha2 fragment. *Chemistry – A European Journal* **2000**, *6*, 3116-3148.

22. Nicolaou, K. C.; Mitchell, H. J.; Rodríguez, R. M.; Fylaktakidou, K. C.; Suzuki, H.; Conley, S. R. Total synthesis of everninomicin 13,384-1—part 3: Synthesis of the de fragment and completion of the total synthesis. *Chemistry – A European Journal* **2000**, *6*, 3149-3165.

23. Nicolaou, K. C.; Rodríguez, R. M.; Mitchell, H. J.; Suzuki, H.; Fylaktakidou, K. C.; Baudoin, O.; van Delft, F. L. Total synthesis of everninomicin 13,384-1—part 1: Retrosynthetic analysis and synthesis of the a1b(a)c fragment. *Chemistry – A European Journal* **2000**, *6*, 3095-3115.

24. Vey, J. L.; Al-Mestarihi, A.; Hu, Y.; Funk, M. A.; Bachmann, B. O.; Iverson, T. M. Structure and mechanism of orf36, an amino sugar oxidizing enzyme in everninomicin biosynthesis. *Biochemistry* **2010**, *49*, 9306-9317.

25. McCulloch, K. M.; McCranie, E. K.; Smith, J. A.; Sarwar, M.; Mathieu, J. L.; Gitschlag, B. L.; Du, Y.; Bachmann, B. O.; Iverson, T. M. Oxidative cyclizations in orthosomycin biosynthesis expand the known chemistry of an oxygenase superfamily. *Proc Natl Acad Sci U S A* **2015**, *112*, 11547-11552.

26. Limbrick, E. M.; Ynigez-Gutierrez, A. E.; Dulin, C. C.; Derewacz, D. K.; Spraggins, J. M.; McCulloch, K. M.; Iverson, T. M.; Bachmann, B. O. Methyltransferase contingencies in the pathway of everninomicin d antibiotics and analogues. *Chembiochem* **2020**, *21*, 3349-3358.

27. Gaisser, S.; Trefzer, A.; Stockert, S.; Kirschning, A.; Bechthold, A. Cloning of an avilamycin biosynthetic gene cluster from streptomyces viridochromogenes tü57. *Journal of Bacteriology* **1997**, *179*, 6271-6278.

28. Gust, B.; Chandra, G.; Jakimowicz, D.; Yuqing, T.; Bruton, C. J.; Chater, K. F.: Λ red-mediated genetic manipulation of antibiotic-producing streptomyces. In *Advances in applied microbiology*; Academic Press, 2004; Vol. Volume 54; pp 107-128.

29. Gust, B.; Challis, G. L.; Fowler, K.; Kieser, T.; Chater, K. F. Pcr-targeted streptomyces gene replacement identifies a protein domain needed for biosynthesis of the sesquiterpene soil odor geosmin. *Proc Natl Acad Sci U S A* **2003**, *100*, 1541-1546.

30. Ganguly, A. K.; Szmulewicz, S.; Sarre, O. Z.; Girijavallabhan, V. M. Structure of everninomicin-2. *J Chem Soc Chem Comm* **1976**, 609-611.

31. Nofiani, R.; Philmus, B.; Nindita, Y.; Mahmud, T. 3-ketoacyl-acp synthase (kas) iii homologues and their roles in natural product biosynthesis. *MedChemComm* **2019**.

32. Weitnauer, G.; Hauser, G.; Hofmann, C.; Linder, U.; Boll, R.; Pelz, K.; Glaser, S. J.; Bechthold, A. Novel avilamycin derivatives with improved polarity generated by targeted gene disruption. *Chemistry & Biology* **2004**, *11*, 1403-1411.

33. Agarwal, V.; Miles, Z. D.; Winter, J. M.; Eustaquio, A. S.; El Gamal, A. A.; Moore, B. S. Enzymatic halogenation and dehalogenation reactions: Pervasive and mechanistically diverse. *Chem Rev* **2017**, *117*, 5619-5674.

34. Xiao, Y.; Li, S.; Niu, S.; Ma, L.; Zhang, G.; Zhang, H.; Zhang, G.; Ju, J.; Zhang, C. Characterization of tiacumicin b biosynthetic gene cluster affording diversified tiacumicin analogues and revealing a tailoring dihalogenase. *Journal of the American Chemical Society* **2011**, *133*, 1092-1105.

35. Franke, J.; Hertweck, C. Biomimetic thioesters as probes for enzymatic assembly lines: Synthesis, applications, and challenges. *Cell Chemical Biology* **2016**, *23*, 1179-1192.

36. Wang, P.; Zhang, Z.; Yu, B. Total synthesis of crm646-a and -b, two fungal glucuronides with potent heparinase inhibition activities. *The Journal of Organic Chemistry* **2005**, *70*, 8884-8889.

37. Moulin, E.; Zoete, V.; Barluenga, S.; Karplus, M.; Winssinger, N. Design, synthesis, and biological evaluation of hsp90 inhibitors based on conformational analysis of radicicol and its analogues. *Journal of the American Chemical Society* **2005**, *127*, 6999-7004.

38. McCoy, J. G.; Johnson, H. D.; Singh, S.; Bingman, C. A.; Lei, I.-K.; Thorson, J. S.; Phillips, G. N. Structural characterization of calo2: A putative orsellinic acid p450 oxidase in the calicheamicin biosynthetic pathway. *Proteins: Structure, Function, and Bioinformatics* **2009**, *74*, 50-60.

39. Bretschneider, T.; Zocher, G.; Unger, M.; Scherlach, K.; Stehle, T.; Hertweck, C. A ketosynthase homolog uses malonyl units to form esters in cervimycin biosynthesis. *Nat Chem Biol* **2011**, *8*, 154-161.

40. He, Q.-L.; Jia, X.-Y.; Tang, M.-C.; Tian, Z.-H.; Tang, G.-L.; Liu, W. Dissection of two acyl-transfer reactions centered on acyl-s-carrier protein intermediates for incorporating 5-chloro-6-methyl-o-methylsalicyclic acid into chlorothricin. *ChemBioChem* **2009**, *10*, 813-819.

41. Sun, H.; Ho, C. L.; Ding, F.; Soehano, I.; Liu, X. W.; Liang, Z. X. Synthesis of (r)-mellein by a partially reducing iterative polyketide synthase. *J Am Chem Soc* **2012**, *134*, 11924-11927.

42. Shao, L.; Qu, X.-D.; Jia, X.-Y.; Zhao, Q.-F.; Tian, Z.-H.; Wang, M.; Tang, G.-L.; Liu, W. Cloning and characterization of a bacterial iterative type i polyketide synthase gene encoding the 6-methylsalicyclic acid synthase. *Biochemical and Biophysical Research Communications* **2006**, *345*, 133-139.

43. Zhang, H.; Tian, X.; Pu, X.; Zhang, Q.; Zhang, W.; Zhang, C. Tiacumicin congeners with improved antibacterial activity from a halogenase-inactivated mutant. *J. Nat. Prod.* **2018**, *81*, 1219-1224.

44. Saxena, G.; Farmer, S.; Towers, G. H. N.; Hancock, R. E. W. Use of specific dyes in the detection of antimicrobial compounds from crude plant extracts using a thin layer chromatography agar overlay technique. *Phytochem. Anal.* **1995**, *6*, 125-129.

45. Meanwell, N. A. Fluorine and fluorinated motifs in the design and application of bioisosteres for drug design. *J Med Chem* **2018**, *61*, 5822-5880.

46. Eichhorn, E.; van der Ploeg, J. R.; Leisinger, T. Characterization of a two-component alkanesulfonate monooxygenase from escherichia coli. *Journal of Biological Chemistry* **1999**, *274*, 26639-26646.

Chapter V

Dissertation Summary and Future Directions

Dissertation Summary

Natural products are powerful molecules engineered by evolution to demonstrate potent bioactivity; however, nature has not optimized these molecules for application to human health resulting in compounds with low solubility, high toxicity, and unsatisfactory pharmacokinetics and dynamics. Given these perceived roadblocks, there has been a recent trend away from natural products and their derivatives in favor of small molecule libraries. Unfortunately, this trend has not been fruitful, especially in regards to the development of antibacterials.[1] This is especially disheartening given the present state of drug resistance in the clinic.[2] The current trend of antibacterial resistance is likely to continue despite initiatives to improve antibiotic stewardship, develop rapid diagnostics, and increase infection prevention. Therefore, the discovery and development of antimicrobial agents with novel scaffolds and mechanisms of action is imperative to refill the therapeutic pipeline.

A key component of our continued reliance on natural products is discovery of novel natural product scaffolds sourced from new sources. We have only scratched the surface of the natural product reservoir and continued discovery efforts will continue to provide compounds to enter the drug development pipeline.[3,4] In addition, genomic analysis has revealed that many microbial producers are host to a large amount of silent biosynthetic gene clusters for which no chemical structures are assigned.[5] This has led many groups, including the Bachmann laboratory, to focus on the activation of these silent gene clusters in the pursuit of novel natural product classes.[6,7]

In addition to these discovery efforts, the revitalization of known natural product classes is also a necessary route to develop clinical therapeutics.

Chapter II discussed numerous case studies highlighting the field's ability to derivatize and improve natural products' scaffolds. Through semi-synthesis, total synthesis, and biosynthetic manipulation, we can continue to develop and advance natural products into the clinic. While some of this development may focus on legacy natural products such as the tetracyclines or macrolides, an important area of development is the rescue of discarded natural product scaffolds. Previous development of a scaffold can often provide researchers with vast amounts of data encompassing MOA, toxicity, and SAR. The orthosomycins are one such class with unique structural features and potent antibacterial activity. Previous work on the everninomicins and avilamycins confirmed a novel MOA, making them excellent candidates for development as clinical therapeutics. Prior development of Evn A (Ziracin) provides insight into key structural features required for activity while also confirming the overall safety and efficacy of this class of molecules. Finally, investigations into the biosynthesis of the avilamycins by the Bechthold group in the producing strain *Streptomyces viridochromogenes* Tü57 provided initial proof that derivatives of these complex compounds can be accessed via biosynthetic manipulation.[8,9]

Prior to the work in this dissertation, the biosynthetic pathway of the everninomicins was only partially annotated. Previous work in the Bachmann laboratory identified and characterized key oxidases responsible for the formation of the unique orthoester linkages as well as the N-oxidation of the evernitrose sugar. This dissertation sought to expand our knowledge about key biosynthetic steps and then apply it to generate novel everninomicin analogs. An ultimate goal of this work was to access new everninomicins with improved pharmacological properties and bioactivity. Chapter III details our development of a robust intergeneric microporous conjugation technique to facilitate targeted genetic deletion in the everninomicin producing strain *M. car.* var. *carbonacea*. We believe this conjugation technique will be applicable to other rare actinomycetes

that do not form spores and may provide an avenue for their genetic manipulation. Using this method, we probed the function of multiple methyltransferases in *M. car.* var. *carbonacea* to generate several late-stage everninomicin intermediates not previously observed. Via analysis of these metabolites, we were able to fully annotate all ten methyltransferases of the everninomicin pathway. The expression and purification of two methyltransferases, EvdM1 and EvdM5, allowed us to confirm *in vitro* that these enzymes act as tailoring proteins to methylate late-stage everninomicin scaffolds. From our positive results in probing the function of the O-methyltransferase EvdM5, we became interested in fully annotating the biosynthesis of dichloroisoeverninic (DCIE) acid to potentially generate analogs focused on this key structural component of the everninomicins.

The work in Chapter IV focuses primarily on our elucidation of DCIE biosynthesis and identification of key biosynthetic enzymes vital for everninomicin derivatization. Functional analysis confirmed the annotation of the three remaining enzymes responsible for DCIE biosynthesis, the iPKS EvdD3, KAS III-like acyltransferase EvdD1, and FDH EvdD2. We identified and characterized three novel metabolites and performed *in vitro* analysis of these enzymes with their respective genetic deletion products. We also identified the key late-stage everninomicin biosynthetic intermediate Evn Q, which lacks the DCIE ring and the evernitrose sugar. Additionally, we determined that the acyltransferase EvdD1 is a vital biosynthetic enzyme responsible for the transfer of the OSA ring from the ACP domain of EvdD3 to Evn Q. Together, access to Evn Q and EvdD1 facilitated the advancement of our stated goal, accessing everninomicin analogs. Using synthesized NAC thioesters, we have established that EvdD1 is a flexible gate-keeper that attaches variable aromatic rings to Evn Q to produce novel analogs. To date, we have utilized EvdD1 to transfer sixteen non-natural aromatic rings to the Evn Q scaffold. Initial analysis of the analogs' bioactivity indicates that many of these compounds at least retain their antibacterial activity and may show improved activity. The identification of Evn

Q and EvdD1 presents a significant advancement in revitalizing the orthosomycin class of natural products.

Future Directions

This dissertation demonstrates a serious expansion of our understanding of orthosomycin biosynthesis and provides multiple pathways forward to their continued development. In order to successfully revitalize this class of natural products, future work should focus on developing the key biosynthetic enzymes described here as synthetic biology tools. While the *in vitro* data from the methyltransferase conversion of late-stage everninomicin metabolites is preliminary, these enzymes could provide a pathway to potentially generate analogs with diverse alkyl groups. The O- and C-methyltransferases in the Evn pathway all require the SAM cofactor, which is unstable with a short half-life. The Thorson group has investigated the application of more stable, non-natural SAM cofactors to increase natural product diversity using methyltransferases as tailoring enzymes.[10,11] A similar strategy could be applied to the late-stage des-methyl Evn analogs we have generated here. The ability of EvdM1, EvdM5, or the other methyltransferases to append non-natural alkyl groups would first need to be established. Additionally, structural characterization of these methyltransferases would facilitate targeted mutagenesis to expand their active sites to accommodate SAM analogs. Such techniques have been utilized to expand the scope of methyltransferases in alkaloid and catechol pathways.[12-14] The annotation of all ten Evn methyltransferases and the ability to access these advanced des-methyl metabolites provides an avenue to probe the SARs between the ribosome and the extended everninomicin structure.

The work presented in Chapter IV also provides an exciting possibility of revitalizing the everninomicins for application in the clinic. The identification of the key biosynthetic enzyme,

EvdD1, now allows for targeted changes to the everninomicin structure. This dissertation demonstrates the inherent substrate flexibility of this enzyme. Future work should continue to fully probe the natural ability of EvdD1 to incorporate non-natural aromatic rings to Evn Q. A wide variety of chemically synthesized NAC thioesters are accessible given the commercial availability of benzoic acid derivatives. Current results indicate that the wildtype enzyme has less capacity to transfer fully substituted aryl groups. However, it appears to tolerate the addition of fluorines well; thus, other fluorine and fluorinated motifs should be evaluated as they often serve as valuable bioisosteres in medicinal chemistry and drug development.[15,16] Structural characterization of EvdD1 via crystallography will also allow for a deeper mechanistic understanding of the aromatic ring transfer and highlight key residues that may be amenable to mutation to alter the enzyme's specificity. Future work should focus on the application of either random mutagenesis or directed evolution to create mutant EvdD1 enzymes with expanded substrate scope. This work could also contribute to an increased understanding and potential application of this class of KAS III-like acyltransferases.[17] While homologs such as PtmR from the pactamycin pathway are known to be flexible in their substrates, structural characterization of EvdD1 may allow for additional members of this family to be exploited to derivatize other natural products. Future work on the acyltransferase EvdD1 also presents the opportunity to fully investigate and exploit the orthosomycins' novel MOA. Previous SAR studies completed for the orthosomycins, such as those in Chapter II, were performed independently of a clear understanding of the drug binding site. Currently, we can use the structures of the orthosomycins bound to the ribosome to generate and test hypotheses regarding the interaction between the DCIE ring, the ribosome, and ribosomal-associated proteins CTC and L16. We now have the synthetic biology tools coupled with a structural map to make targeted alterations to the orthosomycins focused on rehabilitating this powerful class of natural products. The potent

antibacterial activity and the unique MOA of the orthosomycins should encourage future development of these molecules into the clinic.

References

1. Payne, D. J.; Gwynn, M. N.; Holmes, D. J.; Pompliano, D. L. Drugs for bad bugs: Confronting the challenges of antibacterial discovery. *Nat Rev Drug Discov* **2007**, *6*, 29-40.
2. *Antibiotic resistance threats in the united states, 2019*2019.
3. Ling, L. L.; Schneider, T.; Peoples, A. J.; Spoering, A. L.; Engels, I.; Conlon, B. P.; Mueller, A.; Schaberle, T. F.; Hughes, D. E.; Epstein, S.; Jones, M.; Lazarides, L.; Steadman, V. A.; Cohen, D. R.; Felix, C. R.; Fetterman, K. A.; Millett, W. P.; Nitti, A. G.; Zullo, A. M.; Chen, C.; Lewis, K. A new antibiotic kills pathogens without detectable resistance. *Nature* **2015**, *517*, 455-459.
4. Lewis, K. Platforms for antibiotic discovery. *Nat Rev Drug Discov* **2013**, *12*, 371-387.
5. Walsh, C. T.; Fischbach, M. A. Natural products version 2.0: Connecting genes to molecules. *Journal of the American Chemical Society* **2010**, *132*, 2469-2493.
6. Covington, B. C.; Spraggins, J. M.; Ynigez-Gutierrez, A. E.; Hylton, Z. B.; Bachmann, B. O. Response of secondary metabolism of hypogean actinobacterial genera to chemical and biological stimuli. *Applied and Environmental Microbiology* **2018**, *84*, e01125-01118.
7. Derewacz, D. K.; Covington, B. C.; McLean, J. A.; Bachmann, B. O. Mapping microbial response metabolomes for induced natural product discovery. *ACS Chem Biol* **2015**.
8. Weitnauer, G.; Mühlenweg, A.; Trefzer, A.; Hoffmeister, D.; Süßmuth, R. D.; Jung, G.; Welzel, K.; Vente, A.; Girreser, U.; Bechthold, A. Biosynthesis of the orthosomycin antibiotic avilamycin a: Deductions from the molecular analysis of the avi biosynthetic gene cluster of streptomyces viridochromogenes tü57 and production of new antibiotics. *Chemistry & Biology* **2001**, *8*, 569-581.
9. Weitnauer, G.; Hauser, G.; Hofmann, C.; Linder, U.; Boll, R.; Pelz, K.; Glaser, S. J.; Bechthold, A. Novel avilamycin derivatives with improved polarity generated by targeted gene disruption. *Chemistry & Biology* **2004**, *11*, 1403-1411.
10. Zhang, C.; Weller, R. L.; Thorson, J. S.; Rajski, S. R. Natural product diversification using a non-natural cofactor analogue of s-adenosyl-l-methionine. *Journal of the American Chemical Society* **2006**, *128*, 2760-2761.
11. Huber, T. D.; Wang, F.; Singh, S.; Johnson, B. R.; Zhang, J.; Sunkara, M.; Van Lanen, S. G.; Morris, A. J.; Phillips, G. N., Jr.; Thorson, J. S. Functional adomet isosteres resistant to classical adomet degradation pathways. *ACS Chem Biol* **2016**, *11*, 2484-2491.

12. Herbert, A. J.; Shepherd, S. A.; Cronin, V. A.; Bennett, M. R.; Sung, R.; Micklefield, J. Engineering orthogonal methyltransferases to create alternative bioalkylation pathways. *Angew Chem Int Ed Engl* **2020**.

13. Valentic, T. R.; Payne, J. T.; Smolke, C. D. Structure-guided engineering of a scoulerine 9-o-methyltransferase enables the biosynthesis of tetrahydropalmatrubine and tetrahydropalmatine in yeast. *ACS Catalysis* **2020**, *10*, 4497-4509.

14. Adhikari, A.; Teijaro, C. N.; Yan, X.; Chang, C. Y.; Gui, C.; Liu, Y. C.; Crnovcic, I.; Yang, D.; Annaval, T.; Rader, C.; Shen, B. Characterization of tnmh as an o-methyltransferase revealing insights into tiancimycin biosynthesis and enabling a biocatalytic strategy to prepare antibody-tiancimycin conjugates. *J Med Chem* **2020**, *63*, 8432-8441.

15. Zafrani, Y.; Sod-Moriah, G.; Yeffet, D.; Berliner, A.; Amir, D.; Marciano, D.; Elias, S.; Katalan, S.; Ashkenazi, N.; Madmon, M.; Gershonov, E.; Saphier, S. Cf2h, a functional group-dependent hydrogen-bond donor: Is it a more or less lipophilic bioisostere of oh, sh, and ch3? *J Med Chem* **2019**.

16. Meanwell, N. A. Fluorine and fluorinated motifs in the design and application of bioisosteres for drug design. *J Med Chem* **2018**, *61*, 5822-5880.

17. Nofiani, R.; Philmus, B.; Nindita, Y.; Mahmud, T. 3-ketoacyl-acp synthase (kas) iii homologues and their roles in natural product biosynthesis. *MedChemComm* **2019**.

Appendix A. Supporting data for Chapter III

Figure A-1. Genetic map and table of the everninomicin D-G gene cluster from *Micromonospora carbonacea* var. *aurantiaca*. Potential operonal units are minimally defined by transcriptional gene directionality, which is indicated by green (sense) and red (antisense), respectively. (GenBank Nucleotide Accession: CP058322.1, genome region 866393-925867)

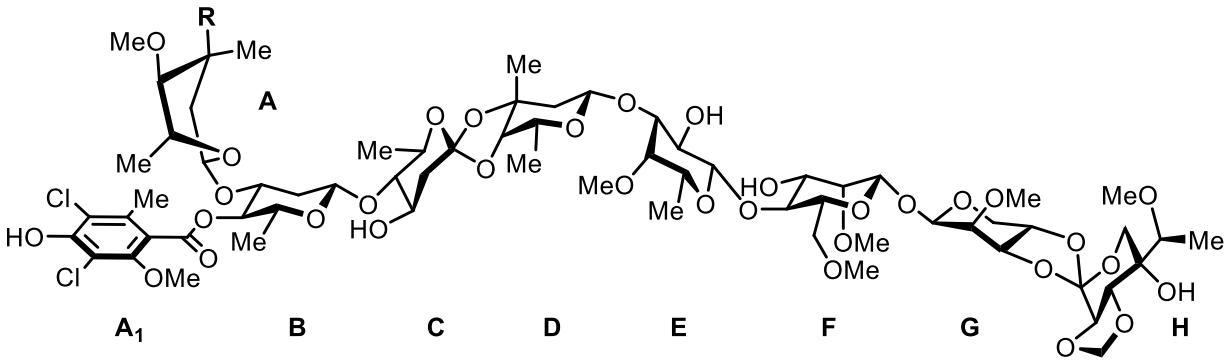

Evn D R = NO_2 **Evn F R = NHOH**

Evn E R = NH_2 **Evn G R = NO**

GenBank Accession #	Start/Stop (bp)	Gene	Size (#aa)	Proposed function	Protein Homolog	Identity	GenBank Accession #
AX574200	753-1	*EvdM1*	250	O-methyltransferase	ApoM1 (*Nocardiopsis* sp. FU40)	71%	AEP40941
	1533-2861	*EvdU1*	442	Unknown	MCAG_03643 (*Micromonospora* sp. ATCC 39149)	76%	ZP_04607386
	2898-4055	*EvdX1*	385	RNA methyltransferase	MCAG_03646 (*Micromonospora* sp. ATCC 39149)	70%	ZP_04607389
	5529-4060	*EvdU2*	489	Unknown	MCAG_03647 (*Micromonospora* sp. ATCC 39149)	77%	ZP_04607390
	6174-6998	*EvdM2*	274	O-methyltransferase	MCAG_03640 (*Micromonospora* sp. ATCC 39149)	79%	ZP_04607383
	7040-8284	*EvdM3*	429	C-methyltransferase	MCAG_03641 (*Micromonospora* sp. ATCC 39149)	72%	ZP_04607384
	8281-9465	*EvdM4*	423	O-methyltransferase	StfMIII O-methyltransferase (*S. steffisburgensis)*	100%	CAJ42340.1
	9472-10491	*EvdGT1*	339	Glycosyltransferase	MCAG_03659 (*Micromonospora* sp. ATCC 39149)	57%	ZP_0460742
	10595-11020	*EvdU3*	137	Unknown	AviX10 (*Streptomyces viridochromogenes* Tue57)	80%	AAK83174
	12020-11076	*EvdS1*	314	4-ketoreductase	ApoH3 (*Nocardiopsis* sp. FU40)	63%	AEP40908
	13056-12061	*EvdM5*	342	O-methyltransferase	MCAG_03673 (*Micromonospora* sp. ATCC 39149)	58%	ZP_04607416
	13912-13082	*EvdU4*	276	Unknown	MCAG_03672 (*Micromonospora* sp. ATCC 39149)	69%	ZP_04607415
	14812-14015	*EvdX2*	265	RNA methyltransferase	VAB18032_26045 (*Verrucosispora maris)*	57%	YP_004406907
	15102-16211	*EvdD1*	344	Acyltransferase	MCAG_03645 (*Micromonospora* sp. ATCC 39149)	75%	ZP_04607388
	17045-16377	*EvdM6*	240	O-methyltransferase	MCAG_03636 (*Micromonospora* sp. ATCC 39149)	67%	ZP_04607379
	18415-17099	*EvdGT2*	438	Glycosyltransferase	ApoGT3 (*Nocardiopsis* sp. FU40)	76%	AEP40907
	19900-18683	*EvdS2*	405	Epimerase	MCAG_03642 (*Micromonospora* sp. ATCC 39149)	74%	ZP_04607385
	20858-19917	*EvdO1*	313	Orthoester synthase	AviO3 (*Streptomyces viridochromogenes*)	73%	AAK83187
	21589-20858	*EvdM7*	243	O-methyltransferase	Mtf (*Catenuloplanes nepalensis)*	82%	ACL80144
	23031-21586	*EvdD2*	481	Halogenase	MCAG_03648 (*Micromonospora* sp. ATCC 39149)	78%	ZP_04607391
	23372-24487	*EvdGT3*	380	Glycosyltransferase	MCAG_03663 (*Micromonospora* sp. ATCC 39149)	61%	ZP_04607406
	24565-25542	*EvdU5*	325	Pyruvate dehydrogenase	Dhg (*Catenuloplanes nepalensis*)	89%	ACL80142

	25547-26509	*EvdU6*	344	Pyruvate dehydrogenase	AviB2 (*Streptomyces viridochromogenes*)	77%	AAK83191
	26515-27570	*EvdGT4*	337	Glycosyltransferase	AviGT3 (*Streptomyces viridochromogenes)*	75%	AAK83192
	27567-28619	*EvdU7*	350	Unknown	MCAG_03660 (*Micromonospora* sp. ATCC 39149)	64%	ZP_04607403
	29397-28639	*EvdO2*	252	Orthoester synthase	MCAG_03658 (*Micromonospora* sp. ATCC 39149)	71%	ZP_04607401
	29752-30681	*EvdS3*	309	Epimerase/dehydratase	UUA_15808 (*Rhodanobacter thiooxydans*)	42%	ZP_10205860
	30879-31946	*EvdS4*	355	Glucose-1-phosphate	MCAG_03630 (*Micromonospora* sp. ATCC 39149)	79%	ZP_04607373
	31946-32935	*EvdS5*	329	4,6-dehydratase	MCAG_03631 (*Micromonospora* sp. ATCC 39149)	78%	ZP_04607374
	32990-34018	*EvdS6*	342	4-epimerase	AviQ2 (*Streptomyces viridochromogenes*)	82%	AAK83170
	34073-35425	*EvdOM1*	450	Oxidase/Methyltransferase	MCAG_03633 (*Micromonospora* sp. ATCC 39149)	77%	ZP_04607376
	39383-35580	*EvdD3*	1267	Polyketide synthase	AviM (*Streptomyces viridochromogenes*)	65%	AAK83194
	39773-40612	*EvdU8*	249	Unknown	MCAG_03657 (*Micromonospora* sp. ATCC 39149)	64%	ZP_04607400
	40609-41532	*EvdS7*	307	4-ketoreductase	MCAG_03656 (*Micromonospora* sp. ATCC 39149)	66%	ZP_04607399
	42326-41511	*EvdGT5*	295	Glycosyltransferase	MCAG_03655 (*Micromonospora* sp. ATCC 39149)	80%	ZP_04607398
	42708-42460	*EvdR1*	82	Regulator	MCAG_03654 (*Micromonospora* sp. ATCC 39149)	82%	ZP_04607397
	44533-43532	*EvdS8*	341	3-ketoreductase	MCAG_03652 (*Micromonospora* sp. ATCC 39149)	68%	ZP_04607395
	45966-44554	*EvdS9*	470	2,3-dehydratase	MCAG_03651 (*Micromonospora* sp. ATCC 39149)	70%	ZP_04607394
	46910-45963	*EvdS10*	346	4,6-dehydratase	MCAG_03650 (*Micromonospora* sp. ATCC 39149)	76%	ZP_04607392
	47878-47207	*EvdX3*	254	RNA Methyltransferase	MCAG_03674 (*Micromonospora* sp. ATCC 39149)	71%	ZP_04607417
AX574200-	48183-48070	*EvdS11*	209	UDP-glucose 4-epimerase	MCAG_03662 (*Micromonospora* sp. ATCC 39149)	74%	ZP_04607405
AX574202	1-1203	*EvdN1*	400	Nitrososynthase	ORF36 (*Micromonospora* sp. ATCC 39149)	80%	ACF94630
	1200-2327	*EvdS12*	375	3-aminotransferase	MCAG_03665 (*Micromonospora* sp. ATCC 39149)	79%	ZP_04607408
	2357-36-7	*EvdM8*	416	C-methyltransferase	MCAG_03666 (*Micromonospora* sp. ATCC 39149)	81%	ZP_04607409
	3616-4239	*EvdS13*	207	3,5-epimerase	MCAG_03667 (*Micromonospora* sp. ATCC 39149)	74%	ZP_04607410
	5169-4060	*EvdS14*	369	4-ketoreductase	StaK (*Streptomyces* sp. TP-A0274)	58%	BAC55215
	6086-5166	*EvdM9*	306	O-methyltransferase	MCAG_03669 (*Micromonospora* sp. ATCC 39149)	71%	ZP_04607412
	7811-6261	*EvdU9*	517	Unknown	MCAG_00021 (*Micromonospora* sp. ATCC 39149)	66%	ZP_04603764
	8746-7889	*EvdR2*	286	Regulator	Amir_6179 (*Actinosynnema mirum*)	61%	YP_003103832
	10035-8764	*EvdR3*	423	Regulator	AMED_3740 (*Amycolatopsis mediterranei*)	63%	YP_003765921

Figure A-2. Map of pSET152ermE, the genetic complementation plasmid. Plasmid map was generated using Savvy (Scalable Vector Graphics & Plasmid Map Copyright© 2001, Malay K Basu) at http://www.bioinformatics.org/savvy/. Hyg is the hygromycin resistance marker hph; oriT is the origin of transfer; int is the phage φC31 integrase; attP is the phage φC31 attachment site; ermE* is the constitutively active promoter directly upstream of the MCS.

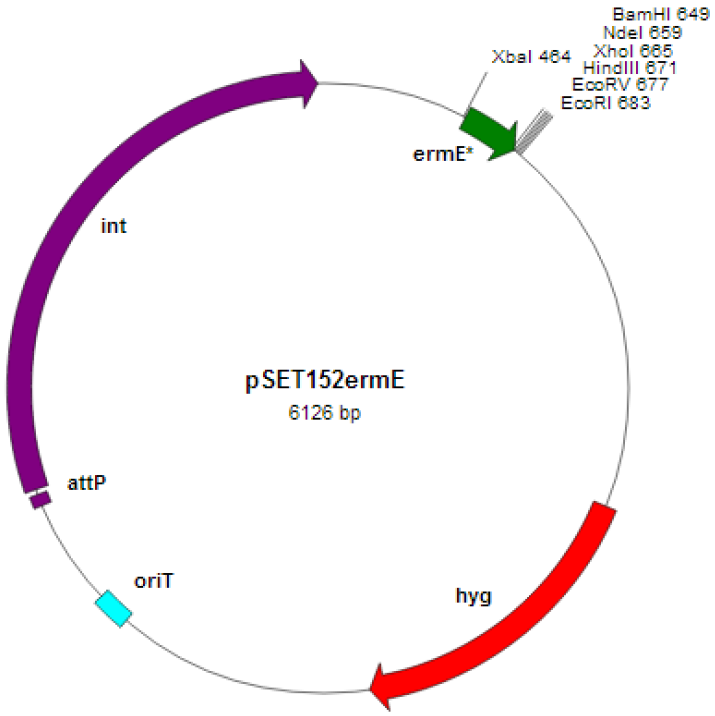

Figure A-3. Southern hybridization and PCR of targeted replacement mutants verifying a double crossover. Ladder is DNA molecular weight marker VII, DIG-labeled (Roche Life Sciences, Product No. 11669940910). WT is wild-type *M. carbonacea* var. *aurantiaca*. Red bar indicates position of gene specific probes. Green bar indicates positions of apramycin cassette specific probes. (A) Southern blot analysis of *ΔevdM2::aac(3)IV*. Diagrams show the expected relative shifts for replacement of *evdM2* with the apramycin cassette. KpnI is the restriction endonuclease used to cleave the genomic DNA into predictable fragments. Predicted shifts were observed experimentally confirming the double crossover. (B) Southern blot analysis of *ΔevdM3::aac(3)IV*. Diagrams show the expected relative shifts for replacement of *evdM3* with the apramycin cassette. BamHI and ApaI are restriction endonucleases used to cleave the genomic DNA into predictable fragments. Predicted shifts were observed experimentally confirming the double crossover. (C) PCR amplification of *ΔevdM1::aac(3)IV*. Amplification with Del and Neo primers showed strain *ΔevdM1-1* to be a double crossover. (D) PCR amplification of *ΔevdM5::aac(3)IV*. Amplification with Del and Neo primers showed strains *ΔevdM5-T2/3* as double crossovers.

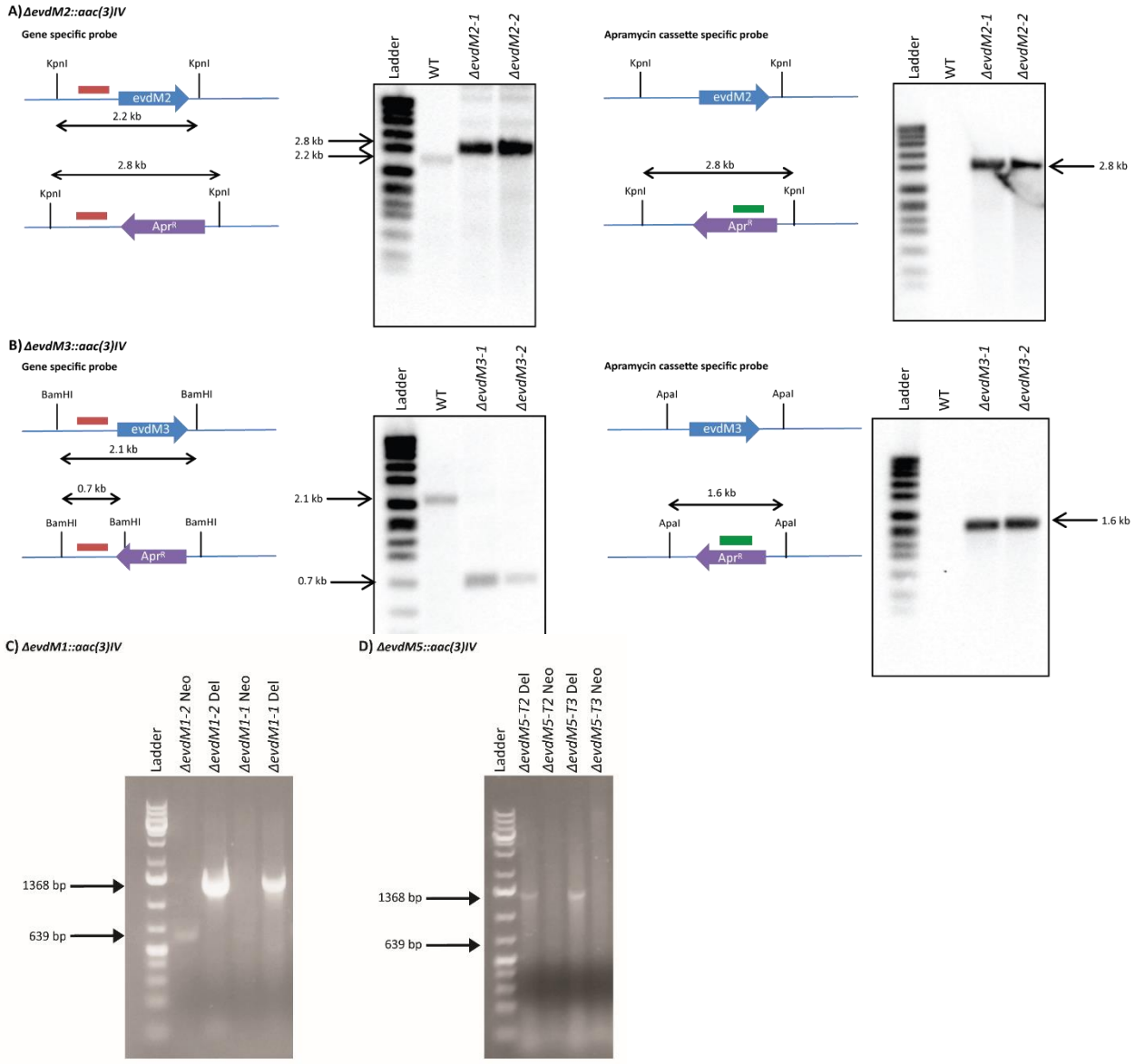

Figure A-4. Mass spectra of everninomicin L. Theoretical mass for Evn L ($C_{65}H_{97}Cl_2NO_{36}$) is 1536.50946. Experimental mass was determined to be 1536.50870. The mass accuracy is 0.5 ppm.

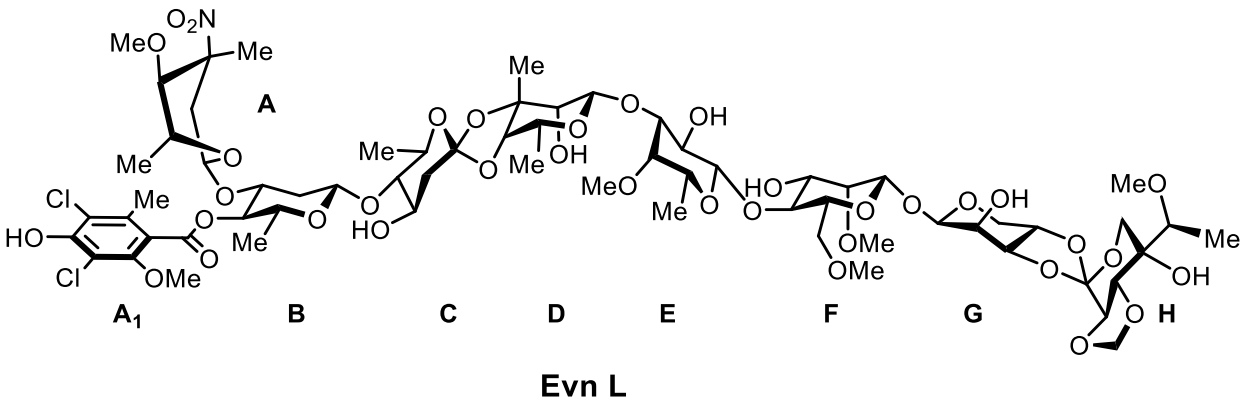

Evn L

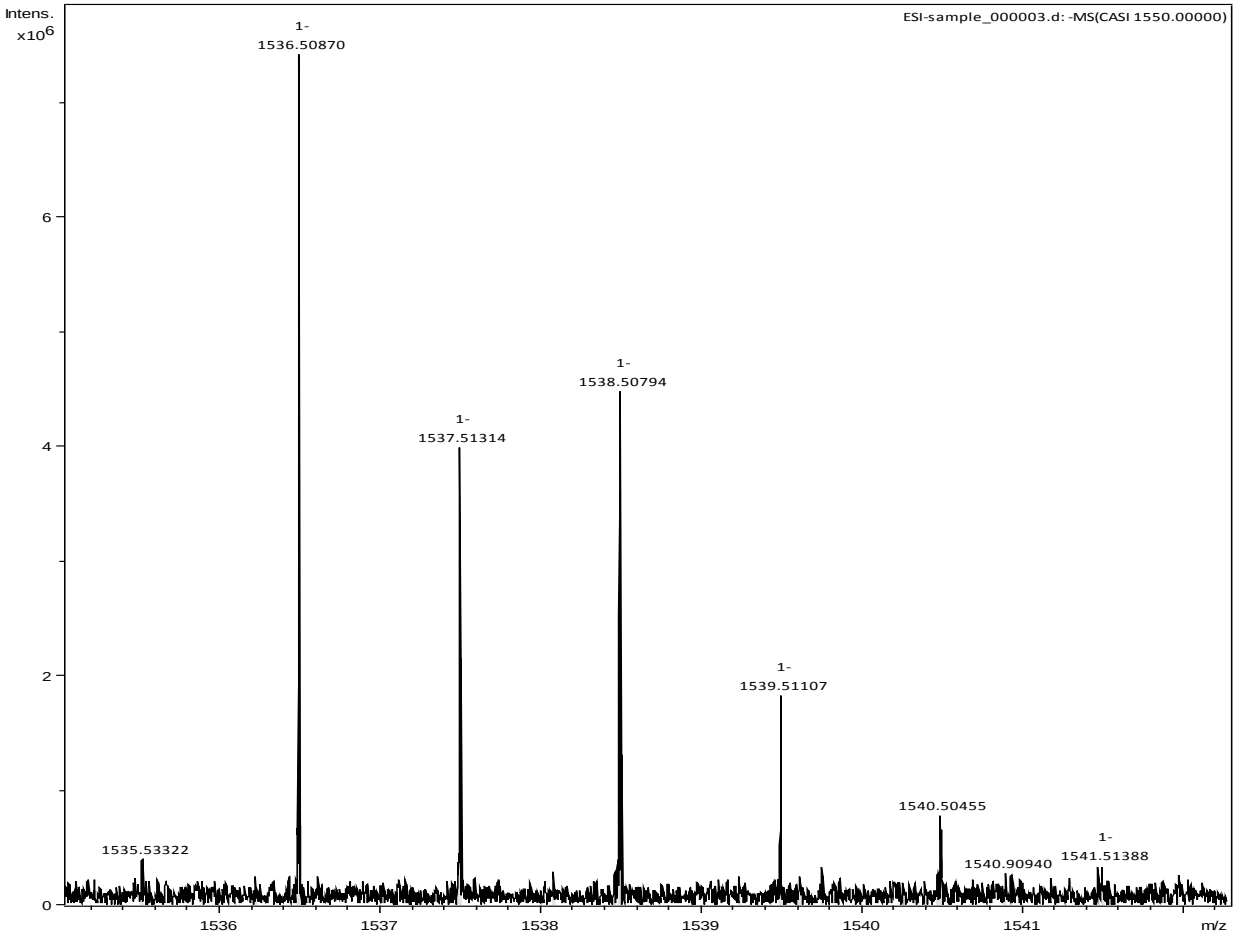

Figure A-5. Fragmentation data of everninomicin J generated using SORI-CID FTICR MS. (A) Mass spectrometric fragmentation pattern for Evn J. Dashed lines indicate positions of cleavage during fragmentation experiments. (B) Spectrum for fragmentation of Evn J (m/z = 1494.5 $[M+H]^+$).

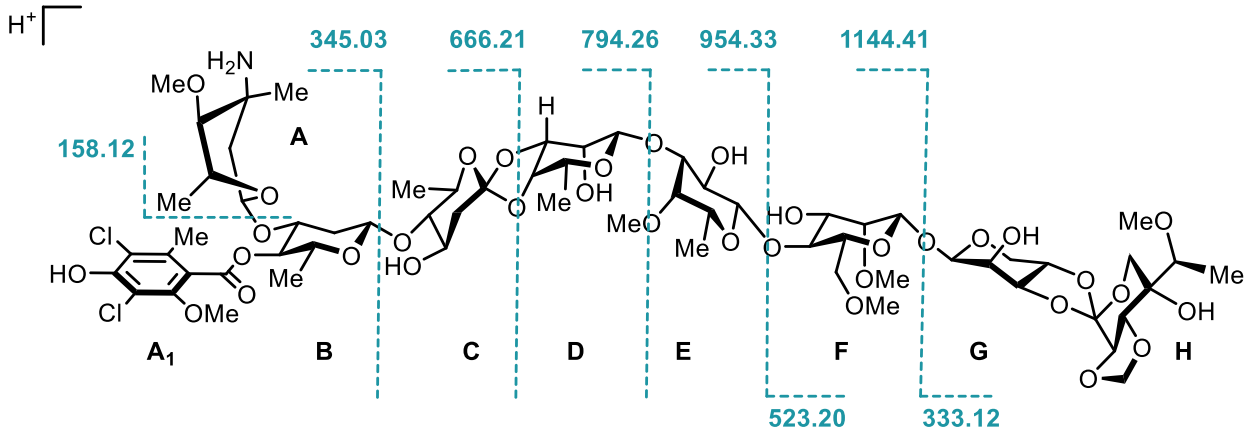

Evn J

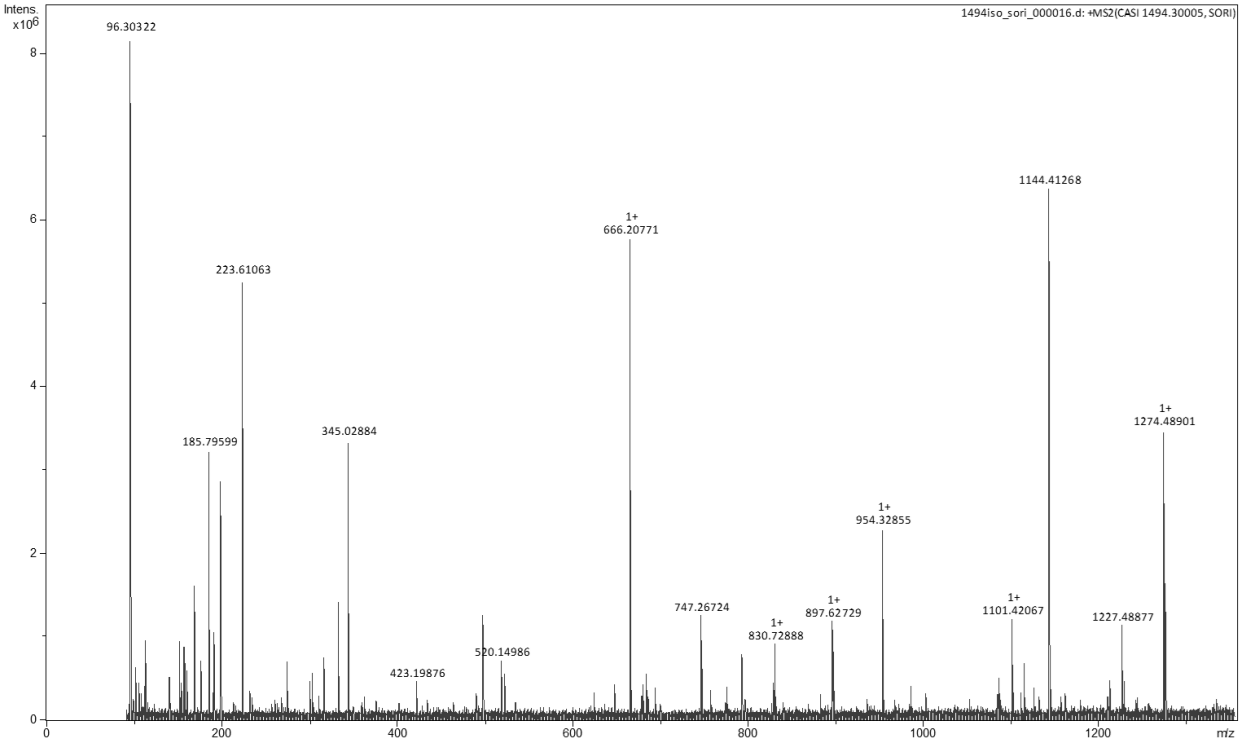

Figure A-6. Fragmentation data of everninomicin K generated using SORI-CID FTICR MS. A) Mass spectrometric fragmentation pattern for Evn K. Dashed lines indicate positions of cleavage during fragmentation experiments. (B) Spectrum for fragmentation of Evn K (m/z = 1508.5 $[M+H]^+$).

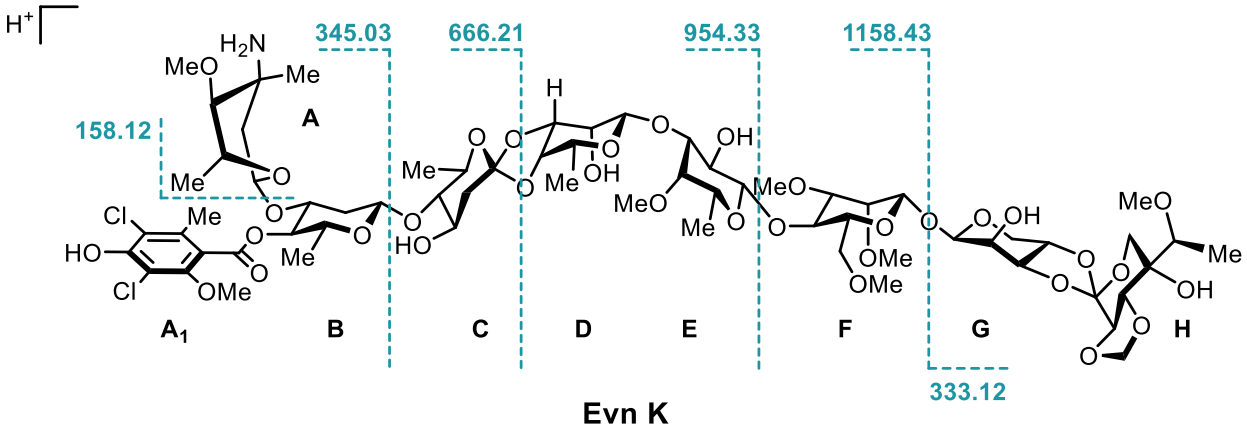

Evn K

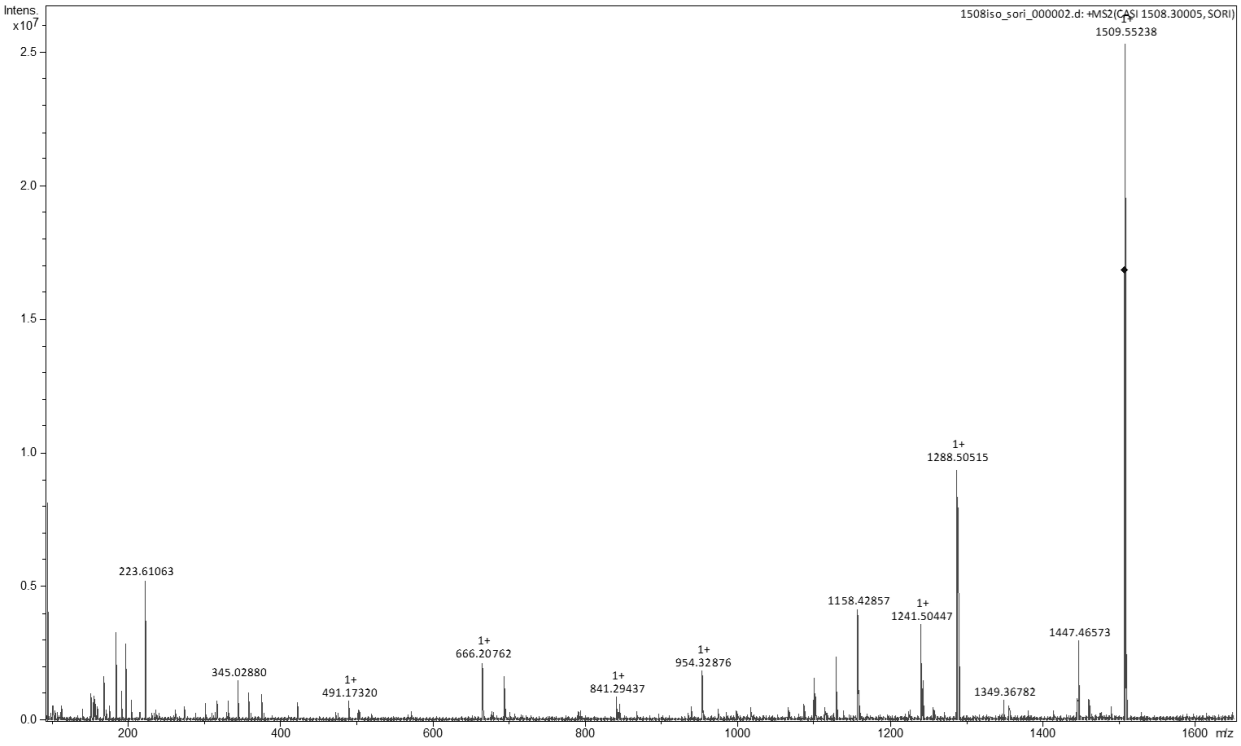

Figure A-7. Fragmentation data of everninomicin H generated using SORI-CID FTICR MS. (A) Mass spectrometric fragmentation pattern for Evn H. Dashed lines indicate positions of cleavage during fragmentation experiments. (B) Spectrum for fragmentation of Evn H (m/z = 1546.5 $[M+Na]^+$).

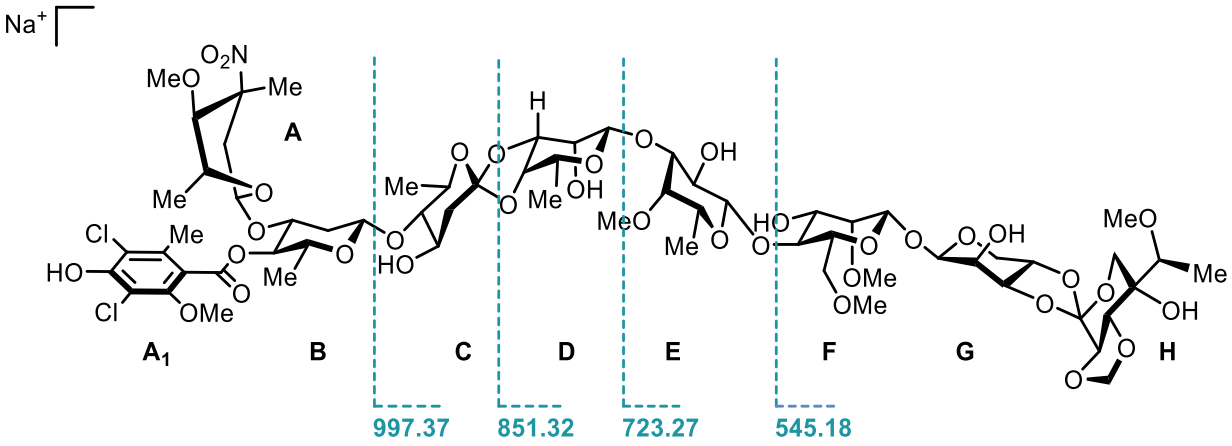

Evn H

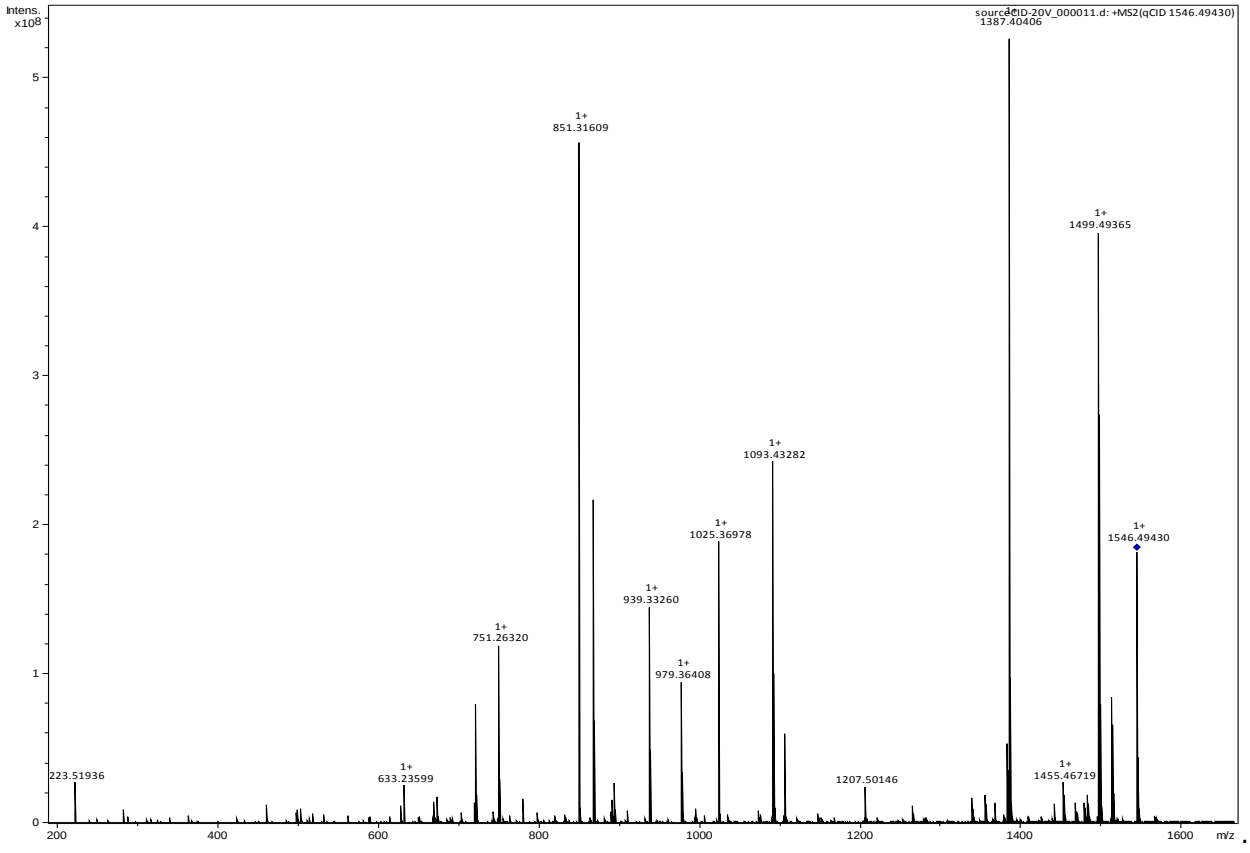

Figure A-8. ^{1}H proton NMR of Evn H in CD_4OD.

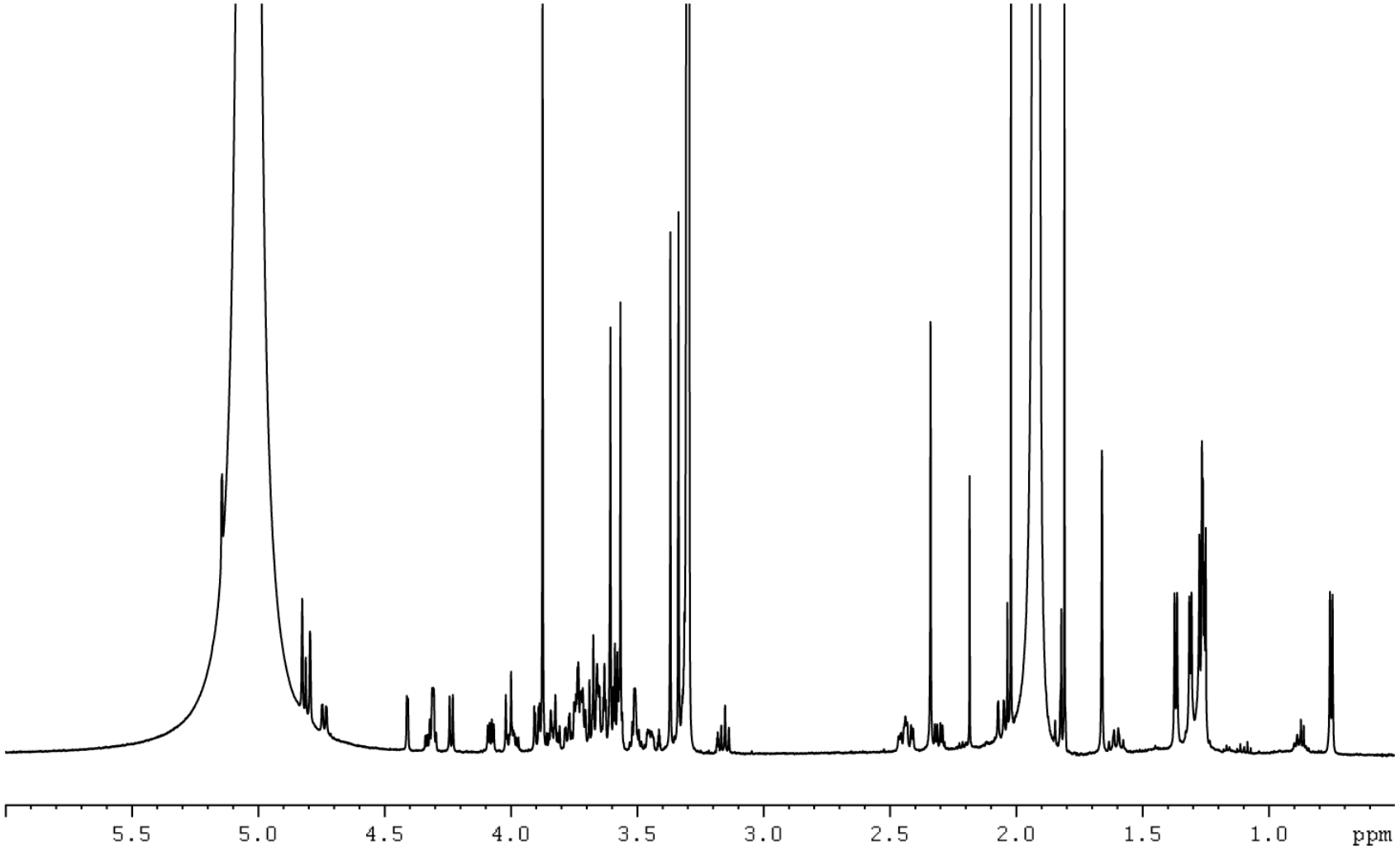

Figure A-9. ^{13}C carbon NMR of Evn H in CD_4OD.

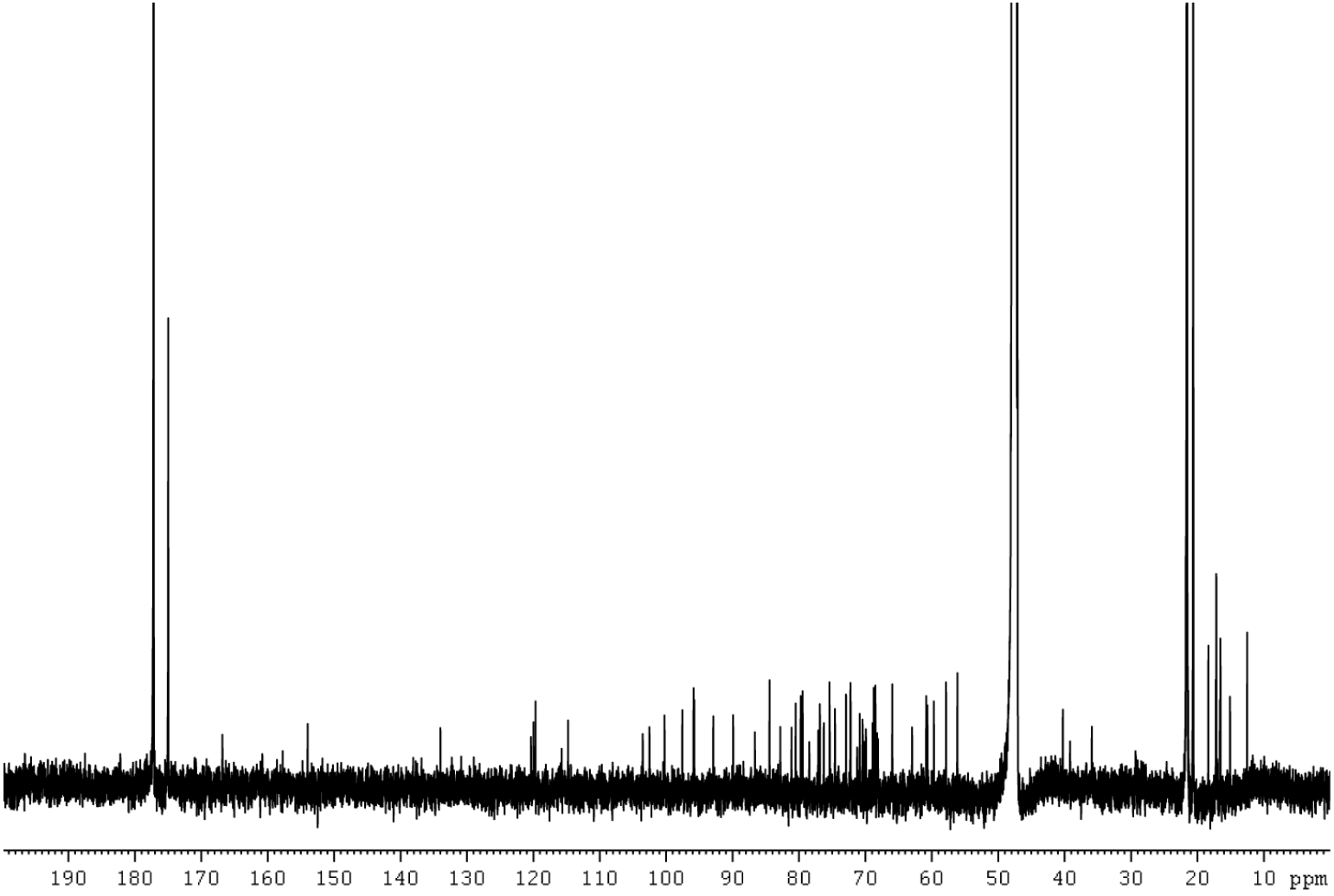

Figure A-10. COSY NMR of Evn H in CD_4OD.

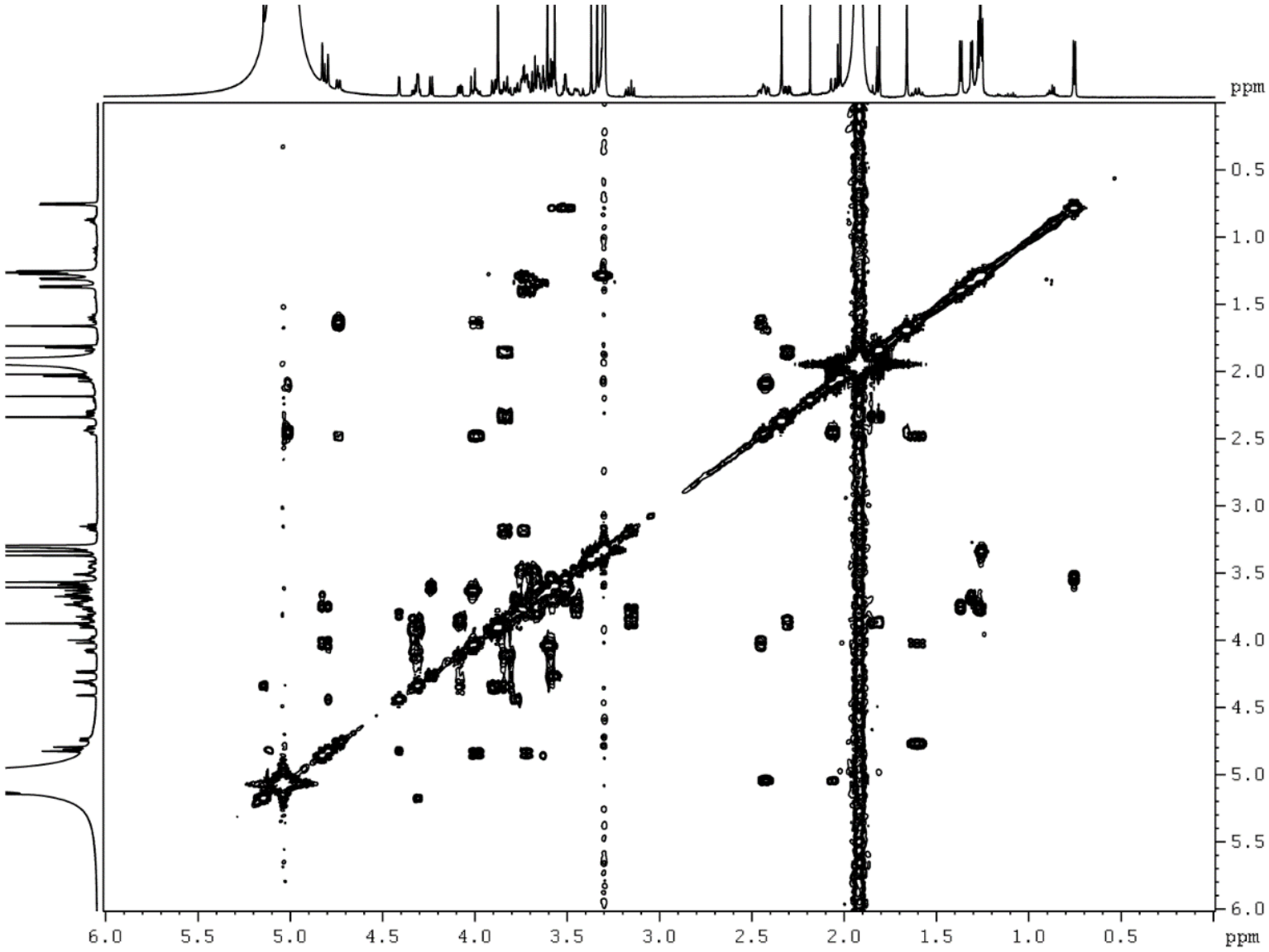

Figure A-11. HSQC NMR of Evn H in CD_4OD.

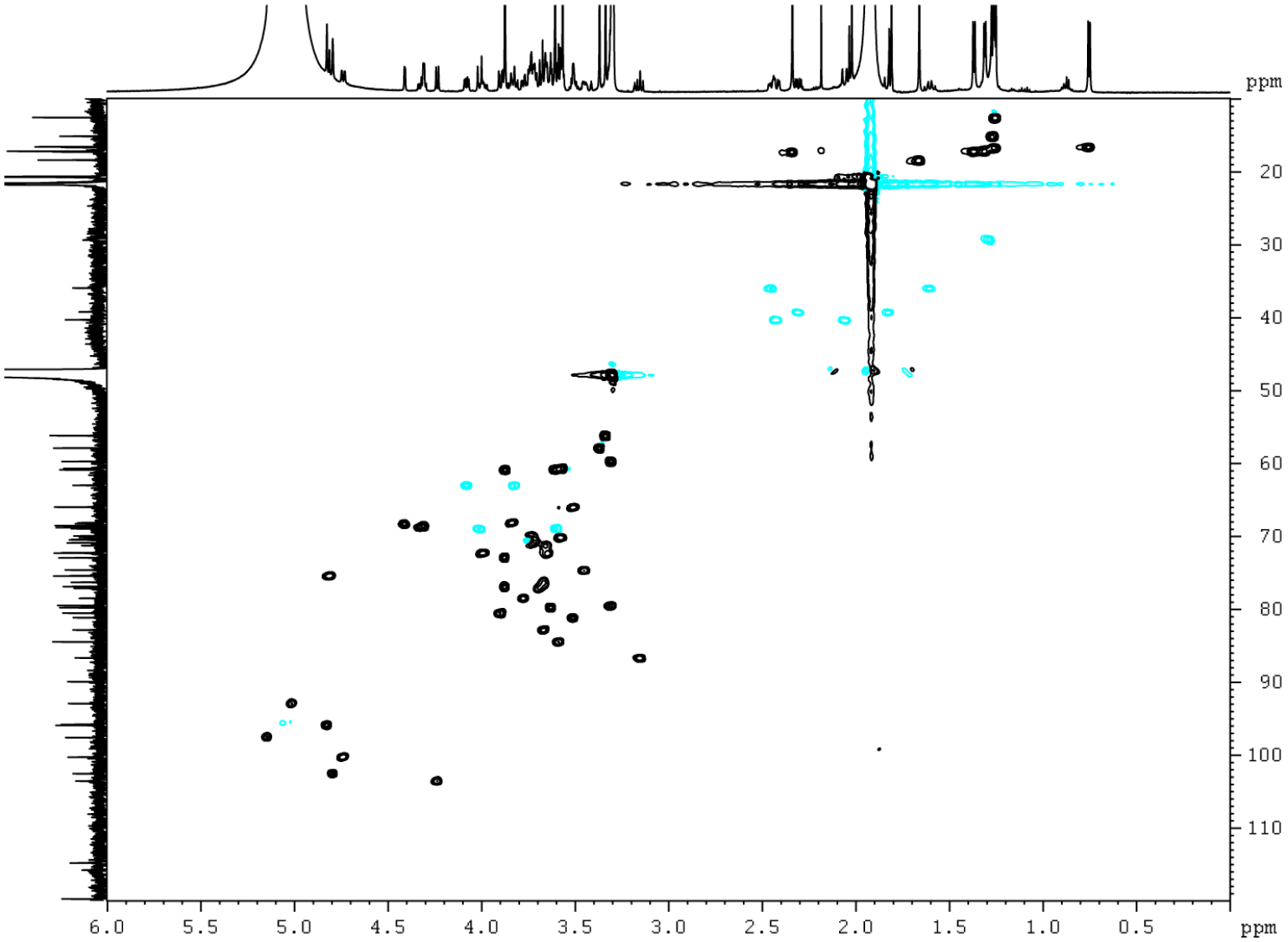

Figure A-12. HMBC NMR of Evn H in CD_4OD.

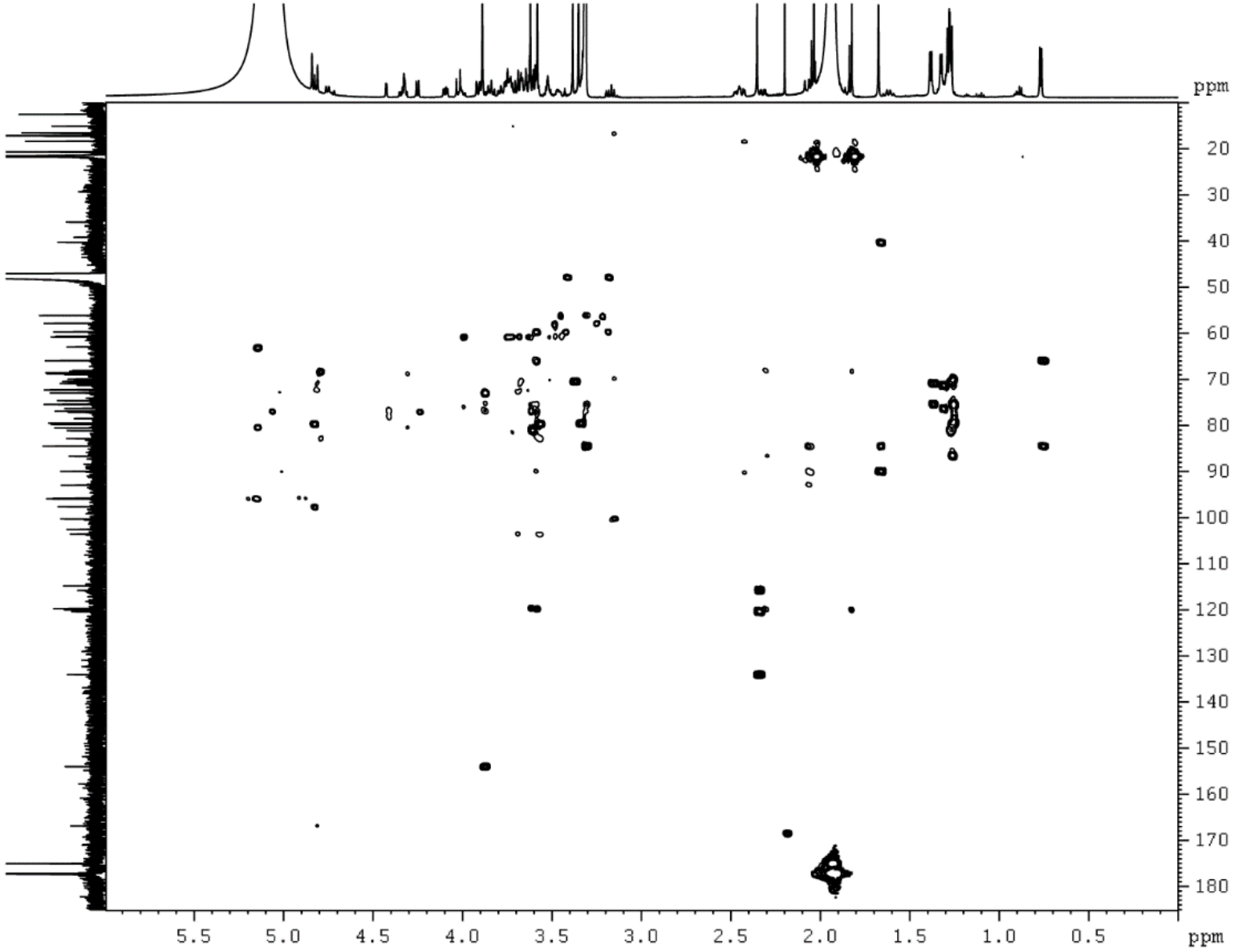

Figure A-13. TOCSY NMR of Evn H in CD_4OD.

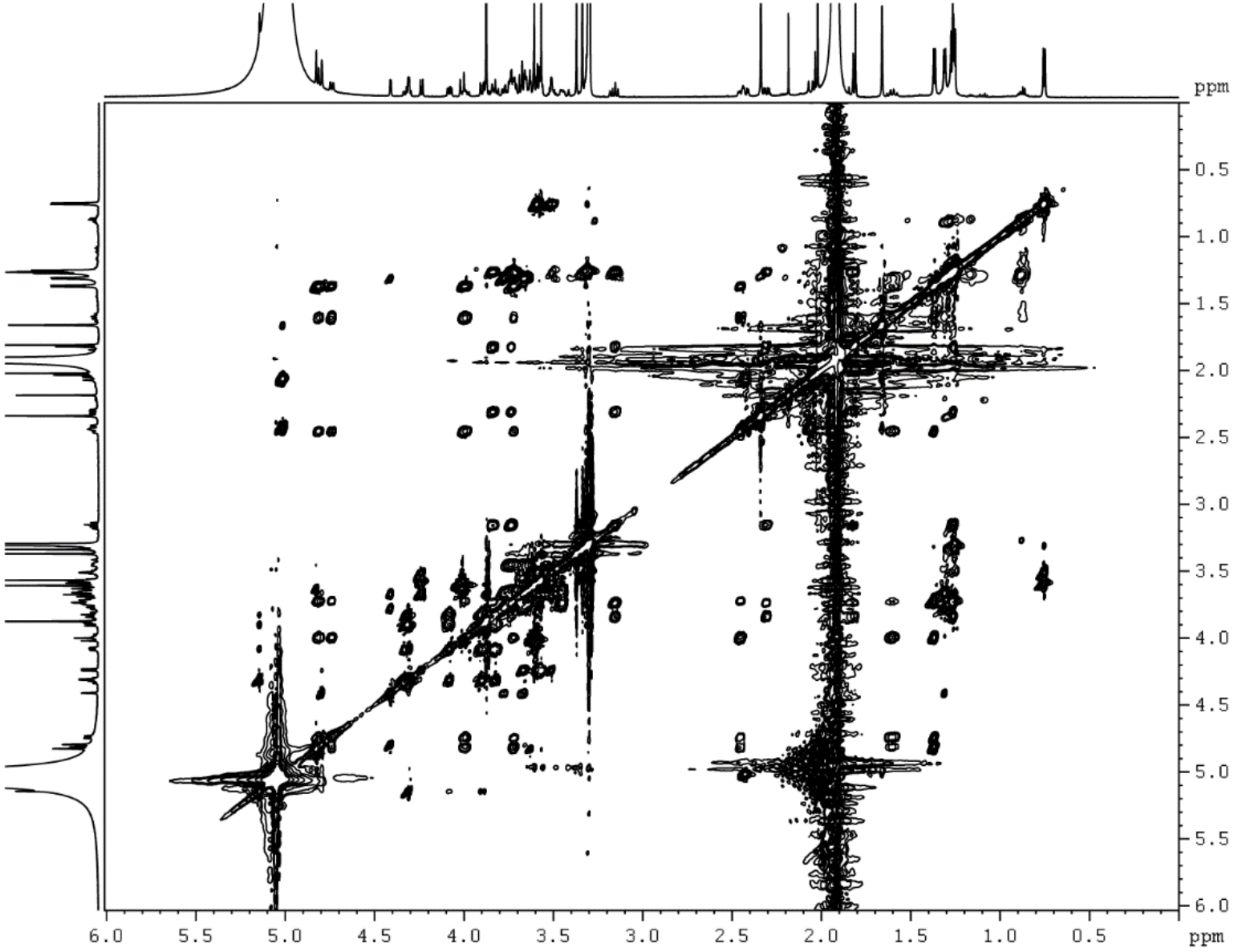

Figure A-14. Mass spectra of everninomicin T. Theoretical mass for Evn T ($C_{65}H_{97}Cl_2O_{35}$) is 1520.51 $[M-H]^-$ or 1539.56 $[M+NH_4]^+$. Experimental mass was determined to be 1520.39 $[M-H]^-$ and 1539.19 $[M+NH_4]^+$.

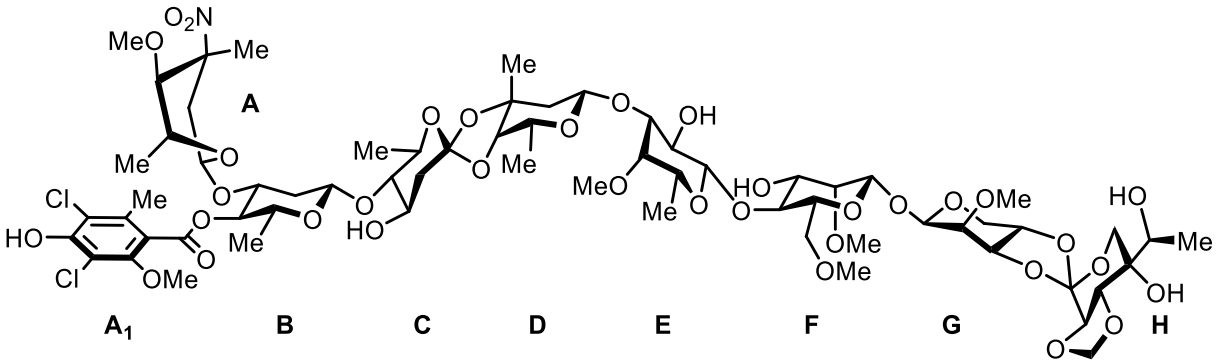

Evn T

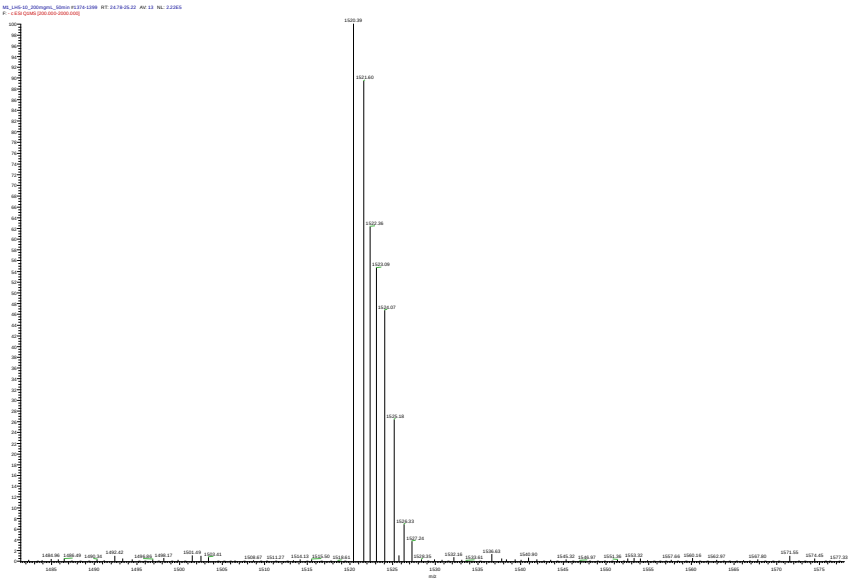

Figure A-15. Fragmentation data of everninomicin U generated using SORI-CID FTICR MS. A) Mass spectrometric fragmentation pattern for Evn U. Dashed lines indicate positions of cleavage during fragmentation experiments. (B) Spectrum for fragmentation of Evn U (m/z = 1492.80 $[M+H]^+$) at 19 V.

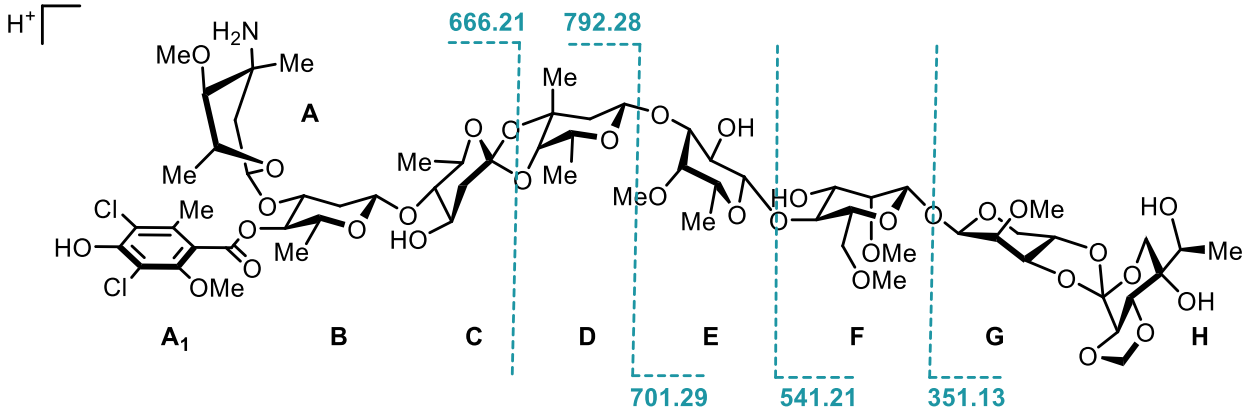

Evn U

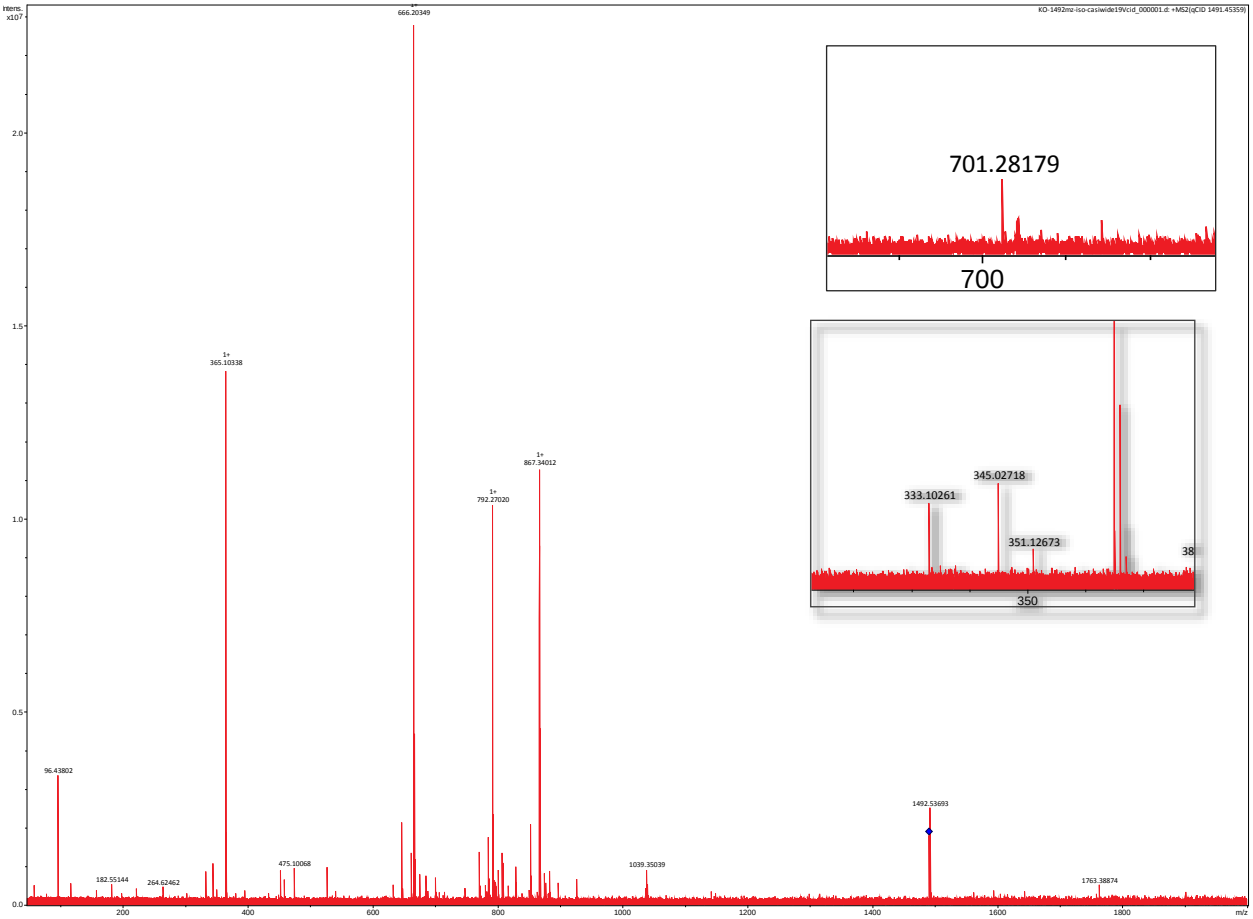

Figure A-16. Mass spectra of everninomicin V. Theoretical mass for Evn V ($C_{65}H_{99}Cl_2O_{34}$) is 1506.54 $[M-H]^-$ or 1508.55 $[M+H]^+$. Experimental mass was determined to be 1506.33 $[M-H]^-$ and 1508.15 $[M+H]^+$.

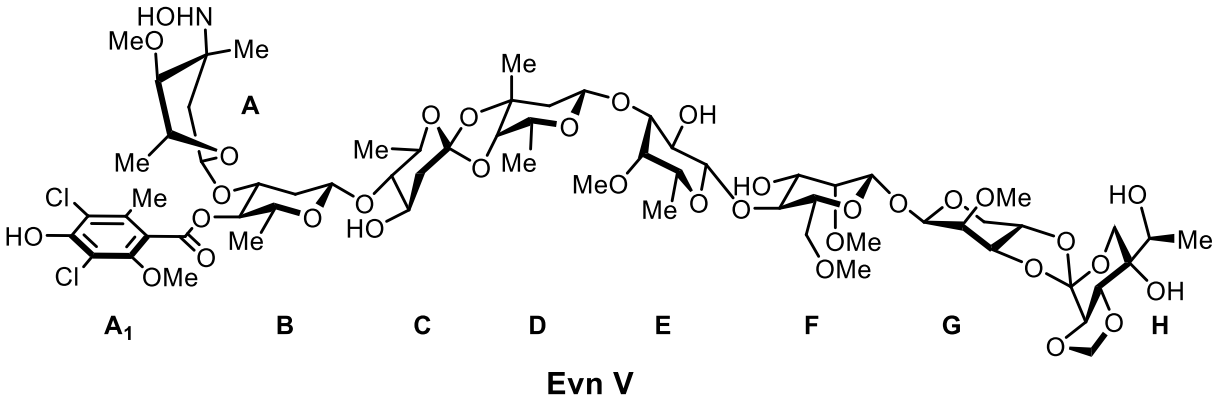

Evn V

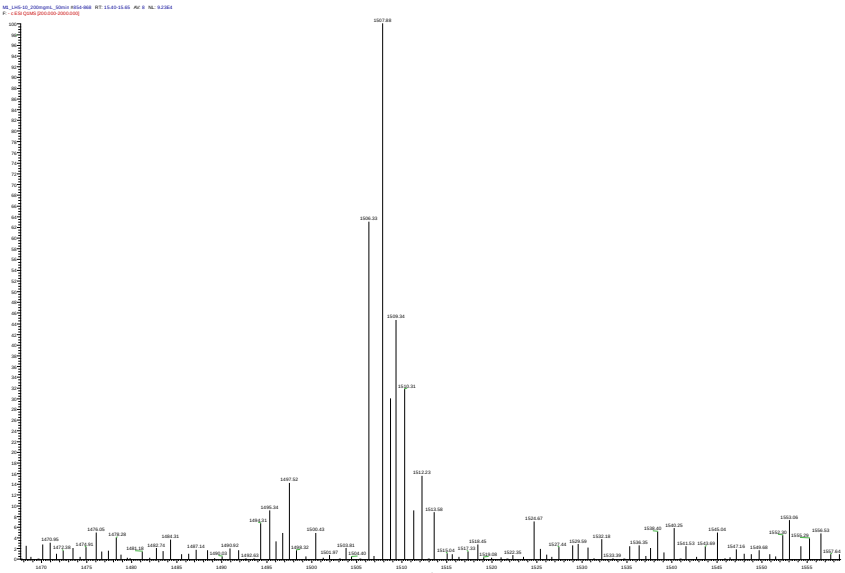

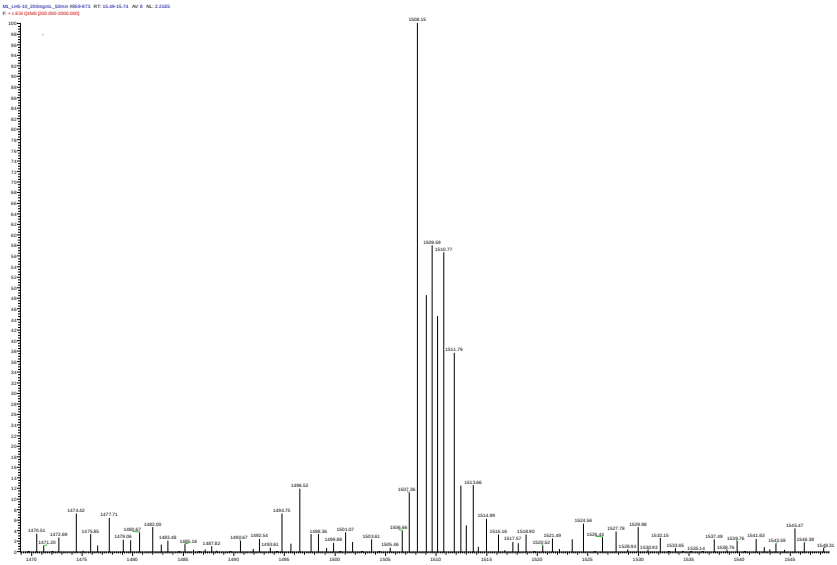

Figure A-17. Mass spectra of everninomicin W. Theoretical mass for Evn W ($C_{65}H_{97}Cl_2O_{34}$) is 1504.52 $[M-H]^-$ or 1523.56 $[M+NH_4]^+$. Experimental mass was determined to be 1504.38 $[M-H]^-$ and 1523.39 $[M+NH_4]^+$.

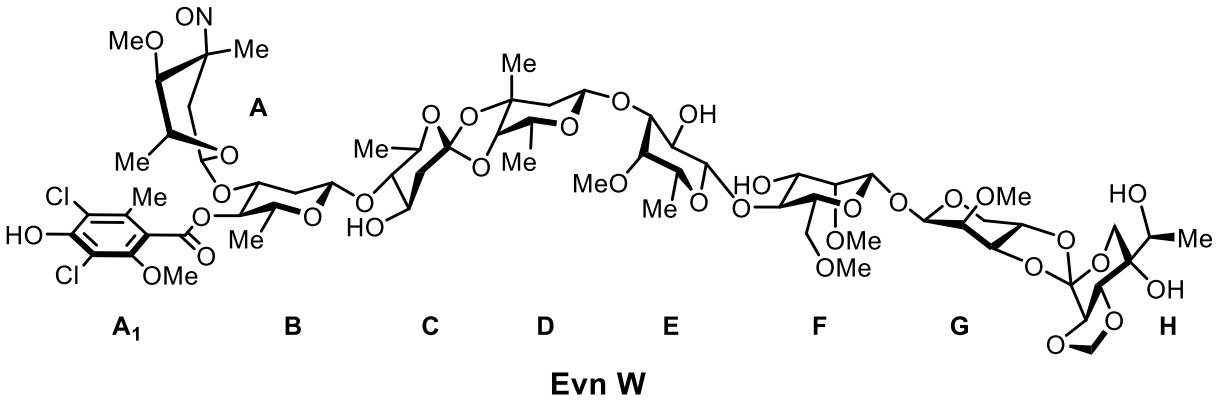

Evn W

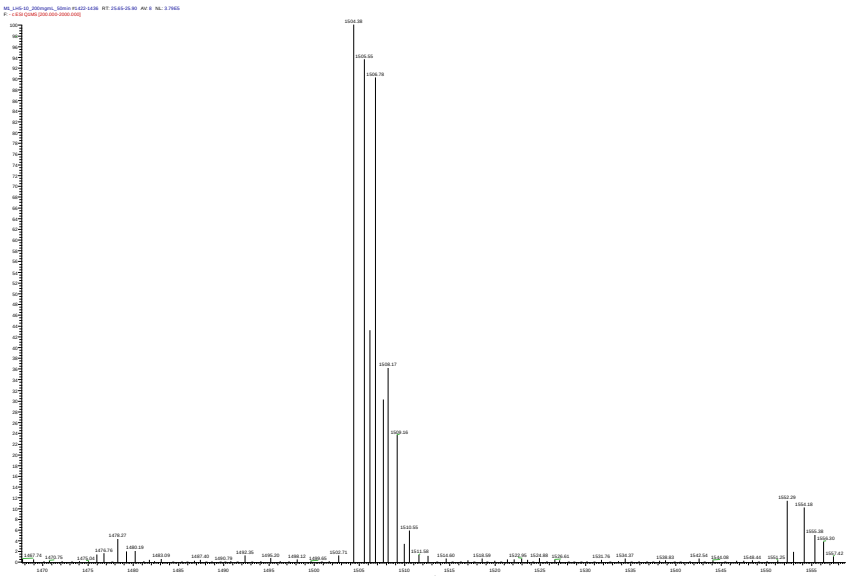

Figure A-18. Fragmentation data of everninomicin AA generated using CID TSQ MS. (A) Mass spectrometric fragmentation pattern for Evn AA. Dashed lines indicate positions of cleavage during fragmentation experiments. (B) Spectrum for fragmentation of Evn AA (m/z = 1539.50 $[M+H]^+$) at 28 volts.

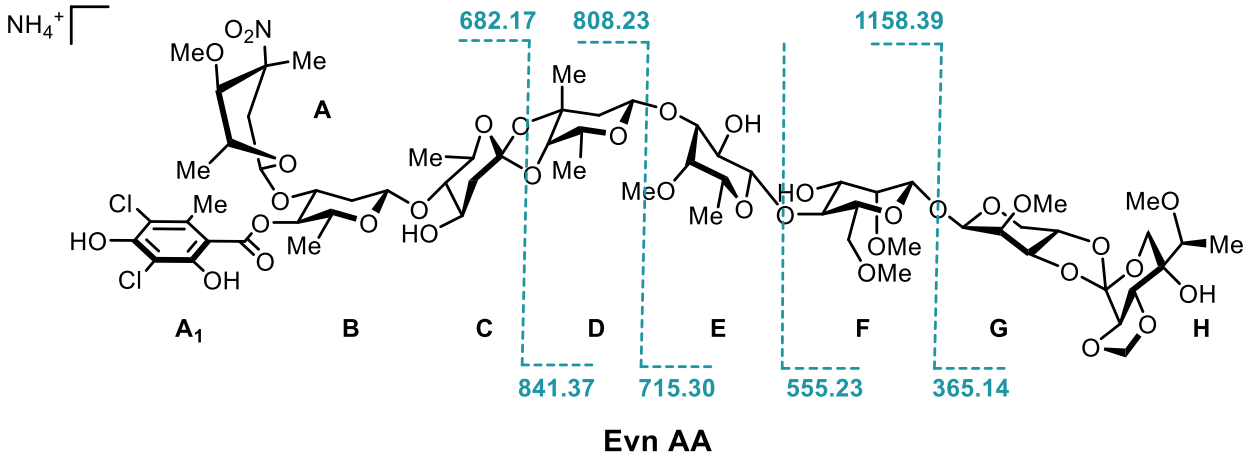

Evn AA

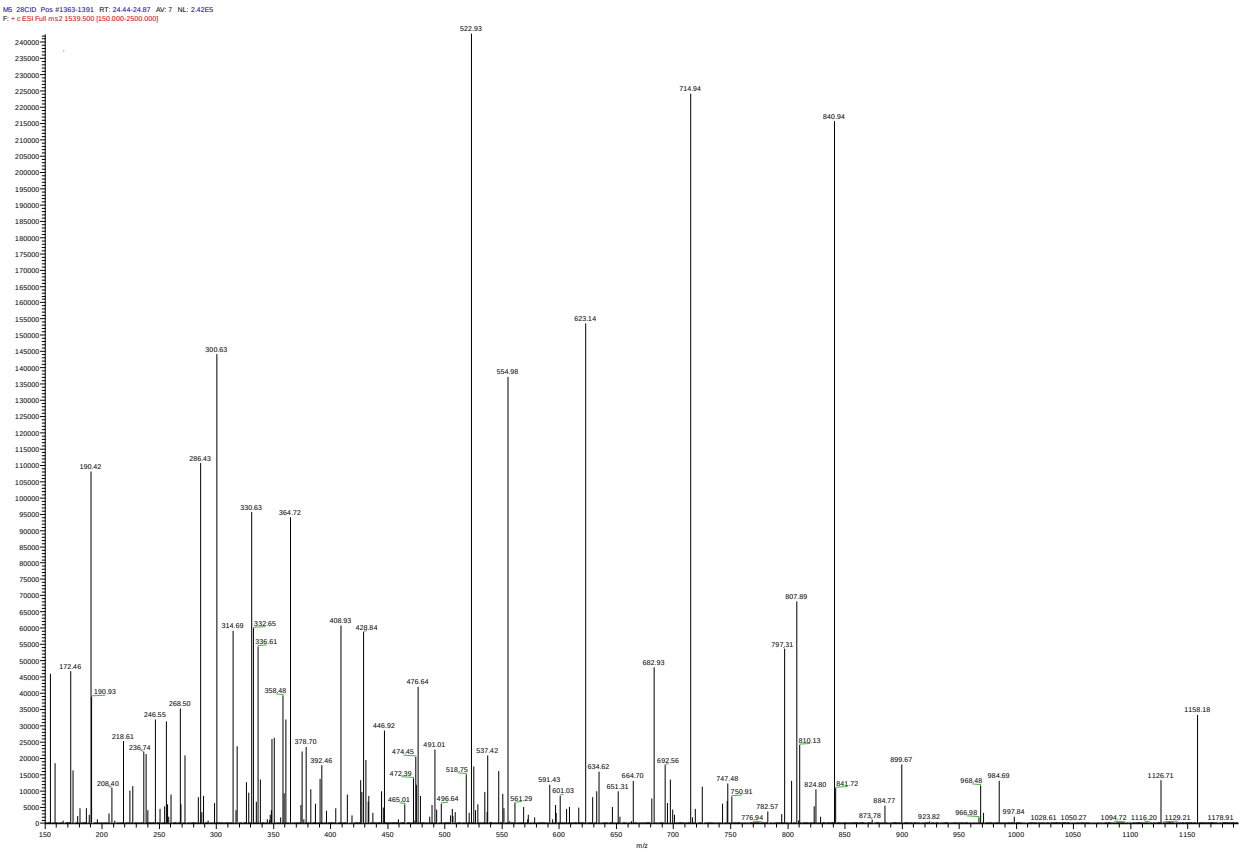

Figure A-19. Fragmentation data of everninomicin AB generated using CID TSQ MS. (A) Mass spectrometric fragmentation pattern for Evn AB. Dashed lines indicate positions of cleavage during fragmentation experiments. (B) Spectrum for fragmentation of Evn AB (m/z = 1492.5 $[M+H]^+$) at 28 volts.

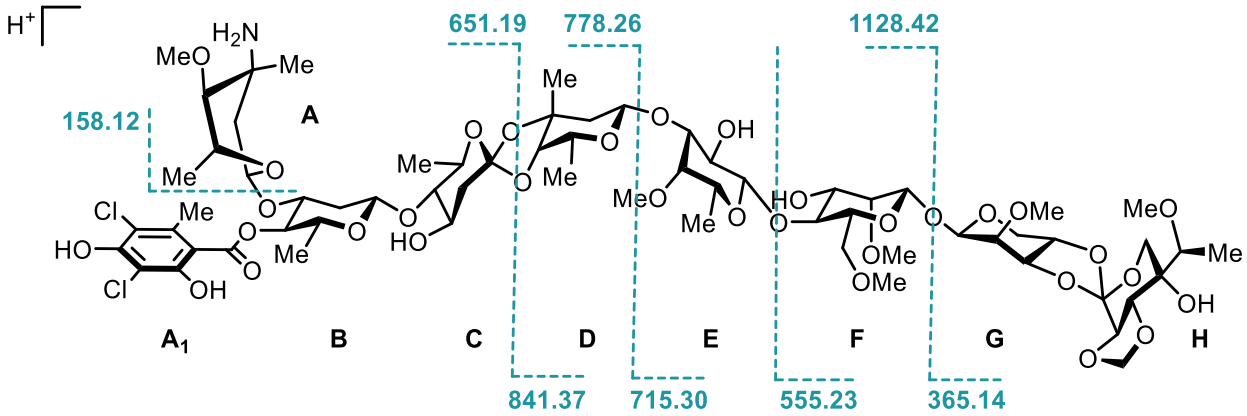

Evn AB

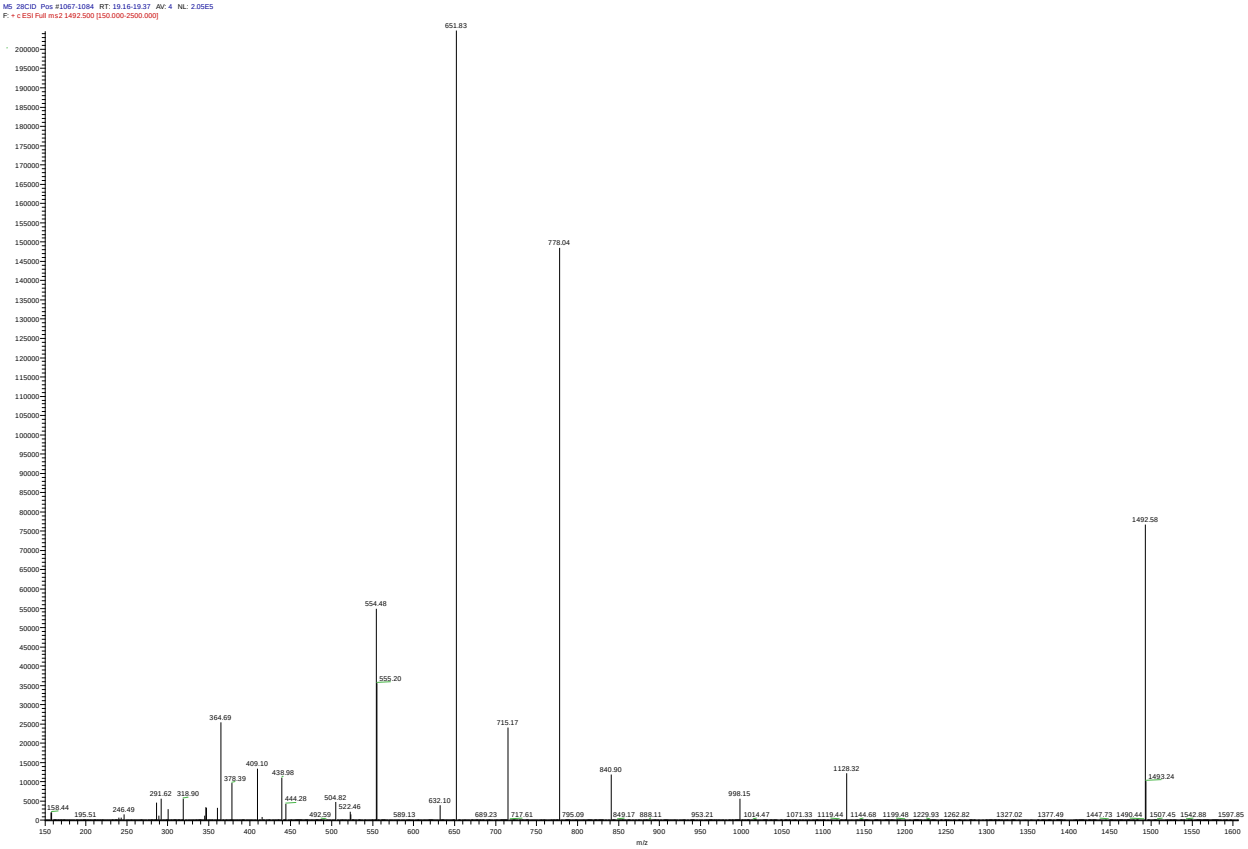

Figure A-20. Fragmentation data of everninomicin AC generated using CID TSQ MS. (A) Mass spectrometric fragmentation pattern for Evn AC. Dashed lines indicate positions of cleavage during fragmentation experiments. (B) Spectrum for fragmentation of Evn AC (m/z = 1505.7 $[M+H]^+$) at 25 volts.

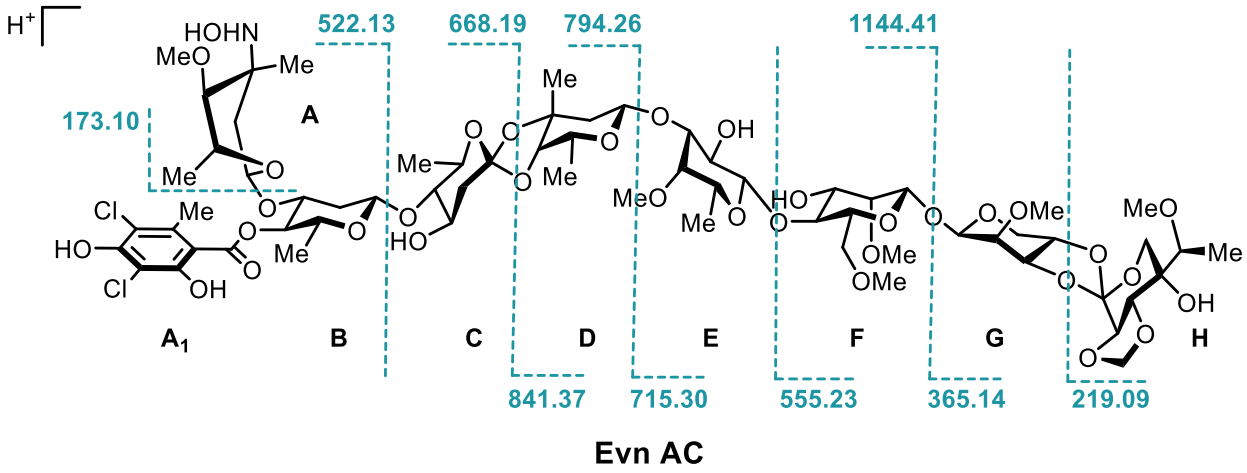

Evn AC

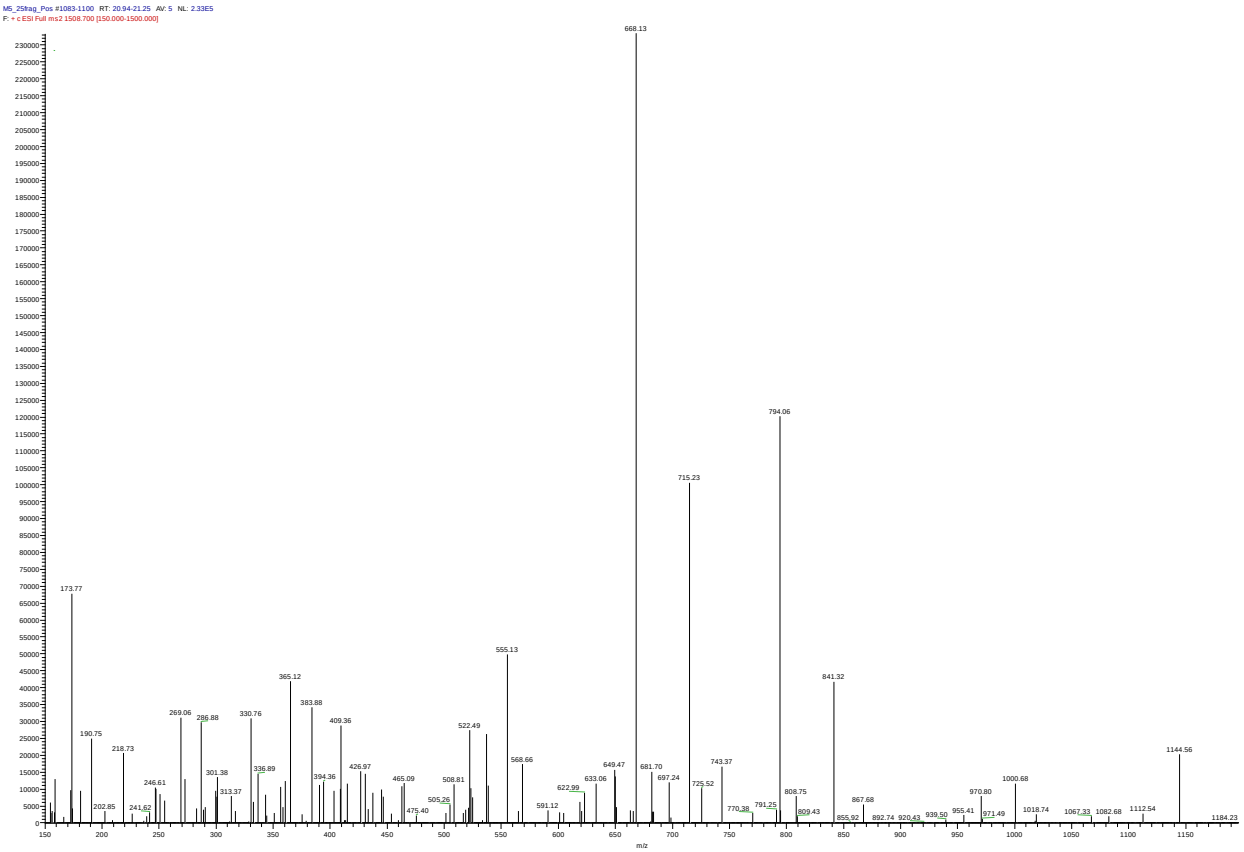

Figure A-21. Fragmentation data of everninomicin AD generated using CID TSQ MS. (A) Mass spectrometric fragmentation pattern for Evn AD. Dashed lines indicate positions of cleavage during fragmentation experiments. (B) Spectrum for fragmentation of Evn AD (m/z = 1523.9 $[M+H]^+$) at 25 volts.

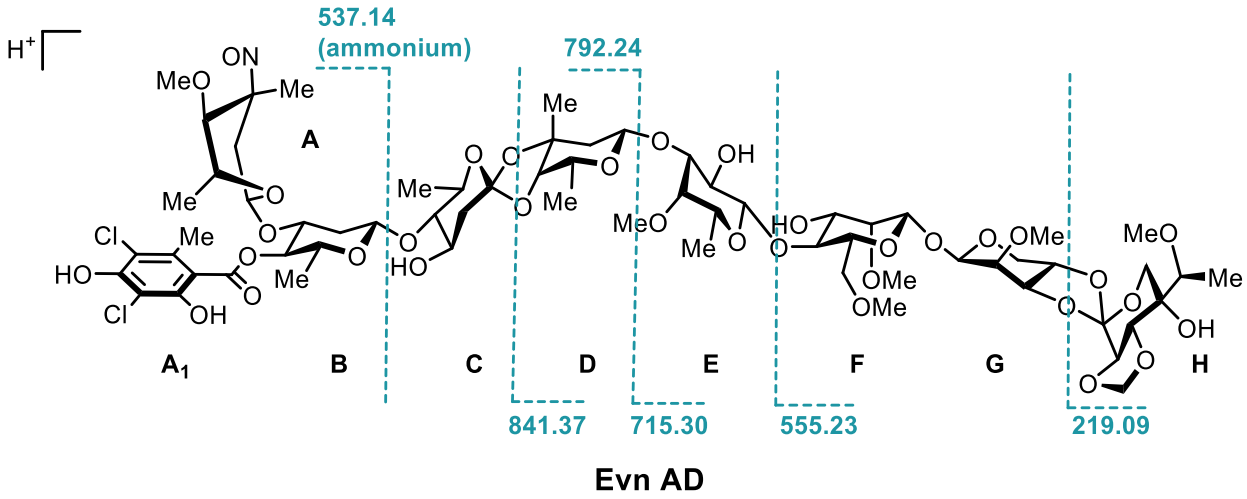

Evn AD

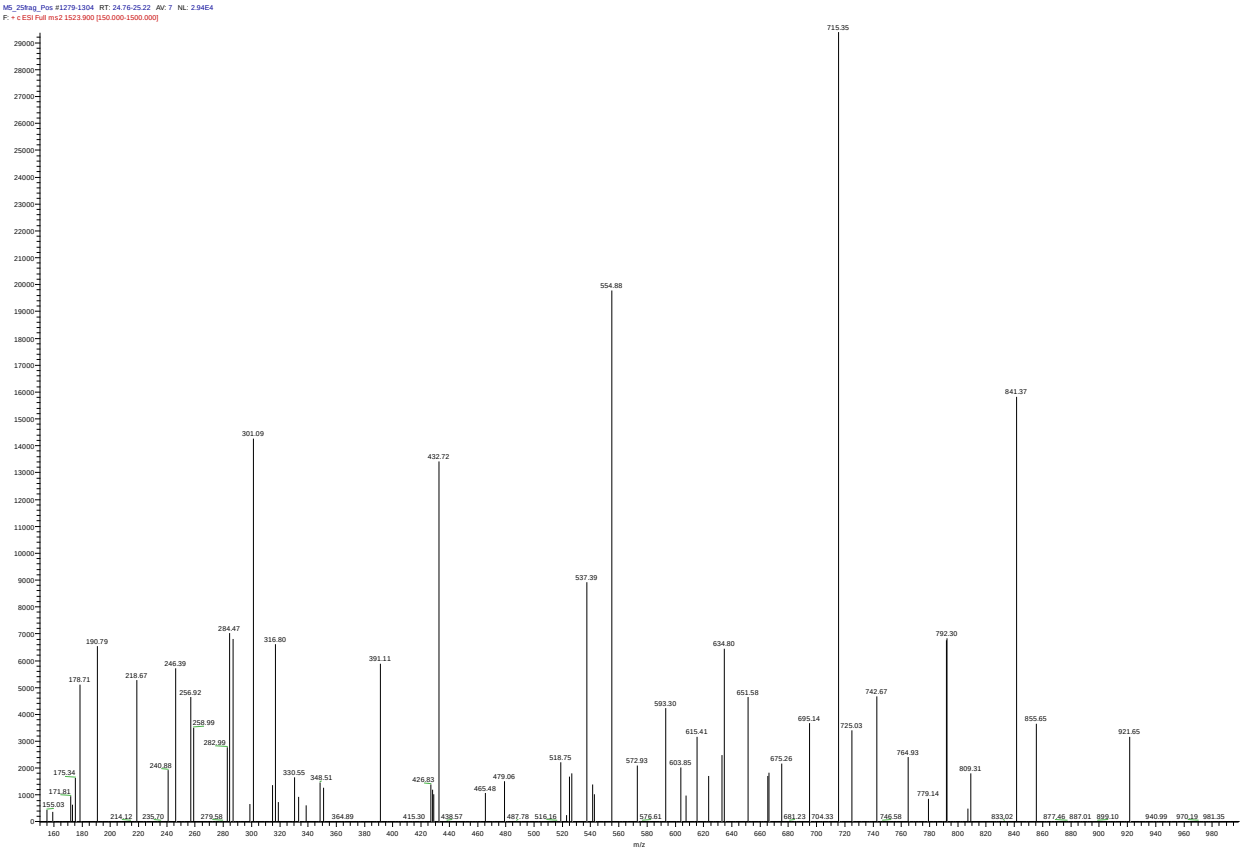

Figure A-22. Mass spectra of everninomicin AE. Theoretical mass for Evn AE ($C_{57}H_{84}Cl_2O_{31}$) is 1333.43 $[M-H]^-$ or 1352.47 $[M+NH_4]^+$. Experimental mass was determined to be 1333.37 $[M-H]^-$ and 1352.53 $[M+NH_4]^+$.

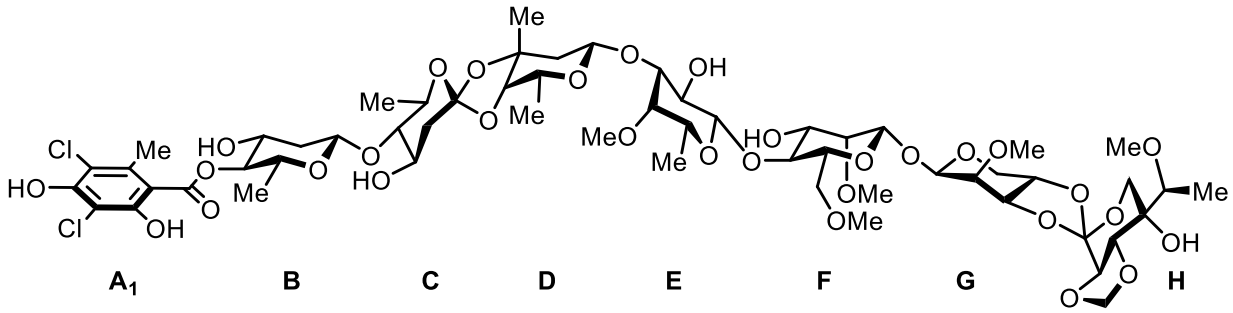

Evn AE

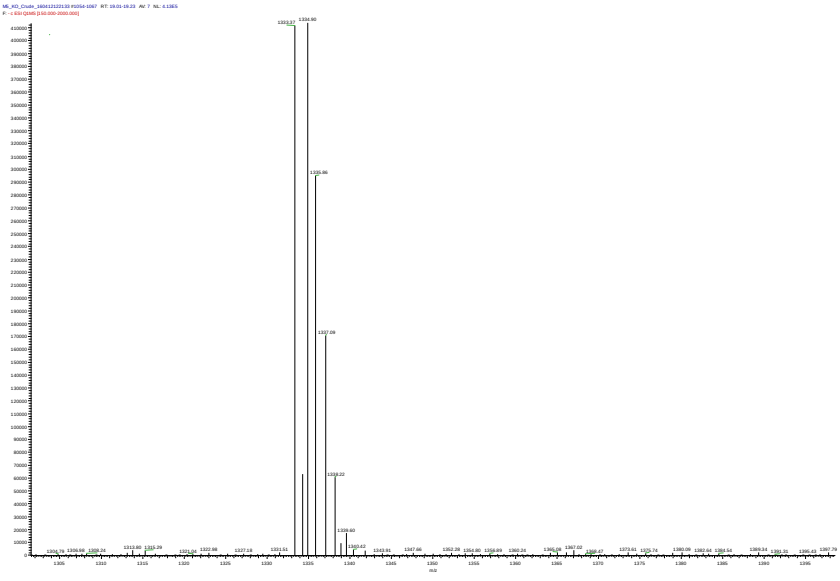

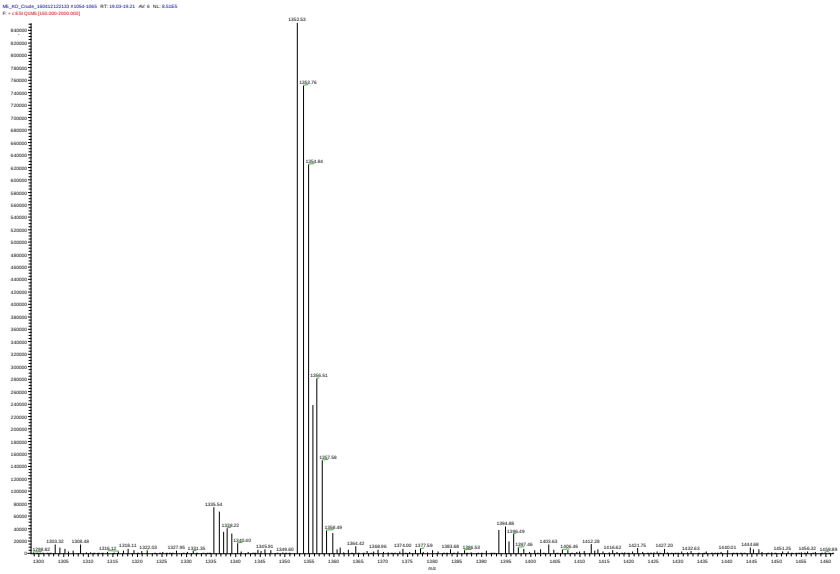

Figure A-23. Expression and purification of methyltransferases EvdM1 and EvdM5 from *E. coli*. Precision Plus Protein Kaleidoscope Prestained Protein Standards (Bio-Rad) used as ladder.

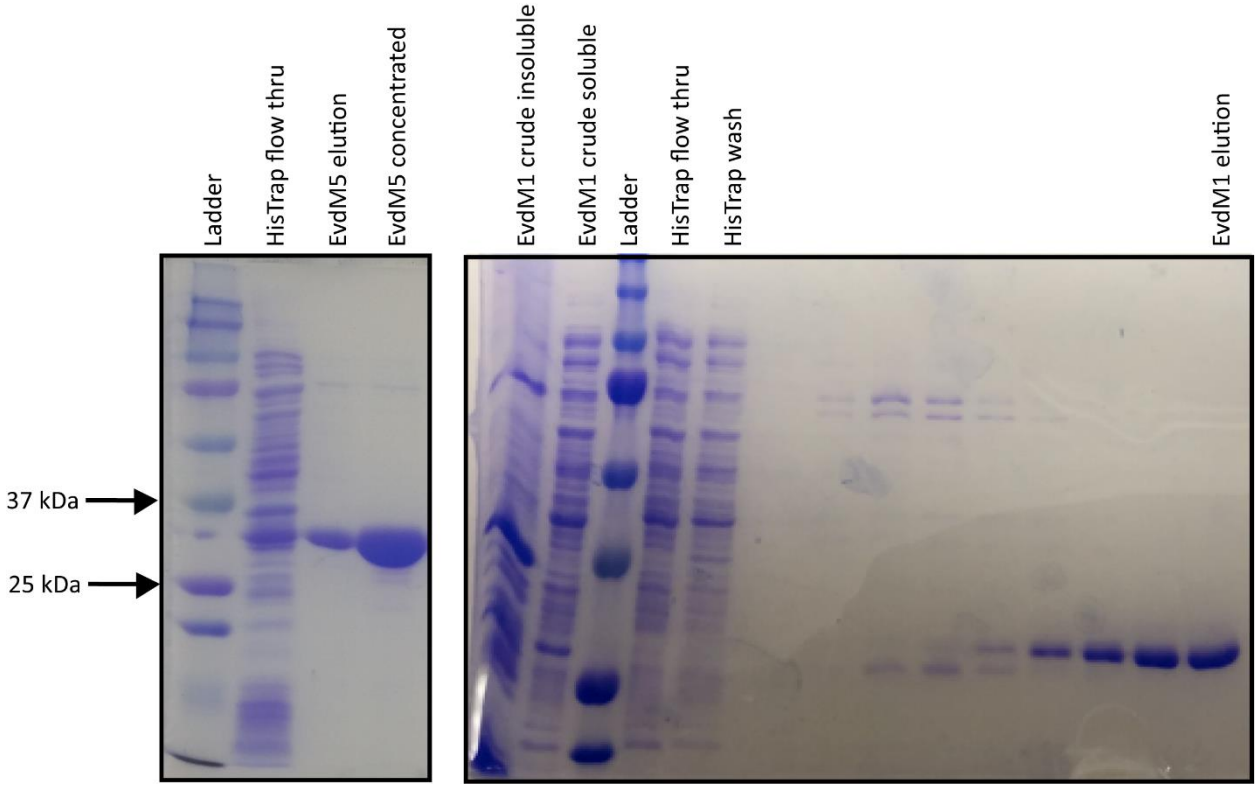

Figure A- 24. Fragmentation data of everninomicin E generated *in vitro* following incubation of everninomicin U with EvdM1 and S-adenosyl methionine. Evn E was fragmented using CID TSQ MS. (A) Mass spectrometric fragmentation pattern for Evn E. Dashed lines indicate positions of cleavage during fragmentation experiments. (B) Spectrum for fragmentation of Evn E (m/z = 1506.57 $[M+H]^+$) at 25 volts.

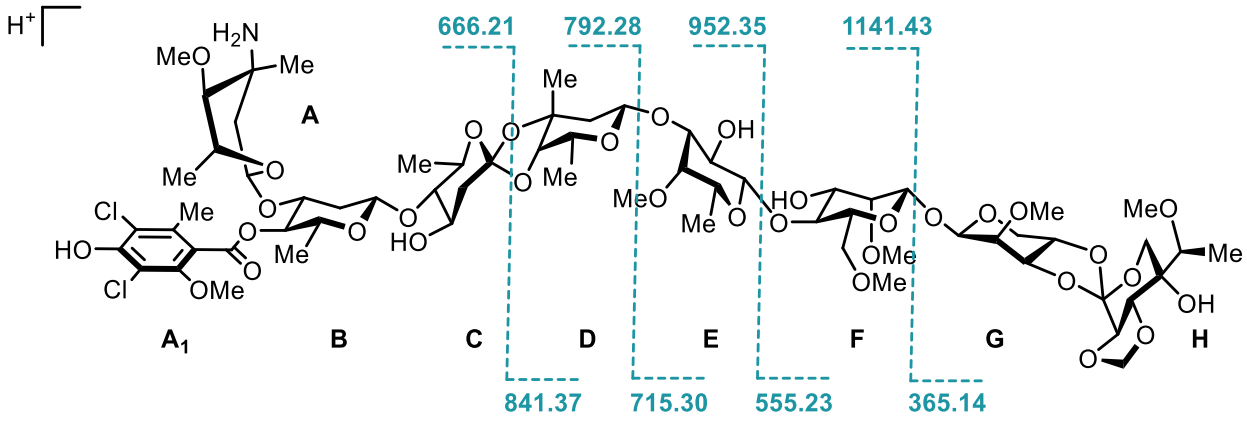

Evn E

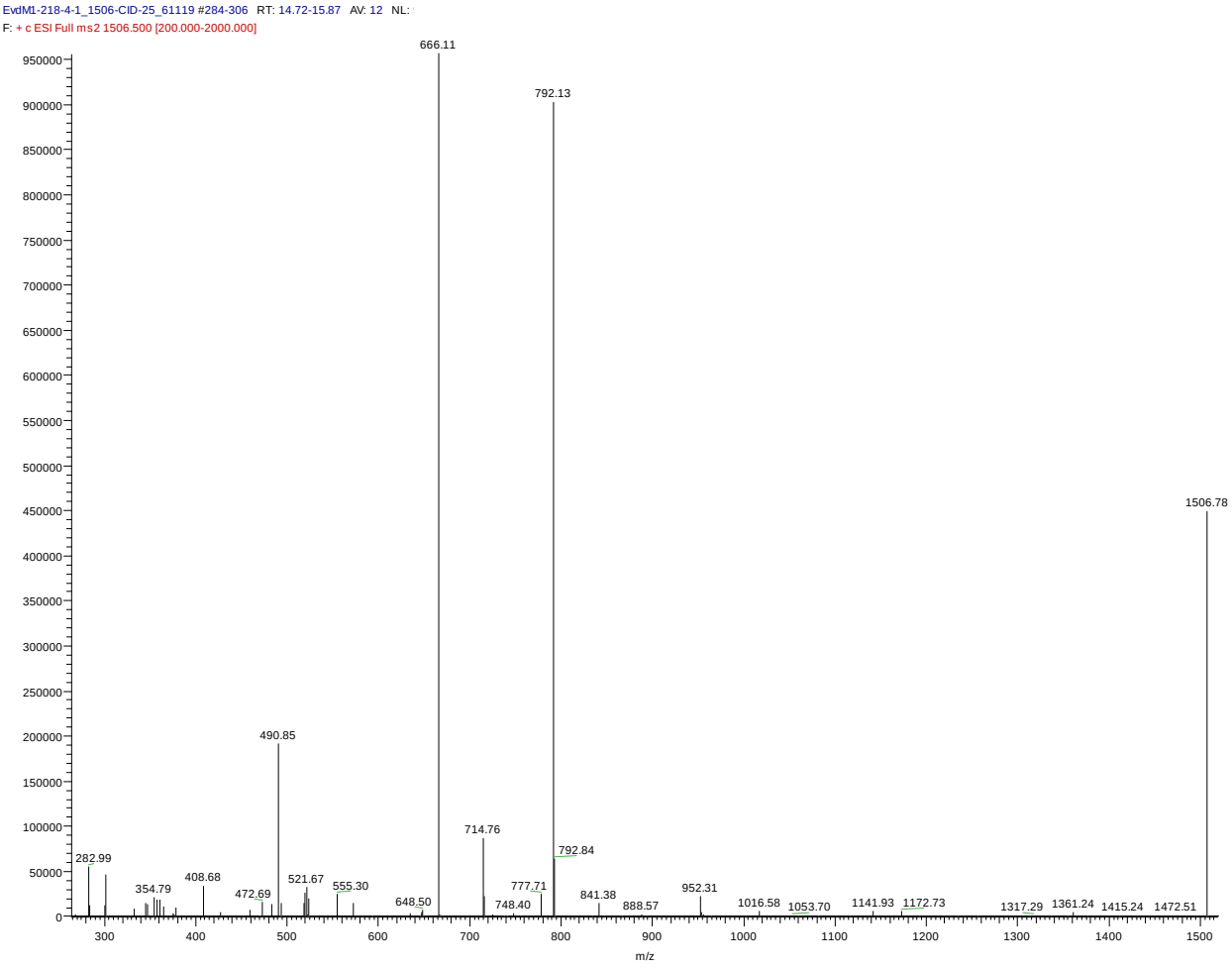

Table

Table A- 1. Masses of everninomicins shown in Chapter III.

Compound	Positive Mode (m/z)	Negative Mode (m/z)
Evn D	1536.5 $[M+H]^+$	1534.5 $[M-H]^-$
Evn E	1506.5 $[M+H]^+$	1504.5 $[M-H]^-$
Evn F	1522.5 $[M+H]^+$	1520.5 $[M-H]^-$
Evn G	1520.5 $[M+H]^+$	1518.5 $[M-H]^-$
Evn H	--	1522.5 $[M-H]^-$
Evn J	1494.5 $[M+H]^+$	1492.5 $[M-H]^-$
Evn K	1508.5 $[M+H]^+$	1506.5 $[M-H]^-$
Evn L	1555.5 $[M+H_2O]^+$	--
Evn T	1539.1 $[M+NH_4]^+$	1520.44 $[M-H]^-$
Evn U	1492.5 $[M+H]^+$	1490.4 $[M-H]^-$
Evn V	1508.7$[M+H]^+$	1506.3 $[M-H]^-$
Evn W	1523.5 $[M+NH_4]^+$	1504.4 $[M-H]^-$
Evn AA	1539.1 $[M+NH_4]^+$	1520.44 $[M-H]^-$
Evn AB	1492.5 $[M+H]^+$	1490.4 $[M-H]^-$
Evn AC	1508.7$[M+H]^+$	1506.3 $[M-H]^-$
Evn AD	1523.5 $[M+NH_4]^+$	1504.4 $[M-H]^-$
Evn AE	1352.5 $[M+NH_4]^+$	1333.3 $[M-H]^-$

Table A- 2. Evn H NMR Data.

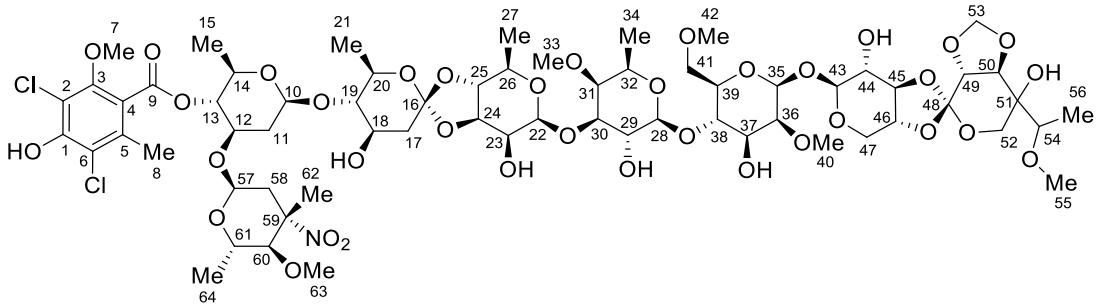

Pos.	^{13}C	^{1}H	HMBC
1	ND		
2	114.8		
3	154.1		
4	115.8		
5	134.2		
6	120.2		
7	60.8	3.88, 3H, s	3
8	17.4	2.34, 3H, s	4, 5, 6
9	166.8		
10	100.2	4.75, 1H, dd (4.7, 10 Hz)	19
11	36.0	1.61, 1H, m	
		2.46, 1H, m	10, 12, 13
12	72.3	3.99, 1H, overlap	13
13	75.4	4.81, 1H, overlap	9, 12, 14
14	70.8	3.72, 1H, m	
15	17.3	1.38, 3H, d (6.4 Hz)	13, 14
16	119.9		
17	39.4	1.84, 1H, dd (9.7, 12.7 Hz)	16, 18
		2.33, 1H, dd (5, 12.7 Hz)	
18	68.1	3.84, 1H, overlap	
19	86.7	3.17, 1H, t (9 Hz)	10, 18, 20, 21
20	69.9	3.73, 1H, m	
21	16.7	1.26, 3H, overlap	19, 20
22	102.5	4.80, 1H, overlap	23, 30
23	68.3	4.41, 1H, dd (1.9, 2.8 Hz)	22, 24, 25
24	78.3	3.78, 1H, overlap	25
25	76.3	3.69, 1H, overlap	
26	71.3	3.66, 1H, m	
27	17.3	1.31, 3H, d (5.5 Hz)	25, 26
28	103.5	4.24, 1H, d (7.8 Hz)	38
29	70.13	3.57, 1H, overlap	28, 30
30	82.8	3.67, 1H, overlap	22, 32
31	81.2	3.51, 1H, overlap	29, 30, 33
32	70.7	3.72, 1H, m	31
33	60.7	3.61, 3H, s	31
34	15.2	1.27, 3H, overlap	31, 32
35	95.8	4.83, 1H, overlap	36, 43
36	79.8	3.63, 1H, overlap	37, 40
37	72.3	3.65, 1H, overlap	
38	77.0	3.69, 1H, overlap	28, 37, 39
39	74.6	3.45, 1H, m	
40	60.7	3.56, 3H, s	36
41	70.5	3.75, 2H, overlap	
42	57.9	3.37, 3H, s	41
43	97.5	5.15, 1H, overlap	35, 44, 47
44	68.6	4.31, 1H, overlap	45, 46
45	80.5	3.89, 1H, dd (2.7, 10.3 Hz)	
46	68.8	4.34, 1H, overlap	

Pos.	^{13}C	^{1}H	HMBC
47	63.0	3.82, 1H, overlap	
		4.08, 1H, dd (4.5, 9.7 Hz)	43, 45, 46
48	119.8		
49	72.8	3.88, 1H, overlap	50
50	77.0	3.87, 1H, overlap	49
51	75.7		
52	68.9	3.61, 1H, overlap	48, 50, 51
		4.01, 1H, d (12.3 Hz)	51
53	95.3	5.02, 1H, overlap	49
		5.06, 1H, overlap	50
54	79.5	3.31, 1H, m	50, 51, 52, 55
55	56.1	3.33, 1H, s	54
56	12.6	1.25, 3H, overlap	51, 54
57	92.8	5.03, 1H, dd	59, 61
58	40.2	2.08, 1H, dd (1, 13 Hz)	57, 59, 60
		2.44, 1H, dd (5, 13.5 Hz)	59, 62
59	89.9		
60	84.4	3.60, 1H, overlap	59, 61, 63
61	65.9	3.51, 1H, m	
62	18.4	1.68, 3H, s	58, 59, 60
63	59.7	3.30, 3H, s	60
64	16.5	0.77, 3H, d (6 Hz)	60, 61

Table A- 3. Primers used in Chapter III.

Primer Name	Used for	Sequence (5'-3')
RED-M2-For	Δ*evdM2*::*aac(3)IV*	GACACCGCCGGTCCACCGTGGGCAGGAGCCCCGGCGGTGATTCCGGGGATCCGTCGACC
RED-M2-Rev	Δ*evdM2*::*aac(3)IV*	CCACGCTCTCGTCATACGCTGATGCGGTCCGACTCACGTTGTAGGCTGGAGCTGCTTC
RED-M3-For	Δ*evdM3*::*aac(3)IV*	CGCCCGGAAACCCCACACGAAGGAGACCGCTACGTGAGTATTCCGGGGATCCGTCGACC
RED-M3-Rev	Δ*evdM3*::*aac(3)IV*	CCGCCGCGGCGAGCAGCCGCTGGACGAGCGAGCCGGTCATGTAGGCTGGAGCTGCTTC
RED-M1-For	Δ*evdM1*::*aac(3)IV*	GTGGCCGCAGCCGATCCCAATGCGCGAAGGACCGTCATGATTCCGGGGATCCGTCGACC
RED-M1-Rev	Δ*evdM1*::*aac(3)IV*	GTGCCGCCGGTCCGGATCCCGTCGGTGGATCGAGGCTCATGTAGGCTGGAGCTGCTTC
RED-M5-For	Δ*evdM5*::*aac(3)IV*	CCGTGGCCGGCAGTGCTGCGGCTGGTGTTCGGCGGGATGATTCCGGGGATCCGTCGACC
RED-M5-Rev	Δ*evdM5*::*aac(3)IV*	ACCTCCTGGACGACGACTCGACCGGTTGGCGGACGGTCATGTAGGCTGGAGCTGCTTC
EvdM2-Southern-For	EvdM2 Southern Probe	CGTTCGGGTAGTCGTAGACC
EvdM2-Southern-Rev	EvdM2 Southern Probe	ACTAGGGTTTCCCCCACAAC
EvdM3-Southern-For	EvdM3 Southern Probe	TACGCGCACTTCATCGATCT
EvdM3-Southern-Rev	EvdM3 Southern Probe	GATACGTGTCCAGGGAGCTG
Apr-Southern-For	Apramycin Southern Probe	ACCGACTGGACCTTCCTTCT
Apr-Southern-Rev	Apramycin Southern Probe	TCGCTATAATGACCCCGAAG
EvdM3-GC-For	pSET152ermE*-evdM3	CATATGGTGAGTCGGACCGCATCA
EvdM3-GC-Rev	pSET152ermE*-evdM3	GATATCTCACGACCCCACCCGCGA
HygBCheck-For	Confirm GC vectors	GATTCGGATGATTCCTACGC
HygBCheck-Rev	Confirm GC vectors	GAAGGCGTTGAGATGCAGTT
Del-Up	Confirm gene replacements	ATTCCGGGGATCCGTCGACC
Del-Dn	Confirm gene replacements	TGTAGGCTGGAGCTGCTTC
Neo-Up	Confirm double crossover	AATATCACGGGTAGCCAACG
Neo-Dn	Confirm double crossover	GTGGAGAGGCTATTCGGCTA
EvdM1-For	EvdM1 Gibson Cloning	CTGGTGCCGCGCGGCAGCATGGAGCATCCCCGAAGTCTCTATCTTGATCTCCT
EvdM1-Rev	EvdM1 Gibson Cloning	GTCGACGGAGCTCGAATTCGTCAGGCCGCCCGCCGCCA
EvdM5-For	EvdM5 PCR Cloning	TTAAATTCATATGGCGACGCACGTGGTC
EvdM5-Rev	EvdM5 PCR Cloning	GGATCCTAATCAATCGGGACAGAGCTCGA

Table A- 4. Methyltransferases and GenBank protein identities utilized for phylogenetic analysis of orthosomycins methyltransferases.

Protein ID	Producing Strain	Associated Secondary Metabolite	Designation
QLD23463	*M. carbonacea* var. *aurantiaca*	Everninomicins (D-G)	EvdM1
QLD23467	*M. carbonacea* var. *aurantiaca*	Everninomicins (D-G)	EvdM2
QLD23468	*M. carbonacea* var. *aurantiaca*	Everninomicins (D-G)	EvdM3
QLD23469	*M. carbonacea* var. *aurantiaca*	Everninomicins (D-G)	EvdM4
QLD28327	*M. carbonacea* var. *aurantiaca*	Everninomicins (D-G)	EvdM5
QLD23476	*M. carbonacea* var. *aurantiaca*	Everninomicins (D-G)	EvdM6
QLD28328	*M. carbonacea* var. *aurantiaca*	Everninomicins (D-G)	EvdM7
QLD28329	*M. carbonacea* var. *aurantiaca*	Everninomicins (D-G)	EvdOM1
QLD23500	*M. carbonacea* var. *aurantiaca*	Everninomicins (D-G)	EvdM8
QLD23502	*M. carbonacea* var. *aurantiaca*	Everninomicins (D-G)	EvdM9
AAK83176	*S. viridochromogenes* Tü57	Avilamycins (A & C)	AviG1
AAK83184	*S. viridochromogenes* Tü57	Avilamycins (A & C)	AviG2
AAK83188	*S. viridochromogenes* Tü57	Avilamycins (A & C)	AviG3
WP_003998210	*S. viridochromogenes* Tü57	Avilamycins (A & C)	AviG4
AAK83180	*S. viridochromogenes* Tü57	Avilamycins (A & C)	AviG5
AAK83186	*S. viridochromogenes* Tü57	Avilamycins (A & C)	AviG6
CAI94729	*S. achromogenes* var. *rubradiris*	Rubradirin	RubN7
CAA11777	*Amycolatopsis orientalis*	Chloroeremomycin	EvaC
5T6B_A	*Antinomadura kijaniata*	Kijanimicin	KijD1
CDI07214	*Rhizobium* sp. IRBG74	Phosphatidylcholines	PmtA

Appendix B Supporting data for Chapter IV

Figure B-1. Fragmentation data of everninomicin Q generated using CID TSQ MS. Mass spectrometric fragmentation pattern for Evn Q. Dashed lines indicate positions of cleavage during fragmentation experiments. Spectrum for fragmentation of Evn Q (*m/z* = 1134.4 $[M+NH_4]^+$) at 20 volts.

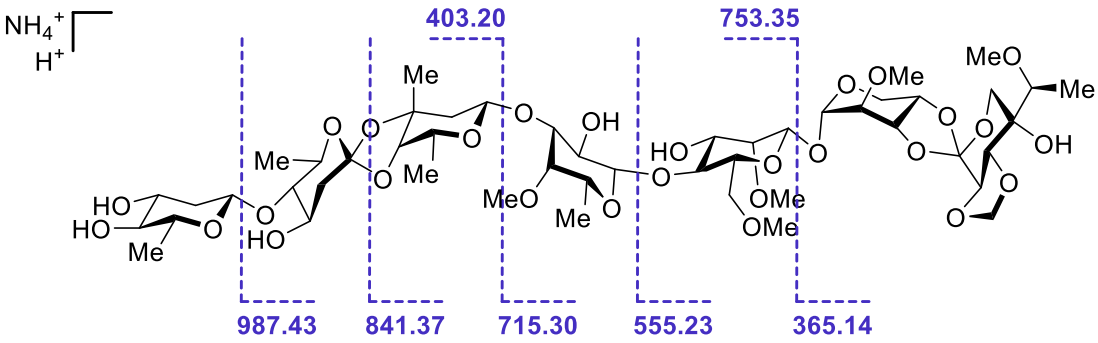

Everninomicin Q

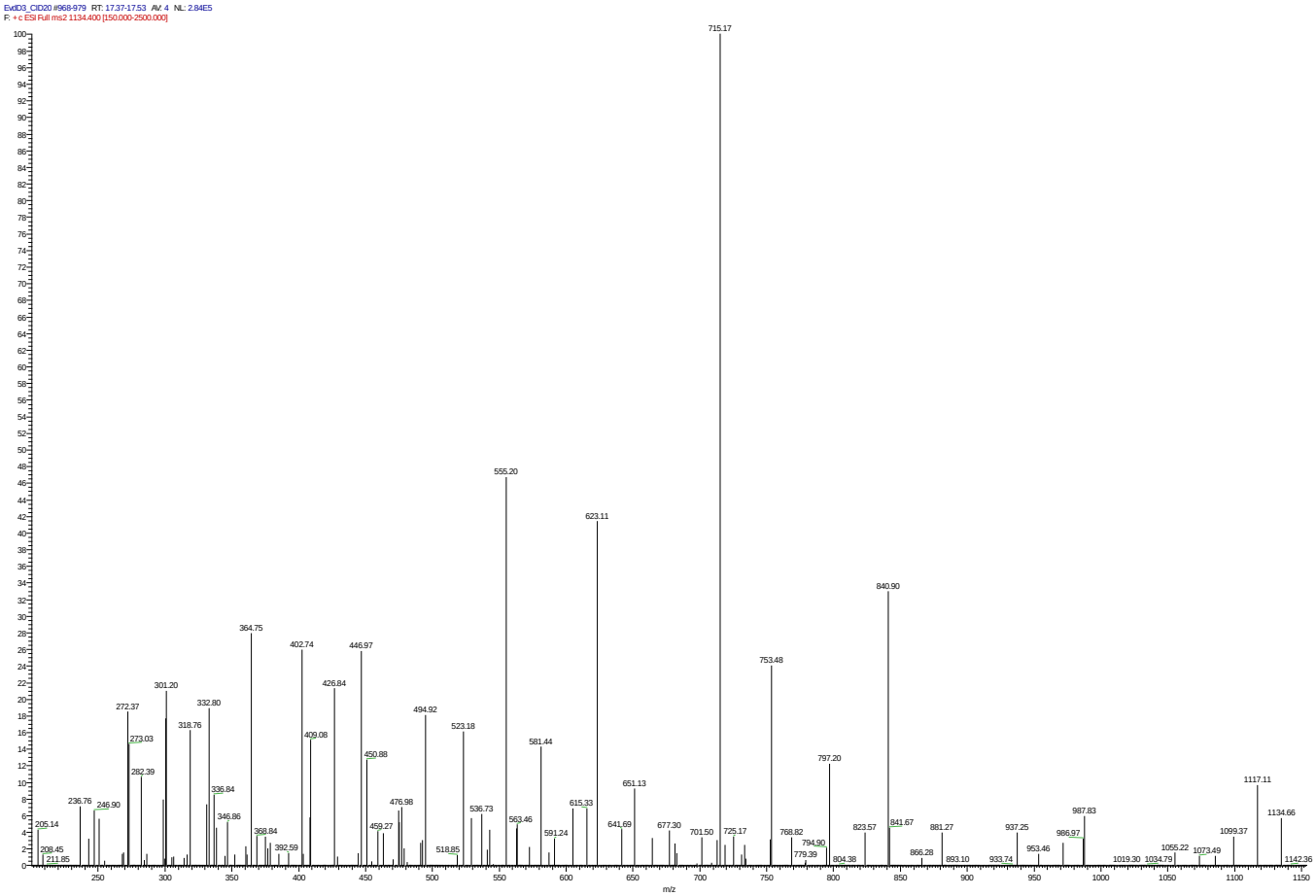

Figure B-2. Fragmentation data of everninomicin R generated using CID TSQ MS. Mass spectrometric fragmentation pattern for Evn R. Dashed lines indicate positions of cleavage during fragmentation experiments. Spectrum for fragmentation of Evn R (*m/z* = 1270.6 $[M+H]^+$) at 20 volts.

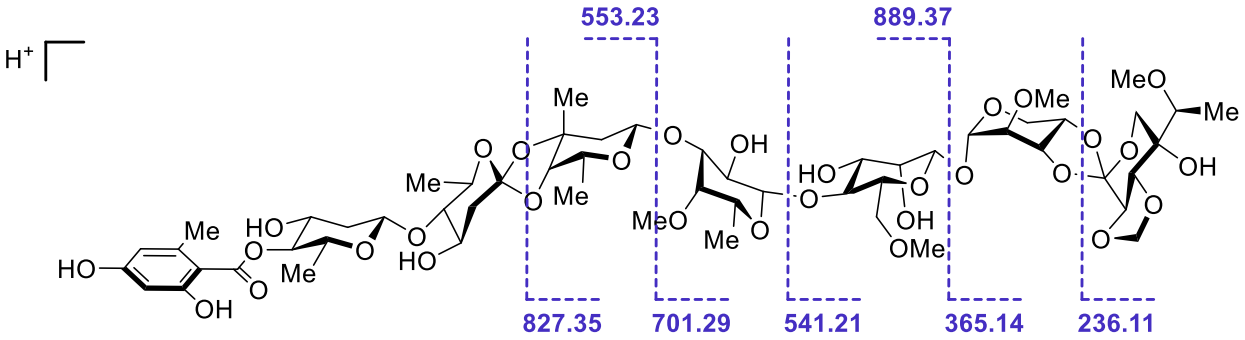

Everninomicin R

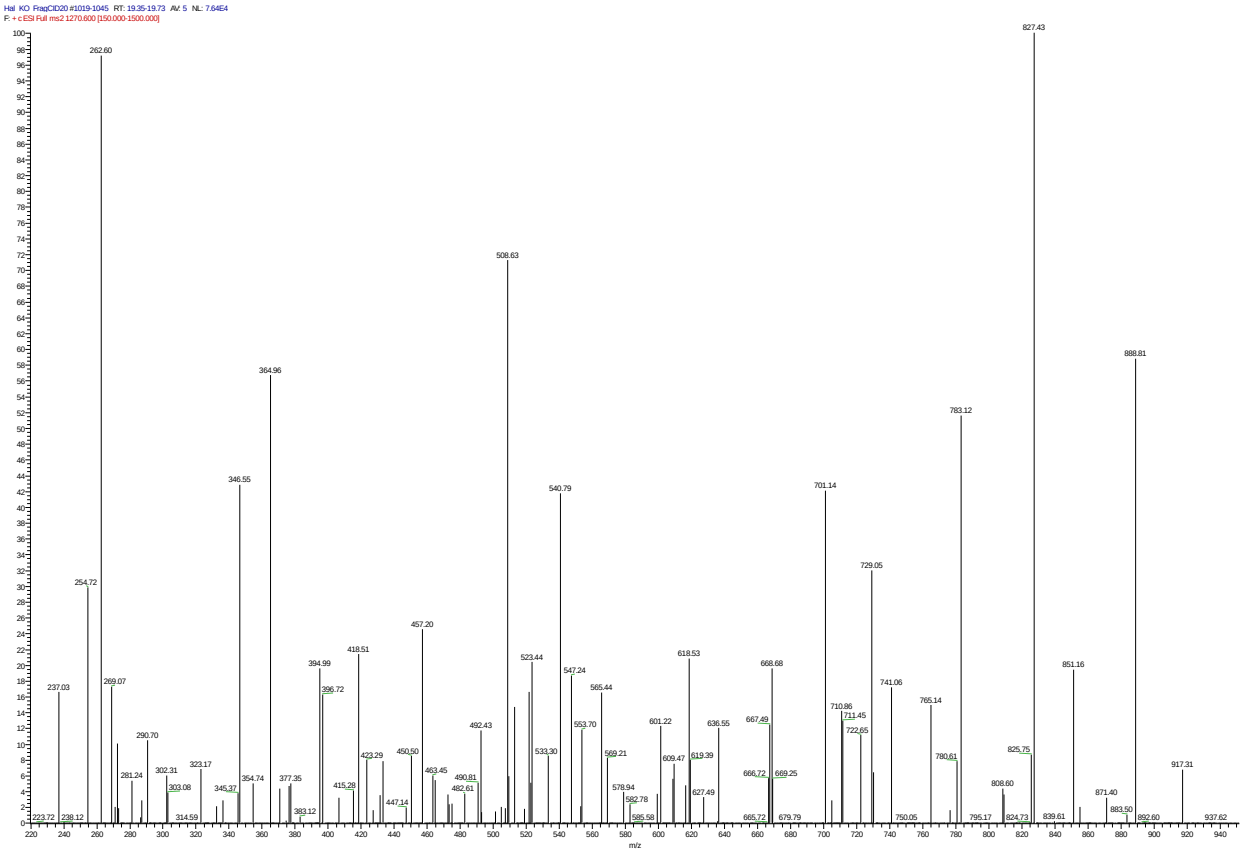

Figure B-3. Fragmentation data of everninomicin S generated using CID TSQ MS. Mass spectrometric fragmentation pattern for Evn S. Dashed lines indicate positions of cleavage during fragmentation experiments. Spectrum for fragmentation of Evn S (*m/z* = 1284.6[M+H]$^+$) at 20 volts.

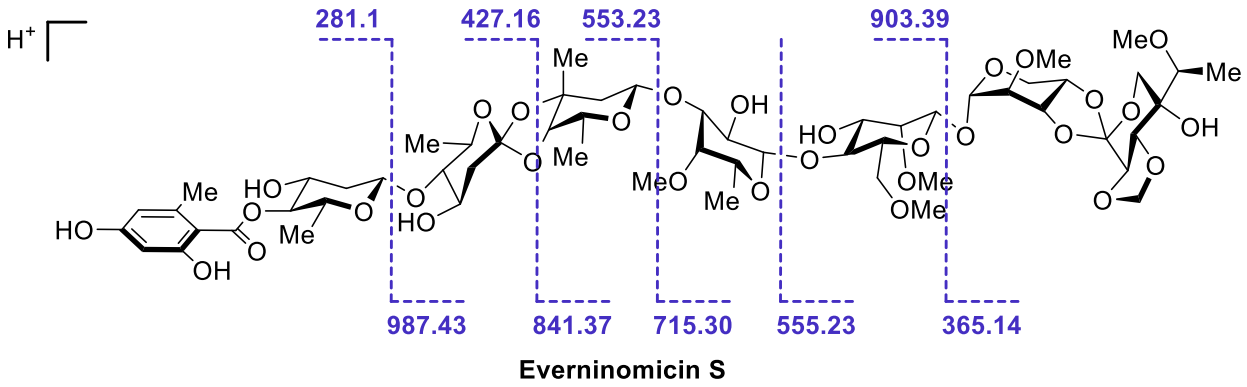

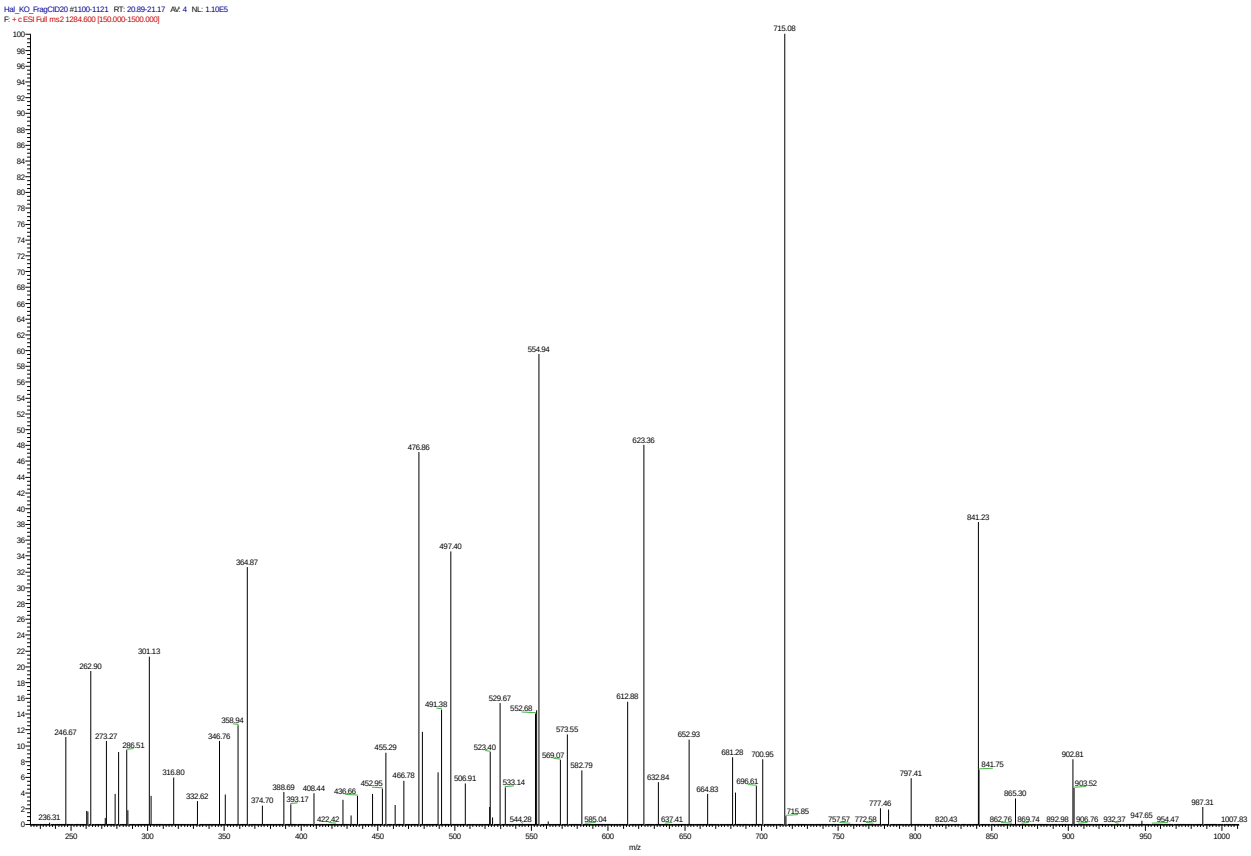

Figure B-4. Map of EvdD1+pET28a(+), the EvdD1 production plasmid. Plasmid map was generated using SnapGene.

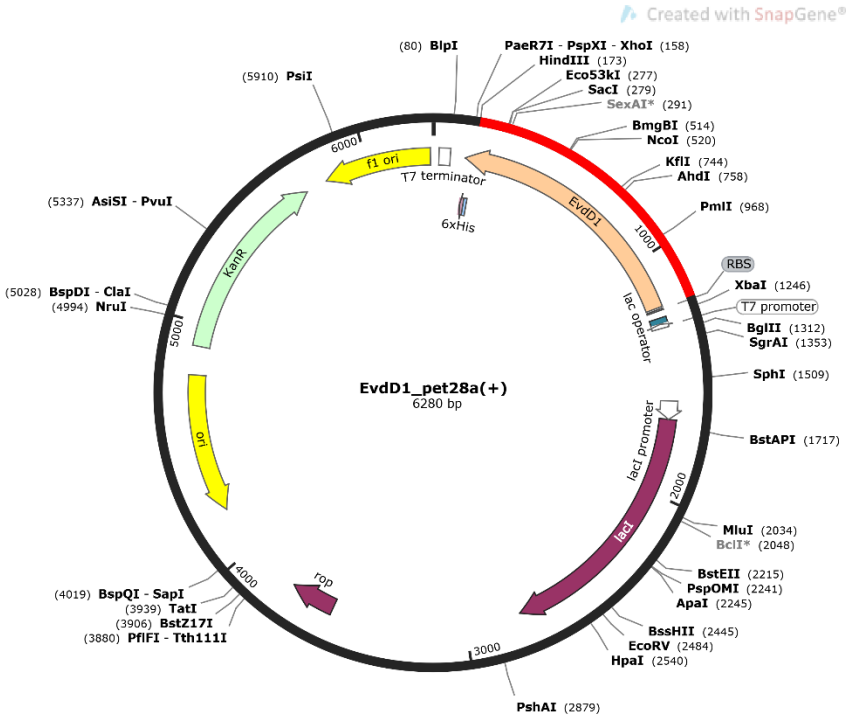

Figure B-5. Map of EvdD2+pET28a(+), the EvdD2 production plasmid. Plasmid map was generated using SnapGene.

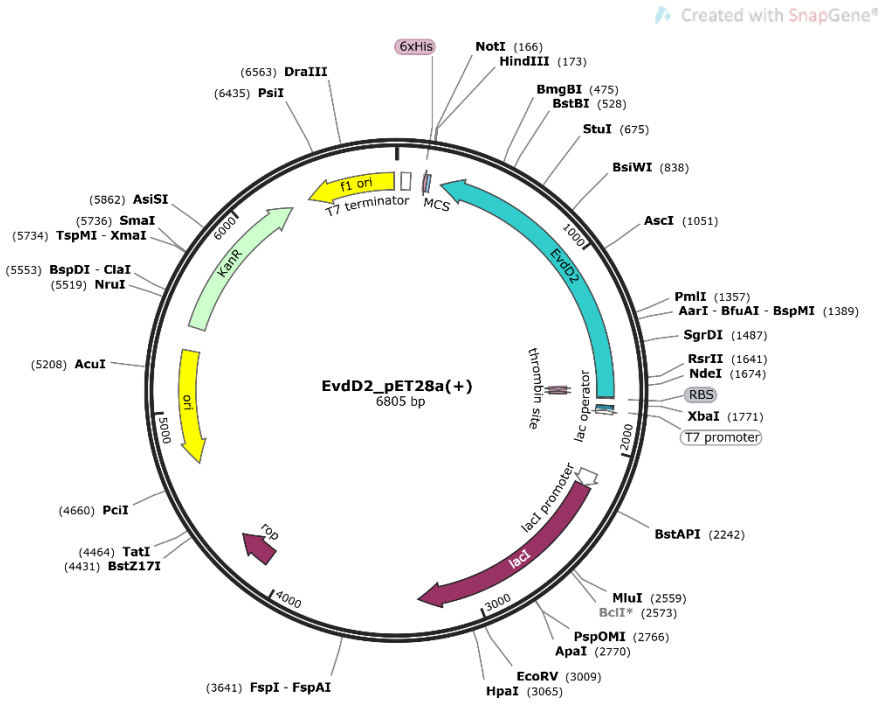

Figure B-6. Map of EvdD3+pET28a(+), the EvdD3 production plasmid. Plasmid map was generated using SnapGene.

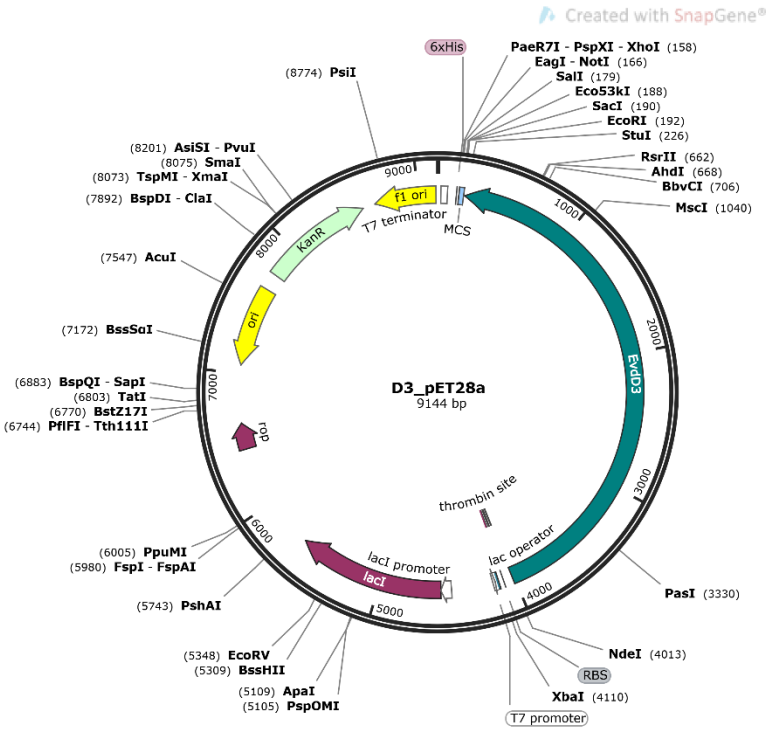

Figure B-7. Map of sfp+CDFDuet, the sfp production plasmid. Plasmid map was generated using SnapGene.

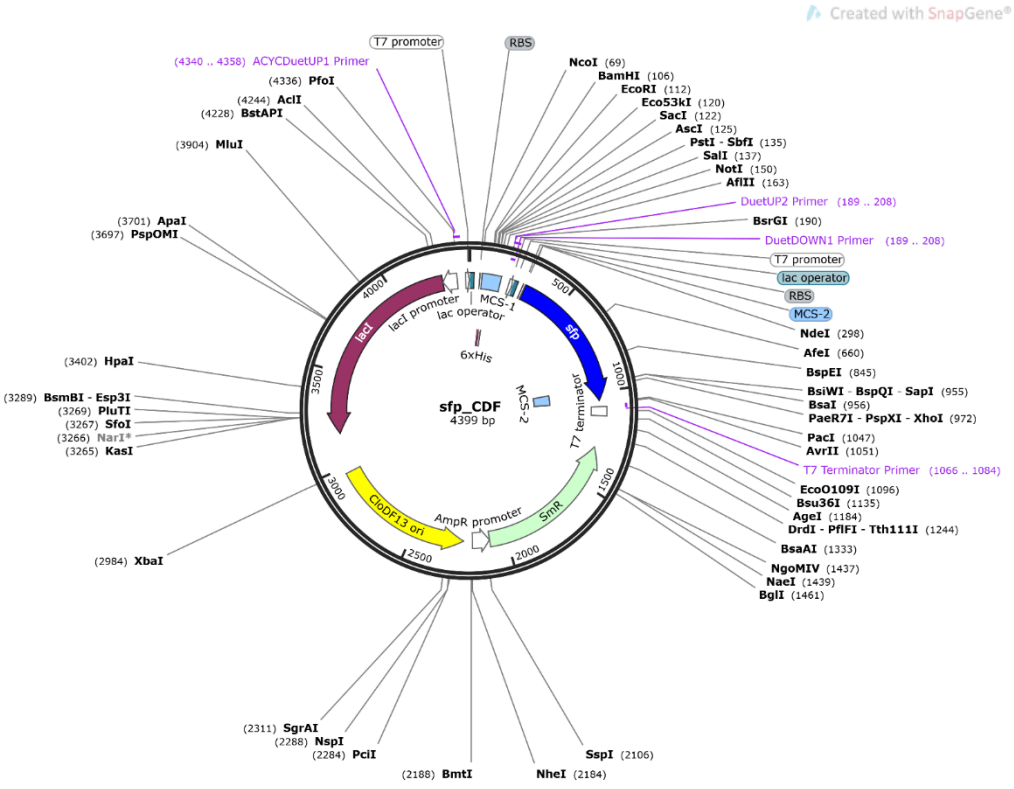

Figure B-8. Synthetic routes for orsellinic acid derivatives Previous route from Nicolaou and coworkers. Our abbreviated route to access both OSA and di-chloro OSA in only two steps.

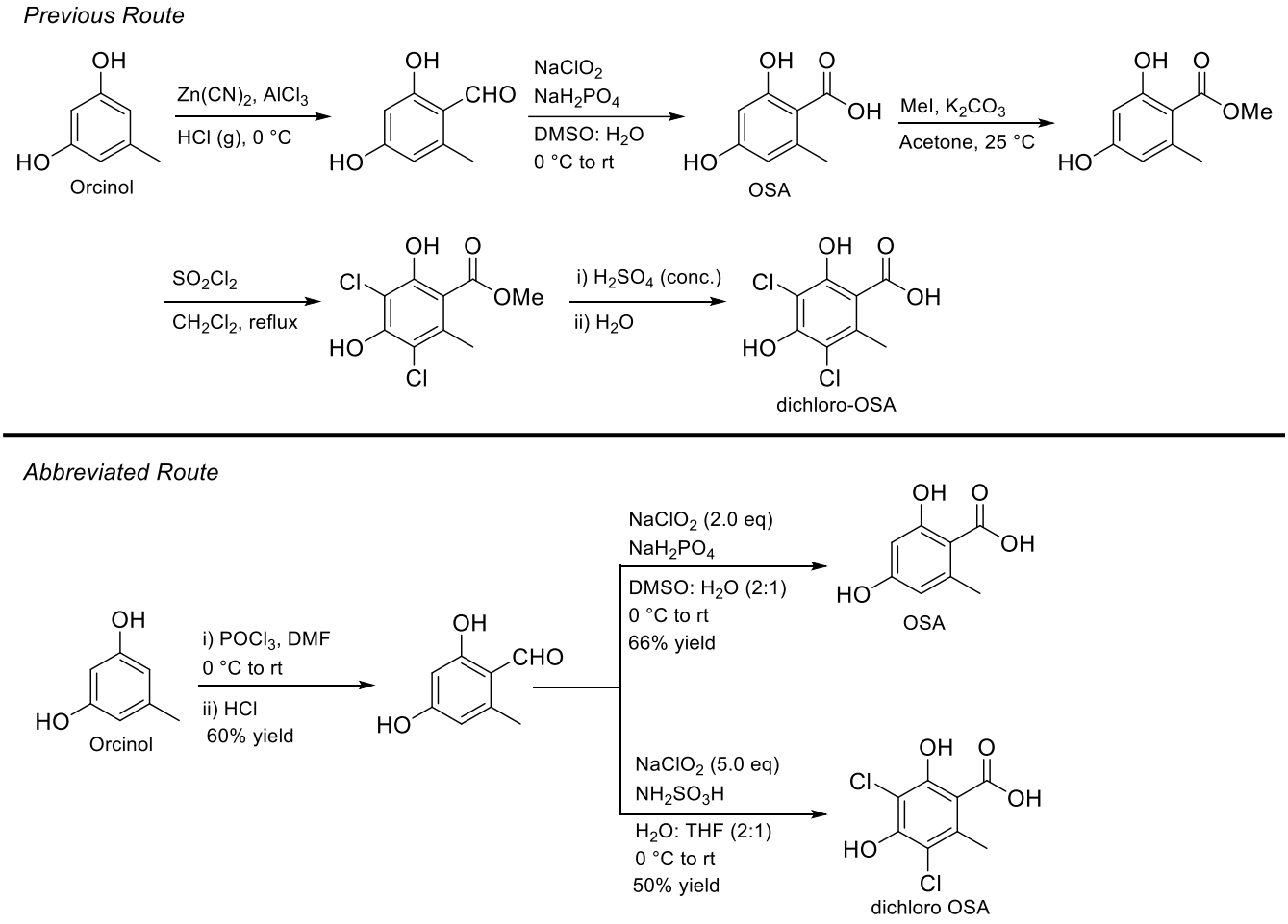

Figure B-9. EIC of everninomicin AE from D2 turnover following incubation with Evn S and the necessary cofactors and auxiliary proteins (Figure 3-3D). Calculated Evn AE *m/z* = 1333.43 $[M-H]^-$.

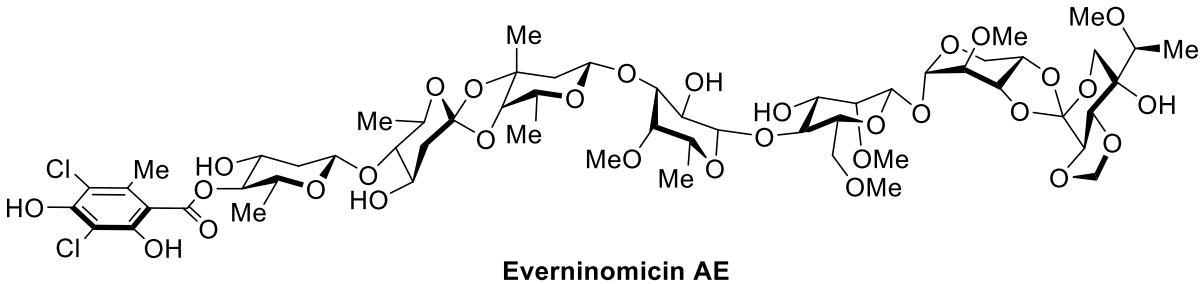

Everninomicin AE

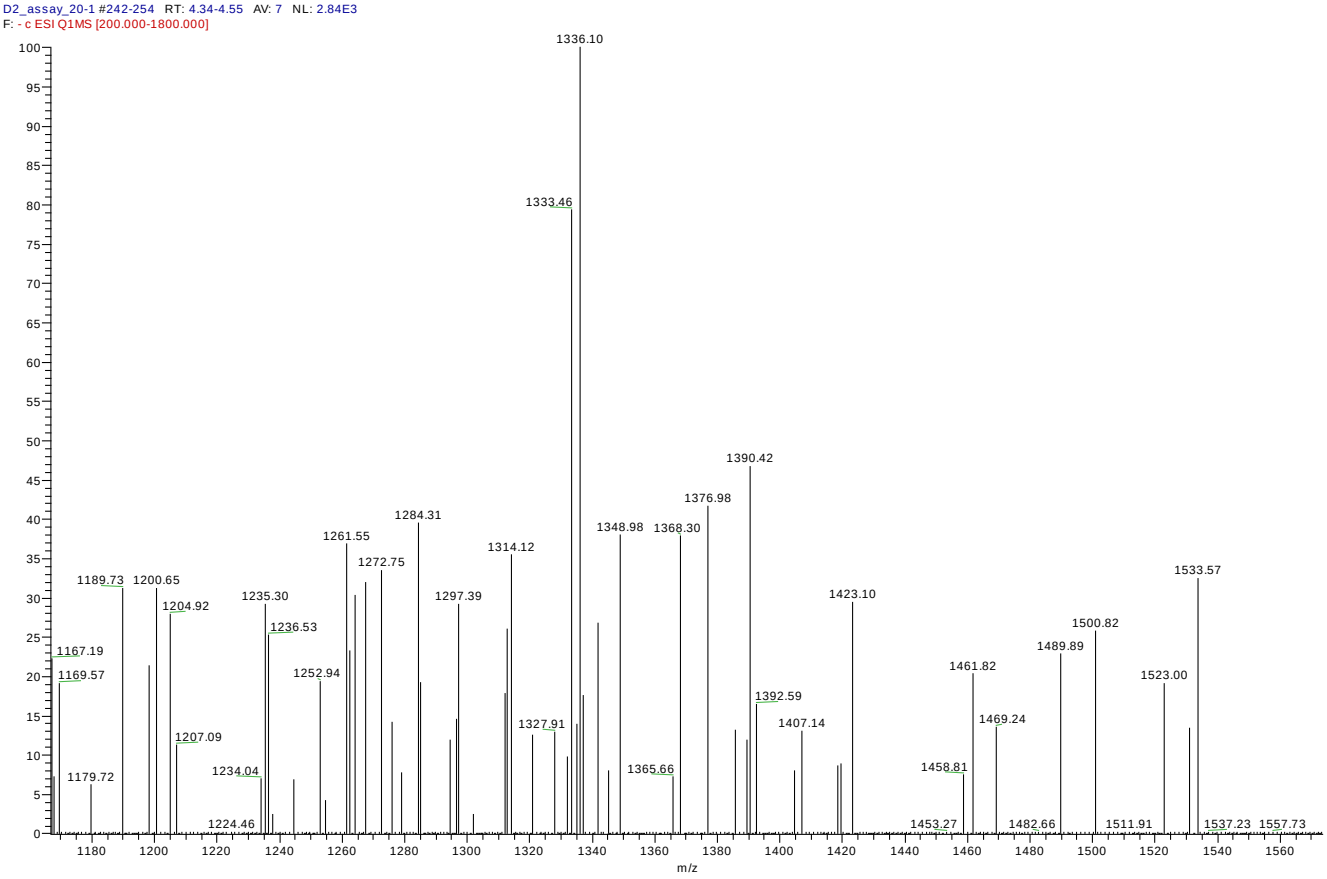

Figure B-10. Structures and NMR assignments for NAC thioesters in Chapter IV.

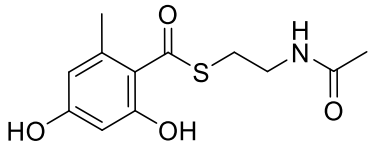

S-(2-acetamidoethyl) 2,4-dihydroxy-6-methylbenzothioate (OSA-NAC): ^{1}H NMR (400 MHz, CD_3OD); δ 6.16 (s, 1H), 6.15 (s, 1H), 3.44 (t, J = 6.8 Hz, 2H), 3.15 (t, J = 6.6 Hz, 2H), 2.27 (s, 3H), 1.94 (s, 3H).

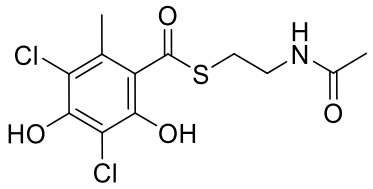

S-(2-acetamidoethyl) 3,5-dichloro-2,4-dihydroxy-6-methylbenzothioate (DC-OSA-NAC): ^{1}H NMR (400 MHz, $CDCl_3$); δ 6.04 (bs, 1 Hz), 3.58 (t, J = 6.1 Hz, 2H), 3.22 (t, J = 6.2 Hz, 2H), 2.45 (s, 3H), 1.99 (s, 3H).

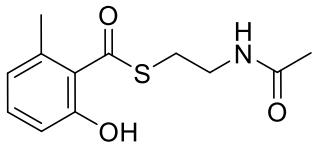

S-(2-acetamidoethyl) 2-hydroxy-6-methylbenzothioate (6MSA-NAC): ^{1}H NMR (400 MHz, $CDCl_3$); δ 7.71 (d, J = 8.2, 1H), 7.34 (d, J = 7.1, 1H), 6.81 (t, J =7.8, 1H), 5.97 (bs, 1H), 3.53 (q, J = 6.0 Hz, 2H), 3.23 (t, J = 6.4 Hz, 2H), 2.26 (s, 3H), 1.98 (s, 3H).

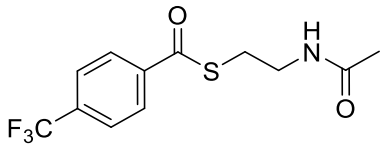

S-(2-acetamidoethyl) 4-(trifluoromethyl)benzothioate (3-CF_3 BA-NAC): ^{1}H NMR (400 MHz, $CDCl_3$); δ 8.06 (d, J = 8.1 Hz, 2H), 7.73 (d, J = 8.2 Hz, 2H), 5.85 (bs, 1H), 3.55 (q, J = 6.3 Hz, 2H), 3.27 (t, J = 6.4 Hz, 2H), 1.98 (s, 3H).

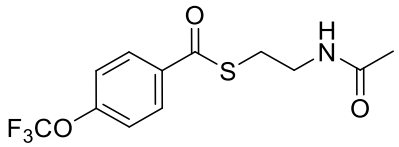

S-(2-acetamidoethyl) 4-(trifluoromethoxy)benzothioate (3-OCF_3 BA-NAC): ^{1}H NMR (400 MHz, $CDCl_3$); δ 8.01 (d, J = 8.7 Hz, 2H), 7.29 (d, J = 8.08 Hz, 2H), 5.88 (bs, 1H), 3.53 (q, J = 6.2 Hz, 2H), 3.24 (t, J = 6.4 Hz, 2H), 1.98 (s, 3H).

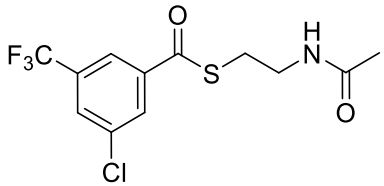

S-(2-acetamidoethyl) 3-chloro-5-(trifluoromethyl)benzothioate (3-Cl-5-CF_3 BA-NAC): ^{1}H NMR (400 MHz, $CDCl_3$); δ 8.08 (s, 1H), 8.065 (s, 1H), 7.80 (s, 1H), 5.99 (bs, 1H), 3.53 (q, J = 6.2 Hz, 2H), 3.27 (t, J = 6.4 Hz, 2H), 1.98 (s, 3H).

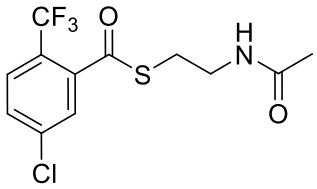

S-(2-acetamidoethyl) 5-chloro-2-(trifluoromethyl)benzothioate (5-Cl-2-CF_3 BA): ^{1}H NMR (400 MHz, $CDCl_3$); δ 7.65 (d, J = 8.4, 1H), 7.62 (d, J = 1.812, 1H), 7.55 (dd, J = 1.2, 8.4, 1H), 6.25 (bs, 1H), 3.51 (q, J = 6.2 Hz, 2H), 3.22 (t, J = 6.4 Hz, 2H), 1.96 (s, 3H).

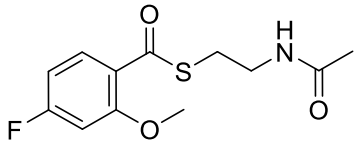

S-(2-acetamidoethyl) 4-fluoro-2-methoxybenzothioate (4-F-2-OCH_3 BA-NAC): ^{1}H NMR (400 MHz, $CDCl_3$); δ 7.84 (t, J = 5.1, 1H), 6.70 (m, 2H), 5.93 (bs, 1H), 3.92 (s, 3H), 3.53 (q, J = 6.1 Hz, 2H), 3.16 (t, J = 6.3 Hz, 2H), 1.97 (s, 3H).

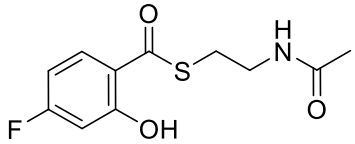

S-(2-acetamidoethyl) 4-fluoro-2-hydroxybenzothioate (4-F-2-OH BA-NAC): ^{1}H NMR (400 MHz, $CDCl_3$); δ 7.86 (dd, J = 5.0, 1H), 6.64 (m, 2H), 5.91 (bs, 1H), 3.53 (q, J = 6.2 Hz, 2H), 3.24 (t, J = 6.4 Hz, 2H), 1.98 (s, 3H).

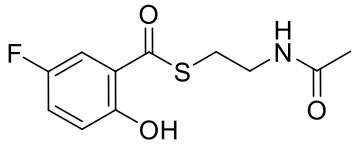

S-(2-acetamidoethyl) 5-fluoro-2-hydroxybenzothioate (5-F-2-OH BA-NAC): ^{1}H NMR (400 MHz, $CDCl_3$); δ 7.52 (dd, J = 8.8, 3.01, 1H), 7.20 (m, 1H), 6.94 (dd, J = 9.2, 4.5, 1H) 6.05 (bs, 1H), 3.52 (q, J = 6.2 Hz, 2H), 3.24 (t, J = 6.4 Hz, 2H), 1.98 (s, 3H).

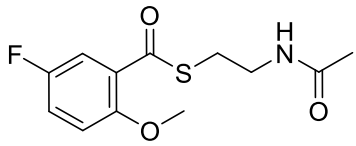

S-(2-acetamidoethyl) 5-fluoro-2-methoxybenzothioate (5-F-2-OCH_3 BA-NAC): ^{1}H NMR (400 MHz, $CDCl_3$); δ 7.47 (dd, J = 8.7, 3.2, 1H), 7.17 (m, 1H), 6.93 (dd, J = 9.1, 4.08, 1H), 6.11 (bs, 1H), 3.88 (s, 3H), 3.50 (q, J = 6.2 Hz, 2H),3.15 (t, J = 6.4 Hz, 2H), 1.95 (s, 3H).

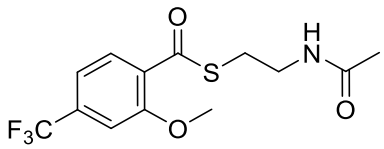

S-(2-acetamidoethyl) 2-methoxy-4-(trifluoromethyl)benzothioate (2-OCH_3-4-CF_3 BA-NAC): ^{1}H NMR (400 MHz, $CDCl_3$); δ 7.81 (d, J = 8.03, 1H), 7.26 (d, J = 7.9, 1H), 7.19 (s, 1H), 5.99 (bs, 1H), 3.96 (s, 3H), 3.52 (q, J = 6.2 Hz, 2H),3.19 (t, J = 6.4 Hz, 2H), 1.97 (s, 3H).

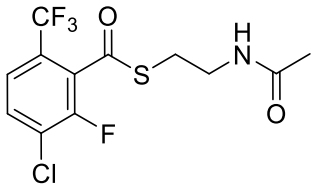

S-(2-acetamidoethyl) 3-chloro-2-fluoro-6-(trifluoromethyl)benzothioate (3-Cl-2-F-6-CF_3 BA): ^{1}H NMR (400 MHz, $CDCl_3$); δ 7.60 (t, J = 7.7, 1H), 7.44 (d, J = 8.5, 1H), 6.09 (bs, 1H), 3.54 (q, J = 6.2 Hz, 2H), 3.22 (t, J = 6.4 Hz, 2H), 1.98 (s, 3H).

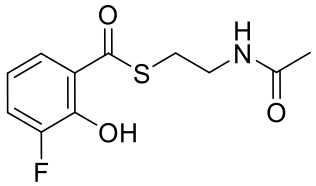

S-(2-acetamidoethyl) 3-fluoro-2-hydroxybenzothioate (3-F-2-OH BA-NAC): ^{1}H NMR (400 MHz, $CDCl_3$); δ 7.63 (td, J = 8.2, 1.3, 1H), 7.29 (m, 1H), 6.84 (dt, J = 8.1, 4.6, 1H), 6.10 (bs, 1H), 3.52 (q, J = 6.3 Hz, 2H), 3.24 (t, J = 6.5 Hz, 2H), 1.95 (s, 3H).

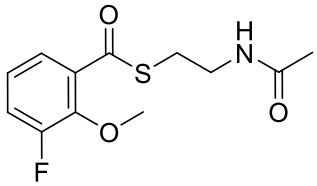

S-(2-acetamidoethyl) 3-fluoro-2-methoxybenzothioate (3-F-2-CH_3 BA-NAC): ^{1}H NMR (400 MHz, $CDCl_3$); δ 7.50 (td, J = 7.9, 1H), 7.26 (m, 1H), 7.08 (dt, J = 8.1, 4.6, 1H), 5.97 (bs, 1H), 4.01 (d, J = 1.97, 1H), 3.54 (q, J = 6.2 Hz, 2H), 3.19 (t, J = 6.4 Hz, 2H), 1.97 (s, 3H).

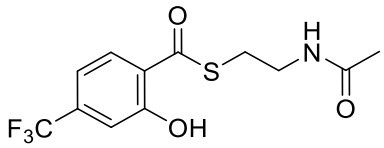

S-(2-acetamidoethyl) 2-hydroxy-4-(trifluoromethyl)benzothioate (2-OH-4-CF_3 BA-NAC): ^{1}H NMR (400 MHz, $CDCl_3$); δ 7.98 (d, J = 8.4, 1H), 7.15 (d, J = 8.4, 1H), 7.19 (s, 1H), 5.82 (bs, 1H), 3.56 (q, J = 6.3 Hz, 2H), 3.29 (t, J = 6.5 Hz, 2H), 2.00 (s, 3H)

Figure B-11. MS spectra (negative mode) of Evn Q incubated with EvdD1 and NAC thioesters orsellinic acid (OSA), 3-methylsalicyclic acid (3MSA), & 6-methylsalicyclic acid (6MSA). Control is a boiled enzyme control. Purple circles show starting material, Evn Q. Teal stars show enzymatic products.

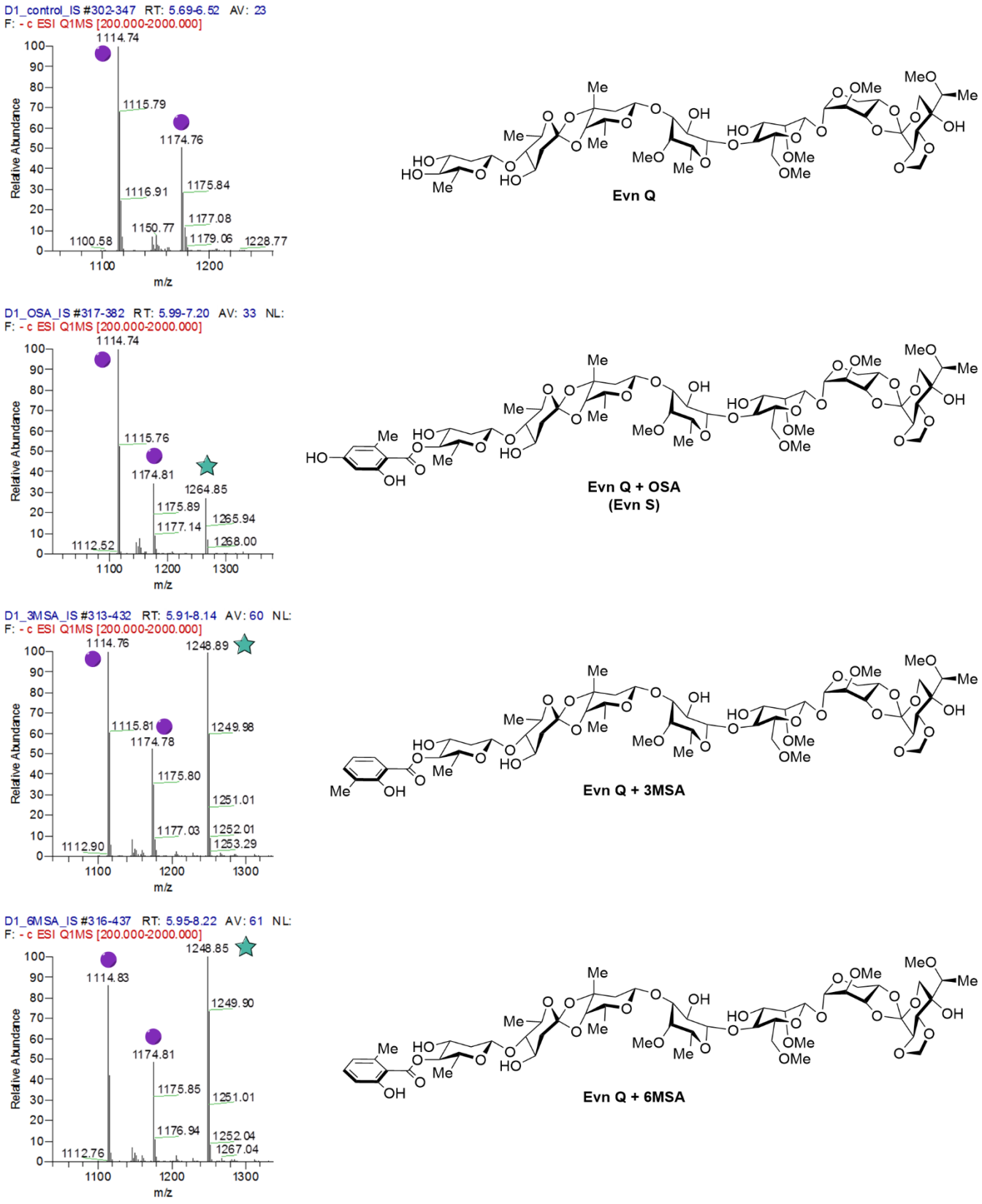

Figure B-12. MS spectra (negative mode) of Evn Q incubated with EvdD1 and NAC thioesters benzoic acid (BA), 4-trifluoromethyl benzoic acid (4-CF_3 BA), 4-trifluoromethoxy benzoic acid (4-OCF_3 BA), & 3-chloro-5-trifluoromethyl benzoic acid (3-Cl-5-CF_3 BA). Purple circles show starting material, Evn Q. Teal stars show enzymatic products.

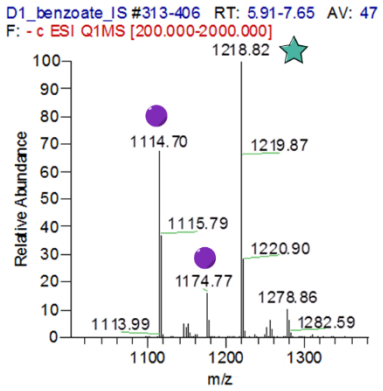

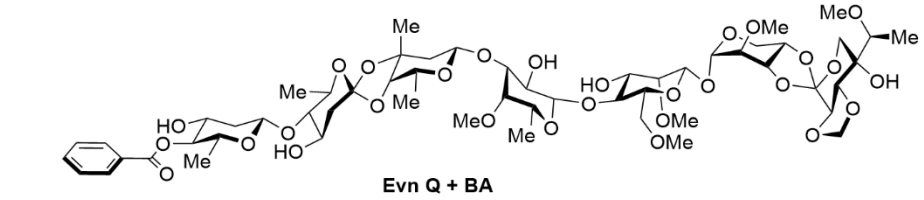
Evn Q + BA

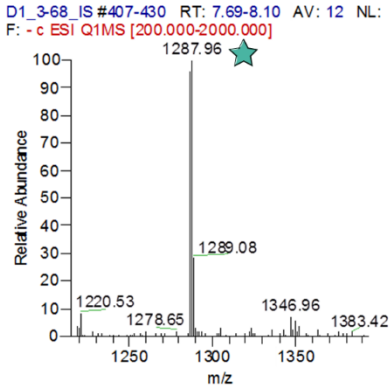

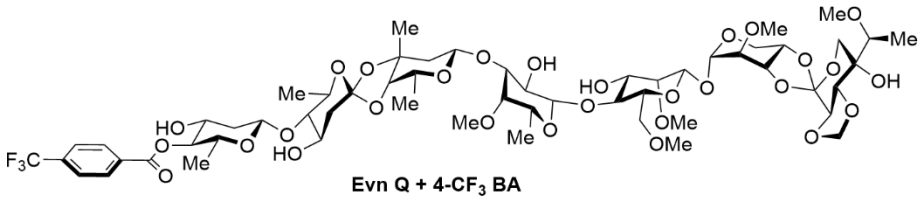
Evn Q + 4-CF_3 BA

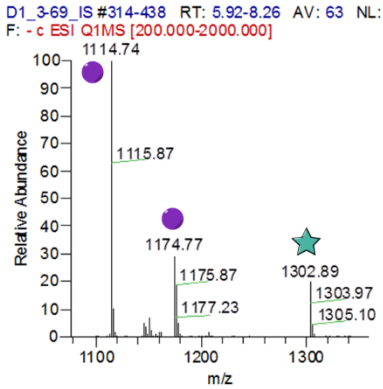

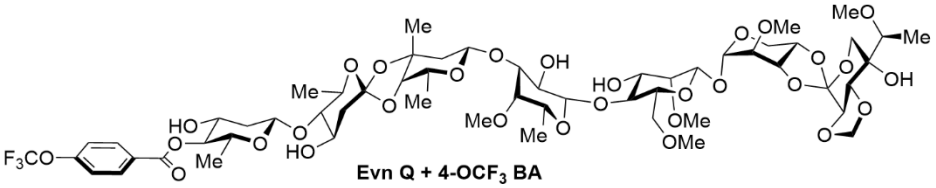
Evn Q + 4-OCF_3 BA

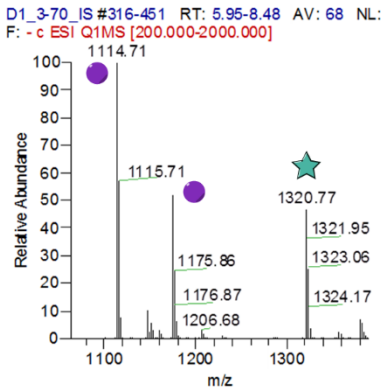

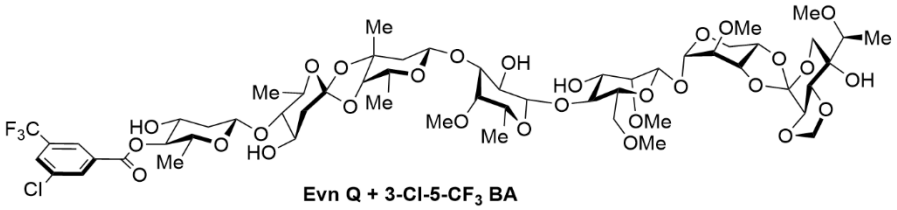
Evn Q + 3-Cl-5-CF_3 BA

Figure B-13. MS spectra (negative mode) of Evn Q incubated with EvdD1 and NAC thioesters 3-chloro-6-trifluoromethyl benzoic acid (3-Cl-6-CF_3 BA), 4-fluoro-2-methoxy benzoic acid (4-F-2-OCH_3 BA), 4-fluoro-2-hydroxyl benzoic acid (4-F-2-OH BA), & 5-fluoro-2-hydroxyl benzoic acid (5-F-2-OH BA). Purple circles show starting material, Evn Q. Teal stars show enzymatic products.

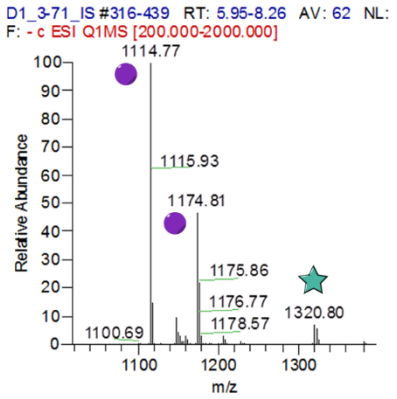

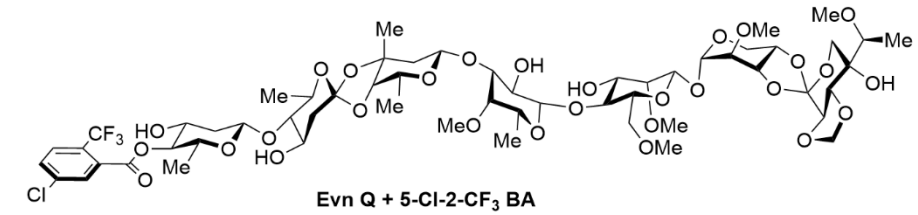

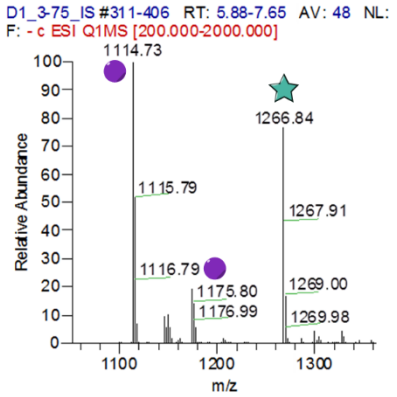

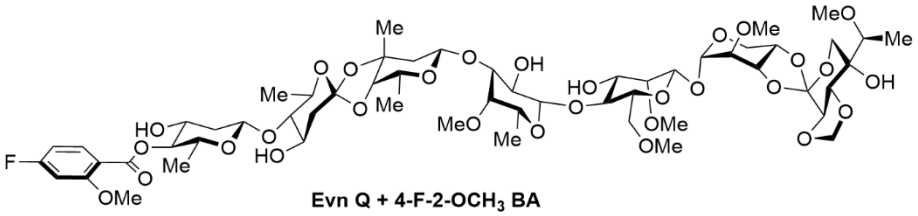

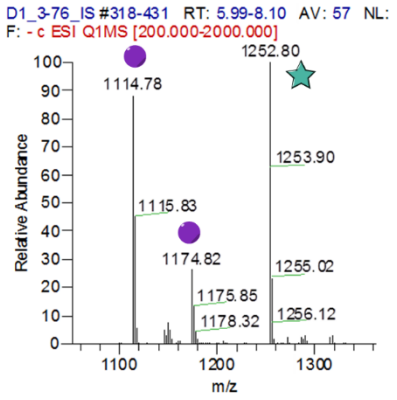

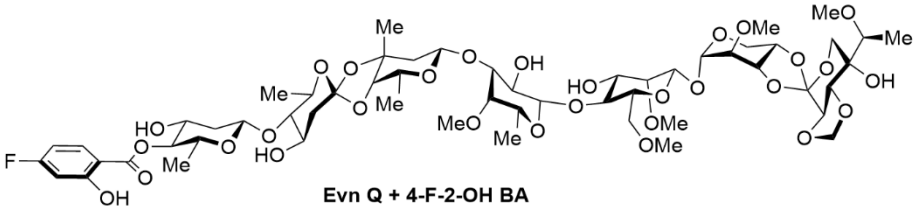

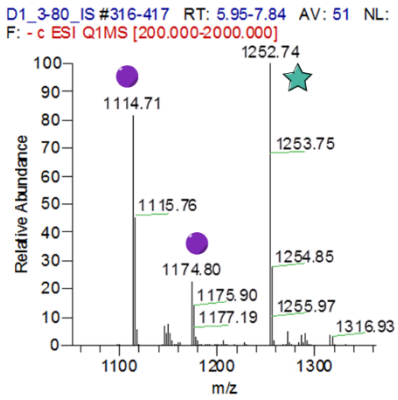

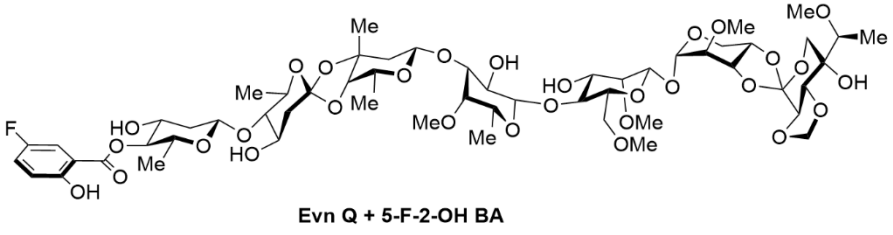

Figure B-14. MS spectra (negative mode) of Evn Q incubated with EvdD1 and NAC thioesters 5-fluoro-2-methoxy benzoic acid (5-F-2-OCH_3 BA), 2-methoxy-4-trifluoromethyl benzoic acid (2-OCH_3-4-CF_3 BA), 3-chloro-2-fluoro-6-trifluoromethyl benzoic acid (3-Cl-2-F-6-CF_3 BA), & 3-fluoro-2-hydroxyl benzoic acid (3-F-2-OH BA). Purple circles show starting material, Evn Q. Teal stars show enzymatic products.

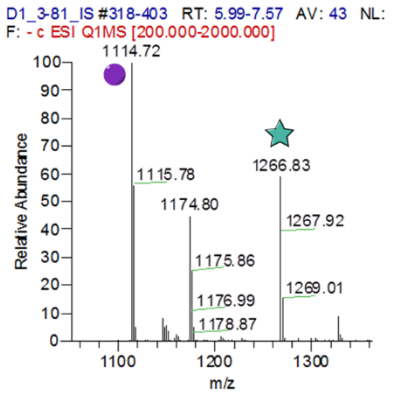

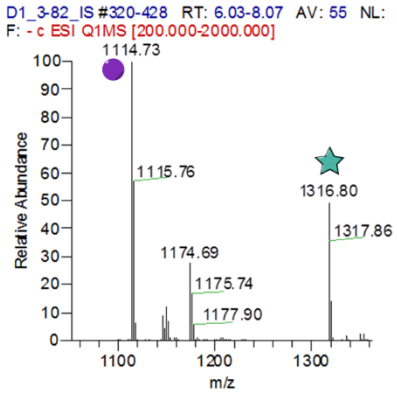

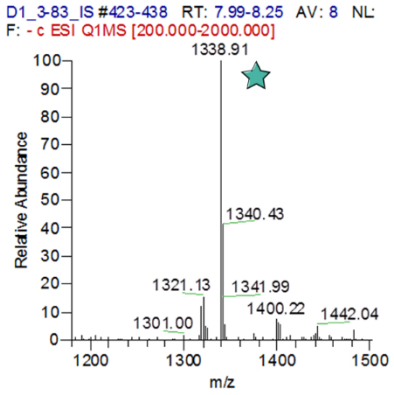

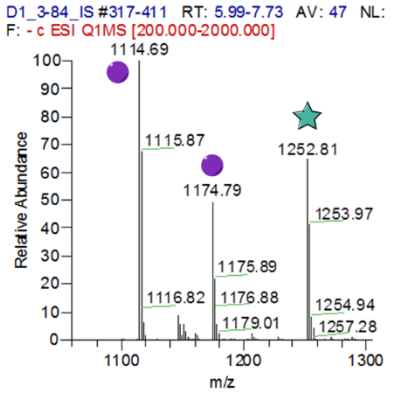

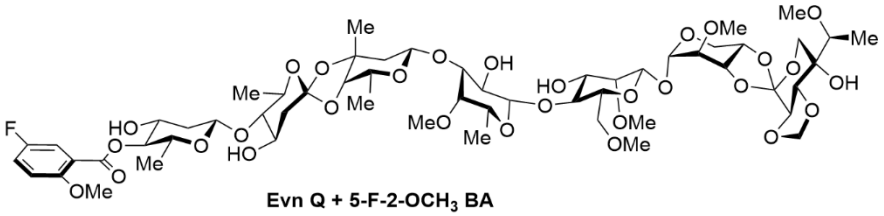

Evn Q + 5-F-2-OCH_3 BA

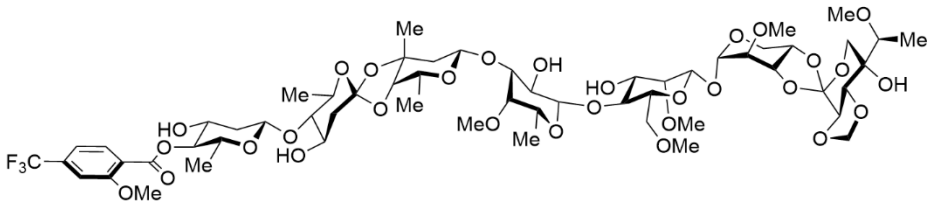

Evn Q + 2-OCH_3-4-CF_3 BA

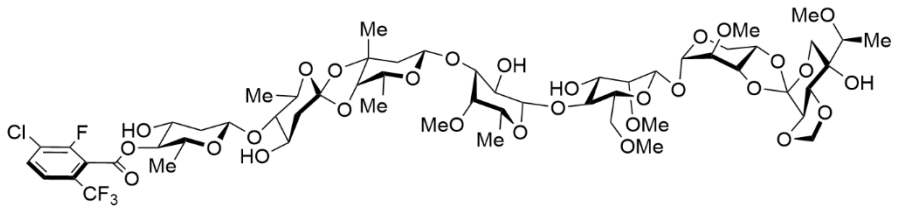

Evn Q + 3-Cl-2-F-6-CF_3 BA

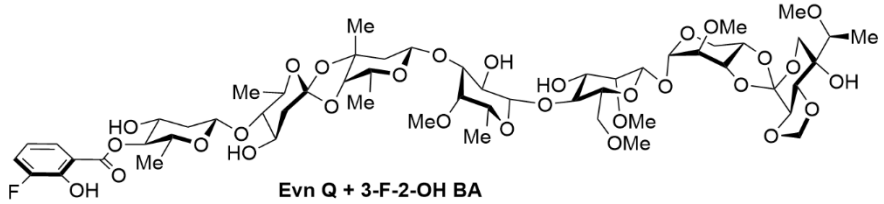

Evn Q + 3-F-2-OH BA

Figure B-15. MS spectra (negative mode) of Evn Q incubated with EvdD1 and NAC thioesters 3-fluoro-2-methoxy benzoic acid (3-F-2-OCH_3 BA) and 2-hydroxyl-4-trifluoromethyl benzoic acid (2-OH-4-CF_3 BA). Purple circles show staritng material, Evn Q. Teal stars show enzymatic products.

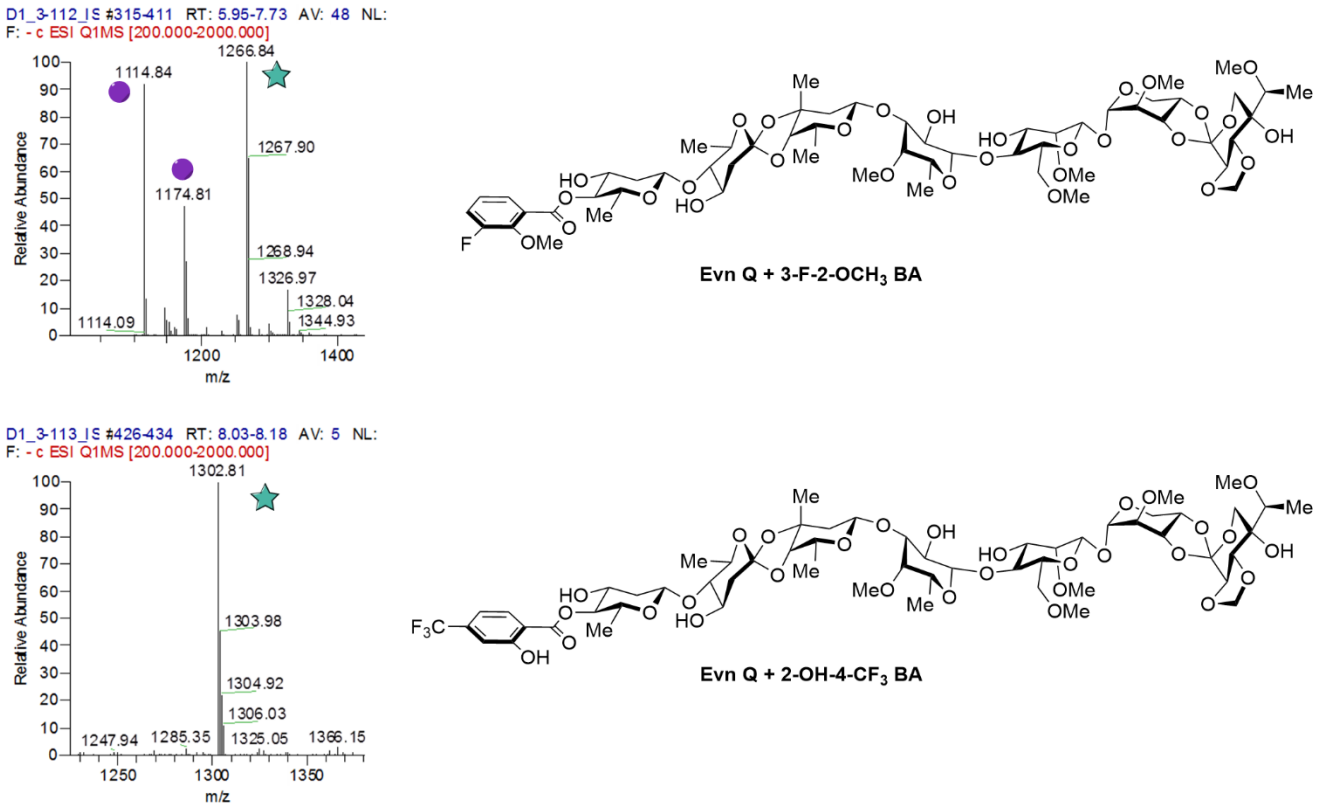

Figure B-16. Chemical complementation of *ΔevdD3* deletion strain. (A) LC/MS analysis of *in vivo* chemical complementation of *ΔevdD3::aac(3)IV* strain with OSA-NAC. (B) LC/MS analysis of *in vivo* chemical complementation of *ΔevdD3::aac(3)IV* strain with BA/3MSA-NAC. Chromatograms show summed ion intensitites for negative mode (dotted lines) and positive mode (solid lines) for Evn analogs. Masses found in Table B-1.

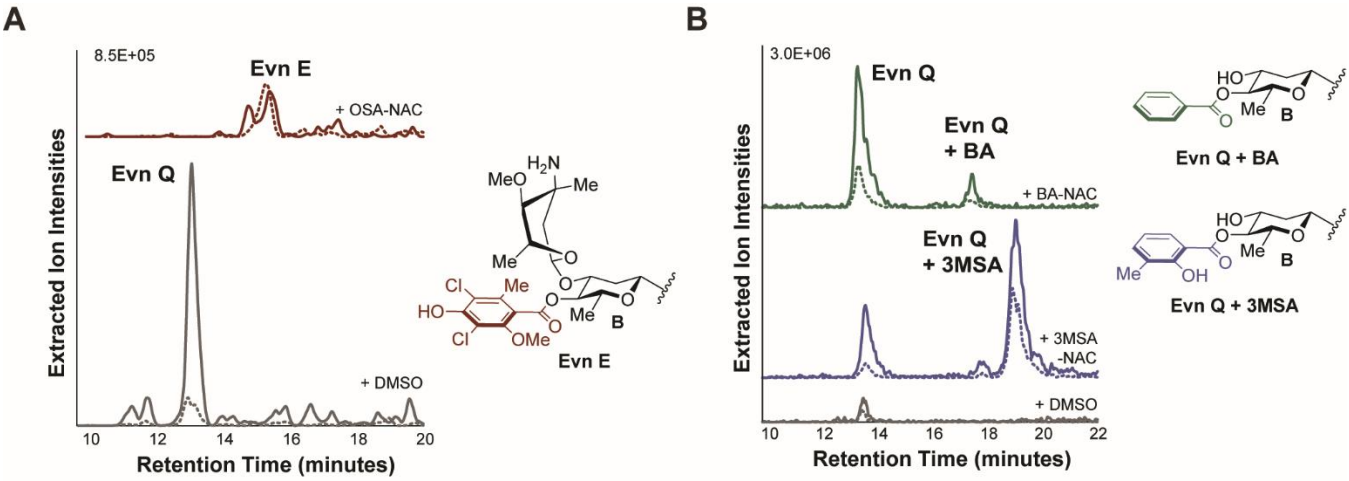

Table B-1. Masses of everninomicins described in Chapter IV.

Compound	Positive Mode (m/z)	Negative Mode (m/z)
Evn D	1536.5 $[M+H]^+$	1534.5 $[M-H]^-$
Evn E	1506.5 $[M+H]^+$	1504.5 $[M-H]^-$
Evn F	1522.5 $[M+H]^+$	1520.5 $[M-H]^-$
Evn G	1520.5 $[M+H]^+$	1518.5 $[M-H]^-$
Evn AE	1352.5 $[M+NH_4]^+$	1333.3 $[M-H]^-$
Evn Q	1117.49 $[M+H]^+$/1134.52 $[M+NH_4]^+$	1115.63 $[M-H]^-$/1175.66 $[M+OAc]^-$
Evn R	1270.73 $[M+NH_4]^+$	1251.57 $[M-H]^-$
Evn S	1284.10 $[M+NH_4]^+$	1265.27 $[M-H]^-$
Evn Q + BA	1238.90 $[M+NH_4]^+$	1219.77 $[M-H]^-$/1279.91 $[M+OAc]^-$
Evn Q + 3MSA	1251.90 $[M+H]^+$/1268.98 $[M+NH_4]^+$	1249.85 $[M-H]^-$

Table B-2. Primers used in Chapter IV.

Primer Name	Used for	Sequence (5'-3')
RED-D1-For	Δ*evdD1*::*aac(3)IV*	GGTGATGATCAACATGAATTGCGAGGAGGAGAATTCATGATTCCGGGGATCCGTCGACC
RED-D1-Rev	Δ*evdD1*::*aac(3)IV*	CCGACGCCGGGGCGGGGGTCCCCCGCCTGCCCGGCGTCATGTAGGCTGGAGCTGCTTC
RED-D2-For	Δ*evdD2*::*aac(3)IV*	GGATCACGTCCCGTCCTCCTCACGATTGGGAGCCTCATGATTCCGGGGATCCGTCGACC
RED-D2-Rev	Δ*evdD2*::*aac(3)IV*	CGTTGCGCTGGGCGGGGTCGGCCGCCAGGGAGCCGCTCATGTAGGCTGGAGCTGCTTC
RED-D3-For	Δ*evdD3*::*aac(3)IV*	CGCCCGACCGTCCGTTCAGGCAATCGACAACAGGGGATGATTCCGGGGATCCGTCGACC
RED-D3-Rev	Δ*evdD3*::*aac(3)IV*	CGATGTCCCGGCCGATCCGTCCGGTGTCCCGGCTCGTCATGTAGGCTGGAGCTGCTTC
Neo_SuperCos_For	Kanamycin cassette primers	GTGGAGAGGCTATTCGGCTA
Neo_SuperCos_Rev	Kanamycin cassette primers	AATATCACGGGTAGCCAACG
Seq-Up	Gene replacement sequencing	TCAGAAGGAAGGTCCAGTCG
Seq-Dn	Gene replacement sequencing	CGGGTGTTCCTCTTCACTG
Del-Up	Apramycin cassette primers	ATTCCGGGGATCCGTCGACC
Del-Dn	Apramycin cassette primers	TGTAGGCTGGAGCTGCTTC
EvdD1-For	EvdD1 Gibson Cloning	CTTTAAGAAGGAGATATACCATGCGGACACCGGACATG
EvdD1-Rev	EvdD1 Gibson Cloning	TCGAGTGCGGCCGCAAGCTTCTTCGTCCAGGCCGGCGATTC
EvdD2-For	EvdD2 PCR Cloning	AAGCTTGTCGGTCGTAGTCCTCGTTG
EvdD2-Rev	EvdD2 PCR Cloning	CAACGAGGACTACGACCGACAAGCTT
EvdD1-C113A For	Directed Mutagenesis	TGGAGATCCGGCAGGGCGCTAACGGTCTGTTCAGC
EvdD1-C113A Rev	Directed Mutagenesis	CGACTTGTCTGGCAATCGCGGGACGGCCTAGAGGT
EvdD1-C113S For	Directed Mutagenesis	TGGAGATCCGGCAGGGCTCTAACGGTCTGTTCAGC
EvdD1-C113S Rev	Directed Mutagenesis	CGACTTGTCTGGCAATCTCGGGACGGCCTAGAGGT
EvdD1-H293A For	Directed Mutagenesis	GTCGCGGGATCGGGGCTTGCGGCGCCAGC
EvdD1-H293A Rev	Directed Mutagenesis	CGACCGCGGCGTTCGGGGCTAGGGCGCTG